

UC San Diego

UC San Diego Electronic Theses and Dissertations

Title

Understanding CXC chemokine receptor 4 activation by CXC chemokine ligand 12

Permalink

<https://escholarship.org/uc/item/3zt5h403>

Author

Stephens, Bryan Scott

Publication Date

2017

Peer reviewed|Thesis/dissertation

UNIVERSITY OF CALIFORNIA SAN DIEGO

Understanding CXC chemokine receptor 4 activation by CXC chemokine ligand 12

A dissertation submitted in partial satisfaction of the
requirements for the degree of Doctor of Philosophy

in

Biomedical Sciences

by

Bryan S. Stephens

Committee in charge:

Professor Tracy M. Handel, Chair
Professor JoAnn Trejo, co-Chair
Professor Marilyn Farquhar
Professor William Joiner
Professor Elizabeth Komives

2017

Copyright

Bryan S. Stephens, 2017

All rights reserved

The dissertation of Bryan S. Stephens is approved,
and it is acceptable in quality and form for publication on
microfilm and electronically:

Co-Chair

Chair

University of California, San Diego

2017

DEDICATION

I dedicate this work to my mother, Kay Taylor.

TABLE OF CONTENTS

Signature page.....	iii
Dedication.....	iv
Table of Contents.....	v
Lists of Figures.....	ix
Lists of Tables.....	xiii
Acknowledgements.....	xiv
Vita.....	xvi
Abstract.....	xviii
Chapter 1 Introduction.....	1
Chemokine Signaling in the Immune System and CXCR4.....	2
G Protein-Coupled Receptors	6
The Structure and Activation of CXCR4.....	10
Chapter 2 Chemokine receptor oligomerization and allostery	19
Introduction.....	21
Background: chemokine structure and interactions with receptors...	22
Evidence for Hetero- and Homo-Oligomerization of Chemokine Receptors	27
Functional Effects of Chemokine Receptor Hetero-Oligomerization on Ligand Binding.....	39

	Effects of Chemokine Hetero- and Homo-Oligomerization on Signaling.....	43
	Heterodimerization of Chemokine Receptors with Nonchemokine Receptors.....	49
	Other Sources of Allostery in Chemokine Receptor Signaling: Chemokine Oligomerization.....	51
	Conclusions and Future Perspectives.....	53
Chapter 3	Stoichiometry and Geometry of the CXC Chemokine Receptor 4 Complex with CXC Ligand 12: Molecular Modeling and Experimental Validation.....	62
	Introduction.....	63
	Results.....	65
	Discussion.....	67
	Materials and Methods.....	69
	Supporting Information.....	73
Chapter 4	What Do Structures Tell Us About Chemokine Receptor Function and Antagonism?.....	77
	Introduction.....	79
	Chemokines: Structure and Biology.....	80

	The Structural Basis of Chemokine Receptor Interactions with Chemokines.....	81
	Insights into Receptor Activation from Experiments Interpreted in the Context of Structures and Models.....	85
	On the Allostery of Chemokine Receptors.....	88
	On the Druggability of Chemokine Receptors.....	92
	Conclusions.....	94
Chapter 5	Anatomy of the CXC chemokine receptor 4 signaling complex with CXCL12.....	103
	Introduction.....	104
	Materials and Methods.....	108
	Results.....	114
	Discussion.....	131
	Figures and Tables.....	146
Chapter 6	Extended speculative discussion and future experimental directions.....	166
	On the need for cautious interpretation of Ca ²⁺ signaling data in chemokine receptor research, and the value of relatively direct measurements of receptor activity	167

Extended interpretation of N-terminal truncations and other CXCR4 perturbations that cause unexpectedly large efficacy deficits in arrestin recruitment	170
Understanding the coupling of G protein, arrestin, and other effectors to CXCR4.....	176
Future experiments.....	177

LIST OF FIGURES

Figure 2.1	Ribbon diagrams of a typical chemokine monomer; a CXC chemokine dimer; a CC chemokine dimer.....	23
Figure 2.2	Two site model of receptor activation.....	25
Figure 2.3	Cartoon of the two-site model where the small molecule antagonist AMD3100 binds CXCR4 in the TM domain CRS2, and displaces the N-terminus of SDF-1/CXCL12.....	26
Figure 2.4	A model for the allosteric ligand binding transinhibition of agonists from chemokine heterodimers as suggested by Springael and coworkers.....	41
Figure 2.5	A model for inhibition of CXCR4 signaling by the EBV viral GPCR, BILF1.....	49
Figure 3.1	Molecular models and experimental designs used in the present study.....	64
Figure 3.2	CXCR4 mutants used in this study.....	66
Figure 3.3	CXCR4 mutants retain ability to dimerize with each other and with WT receptor.....	67
Figure 3.4	The absence of functional rescue when coexpressing two complementary mutants of CXCR4 in CHO-G α_{15} cells.....	68
Figure 3.5	Diluting WT-WT dimers by increasing transfection of loss-of-function mutants does not lead to a decrease in signaling.....	69

Figure 3.6	Cysteine trapping experiment with CXCR4 and CXCL12 coexpressed in insect Sf9 cells.....	70
Figure 3.S1	Design of CXCR4-free cell line for CXCR4 mutant functionality testing. (A–E) Endogenous expression of CXCR4 was detected via flow cytometry following surface staining with anti–CXCR4-PE...	74
Figure 4.1	Topology and oligomerization behavior of chemokines.....	81
Figure 4.2	Chemokine interaction with receptors and other binding partners....	83
Figure 4.3	Insights into chemokine receptor activation.....	87
Figure 4.4	The allosteric nature of chemokine receptor activation and inhibition.....	89
Figure 4.5	Structural basis of small molecule antagonism of chemokine receptors.....	91
Figure 5.1	A full length model of the CXCL12: CXCR4 signaling complex.....	146
Figure 5.2	Mutating CRS2 residues known to be critical to G protein signaling abrogates β arrestin-2 recruitment as well.....	147
Figure 5.3	Residue D262 of CXCR4 is important for potent and efficacious CXCL12-mediated receptor activation.....	148
Figure 5.4	R8E mutation in CXCL12 severely impairs β arrestin-2 recruitment, and recruitment is greatly rescued by both D262K and R mutations in CXCR4.	149

Figure 5.5	Mutagenesis targeting both R30 and E277 impairs CXCR4 signaling, supporting the engagement of both residues with the CXCL12 N-terminus as predicted in the model.....	150
Figure 5.6	Mutating R12 of CXCL12 to glutamate severely impairs its activation of CXCR4, and this effect is substantially reversed by charge-reversing mutation of CXCR4 residue E277.....	151
Figure 5.7	Negatively charged residues in ECL2 of CXCR4 are important for the efficacy of arrestin recruitment.....	152
Figure 5.8	Mutation of the DRY motif residue R134A produces a constitutively active β arrestin-2 recruiting form of CXCR4.....	153
Figure 5.9	Mutating TM5 residues W195 and Q200 causes deficits in signaling that are not easily explained by the CXCL12: CXCR4 model.....	154
Figure 5.10	The effects of mutating charged residues (as well as the putatively sulfated Y21 residue) in the most proximal region of CRS1 reinforce the role of this region in providing for potent CXCL12 association..	155
Figure 5.11	Successively larger truncations of CRS1 produce surprising progressive deficits in β arrestin-2 recruitment efficacy that are not seen in Ca^{2+} mobilization results.....	156
Figure 5.S1	BRET results are unaffected by changes in receptor-RLuc3 expression level within a wide range.....	157
Figure 5.S2	Expression of trans-membrane domain mutant forms of CXCR4 that show differences in signaling from WT receptor.....	158

Figure 5.S3	Expression of N-terminal domain mutant and truncated forms of CXCR4 that show differences in signaling from WT receptor.....	159
Figure 5.S4	Expression of all mutants tested in Ca ²⁺ signaling assays relative to WT receptor tested on the same day, after adjustment of WT receptor DNA amount according to the observed mutant expression range...	160

LIST OF TABLES

Table 2.1	Chemokine receptor oligomers.....	28
Table 2.2	Methods used in studying chemokine receptor oligomerization.....	33
Table 3.S1	Properties of the cell lines tested and generated to identify a background-free CXCR4 mutant testing system.....	75
Table 5.1	Signaling parameters derived from β arrestin-2 recruitment experiments.....	161
Table 5.2	Signaling parameters derived from Ca^{2+} mobilization experiments...	163
Table 5.3	Equiactive bias factors calculated for select mutants.....	164

ACKNOWLEDGEMENTS

Thanks of course to the committee for lending their time and thoughts to my progress frequently. Thanks to Tracy Handel for years of mentoring, which I could not have remotely understood the value of at the outset. I must further thank Tracy for her patience and her own successes that have allowed me to continue working and learning. Two others who deserve individual mention are JoAnn Trejo and Irina Kufareva, who have provided me as much extensive training and guidance to be considered co-mentors. I also very much appreciate both the patience and guidance afforded me by the various post-doctoral scholars, graduate students, and undergraduates who have worked in the laboratory during my time here. I have learned countless lessons from them.

And thanks to my special lady Alex and my mother Kay Taylor, both of whose inexplicable faith in me has given me comfort and motivation in tough times.

Chapter two, in full, is a reprint of a published review article as it appears in Progress in Molecular Biology and Translational Science. (**Stephens, B.** and T. M. Handel (2013). "Chemokine receptor oligomerization and allostery." Prog Mol Biol Transl Sci **115**: 375-420.) The dissertation author was the primary author of this material.

Chapter three, in full, is a reprint of a published research article as it appears in Proceedings of the National Academy of Sciences of the USA. (Kufareva, I., **B. S. Stephens**, L. G. Holden, L. Qin, C. Zhao, T. Kawamura, R. Abagyan and T. M. Handel (2014). "Stoichiometry and geometry of the CXC chemokine receptor 4

complex with CXC ligand 12: molecular modeling and experimental validation." Proc Natl Acad Sci U S A **111**(50): E5363-5372.) The dissertation author was a co-primary researcher and author of this material.

Chapter four, in full, is a reprint of a published review article as it appears in Annual Review of Biophysics. This was a collaboratively written review relying on each experimentalist author's area of expertise. (Kufareva, I., M. Gustavsson, Y. Zheng, **B. S. Stephens** and T. M. Handel (2017). "What Do Structures Tell Us About Chemokine Receptor Function and Antagonism?" Annu Rev Biophys **46**: 175-198.) The dissertation author was among several independent contributors to this material.

Chapter five is adapted from a manuscript currently in preparation for submission for publication. (**Stephens, B. S.**; I. Kufareva and T. M. Handel (2017). "Anatomy of the CXC chemokine receptor 4 signaling complex with CXCL12." in preparation for submission to Science Signaling.) The dissertation author was the primary researcher and author of this material.

VITA

2010 Bachelors of Science, Biochemistry, University of New Mexico

2017 PhD, Biomedical Sciences, University of California San Diego

PUBLICATIONS

Kufareva, I., **B. Stephens**, C. T. Gilliland, B. Wu, G. Fenalti, D. Hamel, R. C. Stevens, R. Abagyan and T. M. Handel (2013). "A novel approach to quantify G-protein-coupled receptor dimerization equilibrium using bioluminescence resonance energy transfer." *Methods Mol Biol* 1013: 93-127.

Stephens, B. and T. M. Handel (2013). "Chemokine receptor oligomerization and allostery." *Prog Mol Biol Transl Sci* 115: 375-420.

Ziarek, J. J., A. E. Getschman, S. J. Butler, D. Taleski, **B. Stephens**, I. Kufareva, T. M. Handel, R. J. Payne and B. F. Volkman (2013). "Sulfopeptide probes of the CXCR4/CXCL12 interface reveal oligomer-specific contacts and chemokine allostery." *ACS Chem Biol* 8(9): 1955-1963.

Kawamura, T., **B. Stephens**, L. Qin, X. Yin, M. R. Does, T. H. Smith, N. Grimsey, R. Abagyan, J. Trejo, I. Kufareva, M. M. Fuster, C. L. Salanga and T. M. Handel (2014). "A general method for site specific fluorescent labeling of recombinant chemokines." *PLoS One* 9(1): e81454.

Kufareva, I., **B. S. Stephens**, L. G. Holden, L. Qin, C. Zhao, T. Kawamura, R. Abagyan and T. M. Handel (2014). "Stoichiometry and geometry of the CXC chemokine receptor 4 complex with CXC ligand 12: molecular modeling and experimental validation." *Proc Natl Acad Sci U S A* 111(50): E5363-5372.

Gustavsson, M., L. Wang, N. van Gils, **B. S. Stephens**, P. Zhang, T. J. Schall, S. Yang, R. Abagyan, M. R. Chance, I. Kufareva and T. M. Handel (2017). "Structural basis of ligand interaction with atypical chemokine receptor 3." *Nat Commun* 8: 14135.

Kufareva, I., M. Gustavsson, Y. Zheng, **B. S. Stephens** and T. M. Handel (2017). "What Do Structures Tell Us About Chemokine Receptor Function and Antagonism?" *Annu Rev Biophys* 46: 175-198.

Ziarek, J. J., A. B. Kleist, N. London, B. Raveh, N. Montpas, J. Bonnetterre, G. St-Onge, C. J. DiCosmo-Ponticello, C. A. Koplinski, I. Roy, **B. Stephens**, S. Thelen, C. T. Veldkamp, F. D. Coffman, M. C. Cohen, M. B. Dwinell, M. Thelen, F. C. Peterson, N. Heveker and B. F. Volkman (2017). "Structural basis for chemokine recognition by a G protein-coupled receptor and implications for receptor activation." *Sci Signal* 10(471).

FIELDS OF STUDY

Major Field: Biomedical Sciences

ABSTRACT OF THE DISSERTATION

Understanding CXC chemokine receptor 4 activation by CXC chemokine ligand 12

by

Bryan S. Stephens

Doctor of Philosophy in Biomedical Sciences

University of California, San Diego, 2017

Professor Tracy M. Handel, Chair

The past several years have seen a rapid advancement in our understanding of how CXCR4 transmits the extracellular CXCL12 signal into intracellular signaling, which ultimately causes cell migration along with other signaling outcomes critical in both immune cell function and various cancers. We began this project uncertain as to the stoichiometry of CXCL12: CXCR4 binding, and through various functional and

structural studies were able to settle on an early complex model with 1:1 stoichiometry (chapters 2&3). An improvement in our ability to model the CXCL12:CXCR4 complex was enabled by the solution of the vMIP-II:CXCR4 crystal structure by our laboratory soon after, and other landmarks in chemokine receptor structural determination (chapter 4) have allowed for a global understanding of chemokine:receptor structure to emerge. At this point the structural link between CXCL12 N-terminus binding and the more conserved intracellular aspects of CXCR4 activation is finally coming into view. In our latest soon to be submitted study, we provide functional evidence decisively supporting the orientation proposed in our current model, as well as revealing previously unrecognized complexity in the nature of CXCR4 activation (chapter 5). In chapter 6, we comprehensively discuss tentative but exciting possible explanations for evidence in our latest findings of greater complexity in chemokine:chemokine receptor signaling than has been appreciated.

We have progressed from a rough understanding of how CXCL12 activates CXCR4 to an experimentally validated full-length CXCL12:CXCR4 signaling complex model. Ultimately, we have made significant contributions to understanding the structure of CXCR4 bound to CXCL12, the precise mechanism whereby CXCL12 stabilizes CXCR4's active state(s), and the complexity of the downstream functional consequences of receptor activation.

Chapter 1

Introduction

Chemokine signaling in the immune system and CXCR4

The chemokine signaling system in humans consists of at least 45 chemokine ligands and 22 chemokine receptors, and enables migration of the receptor-bearing cells across chemokine gradients from areas of low to high concentration (Scholten, Canals et al. 2012). The chemokine system plays critical roles in the development and homeostasis of immune cells as well as in their recruitment to sites of acute inflammation (Sokol and Luster 2015). There is reciprocal promiscuity in the binding of chemokines and their receptors, making the integrated chemokine signaling network quite complex and difficult to tease apart experimentally. In fact most chemokine receptors bind multiple chemokines, although the chemokine receptor CXCR4 only has one chemokine agonist in CXCL12 (Scholten, Canals et al. 2012). CXCR4 and CXCL12 play a role of particularly broad importance in the sequestration and maintenance of hematopoietic stem cells in bone marrow (BM), as well as in their retention and development as they differentiate and mature (Sokol and Luster 2015). As these cells approach maturity, immune cell lineage-specific changes in chemokine receptor expression allow cells to migrate out of BM and into circulation, and ultimately to their final destination in the blood, peripheral tissues, or lymph system. While the maintenance of developing immune cells in BM is dependent on CXCR4, their exit is not simply the result of decreased CXCR4 expression or otherwise down-regulated signaling. Generally, it is the up-regulation of one or more alternative chemokine signaling pathway(s) that is critical to mature immune cells exiting the BM for their ultimate destination (Sokol and Luster 2015). In at least some cases CXCR4

expression is maintained and CXCR4 may be involved in some complex way in the cells' emigration from the BM, and CXCL12 signaling through CXCR4 is definitely involved in establishing pools of immune cells in strategic peripheral locations. Neutrophils in particular up-regulate CXCR4 upon senescence, and this has been hypothesized to allow for their re-uptake into the BM on their course to apoptosis (Sokol and Luster 2015).

Most chemokines are capable of both homo and hetero-oligomerization as well as binding to non-receptor glycosaminoglycans (GAGs), adding a further layer of complexity to their function. In a particularly interesting example, lymph node (LN) immune cell distribution is maintained by expression of both CCL21 and CCL19 (Schumann, Lämmermann et al. 2010). A significant portion of CCL21 is immobilized through anchoring of its extended C-terminus to heparin sulfate, a GAG commonly bound by chemokines. This allows for special highly regulated movement of cells within the lymphatic system, with tethered CCL21 causing cells to crawl slowly through lymphatic vessels, and CCL19 along with the soluble fraction of CCL21 providing the directional cues for precise location within the lymph system (Schumann, Lämmermann et al. 2010). Adding yet another layer of complexity, CCL21 and CCL19 show signaling bias (defined below) relative to one another in their activation of CCR7 (Jørgensen, Rosenkilde et al. 2017). The difference in signaling between the two CCR7-activating chemokines, which is effectively that CCL19 provide a temporally specific burst of signaling compared to the longer sustained signaling for the CCL21-activated receptor state, along with the proteolytic conversion of tethered insoluble CCL21 to soluble CCL21, enables very fine

regulation of the positioning of immune cells within LNs (Jørgensen, Rosenkilde et al. 2017). Generally, the complexity of the chemokine system is such that an immune cell will undergo a series of changes in chemokine receptor expression profiles as it differentiates and matures, and this will typically account for its resting position in the body under homeostatic conditions throughout its lifetime (Sokol and Luster 2015).

Chemokine signaling and the chemokines themselves can be classified as either constitutive, as in the case of the homeostasis-involved chemokine signaling processes discussed above, or inflammatory, based on their pattern of expression. In acute inflammation such as in response to infection, the inflammatorily expressed chemokines act on receptors expressed by various types of mature immune cells and thereby play a large role in both the innate and adaptive immune response. When mature, initially responding immune cells such as macrophages and mast cells prepositioned throughout the blood and peripheral tissues sense infection or tissue damage, and release cytokines and chemokines when an infectious agent is encountered. The secreted chemokine in turn recruit other immune cells such as neutrophils and monocytes to the site of inflammation, which may then also release yet more chemokines. This process can be continued through multiple rounds and provides for significant and rapid amplification in the immune response (Sokol and Luster 2015).

Dendritic cells play the critical role of messengers in initiating the adaptive immune response, and this role is largely dependent on chemokine signaling. A population of mature peripherally distributed DCs, which express multiple chemokine receptors with inflammatory chemokine agonists, allows them to become activated

specifically at sites of inflammation where they will also encounter antigens (Sokol and Luster 2015). When activated, a rapid up-regulation of CCR7 allows for CCL21-directed migration into lymph vessels (and ultimately lymph nodes) where these antigens can be presented to T cells (a critical component of the adaptive immune response), which are themselves pre-positioned in specific areas of the lymph nodes via CCL21 and CCL19 signaling through CCR7 (Schumann et al. 2010, Sokol and Luster 2015).

Chemokines are small (~10 kDa) secreted proteins that signal through G protein-coupled receptors (GPCRs). The basic structure of chemokines is remarkably well-conserved and consists of a disordered short N-terminus connected by an “N-loop” to a three-stranded anti-parallel beta sheet, with a “30s loop” and a “40s loop” connecting the beta strands and a C-terminal helix following the beta sheet, all compactly folded so that the protein appears grossly as a relatively large globular domain with a short disordered region sticking out (the N-terminus) (Scholten, Canals et al. 2012). The chemokine N-terminus is tethered to the beta sheet core of its globular domain at the junction between the N-terminus and the N-loop through one or (in most cases) two disulfide bonds, and the chemokines are named according to the pattern of residues located at this junction (either C, CC, CXC, or CX₃C). The receptors are named according to the type of chemokine ligand they bind (Scholten, Canals et al. 2012).

G protein-coupled receptors

The chemokine receptors are members of the much larger rhodopsin-like (also known as class A) family of GPCRs (Scholten, Canals et al. 2012). GPCRs feature a membrane-spanning domain with seven trans-membrane helices, three connecting intracellular and three extracellular loops, and an intracellular C-terminus that often forms an eighth helix parallel to the membrane. The complete GPCR family comprises over 800 different proteins in humans, making it the largest family of cell surface receptors, with over 700 belonging to the class A family (Heifetz, Schertler et al. 2015). It is understandable given the large role in intracellular signaling played by GPCRs that they are the targets for over 60% of all prescribed drugs (Schöneberg, Schulz et al. 2004).

The extensive study of the class A G protein-coupled β -2 adrenergic receptor (B2AR), originally discovered in the course of understanding the molecular mechanism of adrenaline (epinephrine) and the first GPCR to be successfully cloned (Lefkowitz 2013), provided much of the current understanding of how GPCRs link extracellular ligand binding to intracellular signaling (Rosenbaum, Rasmussen et al. 2009). G proteins are well known as “molecular switches” in various intracellular signaling pathways. The B2AR was among the first GPCRs to be structurally solved by X-ray crystallography (after the light-sensing receptor rhodopsin), and there have since been multiple structures reported for the receptor bound to both agonists and antagonists, as well as a structure for the full ternary complex between an agonist ligand, the receptor, and the trimeric Gs protein coupled to the receptor (Rosenbaum,

Rasmussen and Kobilka 2009, Rosenbaum, Rasmussen and Kobilka 2009, Lefkowitz 2013, (Rasmussen, DeVree et al. 2011). By now more than 20 different GPCRs have been structurally determined (Heifetz, Schertler et al. 2015). Crucially, several have been solved in both agonist-bound and antagonist-bound states, and this along with the multiple B2AR structures have shed light on how exactly ligand binding to the extracellular surface of the receptors leads to G protein activation within the cell.

The putative model that emerged from the decades of research since the initial discovery of the B2AR explained receptor activation in terms of a conformational change from an inactive to an active state, with the active state favored by agonist ligand and thus stabilized by agonist binding (Rosenbaum, Rasmussen and Kobilka 2009). The active state of the receptor has increased potency for coupling to the alpha subunit of inactive (GDP-bound) G proteins, and upon coupling it directly induces a conformational change in the G protein that causes GDP release. The GDP-free state of the G protein alpha subunit is then free to bind GTP and become active. The receptor thereby acts as a ligand-controlled activating GEF for the type of G protein that it couples to, and in this way the receptor links the binding of an extracellular ligand to activation of an intracellular G protein-governed signaling cascade. GPCR signaling is now known to involve multiple families of G proteins, each of which ultimately activates a unique (but in many cases overlapping) set of secondary effector functions (Dorsam and Gutkind 2007).

In addition to the pharmacological observation of dose-responsive activation by ligands, this model explains the multiple observations of constitutive activity in GPCRs through the active/inactive receptor state equilibrium that exists in the absence

of agonists (Rosenbaum, Rasmussen and Kobilka 2009). Antagonism is explained in this model by neutral binding with respect to receptor state (equal affinity to inactive and active states of the target receptor), and according to the same logic, inverse agonists that reduce or eliminate basal receptor activity are explained as preferably binding and stabilizing the inactive state.

With respect to the active and inactive states of the receptors, the situation is more complex than originally appreciated, and this is one of the frontiers of GPCR research. Recent advances in high-resolution dynamic structural experiments have led to the suggestion of at least four distinct states for the B2AR (and likely most other GPCRs), which range from completely inactive (as in the case of an inverse agonist-bound receptor) to the most active case of the full ligand:receptor:G-protein ternary complex (Manglik, Kim et al. 2015). It was observed early on, in fact while the existence of GPCRs was still in question, that the addition of guanine nucleotides reduced adrenaline potency, indeed suggesting a fully cooperative ternary complex between agonist, GPCR, and G protein (Lefkowitz 2013). It was only determined recently (at least in the case of the B2AR), however, that this G protein-mediated increase in activation potency is the result of a conformational change in the receptor upon coupling to an inactive nucleotide-free G protein that ultimately causes an enclosure of the ligand binding site (DeVree, Mahoney et al. 2016). In effect, this G protein-bound state is less accessible to all ligands, but it also greatly extends the residence time of agonists already bound to the receptor, explaining the G protein effect on observed potency through a large decrease in the complex off-rate (DeVree et al. 2016).

Another class of proteins that were discovered early on to interact with GPCRs are arrestins, so named because were originally recognized as G protein signaling desensitization mediators (Lefkowitz 2013). Most commonly, active receptors recruit G protein coupled receptor kinases (GRKs) (after active $G\alpha$ protein subunits dissociate), which then phosphorylate residues in the receptor C-terminus and produce a docking site for arrestins. Once engaged, arrestins sterically prevent G protein coupling to the receptor, and they also recruit internalization machinery to receptors in the course of receptor down-regulation through internalization (Shenoy and Lefkowitz 2011). They have since been discovered to play positive signaling roles as well, with the best established being activation of various kinase signaling pathways (Shukla, Xiao et al. 2011). Recent years have seen rapid advances in our understanding of how and why arrestins interact with receptors (Shukla, Westfield et al. 2014), and in 2015 a crystal structure of rhodopsin in complex with visual arrestin (also known as arrestin-1) was solved (Kang, Zhou et al. 2015).

Along with the discovery that GPCRs can activate multiple intracellular signaling pathways, it has been found that certain ligands can activate one or more particular GPCR-coupled pathway(s) from among a receptor's repertoire with disproportionate effectiveness, which has been termed signaling bias (Lefkowitz 2013). It is not yet clear how common the underlying explanations for the many findings of biased ligands actually are (Klein Herenbrink, Sykes et al. 2016), but in at least some cases the explanation seems to be distinct active receptor states which correspond to activation of one or another coupling effector (Drake, Violin et al. 2008, Reiter, Ahn et al. 2012, Wacker, Wang et al. 2013).

The structure and activation of CXCR4

Given the wide expression and importance of CXCR4 in development and immunity, it is understandable that CXCR4 is quite commonly up-regulated in both haematological and solid tumor cancers (Guo, Wang et al. 2016). In addition to the migratory ability cancer cells exploit CXCR4 to obtain, the stem cell maintenance signaling of CXCR4 makes it also unsurprising that a role in cancer cell survival signaling has been reported as well, and CXCL12/CXCR4 signaling further serves cancer cells through allowing for coordination with tumor-supporting stromal cells (Guo, Wang et al. 2016). Candidates have been numerous but only one approved CXCR4-targeting drug has emerged so far (Danylesko, Sareli et al. 2016), so there is definitely a biomedical need for a better structural understanding of the activation of CXCR4 by CXCL12.

Chemokine receptors also represent an exciting frontier in the field of basic GPCR signaling research owing to the size of chemokines. As multiple receptors have now been solved in various stages of activation, it has become clear that GPCRs can be considered as linking conserved intracellular G protein activation mechanisms with more divergent ligand engagement networks, which is to be expected considering the wide variety of GPCR ligands that exist along with the large degree of commonality in GPCR intracellular activity. Small molecules ultimately activate all of the early class A model receptors that yielded most of our understanding of GPCR structure and activation, whereas chemokines are vastly larger proteins. The nature of the receptor/ligand interaction, and how it is linked to activation of the intracellular region

of the receptor, was thus bound to be quite different in the case of chemokine receptor signaling, making the structural study of chemokine receptors a particularly interesting challenge.

At the outset of the work described herein, understanding of the structural basis for chemokine receptor activation by chemokines was essentially limited to a simplistic chemokine recognition site 1 & 2 (CRS1/CRS2) model (Crump, Gong et al. 1997). In this model, two functionally distinct binding events contribute to the ligand:receptor complex: in the CRS1 interaction the N-terminus of a chemokine receptor binds the globular domain of its chemokine ligand, and in the CRS2 interaction residues in the binding pocket formed by the receptor trans-membrane receptor core domain are responsible for binding the N-terminus of the chemokine. Functionally, the CRS1/CRS2 model states that only the CRS2 interaction is involved in achieving/stabilizing the active state of the receptor upon chemokine binding, whereas the CRS1 interaction only contributes binding affinity necessary for association (Rajagopalan and Rajarathnam 2006, Kleist, Getschman et al. 2016).

There is extensive experimental evidence supportive of the CRS1/CRS2 hypothesis, much of it derived from the study of CXCL12 and CXCR4 in particular. Modification of the CXCL12 N-terminus produced potently binding antagonist variants of CXCL12, suggesting that the extreme chemokine N-terminus is critical for activating the receptor in a way that can be at least partially distinguished from its contribution to binding (Crump, Gong et al. 1997). It was shown next that the N-terminus of CXCL12 alone was capable of eliciting CXCR4 signaling (Loetscher, Gong et al. 1998). It was also suggested by both receptor chimera experiments and the

swapping of N-loop domains between chemokines (including CXCL12) that the receptor N-termini interacting with at least the N-loop of the chemokines are the critical elements for binding affinity and specificity (Kleist, Getschman et al. 2016). Also in agreement with the CRS1/CRS2 hypothesis, multiple acidic residues in the pocket of CXCR4 have long been known to be as critical to signaling as the extreme CXCL12 N-terminal residues K1 and P2 (Brelot, Heveker et al. 2000).

CXCR4 was the first chemokine receptor to be structurally solved in 2010, when our laboratory reported multiple crystal structures for the receptor in complex with both a small molecule and a cyclic peptide antagonist (Wu, Chien et al. 2010). As detailed in chapters 2 and 3 herein, the absence of CXCL12 from the structures along with the crystallization of CXCR4 as a physiologically sensible homodimer allowed for widely varying hypotheses regarding the nature of CXCL12 binding (Wu et al. 2010, (Kufareva, Stephens et al. 2014). While the small molecule and peptide antagonist crystal structures were not at all conclusive as to how CXCL12 binds, a separate NMR-based structure of CXCL12 in combination with the isolated N-terminus of CXCR4 (Veldkamp, Seibert et al. 2008) offered a potential answer to how CRS1 bound CXCL12, and incorporating this proposed orientation into the context of full length CXCR4 led to the hypothesis of a 1:2 CXCL12:CXCR4 binding and activation mechanism. A 1:1 interaction model was also possible but required abandoning the NMR-based CRS1 interaction proposal. Ultimately, our data strongly supported the 1:1 model, and we were able to derive further specific support for the proposed orientation in the form of cysteine mutant disulfide-based crosslinking data.

An exciting step in understanding how CXCL12 binds and activates CXCR4 was made in 2015 with the crystallographic solution of a covalently locked complex between virally encoded antagonist chemokine vMIP-II and CXCR4 (Qin, Kufareva et al. 2015). The crystal structure of the vMIP-II: CXCR4 complex was encouragingly similar in orientation to our previously generated CXCL12: CXCR4 model. Other structural milestones achieved since in the field of chemokine receptors include a chemokine variant-bound CCR5 structure (Zheng, Han et al. 2017) and a CCR2 structure solved in simultaneous complex with both an orthosteric and allosteric antagonists (Zheng, Qin et al. 2016). We review these in the context of our general progress in understanding chemokine signaling structurally in chapter 4. Detailed in chapter 5, we have since improved and extended the model to include all of the CRS1 interaction, and we have generated a large body of experimental evidence that conclusively supports our proposed model.

Ultimately, pharmacology targeting CXCR4 will benefit from better understanding the coordinated but distinct pathways that are initiated by CXCR4. Much of the later mutagenesis data presented herein is arrestin recruitment data, which is lacking in the literature in the case of CXCR4, for which G protein signaling data is overwhelmingly available. We have uncovered multiple interesting cases in which arrestin signaling results differ from Ca^{2+} mobilization-based measurements of G protein signaling. This seems to be largely due to the superior sensitivity of the BRET-based arrestin association measurements to efficacy differences, although there is also evidence for genuinely selective effects of certain receptor perturbations on arrestin versus G protein coupling.

Finally, it should be noted that along the way, I was able to contribute to various projects that while not included herein have made significant contributions to chemokine receptor research in general. In an early team effort, we were able to develop more sophisticated GPCR-dimerization BRET experimental and analytical strategy than was previously available (Kufareva, Stephens et al. 2013). I was second author on the resultant paper. Our laboratory's experience with assaying CXCR4 signaling allowed me to contribute mutagenesis-based support for early modeling by another group of the CRS1 component of the CXCL12: CXCR4 interaction (Ziarek, Getschman et al. 2013). In a separate project, my extensive contributions to the application of fluorescently labeled chemokines that were developed in the lab led to my inclusion as an equally contributing co-first author on the resultant paper (Kawamura, Stephens et al. 2014). More recently, the BRET-based arrestin recruitment experimental platform, which I implemented and developed within our laboratory, enabled functional testing of ACKR3 critical to a recent modeling study led by a post-doctoral scholar working in our laboratory (Gustavsson, Wang et al. 2017).

References

Brelot, A., N. Heveker, M. Montes and M. Alizon (2000). "Identification of residues of CXCR4 critical for human immunodeficiency virus coreceptor and chemokine receptor activities." *J Biol Chem* **275**(31): 23736-23744.

Crump, M. P., J. H. Gong, P. Loetscher, K. Rajarathnam, A. Amara, F. Arenzana-Seisdedos, J. L. Virelizier, M. Baggiolini, B. D. Sykes and I. Clark-Lewis (1997). "Solution structure and basis for functional activity of stromal cell-derived factor-1; dissociation of CXCR4 activation from binding and inhibition of HIV-1." *EMBO J* **16**(23): 6996-7007.

Danylesko, I., R. Sareli, N. Varda-Bloom, R. Yerushalmi, N. Shem-Tov, A. Shimoni and A. Nagler (2016). "Plerixafor (Mozobil): A Stem Cell-Mobilizing Agent for Transplantation in Lymphoma Patients Predicted to Be Poor Mobilizers - A Pilot Study." Acta Haematol **135**(1): 29-36.

DeVree, B. T., J. P. Mahoney, G. A. Vélez-Ruiz, S. G. Rasmussen, A. J. Kuszak, E. Edwald, J. J. Fung, A. Manglik, M. Masureel, Y. Du, R. A. Matt, E. Pardon, J. Steyaert, B. K. Kobilka and R. K. Sunahara (2016). "Allosteric coupling from G protein to the agonist-binding pocket in GPCRs." Nature **535**(7610): 182-186.

Dorsam, R. T. and J. S. Gutkind (2007). "G-protein-coupled receptors and cancer." Nat Rev Cancer **7**(2): 79-94.

Drake, M. T., J. D. Violin, E. J. Whalen, J. W. Wisler, S. K. Shenoy and R. J. Lefkowitz (2008). "beta-arrestin-biased agonism at the beta2-adrenergic receptor." J Biol Chem **283**(9): 5669-5676.

Guo, F., Y. Wang, J. Liu, S. C. Mok, F. Xue and W. Zhang (2016). "CXCL12/CXCR4: a symbiotic bridge linking cancer cells and their stromal neighbors in oncogenic communication networks." Oncogene **35**(7): 816-826.

Gustavsson, M., L. Wang, N. van Gils, B. S. Stephens, P. Zhang, T. J. Schall, S. Yang, R. Abagyan, M. R. Chance, I. Kufareva and T. M. Handel (2017). "Structural basis of ligand interaction with atypical chemokine receptor 3." Nat Commun **8**: 14135.

Heifetz, A., G. F. Schertler, R. Seifert, C. G. Tate, P. M. Sexton, V. V. Gurevich, D. Fourmy, V. Cherezov, F. H. Marshall, R. I. Storer, I. Moraes, I. G. Tikhonova, C. S. Tautermann, P. Hunt, T. Ceska, S. Hodgson, M. J. Bodkin, S. Singh, R. J. Law and P. C. Biggin (2015). "GPCR structure, function, drug discovery and crystallography: report from Academia-Industry International Conference (UK Royal Society) Chicheley Hall, 1-2 September 2014." Naunyn Schmiedebergs Arch Pharmacol **388**(8): 883-903.

Jørgensen, A. S., M. M. Rosenkilde and G. M. Hjortø (2017). "Biased signaling of G protein-coupled receptors - From a chemokine receptor CCR7 perspective." Gen Comp Endocrinol.

Kang, Y., X. E. Zhou, X. Gao, Y. He, W. Liu, A. Ishchenko, A. Barty, T. A. White, O. Yefanov, G. W. Han, Q. Xu, P. W. de Waal, J. Ke, M. H. Tan, C. Zhang, A. Moeller, G. M. West, B. D. Pascal, N. Van Eps, L. N. Caro, S. A. Vishnivetskiy, R. J. Lee, K. M. Suino-Powell, X. Gu, K. Pal, J. Ma, X. Zhi, S. Boutet, G. J. Williams, M. Messerschmidt, C. Gati, N. A. Zatspein, D. Wang, D. James, S. Basu, S. Roy-Chowdhury, C. E. Conrad, J. Coe, H. Liu, S. Lisova, C. Kupitz, I. Grotjohann, R. Fromme, Y. Jiang, M. Tan, H. Yang, J. Li, M. Wang, Z. Zheng, D. Li, N. Howe, Y.

Zhao, J. Standfuss, K. Diederichs, Y. Dong, C. S. Potter, B. Carragher, M. Caffrey, H. Jiang, H. N. Chapman, J. C. Spence, P. Fromme, U. Weierstall, O. P. Ernst, V. Katritch, V. V. Gurevich, P. R. Griffin, W. L. Hubbell, R. C. Stevens, V. Cherezov, K. Melcher and H. E. Xu (2015). "Crystal structure of rhodopsin bound to arrestin by femtosecond X-ray laser." Nature **523**(7562): 561-567.

Kawamura, T., B. Stephens, L. Qin, X. Yin, M. R. Does, T. H. Smith, N. Grimsey, R. Abagyan, J. Trejo, I. Kufareva, M. M. Fuster, C. L. Salanga and T. M. Handel (2014). "A general method for site specific fluorescent labeling of recombinant chemokines." PLoS One **9**(1): e81454.

Klein Herenbrink, C., D. A. Sykes, P. Donthamsetti, M. Canals, T. Coudrat, J. Shonberg, P. J. Scammells, B. Capuano, P. M. Sexton, S. J. Charlton, J. A. Javitch, A. Christopoulos and J. R. Lane (2016). "The role of kinetic context in apparent biased agonism at GPCRs." Nat Commun **7**: 10842.

Kleist, A. B., A. E. Getschman, J. J. Ziarek, A. M. Nevins, P. A. Gauthier, A. Chevigné, M. Szpakowska and B. F. Volkman (2016). "New paradigms in chemokine receptor signal transduction: Moving beyond the two-site model." Biochem Pharmacol **114**: 53-68.

Kufareva, I., B. Stephens, C. T. Gilliland, B. Wu, G. Fenalti, D. Hamel, R. C. Stevens, R. Abagyan and T. M. Handel (2013). "A novel approach to quantify G-protein-coupled receptor dimerization equilibrium using bioluminescence resonance energy transfer." Methods Mol Biol **1013**: 93-127.

Kufareva, I., B. S. Stephens, L. G. Holden, L. Qin, C. Zhao, T. Kawamura, R. Abagyan and T. M. Handel (2014). "Stoichiometry and geometry of the CXC chemokine receptor 4 complex with CXC ligand 12: molecular modeling and experimental validation." Proc Natl Acad Sci U S A **111**(50): E5363-5372.

Lefkowitz, R. J. (2013). "A brief history of G-protein coupled receptors (Nobel Lecture)." Angew Chem Int Ed Engl **52**(25): 6366-6378.

Loetscher, P., J. H. Gong, B. Dewald, M. Baggiolini and I. Clark-Lewis (1998). "N-terminal peptides of stromal cell-derived factor-1 with CXC chemokine receptor 4 agonist and antagonist activities." J Biol Chem **273**(35): 22279-22283.

Manglik, A., T. H. Kim, M. Masureel, C. Altenbach, Z. Yang, D. Hilger, M. T. Lerch, T. S. Kobilka, F. S. Thian, W. L. Hubbell, R. S. Prosser and B. K. Kobilka (2015). "Structural Insights into the Dynamic Process of β 2-Adrenergic Receptor Signaling." Cell **161**(5): 1101-1111.

Qin, L., I. Kufareva, L. G. Holden, C. Wang, Y. Zheng, C. Zhao, G. Fenalti, H. Wu, G. W. Han, V. Cherezov, R. Abagyan, R. C. Stevens and T. M. Handel (2015).

"Structural biology. Crystal structure of the chemokine receptor CXCR4 in complex with a viral chemokine." *Science* **347**(6226): 1117-1122.

Rajagopalan, L. and K. Rajarathnam (2006). "Structural basis of chemokine receptor function--a model for binding affinity and ligand selectivity." *Biosci Rep* **26**(5): 325-339.

Rasmussen, S. G., B. T. DeVree, Y. Zou, A. C. Kruse, K. Y. Chung, T. S. Kobilka, F. S. Thian, P. S. Chae, E. Pardon, D. Calinski, J. M. Mathiesen, S. T. Shah, J. A. Lyons, M. Caffrey, S. H. Gellman, J. Steyaert, G. Skiniotis, W. I. Weis, R. K. Sunahara and B. K. Kobilka (2011). "Crystal structure of the β 2 adrenergic receptor-Gs protein complex." *Nature* **477**(7366): 549-555.

Reiter, E., S. Ahn, A. K. Shukla and R. J. Lefkowitz (2012). "Molecular mechanism of β -arrestin-biased agonism at seven-transmembrane receptors." *Annu Rev Pharmacol Toxicol* **52**: 179-197.

Rosenbaum, D. M., S. G. Rasmussen and B. K. Kobilka (2009). "The structure and function of G-protein-coupled receptors." *Nature* **459**(7245): 356-363.

Scholten, D. J., M. Canals, D. Maussang, L. Roumen, M. J. Smit, M. Wijtmans, C. de Graaf, H. F. Vischer and R. Leurs (2012). "Pharmacological modulation of chemokine receptor function." *Br J Pharmacol* **165**(6): 1617-1643.

Schumann, K., T. Lämmermann, M. Bruckner, D. F. Legler, J. Polleux, J. P. Spatz, G. Schuler, R. Förster, M. B. Lutz, L. Sorokin and M. Sixt (2010). "Immobilized chemokine fields and soluble chemokine gradients cooperatively shape migration patterns of dendritic cells." *Immunity* **32**(5): 703-713.

Schöneberg, T., A. Schulz, H. Biebermann, T. Hermsdorf, H. Römpler and K. Sangkuhl (2004). "Mutant G-protein-coupled receptors as a cause of human diseases." *Pharmacol Ther* **104**(3): 173-206.

Shenoy, S. K. and R. J. Lefkowitz (2011). " β -Arrestin-mediated receptor trafficking and signal transduction." *Trends Pharmacol Sci* **32**(9): 521-533.

Shukla, A. K., G. H. Westfield, K. Xiao, R. I. Reis, L. Y. Huang, P. Tripathi-Shukla, J. Qian, S. Li, A. Blanc, A. N. Oleskie, A. M. Dosey, M. Su, C. R. Liang, L. L. Gu, J. M. Shan, X. Chen, R. Hanna, M. Choi, X. J. Yao, B. U. Klink, A. W. Kahsai, S. S. Sidhu, S. Koide, P. A. Penczek, A. A. Kossiakoff, V. L. W. Jr, B. K. Kobilka, G. Skiniotis and R. J. Lefkowitz (2014). "Visualization of arrestin recruitment by a G-protein-coupled receptor." *Nature* **512**(7513): 218-222.

Shukla, A. K., K. Xiao and R. J. Lefkowitz (2011). "Emerging paradigms of β -arrestin-dependent seven transmembrane receptor signaling." Trends Biochem Sci **36**(9): 457-469.

Sokol, C. L. and A. D. Luster (2015). "The chemokine system in innate immunity." Cold Spring Harb Perspect Biol **7**(5).

Veldkamp, C. T., C. Seibert, F. C. Peterson, N. B. De la Cruz, J. C. Haugner, H. Basnet, T. P. Sakmar and B. F. Volkman (2008). "Structural basis of CXCR4 sulfotyrosine recognition by the chemokine SDF-1/CXCL12." Sci Signal **1**(37): ra4.

Wacker, D., C. Wang, V. Katritch, G. W. Han, X. P. Huang, E. Vardy, J. D. McCorvy, Y. Jiang, M. Chu, F. Y. Siu, W. Liu, H. E. Xu, V. Cherezov, B. L. Roth and R. C. Stevens (2013). "Structural features for functional selectivity at serotonin receptors." Science **340**(6132): 615-619.

Wu, B., E. Y. Chien, C. D. Mol, G. Fenalti, W. Liu, V. Katritch, R. Abagyan, A. Brooun, P. Wells, F. C. Bi, D. J. Hamel, P. Kuhn, T. M. Handel, V. Cherezov and R. C. Stevens (2010). "Structures of the CXCR4 chemokine GPCR with small-molecule and cyclic peptide antagonists." Science **330**(6007): 1066-1071.

Zheng, Y., G. W. Han, R. Abagyan, B. Wu, R. C. Stevens, V. Cherezov, I. Kufareva and T. M. Handel (2017). "Structure of CC Chemokine Receptor 5 with a Potent Chemokine Antagonist Reveals Mechanisms of Chemokine Recognition and Molecular Mimicry by HIV." Immunity **46**(6): 1005-1017.e1005.

Zheng, Y., L. Qin, N. V. Zacarías, H. de Vries, G. W. Han, M. Gustavsson, M. Dabros, C. Zhao, R. J. Cherney, P. Carter, D. Stamos, R. Abagyan, V. Cherezov, R. C. Stevens, A. P. IJzerman, L. H. Heitman, A. Tebben, I. Kufareva and T. M. Handel (2016). "Structure of CC chemokine receptor 2 with orthosteric and allosteric antagonists." Nature **540**(7633): 458-461.

Ziarek, J. J., A. E. Getschman, S. J. Butler, D. Taleski, B. Stephens, I. Kufareva, T. M. Handel, R. J. Payne and B. F. Volkman (2013). "Sulfopeptide probes of the CXCR4/CXCL12 interface reveal oligomer-specific contacts and chemokine allostery." ACS Chem Biol **8**(9): 1955-1963.

Chapter 2

Chemokine receptor oligomerization and allostery



Chemokine Receptor Oligomerization and Allostery

Bryan Stephens, Tracy M. Handel

Skaggs School of Pharmacy and Pharmaceutical Science, University of California, San Diego, La Jolla, California, USA

Contents

1. Introduction	376
2. Background: Chemokine Structure and Interactions with Receptors	377
2.1 Chemokines have conserved tertiary structures but diverse oligomerization states	378
2.2 Evidence for the two-site model of chemokine:receptor binding and activation	379
3. Evidence for Hetero- and Homo-Oligomerization of Chemokine Receptors	382
3.1 Methods used for studying GPCR oligomerization	391
3.2 Chemokine receptor homo- and hetero-oligomerization: Evidence for constitutive ligand-independent oligomer formation early after biosynthesis	395
3.3 Crystal structures of CXCR4 reveal homodimers	396
3.4 Attempts to disrupt receptor dimerization	398
4. Functional Effects of Chemokine Receptor Hetero-Oligomerization on Ligand Binding	399
5. Effects of Chemokine Hetero- and Homo-Oligomerization on Signaling	403
5.1 Transinhibition of signaling by ligands in hetero-oligomeric complexes	403
5.2 Activation of alternative signaling pathways by hetero-oligomers	404
5.3 Modulation of signaling by atypical and virally encoded chemokine receptors	405
6. Heterodimerization of Chemokine Receptors with Nonchemokine Receptors	409
7. Other Sources of Allostery in Chemokine Receptor Signaling: Chemokine Oligomerization	411
8. Conclusions and Future Perspectives	413
Acknowledgments	413
References	414

Abstract

Oligomerization of chemokine receptors has been reported to influence many aspects of receptor function through allosteric communication between receptor protomers. Allosteric interactions within chemokine receptor hetero-oligomers have been shown to cause negative cooperativity in the binding of chemokines and to inhibit receptor activation in the case of some receptor pairs. Other receptor pairs can cause enhanced

signaling and even activate entirely new, hetero-oligomer-specific signaling complexes and responses downstream of receptor activation. Many mechanisms contribute to these effects including direct allosteric coupling between the receptors, G protein-mediated allostery, G protein stealing, ligand sequestration, and recruitment of new intracellular proteins by exposing unique binding interfaces on the oligomerized receptors. These effects present both challenges as well as exciting opportunities for drug discovery. One of the most difficult challenges will involve determining if and when hetero-oligomers versus homomeric receptors are involved in specific disease states.



1. INTRODUCTION

The chemokine family of G protein-coupled receptors (GPCRs) and their protein ligands control the migration, activation, differentiation, and survival of leukocytes in many normal physiological contexts including development, hematopoiesis, immune surveillance, and inflammation. However, inappropriate expression, regulation or exploitation of these proteins contributes to a wide spectrum of inflammatory and autoimmune diseases, cancer, heart disease, and HIV, making chemokine receptors prime targets for therapeutic intervention.¹⁻⁴ Understanding the molecular details that control chemokine receptor interactions with ligands and their signaling responses should contribute to drug discovery efforts, and add to the list of approved therapeutics, which now include the CCR5 HIV entry inhibitor, Maraviroc, and the CXCR4-targeted stem cell mobilizer, Mozobil.

Approximately 45 chemokines have been identified in humans and are classified into four families (CC, CXC, XC, and CX3C) on the basis of the pattern of conserved cysteine residues.⁴ The majority of the ligands are secreted in response to inflammatory signals while others are constitutively produced and involved in homeostatic processes such as lymphopoiesis and immune cell patrol of abnormal physiology. There are 22 known human receptors, most of which couple to heterotrimeric G α i protein complexes. Four of the receptors (D6, DARC, CCX-CCKR1, and CXCR7) are classified as “atypical receptors” that lack canonical DRY boxes and consequently do not signal through G α i. Instead they have scavenging, decoy, transport, presentation, and other accessory functions.^{5,6} CXCR7 has also been reported to be a β -arrestin-biased signaling receptor^{7,8} although a recent report suggests some signaling through G α i in astrocytes and glioma cells.⁹

A subset of the receptors (CXCR4, CXCR6, CCR6, CCR8, and CCR9) have only one known ligand while most have multiple ligands

(~11 in the case of CCR1, ~12 for CCR3). The atypical receptors (DARC, D6) and virally encoded receptors (e.g., US28) tend to be particularly promiscuous with respect to ligand recognition. Similarly, many of the ligands bind multiple receptors making for a complex network of interactions, just considering the receptors and ligands alone (see Refs. 4,10 for an up-to-date matrix of the chemokine receptors and the ligands that they bind). This promiscuous pairing of ligands and receptors initially gave rise to the notion that there is significant redundancy built into the chemokine system for robustness of the immune response.^{11,12} Furthermore, redundancy has been used as a potential explanation for the failure of drug candidates targeting a given receptor for the treatment of specific diseases.^{10,13} However, there are reasons to believe that the system is not as redundant as initially believed,¹⁴ and mechanisms for regulation and fine-tuning of signaling responses are beginning to emerge.

Initially, different spatial and temporal patterns of expression of chemokines and receptors were hypothesized to impose some level of functional non-redundancy.¹⁴ However, there is now extensive evidence for homo- and hetero-oligomerization of chemokine receptors, as well as oligomerization of chemokine receptors with GPCRs outside the chemokine family and with non-GPCR receptors, which can modulate aspects of signaling and cause diverse functional responses, even with the same ligand. In this chapter, we provide examples of the pharmacological effects that these oligomeric interactions have been reported to have on the function of chemokine receptors compared to the receptors in (apparent) isolation. Note that we primarily use the term oligomer rather than dimer to refer to these complexes since it is not known whether they are predominantly dimers or higher-order assemblies.



2. BACKGROUND: CHEMOKINE STRUCTURE AND INTERACTIONS WITH RECEPTORS

Before delving into oligomerization and allostery, it is useful to review concepts regarding chemokine:receptor structure and interactions that prevailed prior to knowledge that they form homo- and hetero-oligomers. Much is known about chemokine structure and function from a wealth of NMR, X-ray, and mutagenesis studies, and recently, the first structure of a chemokine receptor was solved.

2.1. Chemokines have conserved tertiary structures but diverse oligomerization states

Despite their functional diversity, chemokines are small 8–12 kDa proteins with remarkably conserved tertiary structures stabilized by one to three disulfide bonds.¹⁵ The basic ~ 70 residue chemokine module generally consists of a disordered N-terminus, which is a critical signaling domain tethered to a folded α/β core domain (Fig. 9.1). Some chemokines (e.g., SDF-1 γ /CXCL12 γ and SLC/CCL21) also have extended C-terminal domains that are thought to function in binding to glycosaminoglycans (GAGs). The two most unique chemokines (CXCL16 and fractalkine/CX3CL1) are fused to the N-terminus of a large mucin-like stalk that tethers them to the cell membrane and allows them to function as adhesion molecules when membrane bound, and as canonical chemokines after proteolytic release from the transmembrane (TM) domain.

In solution, different chemokines adopt a broad range of oligomerization states with some forming stable monomers (e.g., MCP-3/CCL7, SLC/CCL21), while others form reversible dimers (MCP-1/CCL2, IL-8/CXCL8, SDF-1/CXCL12), tetramers (PF-4/CXCL4), and polymers (MIP-1 α /CCL3,

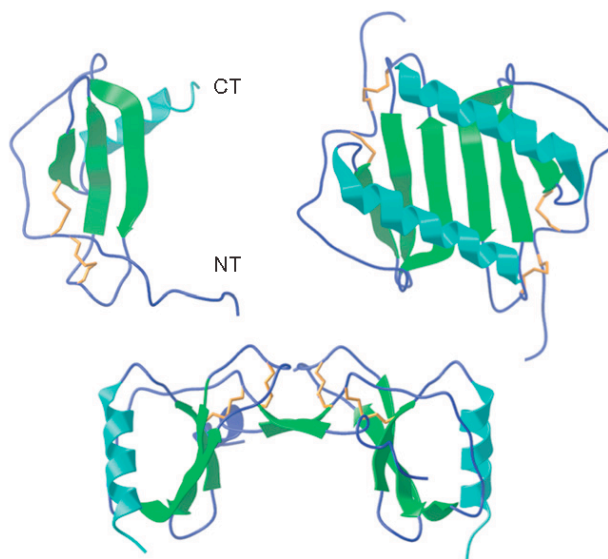


Figure 9.1 Ribbon diagrams of: (top left) a typical chemokine monomer (MCP-1/CCL2, PDB ID 1dol); (top right) a CXC chemokine dimer (IL-8/CXCL8, PDB ID 1il8); and (bottom) a CC chemokine dimer (MCP-1/CCL2, PDB ID 1dok).

MIP-1 β /CCL4, RANTES/CCL5).^{2,16} There are basically two types of dimer structures—CC dimers that are characteristic of the CC chemokine family and CXC-type dimers that are formed predominantly by CXC chemokines (Fig. 9.1). These dimers form the basic substructure of the higher-order oligomers and polymers.^{17,18} Furthermore, interaction of chemokines with GAGs promotes or stabilizes further oligomerization of many if not all chemokines.^{19,20} Oligomerization and interactions with GAGs are important for locally sequestering chemokines on cell surfaces to prevent diffusion and facilitate the formation of chemokine gradients that help guide cell movement. GAG interactions have also been shown to facilitate transcytosis of chemokines across cells, chemokine-mediated signaling, and they can act as cofactors in promoting receptor interactions.^{21–23} Nevertheless, as demonstrated using monomeric variants in bare filter transwell migration assays, the reversibility of chemokine oligomerization is necessary because it is the monomeric form that binds to the receptor with highest affinity and promotes cell migration.^{24,25}

2.2. Evidence for the two-site model of chemokine:receptor binding and activation

Early mutagenesis studies of IL-8/CXCL8 from Clark–Lewis revealed that the chemokine N-terminus is a critical signaling domain, and more specifically, the prominent signaling role of the N-terminal ELR motif in a subset of CXC chemokines.²⁶ Subsequent mutagenesis studies of many chemokines revealed that if the N-terminus is mutated, deleted, or extended, the signaling properties of a given chemokine can be dramatically altered without significantly affecting receptor-binding affinity. For example, deletion of seven residues from MCP-1/CCL2 converts it from an agonist into a high-affinity antagonist,²⁷ as does addition of methionine to RANTES/CCL5 or CCL2,^{28,29} or the introduction of a Pro2Gly or Lys1Arg mutation into CXCL12.³⁰ By contrast, deletion of the first eight residues of HCC-1/CCL14 produces a more potent agonist,³¹ and deletion of 4 and 15 residues from the precursor CTAP-III generates the chemokines β -thromboglobulin and NAP-II/CXCL7, respectively, which have distinct biological activities.³² Chemical and genetic modification of the N-terminus of RANTES/CCL5 has yielded superagonists and antagonists with more potent abilities than the WT chemokine to internalize the receptor CCR5, making these modified chemokines more effective in inhibiting HIV entry into cells.^{33,34} Thus, the N-termini of chemokines are thought to interact with receptor-binding pockets formed primarily by the receptor TM domains (referred to as chemokine recognition site 2, CRS2 in

Ref. 4), perhaps mimicking the binding and activation of other GPCRs by small molecule ligands. In other words, this small domain seems to have the largest influence on the conformational state of the receptor and thus the signaling response.

By contrast, mutations of the chemokine core domain (everything beyond the first cysteine) generally modulate binding affinity and signaling to a proportional extent but without producing dramatic switches in pharmacology such as the conversion of agonists into antagonists. Numerous studies including the structure of a sulfated N-terminal peptide from CXCR4 in complex with SDF-1/CXCL12³⁵ have demonstrated that the core domain interacts with the N-terminus of the receptor (referred to as chemokine recognition site 1, CRS1 in Ref. 4), which is largely unstructured in the absence of ligand engagement. Together, these data along with evidence that the monomeric forms of chemokines promote cell migration have given rise to the concept of a two-site model of receptor activation.³⁶ In this model, the CRS1 binds to the chemokine core domain in an initial docking interaction. This interaction then orients the chemokine N-terminal signaling domain into the receptor CRS2, which triggers the requisite conformational change (Fig. 9.2).

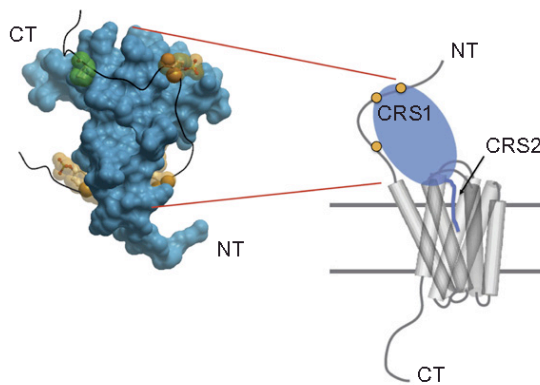


Figure 9.2 Two-site model of receptor activation. On the left is a surface topology model of CXCL12 bound to the N-terminal CRS1 of CXCR4 (black string with sulfated tyrosines side chains shown). The right illustrates the binding of the chemokine core domain to the N-terminus of the receptor (CRS1, circles represent sulfated tyrosines) and the N-terminus of the chemokine binding into the receptor helical bundle (CRS2).

The two-site model has been supported by recent NMR studies of an *in vitro* reconstituted CXCL12: CXCR4 complex.³⁷ In this study, NMR signals from isotopically labeled CXCL12 were broadened beyond detection when in complex with CXCR4; however, when the small molecule antagonist AMD3100 was added, signals from the chemokine N-terminus but not the core domain became visible, presumably because the N-terminus became mobile after being displaced from the receptor by AMD3100, while the core remained bound to CRS1 (Fig. 9.3A). The fact that AMD3100 binds in the TM region of the receptor is consistent with the N-terminus of CXCL12 also binding in this region, although allosteric mechanisms of displacement cannot be ruled out.

In the interpretation of the above studies, it was assumed that the receptor would be monomeric and thus that the functionally relevant form of the complex is 1:1 chemokine:receptor. This hypothesis may well be valid but the accumulating evidence that chemokine receptors homo- and hetero-oligomerize raises the possibility of alternative stoichiometries and modes of binding of monomeric chemokines to oligomerized receptors.

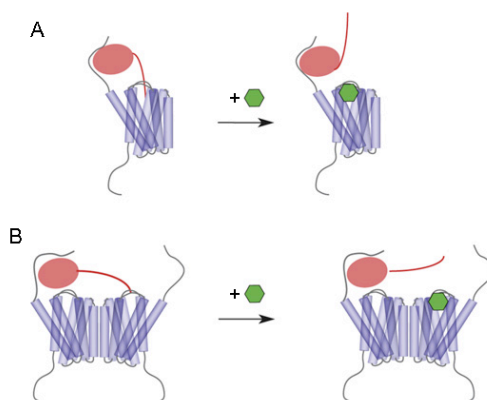


Figure 9.3 Cartoon of the two-site model where the small molecule antagonist AMD3100 (hexagon) binds CXCR4 in the TM domain CRS2 and displaces the N-terminus of SDF-1/CXCL12. Figure A illustrates the hypothetical displacement of the chemokine N-terminus in the context of a 1:1 chemokine-monomer:receptor-monomer interaction. Figure B illustrates the displacement in the context of a 1:2 chemokine-monomer:receptor-dimer interaction. Other stoichiometries are also possible such as 2:2 interactions where two chemokine monomers bind a receptor dimer or one chemokine dimer binds to a receptor dimer.



3. EVIDENCE FOR HETERO- AND HOMO-OLIGOMERIZATION OF CHEMOKINE RECEPTORS

As implied above, for quite some time, GPCRs were assumed to function as monomeric units. Moreover, by reconstituting the β 2-adrenergic receptor, the μ -opioid receptor, and rhodopsin into nanodiscs, it was demonstrated that they can function as monomers with respect to G protein coupling,^{38 40} and in the case of rhodopsin, the monomer is also sufficient for rhodopsin kinase phosphorylation and arrestin binding.⁴¹ However, a large body of evidence suggests that many GPCRs form dimers and higher-order homo- and hetero-oligomers, and chemokine receptors are no exception (Table 9.1). These oligomers may be required for assembling large functional signaling complexes and for allosteric communication within the complexes. For example, natively expressed CXCR4, CCR5, and CD4 have been identified in homogeneous microclusters, predominantly on microvilli, in many cells types.¹⁰⁵ Furthermore, these microclusters were identified in small trans golgi vesicles, suggesting their assembly shortly after synthesis and prior to transport to the cell membrane. The authors proposed that this localization and clustering might facilitate more precise sensing of the microenvironment during cell migration and noted that selectins and integrins, which are also important for cell migration, are located on microvilli. Whether these microclusters contain stable contact-mediated oligomerized receptors was not determined, but it seems likely given the number of studies that have demonstrated homo- and hetero-oligomerization of CXCR4 and CCR5 (Table 9.1).

While the validation of oligomerization in native tissues has yet to be convincingly demonstrated for most chemokine receptors, and the functional relevance of oligomerization on chemokine receptor activity/signaling and dynamics/trafficking is far from well understood, the majority of the chemokine receptors have been reported to homo and/or hetero-oligomerize (Table 9.1). Questions that have been probed in these studies include: (1) What is the affect of ligand binding, the nature of the ligand (agonist vs. antagonist) and the activation state of the receptor on oligomerization? (2) What is the functional significance of homo- and hetero-oligomerization? (3) Is oligomerization required for transport to the membrane surface? (4) What factors regulate receptor oligomerization? (5) Is there allosteric communication between receptors and what are the mechanisms? (6) Are G proteins involved? Answering these questions has

Table 9.1 Chemokine receptor oligomers

Receptors involved	Interesting observations	Methods used	References
Chemokine receptor homomers			
CCR2/CCR2	Homodimerization induced by CCL2	Co-IP with chemical cross-linking, divalent antibody cross-linking	42–44
	Constitutive homodimerization, conformational change caused by CCL2 stimulation	BRET	45,46
	Constitutive, CCL2 stimulation had no effect	BRET	47
	Constitutive, negative cooperativity in agonist binding	BRET	48
	Simultaneous higher-order heteromerization	BiLC-BRET	49
CCR5/CCR5	Trafficking-defective CCR5Δ32 dimerized with WT CCR5 to reduce surface expression	³⁵ S pulse labeling gel analysis IMF Co-IP	50
	Homodimerization induced by CCL5	Co-IP with chemical cross-linking	44,51,52
	CCR5Δ32 mutant defect not related to normal trafficking	Flow cytometry	53
	Divalent antibodies stabilized dimers and promoted internalization	BRET	54
	Constitutive, unaffected by CCL5, BRET signal increased by divalent dimer-stabilizing antibody	BRET	55
	Constitutive	Co-IP	47,56,57

Continued

Table 9.1 Chemokine receptor oligomers—cont'd

Receptors involved	Interesting observations	Methods used	References
	TM1 and TM4 implicated in homodimer interface	FRET-based mutational analysis	58
	Homodimer interface mutations in TM1 and TM4 called into question	BRET	59
	GRK-mediated “cross-phosphorylation” across the homodimer interface	BRET	60
	Constitutive, negative cooperativity in agonist binding, evidence for G protein involvement in negative cooperativity	BRET	48
	Constitutive, homodimer-specific adaptor protein	BiFC	61
	Constitutive, homodimers depend on specific Rabs for cell surface delivery	BiFC	62
	Constitutive, homodimer-specific chaperone	BiFC	63
CXCR1/CXCR1	Constitutive	Co-IP, tr-FRET, single cell FRET, BRET, ER trapping	64
	Homodimers stabilized by CXCL8	FRET	65
CXCR2/CXCR2	Constitutive, TM3 and ICL2 implicated in homodimerization	Co-IP	66
	Disulfide involvement in homodimerization unclear	WB	67
	Constitutive	Co-IP, tr-FRET, single cell FRET, BRET, ER trapping	64
	Homodimers stabilized by CXCL8	FRET	65
CXCR3/CXCR3	Constitutive	Single cell FRET	128

CXCR4/CXCR4	Homodimerization induced by CXCL12	Co-IP with chemical cross-linking	68
	Constitutive	Co-IP, BRET, sucrose gradient centrifugation, BiFC, Bivalent ligand synthesis	61,69–73
	Constitutive, CXCL12 altered FRET signal	FRET	74
	Constitutive, CXCL12 caused conformational change in pre-formed homodimers	BRET	45
	Constitutive, homodimerization reduced by cholesterol depletion and a TM4 synthetic peptide	Single cell FRET, pbFRET	75
	Constitutive, higher-order homo-oligomerization	BRET, BiFC-BRET	76
	Constitutive, signal altered after CXCL12 incubation	PCA	77
	Constitutive, signal modified by ligand stimulation	BRET	7
	Constitutive, signal modified by ligand stimulation	BRET	78
	Simultaneous higher-order heteromerization	BiLC-BRET	49
	Homodimers reconstituted into proteoliposomes	Thermal inactivation	79
	TM 5 and 6 comprised homodimer interface	X-ray crystallography	80
	Constitutive, homodimers depend on specific Rabs for cell surface delivery	BiFC	62
	TM 5 and 6 interface supported with minor adjustments	MD simulation	81
	Sphingomyelin deficiency increased dimerization and signaling, presumably by causing accumulation of receptor in lipid rafts	FRET	82

Continued

Table 9.1 Chemokine receptor oligomers—cont'd

Receptors involved	Interesting observations	Methods used	References
CXCR7/CXCR7	Constitutive, CXCL12-modulated reporter signals	BRET, PCA	7,77,78
DARC/DARC	Constitutive	BRET	83
Chemokine receptor heteromers			
CCR2/CCR5	Required stimulation with both CCL2 and CCL5	Co-IP with chemical cross-linking	43
	CCR2/CCR5 heterodimerization proposed to result from relatively recent gene duplication and resultant high sequence similarity	Correlated mutation analysis	84
	Required co-stimulation with CCL2 and CCR5, cooperative stimulation at lowered chemokine concentrations, distinct signaling proteins recruited and cellular responses elicited	Co-IP with chemical cross-linking	44
	Stimulated by chemokines and divalent antibodies	Co-IP with chemical cross-linking, FRET	85
	No cooperative signaling, negative cooperativity in chemokine binding	BRET	47
	Constitutive, negative cooperativity in agonist binding, evidence for G protein involvement in negative cooperativity	BRET	48
	Gene conversion proposed to be the cause of heterodimerization	Comparative and phylogenetic analysis	86
	Simultaneous higher-order heteromerization and homomerization of CCR2, negative cooperativity in both chemokine and antagonist binding	BiLC-BRET	49
	Heterodimer recruited β -arrestin	GPCR-HIT	87

CCR2/CXCR4	Required stimulation with both CCL2 and CXCL12	Co-IP with chemical cross-linking	43
	Stimulated by chemokines and divalent antibodies	Co-IP with chemical cross-linking, FRET	85
	Constitutive, chemokines caused conformational change	BRET	45
	Constitutive, negative cooperativity in both chemokine and antagonist binding	BRET	88
	Simultaneous higher-order heteromerization and homomerization of CCR2, negative cooperativity in both chemokine and antagonist binding	BiLC-BRET	49
	Heterodimer recruited β -arrestin	GPCR-HIT	87
CCR5/CXCR4	Transinhibition by both agonists and antagonists	Co-IP, BRET, FRET, BiFC	43,49,56,61,89,90
	Heterodimerization seemed to be CD4 expression-dependent	IMF, Co-IP	90
	Constitutive; co-recruited into the Immunological Synapse (IS) of T cells; elicited heterodimer-specific signaling pathways when together in the IS	BRET, BiFC	56,63
	Constitutive, FRET signal modulated by chemokine ligands	FRET	89
	Simultaneous higher-order heteromerization, negative cooperativity in both chemokine and antagonist binding	BRET, BiLC-BRET	49
	Constitutive, distinct adaptor protein from CCR5 homodimer	BiFC	61
	Constitutive, heterodimers depend on specific Rabs for cell surface delivery	BiFC	62

Continued

Table 9.1 Chemokine receptor oligomers—cont'd

Receptors involved	Interesting observations	Methods used	References
CXCR1/CXCR2	Constitutive, signal disrupted by CXCL8	Co-IP, tr-FRET, single cell FRET, BRET, ER trapping	64
	Constitutive, signal altered by CXCL8	FRET	65
CXCR4/CXCR7	Constitutive, CXCR4 signaling was enhanced	Single cell FRET, pbFRET	91
	Constitutive	PCA	77
	CXCR7 impairs CXCR4-mediated G protein signaling	BRET	78
	Increased β -arrestin recruitment, enhanced CXCR4-mediated migration	Co-IP	92
CCR2/CCR5/ CXCR4 Higher-order oligomer	Transinhibition by both agonists and antagonists	BiLC-BRET	49
DARC/CCR5	Constitutive, DARC inhibits CCR5 activation	BRET	83
CCX-CKR/ CXCR3	Inhibits CXCR3 signaling, transinhibition of ligand binding	Single cell FRET	128
CXCR3/CXCR4	Constitutive, transinhibition by agonists in isolated membranes	Co-IP, tr-FRET, BRET, GPCR-HIT	129
Chemokine receptor heteromers with nonchemokine GPCRs			
CXCR2/ α 1A- adrenoceptor	α 1A-AR activation by norepinephrine inhibited by the CXCR2 inverse agonist SB265610; dimerization itself unaffected by ligands	BRET	93
CCR5/ μ -OR CCR5/ δ -OR CCR5/ κ -OR	Cooperative ligand effects	Co-IP with chemical cross-linking	94

CCR5/ μ -OR	Constitutive, negative cooperativity between CCR5 and μ -OR agonists; cross-phosphorylation observed in both directions	Co-IP; bivalent ligand synthesis	95,96
CCR5/C5aR	GRK-mediated "cross-phosphorylation" across the heterodimer interface	BRET	60
CXCR2/AMPA Glu 1	Constitutive	Co-IP	66
	Dimerization reduces activation by CXCL8; CXCL8 modulates AMPA Glu 1 phosphorylation	BRET	97
CXCR2/ δ -OR	CXCR2 antagonists increased δ -OR activation	Co-IP, BRET, FRET	98
CXCR4/ μ -OR CXCR4/ κ -OR	Competed for CXCR4 homodimer formation	FRET	74
CXCR4/ δ -OR	Heterodimerization proposed to silence receptor functions	FRET	99
CCR6/BILF1 CCR7/BILF1 CCR9/BILF1 CCR10/BILF1 CXCR3/BILF1 CXCR4/BILF1 CXCR5/BILF1 CXCR7/BILF1	Constitutive	Co-IP, BRET, tr-FRET	100
CXCR4/BILF1	BILF1 inhibits CXCR4 activation	BiFC, BiLC	101

*Continued***Table 9.1** Chemokine receptor oligomers—cont'd

Receptors involved	Interesting observations	Methods used	References
CXCR5/EBI2	EBI2 inhibits CXCR5 activation	FRET	102
Chemokine receptor heteromers with receptors outside the GPCR family			
CXCR4/CD4	CD4 expression was required for changes in CXCR4 homodimer FRET caused by HIV-1 coat protein gp120IIIB	FRET	74
CXCR4/TCR	Required CXCL12 stimulation; CXCL12 activated downstream signaling pathways through TCR	FRET, Co-IP	103
CCR5/CD4	Constitutive; CCR5 reported to Co-IP with CD4 to a greater extent than CXCR4	Co-IP	104

motivated the development of many methods for investigating receptor oligomerization in living cells as described in the next section.

3.1. Methods used for studying GPCR oligomerization

Many biochemical and biophysical methods have been used to investigate receptor oligomerization, and are summarized in [Table 9.2](#), along with their pros and cons. These methods include chemical cross-linking followed by co-immunoprecipitation (Co-IP), protein fragment complementation (PFC, PCA), and many variants of fluorescence energy transfer (FRET) and bioluminescence energy transfer (BRET) techniques, including time-resolved FRET (tr-FRET, HTRF), bimolecular fluorescence/luminescence complementation BRET (BiFC/BiLC-BRET), and FRET after photobleaching (pbFRET). However, one must be cautious in the interpretation of the data and aware of the artifacts that can arise as a consequence of all of these methods. The biggest criticism is that most methods require heterologous expression of modified receptors, for example, with fluorescent or other tags for detection, or for resonance energy transfer (RET)-based experiments, which can lead to apparent oligomerization due to the unnatural high density of the expressed receptors. The tags may also inhibit interactions with intracellular proteins and alter receptor trafficking. Aggregation of receptors during Co-IP experiments can result in apparent but artificial oligomerization, and chemical cross-linking and protein fragment complementation can stabilize otherwise transient interactions between receptors. These issues have been extensively reviewed,^{1,3,107} and it is now broadly appreciated that methods that identify oligomerization of receptors in native tissues are critically needed. To this end, RET assays based on fluorescent labeling of GPCR ligands rather than the receptors have been developed. However, these ligand-based methods also have limitations because the ligand can modulate the basal state of the receptor. Ligands may alter the oligomerization state, agonists will often cause receptor internalization or modulate receptor trafficking, and allostery between oligomerized receptors can result in transinhibition or cooperative binding of ligands (see [Section 4](#)), leading to a lack of correlation between results from RET experiments and receptor oligomerization. In the case of chemokine receptors, the use of labeled chemokine ligands is also complicated by their propensity to bind to and oligomerize on cell-surface GAGs, although this issue is not relevant to synthetic small molecule ligands.

All of the methods are also fraught with difficulties in quantitative interpretation. For example, although the half maximal BRET signal (BRET₅₀) in saturation experiments has been interpreted as a measure of receptor

Table 9.2 Methods used in studying chemokine receptor oligomerization

Method	Description	Pros and cons	Other notes	Reference(s)
Co-IP	Immunoprecipitation, electrophoresis, and immunoblotting of one receptor followed by immunoblotting of a candidate dimer partner receptor	The most well-established experimental technique used to study GPCR dimerization; requires the least technologically advanced equipment	Sometimes carried out after chemical and/or antibody cross-linking of dimerized receptors; Co-IP methods were the earliest used to establish chemokine receptor dimerization and tended to suggest that dimerization was agonist-induced	3,42
FRET	Dimerization indicated by fluorescence resonance energy transfer between fluorophores (either fluorescent proteins such as CFP and YFP or small organic fluorophores such as Cy3 and Cy5) coupled to candidate receptors	More sensitive than Co-IP methods; requires equipment capable of FRET detection	This method tends to show constitutive dimerization, but the FRET signal is often increased or reduced upon agonist stimulation, which could indicate either a change in dimerization equilibrium or conformational changes within pre-formed dimers	3,65
Single cell FRET	Specific type of FRET in which microscopy is used to collect fluorescent signal from a specific region of a single cell chosen by the experimenter	Can be used in combination with microscopy to analyze specific cellular regions (e.g., plasma membrane, ER); requires microscope capable of FRET detection	In one interesting case, this was used to demonstrate an absence of dimerization where a cell population-average method, BRET, failed to reach the same conclusions	58
tr-FRET	Time-resolved FRET. Specific type of FRET in which a donor with a long fluorescent half-life is used to detect FRET after a time delay	Increased sensitivity over simple FRET due to reduced autofluorescence; often used to detect cell-surface dimerization specifically; and requires	This method is promising for the future, as studies with nonchemokine receptors using long-lived fluorophores coupled to agonists and antagonists have	64,106
	(i.e., after the autofluorescence of the cells being assayed has subsided)	equipment capable of detecting FRET	produced interesting results with respect to ligand:GPCR oligomer stoichiometry. This method can also be used to investigate endogenous receptor oligomers on native cell types of interest	
pbFRET	FRET after photobleaching. This method relies on deducing FRET from recovered donor fluorescence signal after photobleaching the acceptor fluorophore	Can be used in combination with microscopy to analyze specific cellular regions	Usually performed in the context of confocal microscopy-based single cell FRET	75,91
BRET	Similar to FRET, except that a bioluminescent enzyme is used as the donor for resonance energy transfer, so that a chemical substrate is added to produce the observed signal	Increased signal-to-noise ratio over FRET due to the use of a bioluminescent enzyme as a donor rather than a fluorophore that must be excited with light; requires both luminescence and fluorescence detection capabilities	Tends to show constitutive dimerization; this method allows distinction between agonist-mediated disruption/formation of dimers and conformational changes within pre-formed dimers, and agonists are almost always found to cause conformational changes within dimers without affecting the dimer equilibrium	3,45
BiFC-BRET/ BiLC-BRET	Derivative of BRET in which the fluorescent protein (BiFC) and/or bioluminescent enzyme (BiLC) is split, with part of the protein placed on each candidate receptor	Allows the detection of higher-order multimerization; stabilization of split YFP derivatives upon fusion, which will lead to increase in signal unrelated to oligomerization of the actual	These methods have been used to show higher-order homomerization and heteromerization of chemokine receptors	49,76

Continued

Table 9.2 Methods used in studying chemokine receptor oligomerization—cont'd

Method	Description	Pros and cons	Other notes	Reference(s)
		fused GPCRs, may complicate interpretation of results		
GPCR-HIT	BRET-based method in which the fluorescent protein is coupled to one of the candidate GPCRs and the bioluminescent enzyme is fused to β -arrestin	Allows the identification of active, functional heteromers; use is restricted to heterodimer identification	Chemokine receptors were among those used to establish the initial validation of this method	87
PFC (BiFC/BiLC)	Either a bioluminescent enzyme or fluorescent protein is split, with part fused to each candidate receptor, and a functional fluorescent or bioluminescent protein is interpreted to result from dimerization of the candidate receptors	Can be used with microscopy to zoom in on single cells/cellular regions; stabilization of split YFP derivatives upon fusion, which will lead to increase in signal unrelated to oligomerization of the actual fused GPCRs, may complicate interpretation of results	Again, this method tends to show constitutive dimerization, with agonist stimulation often affecting the signal, which could indicate either a change in dimerization equilibrium or conformational changes within pre-formed dimers	77
Radio-ligand displacement	Ligand affinity measured by displacement of radio-labeled ligand	Can be used on live cells; can be used to obtain evidence of allosteric functional effects of receptor oligomerization, such as negative cooperativity; and does not directly establish dimerization	This method has been used several times in recent studies to demonstrate negative cooperativity/transinhibition resulting from chemokine receptor oligomerization	47–49,88

stability, in reality it is not possible to compare different receptors. This is due to the fact that many factors influence the results, including receptor expression levels and cellular localization, which are difficult to control and properly quantify between experiments. For example, the stabilizing or destabilizing effect of mutations on the oligomerization of a given receptor may be difficult to address if they alter stability to an extent that is outside the detection range of BRET, and if receptor expression levels differ but the amount of transfected DNA (the standard protocol) is used as a measure of receptor density.¹⁰⁸ Most methods generally reflect steady state average views of receptor oligomerization over the whole cell although some studies have focused on the cell membrane and subcellular organelles.^{55,58,105} Dynamic, reversible association of receptors is also not captured by the most commonly used approaches, although exciting efforts in this direction have been reported.¹⁰⁹ Nevertheless, these approaches have at least provided leads that oligomerization may have functional relevance for specific receptors, allowing for follow-up studies; and despite the caveats and numerous conflicting reports, much has been learned or at least brought on radar about this fundamentally important feature of GPCRs.

3.2. Chemokine receptor homo- and hetero-oligomerization: Evidence for constitutive ligand-independent oligomer formation early after biosynthesis

Table 9.1 summarizes at least the majority of the reports related to chemokine receptor homo- and hetero-oligomerization along with some of the key observations in these publications. CCR2b was the first chemokine receptor that was shown to oligomerize.⁴² In these studies, chemical cross-linking coupled with Co-IP and western blotting was initially used to demonstrate oligomerization that was induced by binding of its ligand MCP-1/CCL2. Similarly, SDF-1/CXCL12 and RANTES/CCL5 were shown to induce oligomerization of CXCR4 and CCR5, respectively.^{51,68} Subsequently, many reports using RET-based methods showed constitutive association of many receptors without the requirement of ligand binding, and the current consensus is that receptors probably form in the absence of ligand binding.^{4,45,55} Whether the ligand has a significant effect on stabilizing receptor oligomers remains to be seen, as the commonly used RET approaches may not be sufficiently sensitive or quantitative to detect relevant changes. However, BRET studies of CCR2 and CXCR4 homo- and hetero-oligomers suggest that chemokine ligands and small molecule inhibitors affect the conformation but not the basal number of associated receptors

based on observed ligand-induced changes in the $BRET_{max}$ but not $BRET_{50}$.⁴⁵ FRET studies of CCR5/CXCR4 also suggest that the heteromers are preformed in the absence of ligand; however in these studies, stabilization of the hetero-oligomer by CCR5 ligands MIP-1 α /CCL3 and RANTES/CCL5, but destabilization by SDF-1/CXCL12 was reported.⁸⁹ These data are consistent with the early chemical cross-linking/Co-IP results which suggested that chemokines can stabilize receptor dimers.^{42,43,51,68,91} However, it is difficult to judge whether such changes observed in single-expression point FRET studies result from an actual change in the dimerization equilibrium or from conformational changes within constitutive dimers, illustrating a potential advantage of using BRET saturation titration curves.

The presence of basal, ligand-independent formation of chemokine receptor oligomers is consistent with the idea that oligomers form early along the biosynthetic pathway and can be detected during transport through the ER and golgi.^{64,110} The first and most convincing example of this concept was demonstrated with the class C gamma-aminobutyric acid (GABA)_B receptors that form obligate heterodimers: GABA_B-R1 requires dimerization with GABA_B-R2 in the ER in order to traffick to the cell surface, and although GABA_B-R2 can be transported to the cell surface in the absence of GABA_B-R1, it is not functional unless oligomerized with GABA_B-R1.^{111,112} Along these lines, constitutive homo- and hetero-oligomerization of CXCR1 and CXCR2 was demonstrated by a combination of BRET and Co-IP, and a novel-trapping strategy showed interactions between CXCR1 homomers and CXCR1: CXCR2 heteromers in the endoplasmic reticulum (ER). In these experiments, an ER retention signal was added to the C-terminus of CXCR1 and resulted in a significant reduction in the amount of CXCR1 and CXCR2 that was translocated to the cell surface.⁶⁴ Similarly, CCR5 has been shown to oligomerize in a ligand-independent fashion, both at the plasma membrane and in ER subfractions.⁵⁵ More recent studies using both BRET and FRET show constitutive association of virtually all chemokine receptors studied,^{1,3,4,45,47,58,59,90,107,110} and the assumption is, that if these hetero-oligomers are relevant in native cells, they probably form prior to reaching the cell membrane.

3.3. Crystal structures of CXCR4 reveal homodimers

In keeping with earlier biochemical studies that showed that CXCR4 sedimented as a dimer when purified in nondenaturing detergent,⁶⁹ recent crystal structures of CXCR4 have provided structural validation to the

relevance of contact-mediated receptor dimerization rather than simple clustering within the range detectable by RET. In 2010, five structures were reported and in all cases showed a dimer with subunit interactions primarily between TM helices V and VI.⁸⁰ While one cannot exclude that the dimer was due to crystal contacts, the fact that all five structures showed the same dimer interface despite being in different crystal forms, suggests that they are probably not artifacts of crystallization. This data supports numerous cell-based studies that suggest that CXCR4 forms homo- and heterodimers (Table 9.1).

The structures of CXCR4 were in complex with a small molecule antagonist, It1t, and a 16-residue cyclic peptide inhibitor, CVX15. They revealed a rather large acidic binding pocket and showed that It1t bound in the minor pocket involving TM helices I, II, III, and VII while CVX15 bound in the major pocket (TM helices III–VII). These compounds interact with several acidic residues that line the pocket and are known to be involved in binding to SDF-1/CXCL12. Consistent with the two-site model, the current thinking is that the N-terminus of CXCL12 interacts with the pocket CRS2, formed by the TM helices and ECL2, a β -hairpin structure that helps shape the entry to the pocket, and has been highly implicated in chemokine interactions. No density was observed for the receptor N-terminus up to the first cysteine consistent with the hypothesis that in the absence of chemokine, the CRS1 domain is unstructured.

The observed dimers raise questions about the stoichiometry of chemokine:receptor binding in cells. Originally 1:1 chemokine-monomer:receptor-monomer complexes were assumed, but given the CXCR4 dimer structures, it is possible to envision a 1:2 chemokine-monomer:receptor-dimer complex that still conforms to the two-site model (Fig. 9.3B). This issue has yet to be resolved, but it is noteworthy that some biochemical studies suggest that only one chemokine can bind to a receptor dimer at a time (see Section 4 and Refs. 47–49,88). Furthermore, as described in Section 7, CXCL12 dimers can interact with CXCR4 to produce different downstream signals than those stimulated by CXCL12 monomers,¹¹³ suggesting 2:2 chemokine-dimer:receptor-dimer complexes may also be functionally relevant.

Other questions related to the dimer structures include the following: (1) What is the variability and plasticity in chemokine receptor dimer interfaces? Assuming that the CXCR4 structures show a relevant dimer interface, is the TM V/VI interface always the interaction surface in CXCR4 dimers? Or are other interfaces used in higher-order oligomers or with other heteromeric

interactions? (2) Is it possible to engineer non-oligomerizing receptors to answer the functional relevance of chemokine receptor oligomerization? (3) Is there allosteric coupling across the interfaces, what is the functional consequence, and what is the mechanism? (4) Do dimer interfaces make good therapeutic targets?

Answers to these questions are only beginning to emerge. With regard to questions 1, it is worth noting that one of the CXCR4 structures showed an additional interface involving TMS I and II.^{80,108} Furthermore, structures of other GPCRs suggest a great deal of variability in dimer interfaces.¹¹⁴ Regarding question 2, in order to engineer non-oligomerizing receptors, structural knowledge of the interface is obviously useful but even then, identifying appropriate mutations that destabilize oligomeric receptors without affecting receptor stability, folding and ligand binding may be difficult. Quantifying the effect of mutations is also nontrivial as described above and in Ref. 108. Furthermore, the extent to which the stability of oligomerized receptors is affected by intracellular G or other proteins as well as the lipid environment, is unclear. If the receptors exist in assemblies larger than dimers, as has been suggested,^{49,76,101} then more than one interface may need to be simultaneously disrupted to achieve a monomeric status.

3.4. Attempts to disrupt receptor dimerization

In an early attempt to engineer a non-oligomerizing variant of CCR5, a TM I/TM IV dimer interface was predicted in a bioinformatic analysis.⁵⁸ Subsequent mutation of I52V and V150A in TMS I and IV, respectively, were reported to prevent dimerization according to both FRET and cross-linking studies, and TM peptides encompassing Ile52 and Val150 were shown to block dimerization. However, this data was subsequently contested based on BRET analysis by a different group and remains unresolved.⁵⁹ Nevertheless, regardless of the affect on dimerization, in contrast to the WT protein, the mutant CCR5 was unable to signal in calcium flux, chemotaxis, and JAK-STAT activation assays despite retention of binding affinity for RANTES/CCL5.⁵⁸ Similarly, the peptide blocked WT CCR5 receptor function. It therefore remains an open question as to whether the inhibitory effects of the TM peptide and the CCR5 mutant are through the controversial dimer disruption mechanism or through allosteric induction of non-signaling receptor conformations.

More recent BRET studies as well as the report by Lemay⁵⁹ tend to argue for allosteric induction of nonsignaling receptor conformations. In a 1999

report from Tarasova and coworkers, multiple TM peptides from CXCR4 and CCR5 were shown to block signaling of the receptors and to inhibit HIV replication.¹¹⁵ Follow-up studies using BRET suggested that the effects were due to inhibition of ligand-induced conformational changes rather than disruption of receptor dimers, since none of the peptides affected the basal BRET signal but did produce changes in the ligand-induced BRET signals.⁴⁵ The authors reasoned that the inhibitory effect of the TM peptide could best be explained by blockade of the allosteric communication between dimerized receptors. Similarly, in 2006, Wang and coworkers reported that a peptide corresponding to TM IV of CXCR4 blocked the migration of monocytes and cancer cells to CXCL12.⁷⁵ In this case, FRET between CXCR4-CFP and CXCR4-YFP was reduced by the peptide, but again changes in FRET efficiency at a single-expression level of FRET pairs are difficult to assign to reductions in actual numbers of dimers/oligomers versus conformational changes within stable complexes. Whatever the mechanism, the data overall suggest that targeting TM helices (dimer interfaces or otherwise) can be an effective strategy for chemokine receptor inhibition; the question is whether they can be specifically targeted with small molecules.



4. FUNCTIONAL EFFECTS OF CHEMOKINE RECEPTOR HETERO-OLIGOMERIZATION ON LIGAND BINDING

In a series of detailed studies, transinhibition of ligand binding between hetero-oligomerized receptors (CCR2/CCR5, CCR2/CXCR4, and CCR2/CCR5/CXCR4) was demonstrated by BRET and ligand-binding experiments. These studies made a compelling case for the importance of allostery in controlling the function of chemokine receptors, the potential impact that heterodimerization can have on drug efficacy, and provided insight into the mechanism for allosteric communication between receptor subunits. The first of these reports on the heterodimerization of CCR2 and CCR5 showed that these receptors were basally associated in the absence of chemokine agonists.⁴⁷ Furthermore, BRET₅₀ values, which are considered a measure of affinity (with the caveats described in [Section 3.1](#)), were similar for the CCR2 and CCR5 homomers and for the CCR2/CCR5 heteromers suggesting similar propensities for the homo- and hetero-oligomers to form. This is not surprising given the high-sequence conservation between CCR2 and CCR5, especially in their TM domains (78.2% identity, 89.4% similarity). Binding of the respective

chemokine ligands had no effect on the $BRET_{50}$ but affected the $BRET_{max}$ signal, suggesting that the ligands induce conformational changes rather than changes in the number of associated receptors, similar to related studies of CCR2/CXCR4.⁴⁵ Binding of ^{125}I -MCP-1/CCL2 tracer to CCR2 was unaffected by unlabeled CCR5 ligands (MIP-1 α /CCL3, MIP-1 β /CCL4, and RANTES/CCL5) when CCR2 was expressed alone. Similarly, no competitive binding between ^{125}I -MIP-1 β /CCL4 tracer and CCR2 ligands (MCP-1/CCL2 and MCP-2/CCL8) to CCR5 was observed when CCR5 was expressed alone. The surprising finding was that coexpression of the two receptors made the reporter ligands of one receptor susceptible to binding inhibition by the ligands of the other receptor: CCR5 ligands inhibited binding of ^{125}I -MCP-1/CCL2 to cells coexpressing both CCR2 and CCR5, and CCR2 ligands inhibited the binding of ^{125}I -MIP-1 β /CCL4 to the coexpressing cells. Furthermore, the extent of the transinhibition corresponded with the approximate proportion of expressed heterodimers, suggesting some sort of negative binding allostery between the coexpressed receptors. Similar results were observed in both transfected cells as well as T lymphoblasts that naturally express both receptors. These data suggested the potential for allosteric communication between coexpressed and apparently oligomerized CCR2 and CCR5.

To further investigate the mechanism and demonstrate the allosteric nature of the binding inhibition observed for the CCR2/CCR5 hetero-oligomers, a subsequent study used “infinite dilution tracer” experiments.⁴⁸ These experiments showed that dissociation of the CCR2-specific ligand ^{125}I -MCP-1/CCL2 from cells coexpressing CCR2 and CCR5 was accelerated significantly by the CCR5-specific ligand MIP-1 β /CCL4 compared to the dissociation rate from cells expressing CCR2 alone. Likewise, dissociation of ^{125}I -MIP-1 β /CCL4 from CCR5 was accelerated by CCL2 when the cells expressed both receptors compared to CCR5 alone. Again, the results were demonstrated in both transfected cells and in T lymphoblasts suggesting the physiological relevance of the observations. Transinhibition of ligand binding was also demonstrated for CCR2/CXCR4 hetero-oligomers in transfected and primary leukocytes⁸⁸ and for CCR2/CCR5/CXCR4 multimers in transfected cells as well as primary T cells and monocytes.⁴⁹

It has been argued that “G protein stealing” can be the source of transinhibition of ligand binding without the need to invoke heterodimerization.^{107,116,117} The idea here is that many agonists require G protein coupling for high-affinity receptor binding. Thus, independent

of receptor hetero-oligomerization, depletion of G protein due to ligation of one receptor with its agonist can result in the apparent lowering of the affinity of the other receptor for its ligand, especially if the pool of G proteins is limiting. However, the partial agonist [10–68]RANTES/CCL5, and the antagonist MET-RANTES/CCL5 were also effective in promoting dissociation of MCP-1/CCL2 from CCR2 in CCR2/CCR5 coexpressing cells. Similarly, the small molecule CXCR4 antagonist AMD3100 and the CCR2 inverse agonist TAK-779 were able to compete off the binding of chemokine from CCR2 and CXCR4, respectively, but only when the two receptors were coexpressed.⁸⁸ These data are not consistent with a G protein steal since high-affinity binding of antagonists and inverse agonists typically does not require G protein coupling. Along with the results from the infinite dilution tracer experiments, the data suggest that there is direct allosteric communication between hetero-oligomerized receptors (Fig. 9.4).

That is not to say that G proteins do not play a role in the observed transinhibition. Springael and coworkers showed that the addition of pertussis toxin (PTx) or Gpp(NH)p, a nonhydrolyzable analog of GTP, strongly reduced the binding of MIP-1 β /CCL4 to CCR5.⁴⁸ Similarly binding of MIP-1 β /CCL4 was reduced on cells expressing an R126N mutant

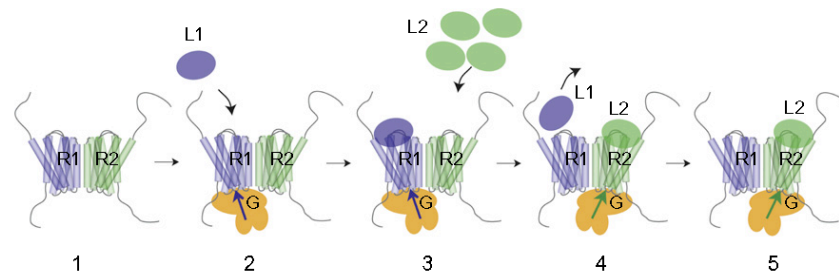


Figure 9.4 A model for the allosteric ligand-binding transinhibition of agonists from chemokine heterodimers as suggested by Springael and coworkers.⁴⁸ (1) Heterodimerization of receptor 1 (R1) and receptor 2 (R2). (2 and 3) Ligand 1 (L1) binds with high affinity to R1 when it is coupled to heterotrimeric G α i proteins (G). The arrow illustrates allosteric coupling between the G protein and R1, which allows R1 to adopt a conformation that leads to high-affinity binding of L1. (3 and 4) Subsequent binding of ligand 2 (L2) to R2 induces a conformational change in R2 that results in the G protein interacting with R2 rather than R1, and subsequently (4 and 5) dissociation of L1 from R1 since G protein is required for high-affinity interaction of L1/R1. Note that the mechanism for transinhibition of agonist by binding of small molecule antagonists does not need to involve changes in G protein coupling but could be explained simply by allosteric communication between the two receptors.⁸⁸

of CCR5 that does not couple to G proteins, indicating the requirement of G proteins for high-affinity binding of CCL4 to CCR5. Although the CCR5-R126N mutant retained the ability to hetero-oligomerize as efficiently with CCR2 as WT CCR5, and CCR5-R126N did not show a dominant negative effect on signaling of coexpressed CCR5 and CCR2 as assessed by calcium flux, MIP-1 β /CCL4 was no longer able to increase the dissociation rate of MCP-1/CCL2 from CCR2 in cells coexpressing both CCR2 and CCR5-R126N. Together the data suggest that the G protein is needed for allosteric communication through the dimer, at least when agonists are involved, and the authors proposed a mechanism for G protein-dependent binding transinhibition (Fig. 9.4). However, since antagonists also promote transinhibition, the requirement for G protein is likely to be first and foremost necessary for high-affinity binding of agonist, regardless of whether the G protein directly contributes to allostery across the heterodimer.

Other conclusions reached from these studies include the fact that (1) ligand binding does not need to induce the activated state of a receptor in order to inhibit ligand binding to the other receptor in the hetero complex^{48,49,88}; (2) that homo and heterodimers likely interact, suggesting larger allosterically coupled arrays of chemokine receptors⁴⁹; (3) that binding transinhibition is not likely due to steric blockade by the competing ligand since small molecules are as effective as chemokines in causing ligand dissociation from the partner receptor; (4) that a receptor heterodimer, and most probably a homodimer, can only bind a single chemokine with high affinity.^{48,49,88} The latter hypothesis is interesting in light of the CXCR4 dimer structure, but further studies are obviously needed to determine chemokine:receptor stoichiometries. Likewise, the stoichiometry between chemokine receptors and downstream signaling partners including G proteins and β -arrestins, may provide key insights that reconcile some of the data.

What is particularly surprising about the results is the fact that ligands with different efficacies and sizes (inverse agonists, antagonists, and agonist variants of small both molecules and chemokines) were all capable of ligand-binding transinhibition. Whether the effect is common or specific to the receptors and ligands reported in these studies remains to be seen. However, it is worth noting that different ligands have been shown to produce different conformational changes in receptor homo- and heterodimers^{45,89}; this suggests that many receptor conformations may produce cross-competition whether it be due to distortions of the binding pocket or perturbations of

G protein coupling that affect the ligand affinity of the opposing oligomeric partner. It will be interesting to see if similar findings are observed with other chemokine receptors that have been shown to heterodimerize (Table 9.1) and in what contexts.

Transinhibition of ligand binding makes sense when there is inhibition of signaling of one receptor by the ligand of the partner receptor as described in the next section. However, there are also examples where the signaling is amplified or completely altered, and how this correlates with ligand binding is an open question. As discussed in Section 5, DARC heterodimerizes with CCR5 and blocks its downstream signaling without affecting ligand binding or CCR5 internalization. The observed combination of effects has functional implications consistent with other behaviors of this atypical chemokine receptor. For example, can chemokine receptor heteromers bind different chemokines than chemokine homomers? Given the known ligand:receptor promiscuity, and the fact that proteolytic processing of chemokines can cause receptor-specificity changes, this scenario would not be difficult to imagine.



5. EFFECTS OF CHEMOKINE HETERO- AND HOMO-OLIGOMERIZATION ON SIGNALING

5.1. Transinhibition of signaling by ligands in hetero-oligomeric complexes

Early reports suggested synergy in calcium flux due to CCR2/CCR5 heterodimers⁴⁴; however, subsequent studies failed to show cooperative calcium signaling with CCR2/CCR5 and with CCR2/CXCR4 and thus this finding remains controversial.^{49,88} Cooperative signaling in cell migration was also not observed with agonists of the coexpressed receptors in transfected as well as native cells. Instead, in both functional assays, small molecule antagonists of one receptor caused inhibition of functional responses of the other receptor to which it does not bind.^{49,88} Thus the CXCR4 antagonist AMD3100 inhibited not only signaling of CXCR4 in response to its ligand SDF-1/CXCL12, but it also blocked signaling of MCP-1/CCL2 to CCR2. Similarly, the CCR2 inverse agonist TAK-779 blocked signaling of SDF-1/CXCL12 in primary CD4+ lymphoblasts coexpressing both CCR2 and CXCR4.⁸⁸ These data are in line with the ligand-binding transinhibition; however, particularly interesting was the fact that the inhibition of functional responses was stronger than the binding cross-competition. The authors proposed that this might reflect allosteric

functional effects across larger arrays of receptors than heterodimers.⁸⁸ Along these lines, subsequent studies showed cooperative interactions and hetero-oligomerization between CCR2, CCR5, and CXCR4 in T lymphoblasts, and similar inhibition of calcium signaling and migration of receptors by antagonists of the orthogonal receptors. This cross-competition also translated into an *in vivo* air pouch migration model in which the small molecule TAK-779 (which antagonizes both CCR5 and CCR2), blocked migration of cells to CXCL12/CXCR4.⁴⁹ The implications for drug discovery here are quite striking; in principal, it may be possible to inhibit the activity of one chemokine receptor indirectly by targeting another receptor with which it oligomerizes.

5.2. Activation of alternative signaling pathways by hetero-oligomers

In addition to inhibiting signaling, Mellado and coworkers subsequently demonstrated that heterodimerization of CCR2 and CCR5 can produce unique signaling responses compared to the classical G α i signals characteristic of chemokine receptors expressed in isolation.⁴⁴ Coexpression of both receptors and stimulation with their respective ligands (RANTES/CCL5 and MCP-1/CCL2) resulted in a PTx-insensitive calcium flux through Gq/11, in contrast to the normal inhibitory effect that PTx has on G α i-mediated calcium flux when the receptors are expressed alone. Furthermore, simultaneous stimulation of the presumed hetero-oligomers by both ligands failed to cause receptor downregulation and produced a delayed and sustained activation of phosphatidylinositol 3-kinase (PI3K). The consequence of the altered signaling was linked to more efficient adhesion instead of cell migration. A plausible interpretation was presented in which the homomers and heteromers cooperate to augment the versatility of the signaling responses, with the ligands and their concentrations controlling the formation/stability of the homo- or hetero-complexes. In the Mellado study, it was suggested that hetero-oligomers might contribute to cell adhesion and “parking,” once the cells reach their destination in tissues, while the homo-oligomers promoted migration.

Subsequent studies showed the relevance of the above findings to the recruitment of CXCR4 and CCR5 into the immunological synapse of T cells, and their role in co-stimulation of the T cell receptor during activation through Gq/G11 mediated responses.¹¹⁸ Similar to the above studies, rather than promoting normal G α i-mediated migration, the recruitment of the receptors resulted in an insensitivity to chemokine gradients, enhanced

adhesion to antigen-presenting cells, and promoted increased proliferation and cytokine production. These results were shown later to be due to the physical association of CXCR4 and CCR5 by BRET and Co-IP; furthermore, it was shown that CXCR4 requires CCR5 for recruitment to the immunological synapse.⁵⁶ Together this series of studies demonstrates the ability of chemokine receptor hetero-complexes to differentially signal compared to the homomeric counterparts, in this case due to specificity changes in coupling with G proteins. These studies represent particularly good examples of signaling versatility bestowed by hetero-oligomerization.

5.3. Modulation of signaling by atypical and virally encoded chemokine receptors

5.3.1 DARC/CCR5

The Duffy antigen for chemokines (DARC), an atypical receptor that does not signal through G proteins, has also been shown to homo-oligomerize and to hetero-oligomerize with CCR5.⁸³ Coexpression of CCR5 and DARC showed a marked attenuation of chemotaxis and calcium flux in response to the CCR5 ligand RANTES/CCL5 (which also binds DARC with equal affinity) as well as to the CCR5-specific CCL3 isoform ligand, LD78 β /CCL3L1. On the other hand, ligand-stimulated CCR5 was internalized to the same extent whether it was coexpressed with DARC or not, even though DARC itself does not internalize upon ligand stimulation or interact with β -arrestin in the cells used in this study. On the basis of these and other data, it was proposed that the DARC/CCR5 interaction inhibits ligand-induced CCR5 signaling by altering the affinity of CCR5 for G proteins or the responsiveness of CCR5 to its ligands, but not by altering its affinity for ligands. One could imagine, for example, that DARC induces a conformation in CCR5 that remains competent for ligand binding and internalization but does not allow CCR5 to adopt conformations required for calcium signaling and chemotaxis. DARC has been suggested to function as a “chemokine rheostat” on endothelial cells by supporting the transport, presentation, and concentration of chemokines to balance the inflammatory response.^{6,119} This study suggests a mechanism by which DARC “rheostats” the function of CCR5, turning it down by blocking signaling through hetero-oligomerization.⁸³ Secondly, the fact that heterodimerization with DARC does not affect CCR5’s high affinity for CCL5 or its ability to internalize (presumably with ligand), adds a second stage to the “dial-down” switch.

5.3.2 CXCR7/CXCR4

It was recently demonstrated that CXCR7 forms hetero-oligomers with CXCR4.^{77,78,91,92} In the original report,⁹¹ hetero-oligomerization coincided with an increased Ca^{2+} flux response to CXCL12 stimulation. Furthermore, it was shown that the time course of ERK activation was altered when CXCR7 was coexpressed in CXCR4-expressing cells. Specifically, when only CXCR4 was present, ERK was activated in a biphasic fashion, whereas when the two receptors were coexpressed, only the second delayed peak in ERK activation was observed.

In a later report, however, coexpression of CXCR7 along with CXCR4 decreased the potency of CXCL12-induced Ca^{2+} flux, though the maximal efficacy was unchanged.⁷⁸ G protein activation as measured by an ^{35}S -GTP- γS binding assay was similarly reduced in potency when the two receptors were coexpressed, and BRET between CXCR4-YFP and $\text{G}\alpha\text{i}1$ -Rluc demonstrated that CXCR7 causes a conformational rearrangement within pre-coupled CXCR4- and $\text{G}\alpha\text{i}$ -containing complexes. Finally, this report demonstrated that CXCR7 knockdown in T lymphocytes, which endogenously express both CXCR4 and CXCR7, led to an increased migratory response to a lower concentration (0.3 nM) of CXCL12, which was attributed to the propensity of CXCR7 to scavenge CXCL12 (discussed below). Overall, it was suggested that the effects of CXCR7 on CXCL12:CXCR4-mediated signaling cell migration was due both to allosteric modulation of CXCR4: $\text{G}\alpha\text{i}$ interactions and hoarding of CXCL12 by CXCR7.

One recent report, which did not directly demonstrate dimerization, nevertheless obtained intriguing results that could involve CXCR4/CXCR7 hetero-oligomerization.¹²⁰ In this study, it was shown that both CXCL11, a chemokine ligand for CXCR7 but not CXCR4, and CCX771, a small molecule inhibitor of CXCR7, were able to inhibit CXCL12-mediate transendothelial migration (TEM), specifically in the case of migrating cells that endogenously expressed both CXCR4 and CXCR7. Since TEM is driven entirely by CXCR4, the most striking observation was that the CXCR7 ligand CCX771, was substantially more potent than the CXCR4 specific ligand AMD3100 in blocking TEM. These results have tremendous ramifications for drug discovery; for example, the authors note that CCX771 might be a particularly potent CXCR4 inhibitor in cells that express both receptors (usually cancer cells) and could provide greater selectivity than blocking CXCR4 indiscriminately with CXCR4 antagonists like AMD3100.

Finally, a recent report demonstrated that CXCR7 coexpression along with CXCR4 decreased the G α i-mediated inhibition of cAMP production resulting from CXCL12 stimulation.⁹² At the same time, coexpression of the receptors greatly increased the resting and CXCL12-induced β -arrestin recruitment to CXCR7. Interestingly, CXCL11 both reversed the decrease in G α i activity and slightly attenuated the increased arrestin recruitment. This study also showed that CXCR7 coexpression increased ERK, p38 MAPK, and SAPK activation upon CXCL12 stimulation, suggesting a broad change in the signaling response elicited in the case of the heteromer. The authors also found that the CXCL12 response of cells in a transwell migration assay was increased when CXCR7 was coexpressed along with CXCR4. The increase in the activation of downstream signaling proteins as well as the increased chemotactic response were dependent upon β -arrestin expression.

As alluded to above, the allosterically regulated functional effects of CXCR4/CXCR7 hetero-oligomerization may be difficult to dissect from other cooperative interactions between the two receptors. In the interpretation of all of the above studies, for example, it should be noted that CXCR7 has significantly higher affinity than CXCR4 for SDF-1/CXCL12. Thus some of the effects, for instance, any increase in CXCR4's responsiveness to CXCL12 when CXCR7 is blocked, could be attributed to the inhibition of CXCR7 from binding and effectively sequestering (from CXCR4) a large proportion of the SDF-1/CXCL12 present. In this regard, it was recently demonstrated that CXCR7 can aid in the pro-migratory, pro-metastatic effects of CXCR4 by scavenging CXCL12 rather than (or in addition to) allosteric modulation of CXCR4 as suggested in the study by Levoye.¹²¹ In this intriguing study, CXCR7 was even shown to affect the function of CXCR4 when it was expressed primarily on different populations of malignant cells compared to CXCR4. *In vivo* imaging demonstrated that CXCR7 reduced SDF-1/CXCL12 levels in the primary tumor microenvironment, which in turn reduced CXCR4 internalization and downregulation. While this scavenging function of CXCR7 would potentially limit the effects of CXCL12:CXCR4 on tumor growth, it was proposed that it allows CXCR4 to maintain responsiveness to external CXCL12 gradients that would draw metastatic cells to other tissues.¹²¹

Several aspects of the above observations are in line with emerging principles of chemokine receptor oligomerization. The ability of CXCR7-specific agonists as well as antagonists to alter signaling responses mediated by CXCR4 is especially compelling evidence of allosteric communication

within receptor oligomers, as CXCR7 does not activate G proteins and as shown by Levoye, likely does not interfere with CXCR4 signaling simply by stealing G proteins.⁷⁸ Furthermore, the change in CXCR4-G α i interaction as well as the increased activation of β -arrestin-mediated signaling proteins (MAPK, ERK, p38, SAPK) suggests that the CXCR4/CXCR7 heteromer is a functionally unique signaling complex. However, not all of the above data can be reconciled with a consistent story, illustrating the dependence on methods and the context dependence of the studies (e.g., the effect of the relative densities of the two receptors as well as cell background).

5.3.3 BILF1/CXCR4

Many viruses, including herpesviruses, encode GPCRs with considerable homology to chemokine receptors.^{122,123} Most of these vGPCRs show significant constitutive activity although they also tend to bind numerous ligands. One of the most famous of these receptors is ORF74 from the Kaposi's sarcoma-associated herpesvirus (HHV-8), which was initially identified as being the cause of the highly vascularized Kaposi's sarcoma lesions in AIDS patients, and other proliferative disorders. It binds to at least 12 chemokine ligands whose activities range from inverse agonists to full agonists. On the other end of the spectrum of known ligands and relationship to chemokines, BILF1 is a GPCR encoded by the Epstein-Barr virus (EBV or HHV-4) that persists in B cells following primary infection and contributes to Burkitt's lymphoma and Hodgkin's lymphoma among other oncogenic disorders.¹²⁴ It has limited homology to chemokine receptors and currently is considered an orphan GPCR with no known ligands. This receptor seems to be involved in immune evasion by a number of mechanisms including downregulation of MHC class I receptors and inhibition of RNA-dependent protein kinase activity that would otherwise put a stop to cellular translation and therefore viral replication.

One of the more recent mechanisms discovered for BILF1 is that it heterodimerizes with a number of chemokine receptors including CXCR4.^{100,101} In fact, by combining bimolecular luminescence complementation and bimolecular fluorescence complementation with BRET measurements, it was shown that heteromeric complexes between BILF1 and CXCR4 consist of the concurrent interaction of at least four GPCR subunits. BILF1 was shown to inhibit binding of SDF-1/CXCL12 to CXCR4 with the consequence of blocking chemokine-mediated signaling. Since BILF1 is a constitutively active receptor and CXCL12 requires G protein coupling for high affinity, it was hypothesized that this

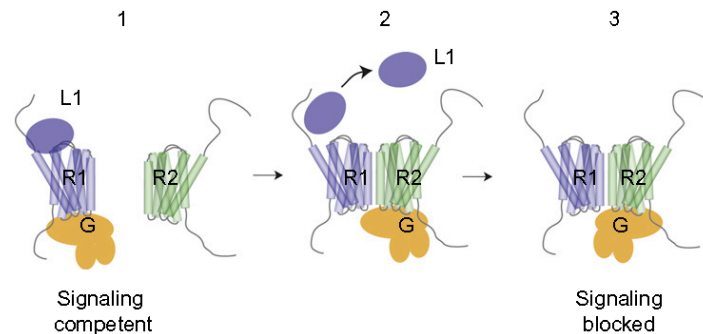


Figure 9.5 A model for inhibition of CXCR4 signaling by the EBV viral GPCR, BILF1.¹⁰¹ (1) CXCR4 (R1), shown here as monomer for simplicity but probably exists as homooligomer, is coupled to heterotrimeric G α i proteins (G) and therefore competent for high affinity binding and signaling in response to SDF-1/CXCL12 (L1). BILF1 is represented as R2. (2) Hetero-oligomerization of CXCR4 (R1) with BILF1 (R2) scavenges the G protein heterotrimer from CXCR4 due to its constitutive activity. The lack of G protein shifts CXCR4 into a low affinity state and CXCL12 dissociates. (3) Uncoupled, ligand-free CXCR4 R1 does not signal.

receptor might scavenge G α i protein from CXCR4, forcing it into a low affinity state for its ligand (Fig. 9.5). Indeed, overexpression of G α i1 restored the ability of CXCL12 to bind and signal through CXCR4. Furthermore, a G protein uncoupled mutant of BILF1 was much less effective in inhibiting CXCL12-mediated signaling. Together these data suggest that inhibition of CXCR4 by BILF1 is a consequence of its constitutive activity, and contrasts with the allosteric mechanisms described above for the ligand-binding transinhibition between CXCR4, CCR2, and CCR5. In principle, this G protein-scavenging mechanism could represent a general mechanism of viral GPCRs for inhibiting the function of chemokine receptors that require G protein coupling for high-affinity binding.



6. HETERODIMERIZATION OF CHEMOKINE RECEPTORS WITH NONCHEMOKINE RECEPTORS

In addition to BILF1, other receptors outside the chemokine receptor family have been shown to hetero-oligomerize with chemokine receptors and impact signaling (Table 9.1). In particular, members of the opioid family of GPCRs have been shown to form heterodimers with CCR5, CXCR4, and CXCR2.^{94,95,98,99} These studies were motivated by the fact that opioid

receptors and chemokine receptors are often coexpressed on immune system cells as well as neurons and glial cells in the brain,⁹⁹ and the fact that opioids have been shown to inhibit migration of leukocytes.¹²⁵ In a study of the μ -opioid receptor (MOR) and CCR5, for example, transinhibition of functional responses was observed.⁹⁵ Whereas cells coexpressing both receptors were responsive to the MOR agonist (DAMGO) and to the CCR5 agonist (RANTES/CCL5) when they were added individually, pre-treatment of the cells with CCL5 inhibited migration to DAMGO, and DAMGO but not the antagonist Naloxone, inhibited migration to CCL5. Similarly DAMGO caused increased phosphorylation of CCR5 and inhibited binding of GTP γ S, while CCL5 treatment caused enhanced phosphorylation and decreased GTP γ S binding to MOR. In contrast to the ligand-binding transinhibition described previously for CCR5, CCR2, and CXCR4, there was no significant bi-directional inhibitory effect on the binding affinity of the agonists. Overall, the data suggest that agonist stimulation of each receptor promoted cross-desensitization of the other receptor.

CXCR4 and the δ -opioid receptor (DOR) have also been shown to hetero-oligomerize. In these studies, hetero-oligomerization and simultaneous stimulation with their respective agonist ligands, SDF-1/CXCL12 and [D-Pen2, D-Pen5]enkephalin (DPDPE), inhibited migration of CXCL12-mediated cell migration and adhesion of primary monocytes and monocytic cell lines. These results were also validated with *in vivo* studies of cell migration into the peritoneal cavity of mice.⁹⁹ In contrast to the above studies of CCR5 and MOR, the inhibitory effect was not due to heterologous desensitization, nor did DPDPE affect the affinity of CXCL12 for CXCR4. Instead the silencing of CXCR4 was shown to be due to the inability of the ligand-engaged heterodimers to activate JAK2, which is a pre-requisite for G α i coupling to CXCR4. While FRET studies showed that the receptors formed oligomers independent of ligand binding, additional studies suggested that the receptors function in a ligand-regulated dynamic equilibrium between homo and hetero-oligomers. Specifically, FRET signals from CXCR4 homomers were disrupted with increasing expression of DOR. Furthermore, the heterodimer formation was reversed by DPDPE but not by simultaneous addition of CXCL12 and DPDPE. Overall the results suggest that CXCL12 or DPDPE alone allows signaling by their respective homomeric receptors, but treatment with both ligands stabilizes the hetero-oligomers and blocks signaling presumably by stabilizing the receptors in inactive conformations. This ligand-dependent

regulation of the heteromers was proposed to provide a mechanism that might have consequences on physiological processes involving pain and inflammation; for example, by increasing sensitivity to pain while simultaneously curtailing migration of cells to sites of inflammation.

Entirely different functional effects were observed in a study of hetero-oligomers between CXCR2 and DOR.⁹⁸ In this case, several complementary methods (BRET, FRET, tr-FRET, and Co-IP) were used to demonstrate heterodimers in transfected cells. Saturation BRET studies suggested that the heterodimers have a greater tendency to associate than the homodimers. Most importantly, the small molecule CXCR2 antagonist resulted in enhanced signaling responsiveness of DOR to agonists, due to allosteric communication between the receptors while the CXCR2 agonist IL-8/CXCL8 did not. That the nature of the ligand matters makes intuitive sense since agonists and antagonists would likely promote different conformations of the partner receptor in the heterodimer.

In contrast, the Epstein-Barr virus-induced receptor 2 (EBI2) exerts a negative allosteric effect on the function of CXCR5.¹⁰² In these studies coexpression of EBI2 lead to decreased responsiveness to CXCL13, as measured by Ca^{+2} flux, chemotaxis, and ERK1/2 phosphorylation. These results were attributed to the reduced affinity of CXCR5 for its ligand CXCL13 when the two receptors were coexpressed. Whether the ligand affinity was reduced due to a direct allosteric modulation of EBI2 on the CXCR5-binding pocket, the coupling with G protein, or a combination of both mechanisms was not determined. The cooperation between these two receptors is thought to regulate B cell movement into lymphoid follicles.

CXCR2 has also been shown to associate with the α 1A-adrenoreceptor.⁹³ In this case, heterodimerization with CXCR2 changes the pharmacology of α 1A such that it strongly recruits β -arrestin upon stimulation with norepinephrine. This effect was inhibited not only by the α 1A antagonist Terazosin, but also by a CXCR2-specific small molecule inverse agonist, SB265610.



7. OTHER SOURCES OF ALLOSTERY IN CHEMOKINE RECEPTOR SIGNALING: CHEMOKINE OLIGOMERIZATION

The bulk of this review has been focused on chemokine receptor oligomerization and its functional consequences. However, there are many other sources of allostery related to ligands that are worth noting. Similar to small molecule agonists of GPCRs, functional selectivity of different chemokine

ligands of the same receptor have been reported. One of the best examples involves the ligands of CCR7, SLC/CCL21, and ELC/CCL19, which work together to allow for temporally and spatially distinct responses of CCR7-expressing T cells.¹²⁶ Both of these ligands show a similar binding affinity for CCR7 and equipotent ability to activate G proteins and cause calcium flux. However, only CCL19 promotes robust desensitization and phosphorylation of the receptor, as well as β -arrestin recruitment and ERK1/2 activation. This finding and the fact that these ligands are differentially expressed *in vivo* has been used to explain how CCR7 can produce the diverse responses of T cells as they migrate into the T cell zones of peripheral lymph nodes. CCL21 is expressed on the high endothelial venules, and thus it makes sense that it would not cause desensitization, allowing subsequent migration of the cells into T cell zones where CCL19 is expressed.

Another important example is that of synthetic N-terminally modified variants of RANTES/CCL5 that can cause internalization of CCR5 and inhibit it from being recycled back to the cell surface. These studies have provided proof of concept that engineering this type of allosteric functional selectivity can be a powerful approach to inhibiting HIV. There are also many reports of allosteric small molecules of chemokine receptors (for an excellent review see Ref. 4).

All of the above examples of functionally selective ligands fit into the classic view of chemically different variants of related ligands. However, recently in the chemokine field, it has been shown that different oligomerization states of the same ligand can also show biased signaling. Early investigations of RANTES/CCL5 showed that although oligomerization-deficient mutants were equally capable as WT CCL5 in promoting transendothelial cell migration, only the oligomerizing WT chemokine could promote monocyte arrest.¹²⁷ More recent studies of an obligate disulfide-locked dimer of SDF-1/CXCL12 have shown that it is capable of binding CXCR4 but it has a different signaling profile than WT CXCL12 (which is effectively monomeric below millimolar concentrations). Whereas WT CXCL12 stimulated calcium flux, inhibited cAMP, and promoted cell migration and β -arrestin association, dimeric CXCL12 was impaired in its ability to stimulate cell migration and recruit β -arrestin.¹¹³ Whether dimeric CXCL12 binds and stabilizes monomeric or dimeric CXCR4 remains to be seen, but one can imagine an effect of the oligomerization state of the CXCL12 on the homo or hetero-oligomerization state of CXCR4 and vice versa—that the state of CXCR4 affects whether monomeric or dimeric CXCL12 binds to CXCR4.



8. CONCLUSIONS AND FUTURE PERSPECTIVES

In the last decade, there has been an explosion in the number of studies focused on demonstrating the presence and functional relevance of chemokine receptor homo- and hetero-oligomerization. Notwithstanding acknowledgement of the fact that there are conflicting reports and perhaps erroneous conclusions because of limitations in methods used, it appears that receptor oligomerization, particularly hetero-oligomerization, can result in many different types of pharmacological responses compared to chemokine receptors in isolation, and as a consequence of many different types of cellular mechanisms. These functional effects and mechanisms include (1) transinhibition of ligand binding whether it be through a G protein steal when the pool of G proteins is limiting, or purely from allosteric effects because of changes in the conformation of a given receptor (R1) due to the presence of the second receptor (R2) and/or the presence of the agonist or antagonist ligand of R1 or R2; (2) activation of receptor functional responses whether it be through ligand-dependent or independent effects; (3) inhibition of functional responses that are ligand independent, or dependent on ligands of one or both of the interacting receptors; (4) ligand-regulated formation of receptor heteromers or destabilization of receptor heteromers.

In addition to these functional effects, the next level of complexity and a key issue is whether there are cell- and tissue-dependent effects given differences in receptor expression levels, intracellular signaling partners, and intra- and inter-cellular microenvironments. The idea that these effects can impact drug discovery seems indisputable and while it complicates high-throughput screening campaigns, in principle there are major opportunities for drug discovery if the biology of the disease and detailed pharmacology of the receptors in question are understood. Technology development to validate the presence of interacting receptors, their functional consequences and mechanisms of action, and determining their role in disease will be required to capitalize on these new insights into the complex function and regulation of chemokine receptors and other GPCRs.

ACKNOWLEDGMENTS

The authors acknowledge support from the National Institutes of Health/National Institute of General Medical Sciences U01GM094612 and R01GM081763 to T. M. H., and the Graduate Training Program in Cellular and Molecular Pharmacology T32GM007752, which supports B. S. We also thank Catherina L. Salanga for assistance with figure preparation.

REFERENCES

1. Munoz LM, Lucas P, Holgado BL, Barroso R, Vega B, Rodriguez-Frade JM, et al. Receptor oligomerization: a pivotal mechanism for regulating chemokine function. *Pharmacol Ther* 2011;**131**:351–8.
2. Salanga CL, Handel TM. Chemokine oligomerization and interactions with receptors and glycosaminoglycans: the role of structural dynamics in function. *Exp Cell Res* 2011;**317**:590–601.
3. Munoz LM, Holgado BL, Martinez AC, Rodriguez-Frade JM, Mellado M. Chemokine receptor oligomerization: a further step toward chemokine function. *Immunol Lett* 2012;**145**:23–9.
4. Scholten DJ, Canals M, Maussang D, Roumen L, Smit MJ, Wijtmans M, et al. Pharmacological modulation of chemokine receptor function. *Br J Pharmacol* 2012;**165**:1617–43.
5. Graham GJ. D6 and the atypical chemokine receptor family: novel regulators of immune and inflammatory processes. *Eur J Immunol* 2009;**39**:342–51.
6. Graham GJ, Locati M, Mantovani A, Rot A, Thelen M. The biochemistry and biology of the atypical chemokine receptors. *Immunol Lett* 2012;**145**:30–8.
7. Kalatskaya I, Berchiche YA, Gravel S, Limberg BJ, Rosenbaum JS, Heveker N. AMD3100 is a CXCR7 ligand with allosteric agonist properties. *Mol Pharmacol* 2009;**75**:1240–7.
8. Zabel BA, Lewen S, Berahovich RD, Jaen JC, Schall TJ. The novel chemokine receptor CXCR7 regulates trans-endothelial migration of cancer cells. *Mol Cancer* 2011;**10**:73.
9. Odemis V, Lipfert J, Kraft R, Hajek P, Abraham G, Hattermann K, et al. The presumed atypical chemokine receptor CXCR7 signals through G(i/o) proteins in primary rodent astrocytes and human glioma cells. *Glia* 2012;**60**:372–81.
10. Schall TJ, Proudfoot AE. Overcoming hurdles in developing successful drugs targeting chemokine receptors. *Nat Rev Immunol* 2011;**11**:355–63.
11. Lukacs NW, Oliveira SH, Hogaboam CM. Chemokines and asthma: redundancy of function or a coordinated effort? *J Clin Invest* 1999;**104**:995–9.
12. Mantovani A. The chemokine system: redundancy for robust outputs. *Immunol Today* 1999;**20**:254–7.
13. Proudfoot AE, Power CA, Schwarz MK. Anti-chemokine small molecule drugs: a promising future? *Expert Opin Investig Drugs* 2010;**19**:345–55.
14. Devalaraja MN, Richmond A. Multiple chemotactic factors: fine control or redundancy? *Trends Pharmacol Sci* 1999;**20**:151–6.
15. Handel TM, Lau EK. Chemokine structure and receptor interactions. *Emst Scher Res Found Workshop* 2004;**45**:101–24.
16. Ray P, Lewin SA, Mihalko LA, Leshner-Perez SC, Takayama S, Luker KE, et al. Secreted CXCL12 (SDF-1) forms dimers under physiological conditions. *Biochem J* 2012;**442**:433–42.
17. Ren M, Guo Q, Guo L, Lenz M, Qian F, Koenen RR, et al. Polymerization of MIP-1 chemokine (CCL3 and CCL4) and clearance of MIP-1 by insulin-degrading enzyme. *EMBO J* 2010;**29**:3952–66.
18. Wang X, Watson C, Sharp JS, Handel TM, Prestegard JH. Oligomeric structure of the chemokine CCL5/RANTES from NMR, MS, and SAXS data. *Structure* 2011;**19**:1138–48.
19. Hoogewerf AJ, Kuschert GS, Proudfoot AE, Borlat F, Clark-Lewis I, Power CA, et al. Glycosaminoglycans mediate cell surface oligomerization of chemokines. *Biochemistry* 1997;**36**:13570–8.

-
20. Lau EK, Paavola CD, Johnson Z, Gaudry JP, Geretti E, Borlat F, et al. Identification of the glycosaminoglycan binding site of the CC chemokine, MCP-1: implications for structure and function in vivo. *J Biol Chem* 2004;**279**:22294–305.
 21. Vega B, Munoz LM, Holgado BL, Lucas P, Rodriguez-Frade JM, Calle A, et al. Technical advance: surface plasmon resonance-based analysis of CXCL12 binding using immobilized lentiviral particles. *J Leukoc Biol* 2011;**90**:399–408.
 22. Wang L, Fuster M, Sriramarao P, Esko JD. Endothelial heparan sulfate deficiency impairs L-selectin- and chemokine-mediated neutrophil trafficking during inflammatory responses. *Nat Immunol* 2005;**6**:902–10.
 23. Yin X, Truty J, Lawrence R, Johns SC, Srinivasan RS, Handel TM, et al. A critical role for lymphatic endothelial heparan sulfate in lymph node metastasis. *Mol Cancer* 2010;**9**:316.
 24. Proudfoot AE, Handel TM, Johnson Z, Lau EK, LiWang P, Clark-Lewis I, et al. Glycosaminoglycan binding and oligomerization are essential for the in vivo activity of certain chemokines. *Proc Natl Acad Sci USA* 2003;**100**:1885–90.
 25. Rajarathnam K, Sykes BD, Kay CM, Dewald B, Geiser T, Baggiolini M, et al. Neutrophil activation by monomeric interleukin-8. *Science* 1994;**264**:90–2.
 26. Clark-Lewis I, Kim KS, Rajarathnam K, Gong JH, Dewald B, Moser B, et al. Structure-activity relationships of chemokines. *J Leukoc Biol* 1995;**57**:703–11.
 27. Zhang Y, Rollins BJ. A dominant negative inhibitor indicates that monocyte chemoattractant protein 1 functions as a dimer. *Mol Cell Biol* 1995;**15**:4851–5.
 28. Proudfoot AE, Power CA, Hoogewerf AJ, Montjovent MO, Borlat F, Offord RE, et al. Extension of recombinant human RANTES by the retention of the initiating methionine produces a potent antagonist. *J Biol Chem* 1996;**271**:2599–603.
 29. Jarnagin K, Grunberger D, Mulkins M, Wong B, Hemmerich S, Paavola C, et al. Identification of surface residues of the monocyte chemotactic protein 1 that affect signaling through the receptor CCR2. *Biochemistry* 1999;**38**:16167–77.
 30. Crump MP, Gong JH, Loetscher P, Rajarathnam K, Amara A, Arenzana-Seisdedos F, et al. Solution structure and basis for functional activity of stromal cell-derived factor-1; dissociation of CXCR4 activation from binding and inhibition of HIV-1. *EMBO J* 1997;**16**:6996–7007.
 31. Blain KY, Kwiatkowski W, Zhao Q, La Fleur D, Naik C, Chun TW, et al. Structural and functional characterization of CC chemokine CCL14. *Biochemistry* 2007;**46**:10008–15.
 32. Brandt E, Van Damme J, Flad HD. Neutrophils can generate their activator neutrophil-activating peptide 2 by proteolytic cleavage of platelet-derived connective tissue-activating peptide III. *Cytokine* 1991;**3**:311–21.
 33. Mack M, Luckow B, Nelson PJ, Cihak J, Simmons G, Clapham PR, et al. Amino-oxy-pentane-RANTES induces CCR5 internalization but inhibits recycling: a novel inhibitory mechanism of HIV infectivity. *J Exp Med* 1998;**187**:1215–24.
 34. Gaertner H, Cerini F, Escola JM, Kuenzi G, Melotti A, Offord R, et al. Highly potent, fully recombinant anti-HIV chemokines: reengineering a low-cost microbicide. *Proc Natl Acad Sci USA* 2008;**105**:17706–11.
 35. Veldkamp CT, Seibert C, Peterson FC, De la Cruz NB, Haugner 3rd JC, Basnet H, et al. Structural basis of CXCR4 sulfotyrosine recognition by the chemokine SDF-1/CXCL12. *Sci Signal* 2008;**1**:ra4.
 36. Blanpain C, Doranz BJ, Bondue A, Govaerts C, De Leener A, Vassart G, et al. The core domain of chemokines binds CCR5 extracellular domains while their amino terminus interacts with the transmembrane helix bundle. *J Biol Chem* 2003;**278**:5179–87.
 37. Kofuku Y, Yoshiura C, Ueda T, Terasawa H, Hirai T, Tominaga S, et al. Structural basis of the interaction between chemokine stromal cell-derived factor-1/CXCL12 and its G-protein-coupled receptor CXCR4. *J Biol Chem* 2009;**284**:35240–50.

-
38. Kuzsak AJ, Pitchiaya S, Anand JP, Mosberg HI, Walter NG, Sunahara RK. Purification and functional reconstitution of monomeric mu-opioid receptors: allosteric modulation of agonist binding by Gi2. *J Biol Chem* 2009;**284**:26732–41.
 39. Whorton MR, Bokoch MP, Rasmussen SG, Huang B, Zare RN, Kobilka B, et al. A monomeric G protein-coupled receptor isolated in a high-density lipoprotein particle efficiently activates its G protein. *Proc Natl Acad Sci USA* 2007;**104**:7682–7.
 40. Whorton MR, Jastrzebska B, Park PS, Fotiadis D, Engel A, Palczewski K, et al. Efficient coupling of transducin to monomeric rhodopsin in a phospholipid bilayer. *J Biol Chem* 2008;**283**:4387–94.
 41. Bayburt TH, Vishnivetskiy SA, McLean MA, Morizumi T, Huang CC, Tesmer JJ, et al. Monomeric rhodopsin is sufficient for normal rhodopsin kinase (GRK1) phosphorylation and arrestin-1 binding. *J Biol Chem* 2011;**286**:1420–8.
 42. Rodriguez-Frade JM, Vila-Coro AJ, de Ana AM, Albar JP, Martinez AC, Mellado M. The chemokine monocyte chemoattractant protein-1 induces functional responses through dimerization of its receptor CCR2. *Proc Natl Acad Sci USA* 1999;**96**:3628–33.
 43. Mellado M, Rodriguez-Frade JM, Vila-Coro AJ, de Ana AM, Martinez AC. Chemokine control of HIV-1 infection. *Nature* 1999;**400**:723–4.
 44. Mellado M, Rodriguez-Frade JM, Vila-Coro AJ, Fernandez S, Martin de Ana A, Jones DR, et al. Chemokine receptor homo- or heterodimerization activates distinct signaling pathways. *EMBO J* 2001;**20**:2497–507.
 45. Percherancier Y, Berchiche YA, Slight I, Volkmer-Engert R, Tamamura H, Fujii N, et al. Bioluminescence resonance energy transfer reveals ligand-induced conformational changes in CXCR4 homo- and heterodimers. *J Biol Chem* 2005;**280**:9895–903.
 46. Berchiche YA, Gravel S, Pelletier ME, St-Onge G, Heveker N. Different effects of the different natural CC chemokine receptor 2b ligands on beta-arrestin recruitment, G α signaling, and receptor internalization. *Mol Pharmacol* 2011;**79**:488–98.
 47. El-Asmar L, Springael JY, Ballet S, Andrieu EU, Vassart G, Parmentier M. Evidence for negative binding cooperativity within CCR5-CCR2b heterodimers. *Mol Pharmacol* 2005;**67**:460–9.
 48. Springael JY, Le Minh PN, Urizar E, Costagliola S, Vassart G, Parmentier M. Allosteric modulation of binding properties between units of chemokine receptor homo- and hetero-oligomers. *Mol Pharmacol* 2006;**69**:1652–61.
 49. Sohy D, Yano H, de Nadai P, Urizar E, Guillabert A, Javitch JA, et al. Hetero-oligomerization of CCR2, CCR5, and CXCR4 and the protean effects of “selective” antagonists. *J Biol Chem* 2009;**284**:31270–9.
 50. Benkirane M, Jin DY, Chun RF, Koup RA, Jeang KT. Mechanism of transdominant inhibition of CCR5-mediated HIV-1 infection by ccr5delta32. *J Biol Chem* 1997;**272**:30603–6.
 51. Vila-Coro AJ, Mellado M, Martin de Ana A, Lucas P, del Real G, Martinez AC, et al. HIV-1 infection through the CCR5 receptor is blocked by receptor dimerization. *Proc Natl Acad Sci USA* 2000;**97**:3388–93.
 52. Rodriguez-Frade JM, Vila-Coro AJ, Martin A, Nieto M, Sanchez-Madrid F, Proudfoot AE, et al. Similarities and differences in RANTES- and (AOP)-RANTES-triggered signals: implications for chemotaxis. *J Cell Biol* 1999;**144**:755–65.
 53. Chelli M, Alizon M. Determinants of the trans-dominant negative effect of truncated forms of the CCR5 chemokine receptor. *J Biol Chem* 2001;**276**:46975–82.
 54. Blanpain C, Vanderwinden JM, Cihak J, Wittamer V, Le Poul E, Issafras H, et al. Multiple active states and oligomerization of CCR5 revealed by functional properties of monoclonal antibodies. *Mol Biol Cell* 2002;**13**:723–37.
 55. Issafras H, Angers S, Bulenger S, Blanpain C, Parmentier M, Labbe-Jullie C, et al. Constitutive agonist-independent CCR5 oligomerization and antibody-mediated clustering occurring at physiological levels of receptors. *J Biol Chem* 2002;**277**:34666–73.

-
56. Contento RL, Molon B, Boularan C, Pozzan T, Manes S, Marullo S, et al. CXCR4-CCR5: a couple modulating T cell functions. *Proc Natl Acad Sci USA* 2008;**105**:10101–6.
 57. Chelli M, Alizon M. Rescue of HIV-1 receptor function through cooperation between different forms of the CCR5 chemokine receptor. *J Biol Chem* 2002;**277**:39388–96.
 58. Hernanz-Falcon P, Rodriguez-Frade JM, Serrano A, Juan D, del Sol A, Soriano SF, et al. Identification of amino acid residues crucial for chemokine receptor dimerization. *Nat Immunol* 2004;**5**:216–23.
 59. Lemay J, Marullo S, Jockers R, Alizon M, Brelot A. On the dimerization of CCR5. *Nat Immunol* 2005;**6**:535 Author reply 535–536.
 60. Huttenrauch F, Pollok-Kopp B, Oppermann M. G protein-coupled receptor kinases promote phosphorylation and beta-arrestin-mediated internalization of CCR5 homo- and hetero-oligomers. *J Biol Chem* 2005;**280**:37503–15.
 61. Hammad MM, Kuang YQ, Yan R, Allen H, Dupre DJ. Na⁺/H⁺ exchanger regulatory factor-1 is involved in chemokine receptor homodimer CCR5 internalization and signal transduction but does not affect CXCR4 homodimer or CXCR4-CCR5 heterodimer. *J Biol Chem* 2010;**285**:34653–64.
 62. Charette N, Holland P, Frazer J, Allen H, Dupre DJ. Dependence on different Rab GTPases for the trafficking of CXCR4 and CCR5 homo or heterodimers between the endoplasmic reticulum and plasma membrane in Jurkat cells. *Cell Signal* 2011;**23**:1738–49.
 63. Kuang YQ, Charette N, Frazer J, Holland PJ, Attwood KM, Delleire G, et al. Dopamine receptor-interacting protein 78 acts as a molecular chaperone for CCR5 chemokine receptor signaling complex organization. *PLoS One* 2012;**7**:e40522.
 64. Wilson S, Wilkinson G, Milligan G. The CXCR1 and CXCR2 receptors form constitutive homo- and heterodimers selectively and with equal apparent affinities. *J Biol Chem* 2005;**280**:28663–74.
 65. Martinez Munoz L, Lucas P, Navarro G, Checa AI, Franco R, Martinez AC, et al. Dynamic regulation of CXCR1 and CXCR2 homo- and heterodimers. *J Immunol* 2009;**183**:7337–46.
 66. Trettel F, Di Bartolomeo S, Lauro C, Catalano M, Ciotti MT, Limatola C. Ligand-independent CXCR2 dimerization. *J Biol Chem* 2003;**278**:40980–8.
 67. Limatola C, Di Bartolomeo S, Catalano M, Trettel F, Fucile S, Castellani L, et al. Cysteine residues are critical for chemokine receptor CXCR2 functional properties. *Exp Cell Res* 2005;**307**:65–75.
 68. Vila-Coro AJ, Rodriguez-Frade JM, Martin De Ana A, Moreno-Ortiz MC, Martinez AC, Mellado M. The chemokine SDF-1alpha triggers CXCR4 receptor dimerization and activates the JAK/STAT pathway. *FASEB J* 1999;**13**:1699–710.
 69. Babcock GJ, Farzan M, Sodroski J. Ligand-independent dimerization of CXCR4, a principal HIV-1 coreceptor. *J Biol Chem* 2003;**278**:3378–85.
 70. Hamdan FF, Percherancier Y, Breton B, Bouvier M. Monitoring protein-protein interactions in living cells by bioluminescence resonance energy transfer (BRET). *Curr Protoc Neurosci* 2006; Chapter 5, Unit 5 23.
 71. Lagane B, Chow KY, Balabanian K, Levoye A, Harriague J, Planchenault T, et al. CXCR4 dimerization and beta-arrestin-mediated signaling account for the enhanced chemotaxis to CXCL12 in WHIM syndrome. *Blood* 2008;**112**:34–44.
 72. Tanaka T, Nomura W, Narumi T, Masuda A, Tamamura H. Bivalent ligands of CXCR4 with rigid linkers for elucidation of the dimerization state in cells. *J Am Chem Soc* 2010;**132**:15899–901.
 73. Choi WT, Kumar S, Madani N, Han X, Tian S, Dong CZ, et al. A novel synthetic bivalent ligand to probe chemokine receptor CXCR4 dimerization and inhibit HIV-1 entry. *Biochemistry* 2012;**51**:7078–86.

-
74. Toth PT, Ren D, Miller RJ. Regulation of CXCR4 receptor dimerization by the chemokine SDF-1alpha and the HIV-1 coat protein gp120: a fluorescence resonance energy transfer (FRET) study. *J Pharmacol Exp Ther* 2004;**310**:8–17.
 75. Wang J, He L, Combs CA, Roderiquez G, Norcross MA. Dimerization of CXCR4 in living malignant cells: control of cell migration by a synthetic peptide that reduces homologous CXCR4 interactions. *Mol Cancer Ther* 2006;**5**:2474–83.
 76. Hamatake M, Aoki T, Futahashi Y, Urano E, Yamamoto N, Komano J. Ligand-independent higher-order multimerization of CXCR4, a G-protein-coupled chemokine receptor involved in targeted metastasis. *Cancer Sci* 2009;**100**:95–102.
 77. Luker KE, Gupta M, Luker GD. Imaging chemokine receptor dimerization with firefly luciferase complementation. *FASEB J* 2009;**23**:823–34.
 78. Levoye A, Balabamian K, Baleux F, Bachelerie F, Lagane B. CXCR7 heterodimerizes with CXCR4 and regulates CXCL12-mediated G protein signaling. *Blood* 2009;**113**:6085–93.
 79. Zhukovsky MA, Basmaciogullari S, Pacheco B, Wang L, Madani N, Haim H, et al. Thermal stability of the human immunodeficiency virus type 1 (HIV-1) receptors, CD4 and CXCR4, reconstituted in proteoliposomes. *PLoS One* 2010;**5**:e13249.
 80. Wu B, Chien EY, Mol CD, Fenalti G, Liu W, Katritch V, et al. Structures of the CXCR4 chemokine GPCR with small-molecule and cyclic peptide antagonists. *Science* 2010;**330**:1066–71.
 81. Rodriguez D, Gutierrez-de-Teran H. Characterization of the homodimerization interface and functional hotspots of the CXCR4 chemokine receptor. *Proteins* 2012;**80**:1919–28.
 82. Asano S, Kitatani K, Taniguchi M, Hashimoto M, Zama K, Mitsutake S, et al. Regulation of cell migration by sphingomyelin synthases: sphingomyelin in lipid rafts decreases responsiveness to signaling by the CXCL12/CXCR4 pathway. *Mol Cell Biol* 2012;**32**:3242–52.
 83. Chakera A, Seeber RM, John AE, Eidne KA, Greaves DR. The duffy antigen/receptor for chemokines exists in an oligomeric form in living cells and functionally antagonizes CCR5 signaling through hetero-oligomerization. *Mol Pharmacol* 2008;**73**:1362–70.
 84. Gouldson PR, Dean MK, Snell CR, Bywater RP, Gkoutos G, Reynolds CA. Lipid-facing correlated mutations and dimerization in G-protein coupled receptors. *Protein Eng* 2001;**14**:759–67.
 85. Rodriguez-Frade JM, del Real G, Serrano A, Hernanz-Falcon P, Soriano SF, Vila-Coro AJ, et al. Blocking HIV-1 infection via CCR5 and CXCR4 receptors by acting in trans on the CCR2 chemokine receptor. *EMBO J* 2004;**23**:66–76.
 86. Vazquez-Salat N, Yuhki N, Beck T, O'Brien SJ, Murphy WJ. Gene conversion between mammalian CCR2 and CCR5 chemokine receptor genes: a potential mechanism for receptor dimerization. *Genomics* 2007;**90**:213–24.
 87. See HB, Seeber RM, Kocan M, Eidne KA, Pflieger KD. Application of G protein-coupled receptor-heteromer identification technology to monitor beta-arrestin recruitment to G protein-coupled receptor heteromers. *Assay Drug Dev Technol* 2011;**9**:21–30.
 88. Sohy D, Parmentier M, Springael JY. Allosteric transinhibition by specific antagonists in CCR2/CXCR4 heterodimers. *J Biol Chem* 2007;**282**:30062–9.
 89. Isik N, Hereld D, Jin T. Fluorescence resonance energy transfer imaging reveals that chemokine-binding modulates heterodimers of CXCR4 and CCR5 receptors. *PLoS One* 2008;**3**:e3424.
 90. Wang J, Alvarez R, Roderiquez G, Guan E, Norcross MA. Constitutive association of cell surface CCR5 and CXCR4 in the presence of CD4. *J Cell Biochem* 2004;**93**:753–60.
 91. Sierro F, Biben C, Martinez-Munoz L, Mellado M, Ransohoff RM, Li M, et al. Disrupted cardiac development but normal hematopoiesis in mice deficient in the second CXCL12/SDF-1 receptor, CXCR7. *Proc Natl Acad Sci USA* 2007;**104**:14759–64.

-
92. Decaillot FM, Kazmi MA, Lin Y, Ray-Saha S, Sakmar TP, Sachdev P. CXCR7/CXCR4 heterodimer constitutively recruits beta-arrestin to enhance cell migration. *J Biol Chem* 2011;**286**:32188–97.
 93. Mustafa S, See HB, Seeber RM, Armstrong SP, White CW, Ventura S, et al. Identification and profiling of novel alpha1A-adrenoceptor-CXC chemokine receptor 2 heteromer. *J Biol Chem* 2012;**287**:12952–65.
 94. Suzuki S, Chuang LF, Yau P, Doi RH, Chuang RY. Interactions of opioid and chemokine receptors: oligomerization of mu, kappa, and delta with CCR5 on immune cells. *Exp Cell Res* 2002;**280**:192–200.
 95. Chen C, Li J, Bot G, Szabo I, Rogers TJ, Liu-Chen LY. Heterodimerization and cross-desensitization between the mu-opioid receptor and the chemokine CCR5 receptor. *Eur J Pharmacol* 2004;**483**:175–86.
 96. Yuan Y, Arnatt CK, Li G, Haney KM, Ding D, Jacob JC, et al. Design and synthesis of a bivalent ligand to explore the putative heterodimerization of the mu opioid receptor and the chemokine receptor CCR5. *Org Biomol Chem* 2012;**10**:2633–46.
 97. Catalano M, Trettel F, Cipriani R, Lauro C, Sobrero F, Eusebi F, et al. Chemokine CXCL8 modulates GluR1 phosphorylation. *J Neuroimmunol* 2008;**198**:75–81.
 98. Parenty G, Appelbe S, Milligan G. CXCR2 chemokine receptor antagonism enhances DOP opioid receptor function via allosteric regulation of the CXCR2-DOP receptor heterodimer. *Biochem J* 2008;**412**:245–56.
 99. Pello OM, Martinez-Munoz L, Parrillas V, Serrano A, Rodriguez-Frade JM, Toro MJ, et al. Ligand stabilization of CXCR4/delta-opioid receptor heterodimers reveals a mechanism for immune response regulation. *Eur J Immunol* 2008;**38**:537–49.
 100. Vischer HF, Nijmeijer S, Smit MJ, Leurs R. Viral hijacking of human receptors through heterodimerization. *Biochem Biophys Res Commun* 2008;**377**:93–7.
 101. Nijmeijer S, Leurs R, Smit MJ, Vischer HF. The Epstein-Barr virus-encoded G protein-coupled receptor BILF1 hetero-oligomerizes with human CXCR4, scavenges Galphai proteins, and constitutively impairs CXCR4 functioning. *J Biol Chem* 2010;**285**:29632–41.
 102. Barroso R, Martinez Munoz L, Barrondo S, Vega B, Holgado BL, Lucas P, et al. EBI2 regulates CXCL13-mediated responses by heterodimerization with CXCR5. *FASEB J* 2012;**26**:4841–54.
 103. Kumar A, Humphreys TD, Kremer KN, Bramati PS, Bradfield L, Edgar CE, et al. CXCR4 physically associates with the T cell receptor to signal in T cells. *Immunity* 2006;**25**:213–24.
 104. Xiao X, Wu L, Stantchev TS, Feng YR, Ugolini S, Chen H, et al. Constitutive cell surface association between CD4 and CCR5. *Proc Natl Acad Sci USA* 1999;**96**:7496–501.
 105. Singer II, Scott S, Kawka DW, Chin J, Daugherty BL, DeMartino JA, et al. CCR5, CXCR4, and CD4 are clustered and closely apposed on microvilli of human macrophages and T cells. *J Virol* 2001;**75**:3779–90.
 106. Doumazane E, Scholler P, Zwier JM, Trinquet E, Rondard P, Pin JP. A new approach to analyze cell surface protein complexes reveals specific heterodimeric metabotropic glutamate receptors. *FASEB J* 2011;**25**:66–77.
 107. Vischer HF, Watts AO, Nijmeijer S, Leurs R. G protein-coupled receptors: walking hand-in-hand, talking hand-in-hand? *Br J Pharmacol* 2011;**163**:246–60.
 108. Kufareva I, Stephens B, Gilliland CT, Wu B, Fenalti G, Hamel D, et al. Novel approach to quantify GPCR dimerization equilibrium using bioluminescence resonance energy transfer. *Methods Mol Biol* 2012. In press.
 109. Hern JA, Baig AH, Mashanov GI, Birdsall B, Corrie JE, Lazareno S, et al. Formation and dissociation of M1 muscarinic receptor dimers seen by total internal reflection fluorescence imaging of single molecules. *Proc Natl Acad Sci USA* 2010;**107**:2693–8.

-
110. Milligan G. G protein-coupled receptor hetero-dimerization: contribution to pharmacology and function. *Br J Pharmacol* 2009;**158**:5–14.
 111. Jones KA, Borowsky B, Tamm JA, Craig DA, Durkin MM, Dai M, et al. GABA(B) receptors function as a heteromeric assembly of the subunits GABA(B)R1 and GABA(B)R2. *Nature* 1998;**396**:674–9.
 112. White JH, Wise A, Main MJ, Green A, Fraser NJ, Disney GH, et al. Heterodimerization is required for the formation of a functional GABA(B) receptor. *Nature* 1998;**396**:679–82.
 113. Drury LJ, Ziarek JJ, Gravel S, Veldkamp CT, Takekoshi T, Hwang ST, et al. Monomeric and dimeric CXCL12 inhibit metastasis through distinct CXCR4 interactions and signaling pathways. *Proc Natl Acad Sci USA* 2011;**108**:17655–60.
 114. Milligan G, Wilson S, Lopez-Gimenez JF. The specificity and molecular basis of alpha1-adrenoceptor and CXCR chemokine receptor dimerization. *J Mol Neurosci* 2005;**26**:161–8.
 115. Tarasova NI, Rice WG, Michejda CJ. Inhibition of G-protein-coupled receptor function by disruption of transmembrane domain interactions. *J Biol Chem* 1999;**274**:34911–5.
 116. Chabre M, Deterre P, Antonny B. The apparent cooperativity of some GPCRs does not necessarily imply dimerization. *Trends Pharmacol Sci* 2009;**30**:182–7.
 117. Birdsall NJ. Class A GPCR heterodimers: evidence from binding studies. *Trends Pharmacol Sci* 2010;**31**:499–508.
 118. Molon B, Gri G, Bettella M, Gomez-Mouton C, Lanzavecchia A, Martinez AC, et al. T cell costimulation by chemokine receptors. *Nat Immunol* 2005;**6**:465–71.
 119. Pruenster M, Rot A. Throwing light on DARC. *Biochem Soc Trans* 2006;**34**:1005–8.
 120. Zabel BA, Wang Y, Lewen S, Berahovich RD, Penfold ME, Zhang P, et al. Elucidation of CXCR7-mediated signaling events and inhibition of CXCR4-mediated tumor cell transendothelial migration by CXCR7 ligands. *J Immunol* 2009;**183**:3204–11.
 121. Luker KE, Lewin SA, Mihalko LA, Schmidt BT, Winkler JS, Coggins NL, et al. Scavenging of CXCL12 by CXCR7 promotes tumor growth and metastasis of CXCR4-positive breast cancer cells. *Oncogene* 2012;**45**:4750–8.
 122. Maussang D, Vischer HF, Schreiber A, Michel D, Smit MJ. Pharmacological and biochemical characterization of human cytomegalovirus-encoded G protein-coupled receptors. *Methods Enzymol* 2009;**460**:151–71.
 123. Slinger E, Langemeijer E, Siderius M, Vischer HF, Smit MJ. Herpesvirus-encoded GPCRs rewire cellular signaling. *Mol Cell Endocrinol* 2011;**331**:179–84.
 124. Hsu JL, Glaser SL. Epstein-barr virus-associated malignancies: epidemiologic patterns and etiologic implications. *Crit Rev Oncol Hematol* 2000;**34**:27–53.
 125. Miyagi T, Chuang LF, Lam KM, Kung H, Wang JM, Osburn BI, et al. Opioids suppress chemokine-mediated migration of monkey neutrophils and monocytes - an instant response. *Immunopharmacology* 2000;**47**:53–62.
 126. Kohout TA, Nicholas SL, Perry SJ, Reinhart G, Junger S, Struthers RS. Differential desensitization, receptor phosphorylation, beta-arrestin recruitment, and ERK1/2 activation by the two endogenous ligands for the CC chemokine receptor 7. *J Biol Chem* 2004;**279**:23214–22.
 127. Baltus T, Weber KS, Johnson Z, Proudfoot AE, Weber C. Oligomerization of RANTES is required for CCR1-mediated arrest but not CCR5-mediated transmigration of leukocytes on inflamed endothelium. *Blood* 2003;**102**:1985–8.
 128. Vinet J, van Zwam M, Dijkstra IM, Brouwer N, van Weering HR, Watts A, et al. Inhibition of CXCR3-mediated chemotaxis by the human chemokine receptor-like protein CCX-CKR. *Br J Pharmacol* 2012. Epub ahead of print.
 129. Watts AO, van Lipzig MM, Jaeger WC, Seeber RM, van Zwam M, Vinet J, et al. Identification and profiling of CXCR3-CXCR4 chemokine receptor heteromer complexes. *Br J Pharmacol* 2012. Epub ahead of print.

Acknowledgement

Chapter two, in full, is a reprint of a published review article as it appears in Progress in Molecular Biology and Translational Science. (**Stephens, B.** and T. M. Handel (2013). "Chemokine receptor oligomerization and allostery." Prog Mol Biol Transl Sci **115**: 375-420.) The dissertation author was the primary author of this material.

Chapter 3

Stoichiometry and geometry of the CXC chemokine receptor 4 complex with CXC ligand 12: molecular modeling and experimental validation.



Stoichiometry and geometry of the CXC chemokine receptor 4 complex with CXC ligand 12: Molecular modeling and experimental validation

Irina Kufareva^{1,2}, Bryan S. Stephens¹, Lauren G. Holden¹, Ling Qin, Chunxia Zhao, Tetsuya Kawamura, Ruben Abagyan, and Tracy M. Handel²

Skaggs School of Pharmacy and Pharmaceutical Sciences, University of California, San Diego, La Jolla, CA 92093

Edited by K. Christopher Garcia, Stanford University, Stanford, CA, and approved November 13, 2014 (received for review September 3, 2014)

Chemokines and their receptors regulate cell migration during development, immune system function, and in inflammatory diseases, making them important therapeutic targets. Nevertheless, the structural basis of receptor:chemokine interaction is poorly understood. Adding to the complexity of the problem is the persistently dimeric behavior of receptors observed in cell-based studies, which in combination with structural and mutagenesis data, suggest several possibilities for receptor:chemokine complex stoichiometry. In this study, a combination of computational, functional, and biophysical approaches was used to elucidate the stoichiometry and geometry of the interaction between the CXC-type chemokine receptor 4 (CXCR4) and its ligand CXCL12. First, relevance and feasibility of a 2:1 stoichiometry hypothesis was probed using functional complementation experiments with multiple pairs of complementary nonfunctional CXCR4 mutants. Next, the importance of dimers of WT CXCR4 was explored using the strategy of dimer dilution, where WT receptor dimerization is disrupted by increasing expression of nonfunctional CXCR4 mutants. The results of these experiments were supportive of a 1:1 stoichiometry, although the latter could not simultaneously reconcile existing structural and mutagenesis data. To resolve the contradiction, cysteine trapping experiments were used to derive residue proximity constraints that enabled construction of a validated 1:1 receptor:chemokine model, consistent with the paradigmatic two-site hypothesis of receptor activation. The observation of a 1:1 stoichiometry is in line with accumulating evidence supporting monomers as minimal functional units of G protein-coupled receptors, and suggests transmission of conformational changes across the dimer interface as the most probable mechanism of altered signaling by receptor heterodimers.

chemokine receptor | GPCR dimerization | molecular docking | functional complementation | cysteine trapping

The chemokine receptor CXCR4 regulates cell migration during many developmental processes (1, 2). Along with CCR5, it serves as one of the principal coreceptors for HIV entry into leukocytes (3), and is one of the most important chemokine receptors involved in cancer metastasis (4). Stromal-cell derived factor 1 (SDF-1 or CXCL12) was its only known ligand until recently, when CXCR4 was also shown to bind CXCL14 (5) and extracellular ubiquitin (6). Although structures of CXCR4 (7) and CCR5 (8) have been solved with synthetic antagonists, the structural basis for the interaction of CXCR4 (or any other chemokine receptor) with their natural ligands has yet to be determined. Numerous mutagenesis and NMR studies indicate that receptor:chemokine interactions involve two distinct sites (9–12), which has led to a two-site hypothesis of receptor activation (13). The so-called chemokine recognition site 1 (CRS1) (14) includes the N terminus of the receptor interacting with the globular core of the chemokine, whereas chemokine recognition site 2 (CRS2), located within the transmembrane (TM) domain pocket of the receptor, accommodates the flexible N terminus of

the chemokine. Mutations in CRS1 typically reduce the binding affinity of the chemokine, whereas CRS2 is critical not only for binding but also for chemokine-induced activation (9, 10, 12, 15–20). Similarly, mutations to the core domain of the chemokine generally affect receptor-binding affinity, but truncations or modifications of as little as one amino acid in the N-terminal “signaling” domain frequently alter both ligand binding and pharmacology.

The two-site model has been envisioned in the context of a monomeric receptor. However, like many other G protein-coupled receptors (GPCRs) (21), CXCR4 has been shown to dimerize in cell membranes. Evidence supporting CXCR4 dimerization includes immunoprecipitation (22), bioluminescence and fluorescence resonance energy transfer [BRET (23) and FRET (24), respectively], fluorescence and luminescence complementation assays (25), and bivalent ligands (26). Dimerization of a WT CXCR4 with a C-terminally truncated mutant causing the “warts, hypogammaglobulinemia, infections and myelokathexis” (WHIM) syndrome has been implicated in its resistance to desensitization and enhanced signaling in heterozygous WHIM patients (27). CXCR4 has also been shown to heterodimerize with other chemokine receptors and with GPCRs outside the chemokine family (28–32), with consequences including transinhibition of ligand binding (28) and changes in G protein and β -arrestin coupling

Significance

The chemokine receptor axis plays a critical role in numerous physiological and pathological processes, yet the structural basis of receptor interaction with chemokines is poorly understood. Although the community agrees on the existence of two distinct epitopes for recognition of receptors by chemokines, conflicting evidence from structural and mutagenesis studies suggested several possibilities for receptor:chemokine complex stoichiometry. We use a combination of computational, functional, and biophysical approaches to show that despite its dimeric nature, chemokine receptor CXCR4 interacts with its chemokine ligand, CXCL12, in a 1:1 stoichiometry. This result is also likely relevant for other receptor:chemokine pairs. Structural modeling informed by restraints derived from cysteine trapping experiments enabled determination of the receptor:chemokine complex geometry at a medium resolution level.

Author contributions: I.K., B.S.S., L.G.H., R.A., and T.M.H. designed research; I.K., B.S.S., L.G.H., L.Q., and C.Z. performed research; T.K. contributed new reagents/analytic tools; I.K., B.S.S., and L.G.H. analyzed data; and I.K., B.S.S., L.G.H., and T.M.H. wrote the paper.

The authors declare no conflict of interest.

This article is a PNAS Direct Submission.

¹I.K., B.S.S., and L.G.H. contributed equally to this work.

²To whom correspondence may be addressed. Email: ikufareva@ucsd.edu or thandel@ucsd.edu

This article contains supporting information online at www.pnas.org/lookup/suppl/doi:10.1073/pnas.1417037111/-/DCSupplemental.

(30, 33, 34). These observations establish the dimeric nature of CXCR4; however, the functional role of CXCR4 dimers has yet to be elucidated.

In agreement with its persistently dimeric behavior, CXCR4 formed structurally similar parallel dimers in five crystal structures (7), despite being solved in different space groups and with different synthetic ligands. The cell-based and structure-based observations of CXCR4 dimers raised the key question as to whether CXCL12 binds to a single receptor subunit or to both subunits of the dimer, in a manner consistent with the two-site model. Several possible stoichiometries of the complex were suggested (7, 35, 36); among them, a 1:1 receptor:chemokine stoichiometry, a 2:1 stoichiometry with one chemokine molecule simultaneously binding to both subunits of a CXCR4 dimer, and a 2:2 stoichiometry with a chemokine dimer binding to the CXCR4 dimer. With respect to the latter, although CXCL12 dimers bind and act as partial agonists of CXCR4 (37), full agonist signaling requires a monomeric chemokine (37, 38). Con-

sequently, the distinction between a 1:1 and a 2:1 receptor:chemokine stoichiometry is the most relevant question, and constituted the focus of the present study.

Our initial molecular modeling efforts encompassed the available structural information in the form of (i) the NMR structure of a cross-linked CXCL12 dimer in complex with an N-terminal peptide of CXCR4 (residues M1-K38) (39), and (ii) the X-ray structures of full-length CXCR4 (7). The former structure contains components of the CRS1 interaction (Fig. 1*A*), whereas the latter contains the receptor side of the CRS2 interaction. Although the crystallization constructs used in the CXCR4 X-ray study contained the intact N terminus of the receptor, only residues P27–S19 could be detected in the electron density; thus, the overlap between the NMR and X-ray structures was limited to residues P27–K38. Modeling demonstrated that a 2:1 receptor:chemokine model with decoupled CRS1 and CRS2 best accommodated the structural and mutagenesis data. In this model, the globular core of the chemokine interacts with the CRS1

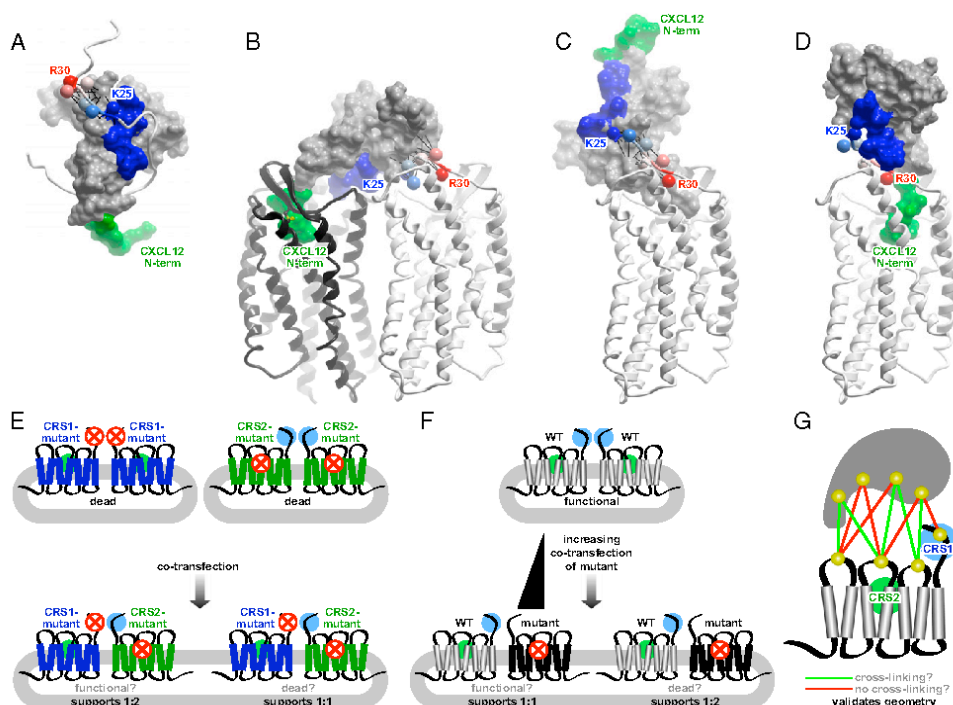


Fig. 1. Molecular models and experimental designs used in the present study. (*A*) NMR structure of CXCL12 (skin mesh) in complex with the N terminus of CXCR4 (residues M1–K38, ribbon) (39). Chemokine N terminus (green) and N-loop (blue) correspond to the expected interactions in CRS2 and CRS1, respectively. Receptor residues K25–R30 are shown as spheres, labeled, and colored in order from blue to red. CRS1 residue proximities observed in the NMR structure and maintained throughout the docking simulations include the interaction of CXCR4 K25 (blue sphere) with CXCL12 S16, while the subsequent receptor residues up to R30 (red sphere) are directed away from the chemokine N-loop (blue surface) toward the chemokine C-terminal helix; these proximities are shown as thin black lines. (*B*) A hybrid 2:1 model of the receptor:chemokine interaction accommodates both NMR proximity restraints (black lines) and the mutagenesis data. (*C*) A hybrid 1:1 model that accommodates NMR proximity restraints (black lines) is inconsistent with mutagenesis and with the two-site interaction hypothesis, because the N terminus of the chemokine invariably points away from the receptor CRS2. (*D*) A 1:1 model consistent with the two-site interaction hypothesis contradicts NMR proximity restraints, as receptor residues K25–R30 are directed along the chemokine N-loop toward its N terminus. (*E–G*) Conceptual designs of the functional complementation (*E*), dimer dilution (*F*), and cysteine trapping (*G*) experiments used in this study to probe the receptor:chemokine stoichiometry and geometry hypotheses.

of one receptor subunit and the N-terminal residues of the chemokine reach into CRS2 of its dimeric partner (Fig. 1*B*). In addition to being spatially consistent, this model provides a direct explanation for the negative cooperativity in chemokine binding that is frequently observed with receptor heterodimers (28, 40), and with the notion that CXCL12 triggers CXCR4 dimerization (41), stabilizes preformed dimers (42), or induces conformational changes within the dimers (23). The model is also consistent with the original two-site hypothesis of receptor activation. On the other hand, a 1:1 model, in which CXCL12 interacts with CRS1 and CRS2 of the same receptor subunit, required significant deviations from the CRS1 component of the CXCR4: CXCL12 interaction suggested by the NMR structure (39) to orient the CXCL12 N-terminal signaling domain toward the receptor binding pocket (Fig. 1*C* and *D*).

Three strategies were devised to elucidate the stoichiometry of the receptor:chemokine interaction. The first approach was based on functional complementation and designed to specifically probe the relevance of the 2:1 hypothesis. Functional complementation provides one of the strongest arguments for the existence and physiological role of GPCR dimers. In this type of experiment, different aspects of receptor function are restored by coexpression of two mutants of the receptor in question, each of which is incapable of producing the functional response when expressed alone (Fig. 1*E*). Functional rescue through dimerization has been demonstrated for several GPCRs. For example, domain swapping of histamine H1 receptor dimers reconstituted functional receptors from nonfunctional mutant components (43), and a related mechanism led to reconstitution of functional muscarinic and adrenergic receptors from receptor chimeras (44). Similarly, the binding site in the angiotensin II receptor was successfully reconstituted (45), and the function of the luteinizing hormone receptor was rescued by coexpression of two nonfunctional mutants (46). In the present study, the functional complementation strategy was used to probe the possibility of simultaneous interaction of CXCL12 with two CXCR4 monomers in the dimer.

Another strategy for exploring the role of dimers in general, and the stoichiometry of GPCR interactions with ligands and effectors in particular, is based on dimer dilution. In this approach, functional responses or binding events that are dependent on GPCR dimers are reduced or completely ablated by introducing increasing amounts of a mutant that is capable of dimerizing with the WT receptor but incapable of mediating the functional or binding response (Fig. 1*F*). The mutant receptors compete with WT receptors for dimer formation and lead to an increase in the surface density of WT/mutant dimers, with a simultaneous decrease in WT/WT dimers (47). In contrast, if dimers are unnecessary for the functional response or binding event, one should see no change with increasing concentration of mutant; thus, this approach distinguishes 1:1 vs. 2:1 interactions. There are important caveats associated with this strategy, as increasing expression of mutant receptors may interfere not only with formation of WT/WT dimers, but also with the expression of WT receptors because of expression competition. In this study, a modified dimer dilution strategy that addressed these problems was designed.

The above strategies are based on functional readouts and provide indirect evidence in favor of, or against, the different stoichiometries. We therefore complemented them by cysteine trapping studies, where pairs of cysteine mutations are introduced at different positions in the ligand and in the receptor, and spontaneous formation of disulfide bonds is monitored. These studies provide direct spatial proximity restraints that can be combined with modeling to determine the stoichiometry and geometry of the receptor:chemokine complex (Fig. 1*G*).

The results of all three complementary experimental strategies were supportive of a 1:1 and not a 2:1 receptor:chemokine stoichiometry. These results also informed further molecular

modeling efforts, which led to construction of an experimentally validated model of the CXCR4: CXCL12 complex. The model elucidates key features of the receptor:chemokine interaction and may facilitate further structure-function studies to understand the molecular basis for CXCR4: CXCL12 signaling.

Results

Structural Constraints Are Incompatible with Mutagenesis in the Context of a 1:1 CXCR4: CXCL12 Model. Using molecular modeling and chemical field-guided docking (48), we attempted reconstruction of the hybrid structure of the CXCR4: CXCL12 complex by simultaneously satisfying restraints from the X-ray structure of the CXCR4 TM domain (7) and the NMR structure of the CXCL12 dimer in complex with a CXCR4 N-terminal peptide (39) (Fig. 1*A*). The former set of restraints included the relative positioning of the CXCR4 TM helices, as well as a disulfide bond between the N-terminal cysteine (C28) of the receptor and its extracellular loop 3. The latter set involved harmonic distance restraints (thin black lines in Fig. 1*A-C*) imposed between the C β atoms in the least uncertain portion of the receptor N terminus in the NMR structure (residues K25–R30, shown as spheres in Fig. 1*A-D* and colored in order from blue to red) and the C α atoms of proximal chemokine residues F14–S16 (N-loop), I51–K56 (the loop connecting β_3 and the C-terminal helix), and I58–E60 (C-terminal helix). As observed in the NMR structure, these restraints included the interaction of the receptor residue K25 (blue sphere in Fig. 1*A-D*) with residue S16 in the chemokine N-loop (blue patch in Fig. 1*A-D*), whereas the subsequent receptor residues up to R30 (red sphere in Fig. 1*A-D*) were directed away from the N-loop and toward the chemokine C-terminal helix (Fig. 1*A*).

Docking simulations were carried out by explicit conformational sampling of CXCL12 and the N-terminal residues K25–R30 of CXCR4 in internal coordinates (49), with the remaining parts of the receptor represented by the potential grid maps (50). These simulations sought to optimize electrostatic, van der Waals, hydrogen bonding, and surface interactions within and between the two molecules while simultaneously satisfying the constraints from the existing structures. Despite allowing full flexibility in the N-terminal parts of both molecules, the simulations invariably resulted in models that were inconsistent with existing mutagenesis studies (9, 16, 18–20, 51–54) when undertaken in the context of the 1:1 stoichiometry hypothesis. Specifically, the N-terminal signaling domain of the chemokine was forced out of the receptor CRS2, separating the critical interacting residues by as much as 50 Å (Fig. 1*C*). In contrast, models built to test the 2:1 stoichiometry hypothesis appeared spatially compatible with the mutagenesis, as the N terminus of the chemokine could be freely directed into the CRS2 of one CXCR4 dimer partner when the core domain was bound to CRS1 of the other (Fig. 1*B*). Although coarse-grained and approximate, this modeling exercise raised the question of what the actual interaction stoichiometry is.

Design and Testing of a CXCR4-Free Cell Line for Functional Complementation Experiments. For the purpose of testing loss-of-function CXCR4 mutant pairs in the functional complementation experiments, it was essential to use a cell line devoid of endogenous CXCR4 expression. However, we discovered that many cells commonly used in chemokine functional assays endogenously express CXCR4 (Fig. S1*A-E* and Table S1) and mobilize calcium in response to CXCL12 (Fig. S1*F-I* and Table S1). Among the few immortalized cell lines that did not express endogenous CXCR4, only Chinese hamster ovary (CHO) cells displayed both a robust transfection efficiency and signaling response using Ca²⁺ mobilization as a readout (Fig. S1*E* and *J*). The latter was significantly improved when the cells were stably transfected with human G α_{15} protein (55) (Fig. S1*J-P*), which resulted in creation of a CHO-G α_{15} cell line.

Design, Surface Expression, and Function of CXCR4 Point Mutants in CHO-G α_{15} . CXCR4 mutants defective in chemokine binding and signaling were designed taking into account earlier mutagenesis studies (9, 16, 18–20, 51–54) and the residue contacts in the structural models of the complex. To disrupt CXCR4: CXCL12 interactions in CRS1, two mutants were generated: one with alanine substitutions in the positions of the three sulfotyrosines known to affect ligand binding (56) and signaling (57) (Y7A/Y12A/Y21A, further referred to as YYY), and another where I4 and I6 were also mutated to alanine (37) (I4A/I6A/Y7A/Y12A/Y21A, further referred to as IYYYY). To disrupt interactions in CRS2, the following mutations were introduced one at a time: D97N, D171A, D187A, and E288A (Fig. 2A). Mutants were cloned into multiple receptor constructs as described in *SI Text*.

It was expected that CRS1 mutations would impact CXCL12 binding affinity without affecting the maximal signaling capacity of the receptor, whereas CRS2 mutations would mainly disrupt signaling. Some of the CRS2 mutants have been shown to bind CXCL12 with affinities similar to the WT receptor; specifically, E288A and D187A bind CXCL12 with IC₅₀ values of 4.4 nM and 4.7 nM, respectively, compared with 2.2 nM for WT CXCR4 in a radioligand competition binding assay (19). Similarly, Wong et al. reported K_d values of 47.6 nM and 44.1 nM for D97N and E288A, respectively, compared with 35.8 nM for WT CXCR4 in competition binding assays (20).

Using flow cytometry experiments described in *SI Text*, we found that all mutants were expressed similarly to WT when transiently transfected in CHO-G α_{15} cells (Fig. 2B). The CRS1 YYY and IYYYY mutants were able to elicit a full Ca²⁺ mobilization response at high CXCL12 concentrations but had an ~10-fold lower EC₅₀ than WT CXCR4. Two of the CRS2 mutations, D171A and D187A, were significantly impaired in both EC₅₀ and maximal Ca²⁺ responses, whereas the remaining two, D97N and E288A, were completely signaling-dead (Fig. 2C). These mutants therefore seemed viable candidates for use in the functional complementation and dimer dilution experiments.

CXCR4 Mutants Dimerize with Each Other and with WT CXCR4. An important control for the functional complementation and dimer dilution experiments is that the mutants retain the ability to form dimers. BRET YFP titration experiments, which are commonly used to assess GPCR dimerization (58, 59), confirmed that none of the above mutations affected the oligomerization propensity of the receptor (Fig. 3). In these experiments, receptors C-terminally tagged with *Renilla* luciferase (Rluc) are expressed at a constant level, whereas expression of YFP-tagged receptors is increased. This results in a hyperbolic increase in BRET_{net} values if the interaction is specific; in contrast, a low linearly increasing signal is indicative of a nonspecific random interaction (60). The fluorescence/luminescence ratio at which the BRET_{net} value is half maximal (BRET₅₀) is an indicator of affinity, whereas the BRET_{max} value depends on the conformation of the interacting receptors as well as the distance between the YFP and Rluc molecules in the complex (58). Mutant/mutant and mutation/WT combinations used in functional complementation and dimer dilution experiments are shown in Fig. 3A and B, respectively. The BRET₅₀ values for the different combinations indicate that none of the mutations adversely affected receptor dimerization capacity.

Dimerization of mutant and WT receptors was also confirmed using coimmunoprecipitation (Fig. 3C). Following precipitation with anti-Flag affinity resin, bands indicating the presence of HA-tagged receptors were found in all samples coexpressing Flag-tagged WT and HA-tagged WT or mutant receptors, with the intensity of the bands correlating with the amount of transfected HA-tagged receptor. No coimmunoprecipitation was observed in the control sample where lysates of cells independently expressing the two types of receptors were mechanically mixed.

Mutant Functional Complementation Experiments Do Not Support 2:1 Model. Functional complementation experiments were designed to specifically test the 2:1 model of the CXCR4: CXCL12 interaction shown in Fig. 1B. In the model, the globular core of CXCL12 interacts with CRS1 of one CXCR4 subunit in a dimer, and the N terminus of CXCL12 interacts with CRS2 of the other

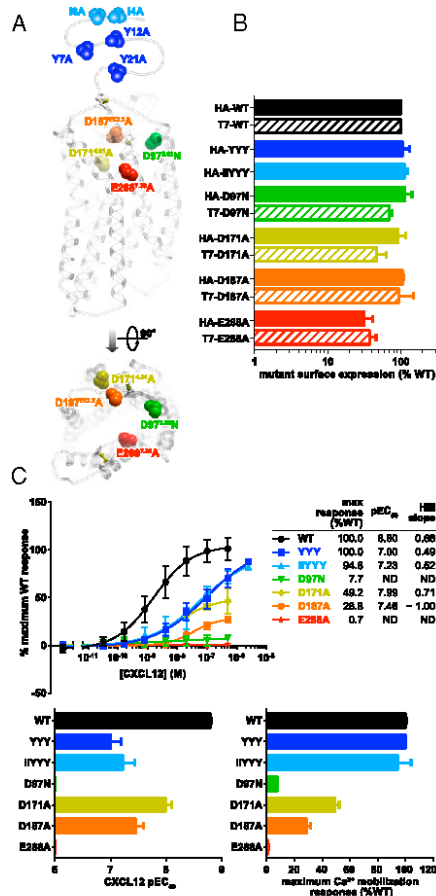


Fig. 2. CXCR4 mutants used in this study. (A) Location of mutated residues in the CXCR4 structure. Side view along the membrane plane and top view across the membrane plane from the extracellular side are shown. (B) Surface expression of mutants in HA-tagged and T7-tagged constructs when transiently expressed in CHO-G α_{15} cells as determined by flow cytometry analysis of anti-HA and anti-T7 antibody staining. Data are presented as percent of WT receptor expression and represents the average and SD of relative geometric mean fluorescence intensity in at least two independent experiments. (C) Mutant functionality measured as the ability of CHO-G α_{15} cells transiently transfected with the mutants to mobilize intracellular Ca²⁺ in response to stimulation with varying concentrations of CXCL12. Data are presented as percent maximal response elicited by the WT receptor and represents the average and SD of all replicates from at least two independent experiments.

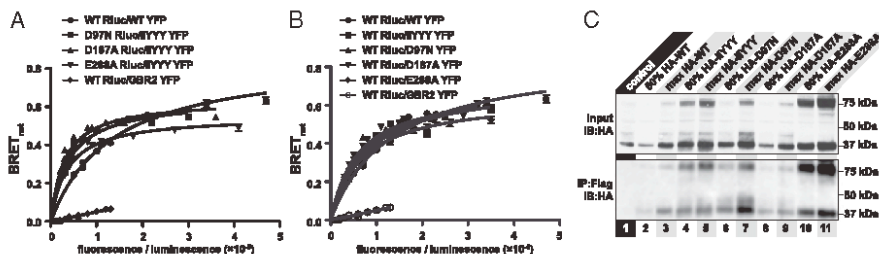


Fig. 3. CXCR4 mutants retain ability to dimerize with each other (A) and with WT receptor (B and C). In A and B, BRET saturation experiments were performed in HEK293T cells as described in *Materials and Methods*. The resulting BRET_{max} ratio is plotted against the fluorescence/luminescence ratio. The BRET pair WT CXCR4-Rluc with CXCR4-YFP was used as a positive control and WT CXCR4-Rluc and G8R2-YFP was used as a negative control for nonspecific BRET. Data are from three independent experiments. In C, HA-tagged mutant receptors were pulled down with Flag-tagged WT receptors using anti-Flag affinity resin when the receptors were coexpressed in HEK293T cells, but not when lysates of two cell populations independently expressing the receptors were mixed (control). The amount of coimmunoprecipitated mutant receptor correlated with the levels of transfection (maximum vs. 50% max HA-tagged mutant).

subunit. Therefore, these experiments were designed such that a binding-deficient CRS1 mutant was coexpressed with a non-functional CRS2 mutant. If the 2:1 hypothesis is correct, one would expect that coexpression would partially rescue the Ca²⁺ mobilization response to CXCL12 stimulation (Fig. 1E). However, no rescue response was observed with any of the CRS1/CRS2 mutant combinations tested (four representative combinations are shown in Fig. 4 A–D). As a control experiment, mutant coexpression was monitored by costaining the cells with antibodies conjugated to different fluorophores and specific to the two tags on the mutants; such coexpression was found efficient in all cases (Fig. 4 E–H). These data therefore suggest that the 2:1 receptor:chemokine hypothesis is incorrect, and that the CXCR4: CXCL12 stoichiometry is more likely 1:1.

Dimer Dilution Experiments Support the 1:1 Model. To confirm that the stoichiometry of the CXCR4: CXCL12 complex is 1:1, dimer dilution experiments were performed in which nonfunctional CXCR4 mutant expression was systematically increased by transient transfection into HEK293 cells that stably express WT CXCR4, effectively “diluting” WT/WT CXCR4 homodimers with nonfunctional mutants (Fig. 1F). Empty vector complementation was used so that all cells were transfected with the same amount of DNA. The Ca²⁺ mobilization response of these cells was then tested after addition of 20 nM or a saturating concentration (100 nM) of CXCL12. If the 1:1 stoichiometry hypothesis is correct, then increasing amounts of mutant receptor to dilute WT CXCR4 homodimers should not reduce the signaling response. Indeed, there was no significant change in Ca²⁺ mobilization after diluting with either CRS1 or CRS2 mutants (Fig. 5 A–D). Importantly, we established that increasing expression of mutant receptors did not alter WT CXCR4 expression (which may have artificially resulted in decreased signaling), and moreover that the amount of mutant receptor exceeded that of WT CXCR4 by a factor sufficient to effectively dilute WT/WT dimers (Fig. 5 E–H). By costaining the cell population with antibodies conjugated to different fluorophores and directed against distinct tags on WT and mutant receptors, it was possible to ensure that the expression of WT CXCR4 was constant whereas the mutant CXCR4 constructs systematically increased, and that both constructs were coexpressed in the vast majority of cells (Fig. 5 I–L). Taken together, these data strongly support the 1:1 stoichiometry of interaction of monomeric CXCL12 with CXCR4.

Cysteine Trapping Experiments Support the 1:1 Stoichiometry and Guide 1:1 Model Development. To obtain validation of the 1:1 CXCR4: CXCL12 complex stoichiometry and insight into the

structure of the complex, cysteine trapping experiments were developed. In these experiments, individual residues of CXCL12 and CXCR4 were mutated to cysteine, and the mutant pairs were coexpressed in *Spodoptera frugiperda* (Sf9) insect cells, purified by a His-tag on the receptor, and analyzed by SDS/PAGE and Western blotting for the presence of copurified chemokine. This approach assumes that when coexpressed, mutant receptors and chemokines bind in near-native geometry; and if this geometry brings the artificially introduced cysteines in proximity to one another, a disulfide bond spontaneously forms, resulting in an irreversible complex. As shown in Fig. 6A, cysteine trapping confirmed the proximity of K25 in CXCR4 with S16 in CXCL12, consistent with their relative orientation in the NMR structure (39) (Fig. 6D). However, multiple other residue pairs that were proximal in the NMR structure did not cross-link. Negative results were obtained for the following CXCR4: CXCL12 pairs: 16/N30, T8/L29, S9/L29, Y12/T31, P27/Q59, and F29/Q59 (Fig. 6 A and D). Systematic exploration of proximities in the CXCL12 region E15–V18 to CXCR4 K25 confirmed the initial finding of K25/S16; the nearby residues showed less or no cross-linking, providing evidence of specificity (Fig. 6B).

Based on this finding, we constructed second-generation 1:1 complex models by molecular docking, as described above, with one modification involving the introduction of a single disulfide bond between CXCR4 K25C and CXCL12 S16C instead of the NMR proximity restraints (Figs. 1D and 6F). The obtained models still featured the interaction of receptor residue K25 with S16 in the chemokine N-loop; however, the subsequent receptor residues up to R30 were directed along the N-loop, toward the chemokine N terminus, and away from the chemokine C-terminal helix. To functionally validate this prediction, we attempted cysteine trapping of residue pairs that were distant in the NMR structure but proximal in the new models (Fig. 6D). This included pairs of F29/F13, E31/R8, and E32/R8, which all showed positive cross-linking (although less efficient than with K25/S16) (Fig. 6 C, D, and F). We therefore concluded that the interactions observed in the NMR structure between the CXCL12 dimer and the N-terminal peptide of CXCR4 are different from those in the context of the full-length receptor. Our data suggest that the approximate complex geometry CXCL12 with full-length CXCR4 may be better represented by the computational model shown in Figs. 1D and 6F.

Discussion

Evidence firmly establishing class A GPCR dimerization in general, and chemokine receptor dimerization in particular, has accumulated for over a decade (23, 28, 41, 61). However, for most GPCRs, the functional purpose of dimerization is unclear.

In the case of chemokine receptors, despite numerous reports suggesting functional interactions between receptors in both homodimers and heterodimers, the structural causes and functional consequences of such interactions remain unknown. CXCL12 stimulation was shown to cause conformational changes in the CXCR4 homodimer (23). Furthermore, chemokines and

small-molecule antagonists were shown to transinhibit other receptors within heterodimers of chemokine receptors (28, 62), and chemokine receptors with other GPCRs (63, 64). The first report of a chemokine receptor crystal structure also showed that CXCR4 formed dimers (7), and moreover suggested that based on existing data, a 2:1 receptor:chemokine stoichiometry was a viable alternative to 1:1. Interesting examples in which a single GPCR agonist binds and activates a receptor homodimer with 2:1 receptor:ligand stoichiometry have been reported (46, 65). If confirmed for chemokine receptors, 2:1 stoichiometry could explain the observed dimer-mediated alteration of ligand binding and responses. On the other hand, definitively demonstrating a 1:1 stoichiometry between chemokines and their receptors would provide the impetus for investigating other, more complicated explanations for these phenomena.

Of the two possibilities, only the 2:1 stoichiometry was consistent with the NMR-based CXCL12 structure, the CXCR4 crystal structure, and the prevailing two-site model of receptor activation. Functional complementation experiments were designed to validate the 2:1 model, but the lack of functional rescue strongly suggested that such a model is incorrect and that the stoichiometry is more likely 1:1. Furthermore, dimer dilution experiments also supported the 1:1 interaction stoichiometry. Of note, although studying the functional importance of dimerization by coexpressing WT and nonfunctional mutant receptors is not new (27, 47, 64, 66, 67), care must be taken to ensure that the expression level of the WT receptor stays constant with increasing expression of mutant, and that the expression levels of the mutants are sufficient to effectively dilute WT/WT dimers. In the present study, such precautions were taken such that we could confidently conclude that dimerization of WT CXCR4 with CRS1 or CRS2 mutants does not alter its functional response, consistent with the 1:1 stoichiometry.

Finally, we used cysteine trapping experiments to elucidate the geometry of the 1:1 CXCR4:CXCL12 complex. These experiments confirmed that in the context of the full-length receptor, the pairwise residue proximity is different from that observed in the NMR structure (39) and is more consistent with a 1:1 model generated by computational docking with a single disulfide restraint. Similar contradictions are also present in other computationally generated 1:1 models of chemokine:receptor complexes (68, 69). One possible explanation for the inconsistency is that the NMR structure contains a dimer of CXCL12 in complex with two copies of the N-terminal CXCR4 peptide, rather than a monomer of CXCL12 complexed to a single receptor peptide. In fact, the CXCL12 dimer is known to be a partial agonist of CXCR4, and the NMR complex may be more representative of this alternative signaling complex (39). Alternatively, in the context of the full-length receptor, there may be some sort of rearrangement after docking of the CXCL12 globular domain to the CXCR4 N terminus, and engagement of the CXCL12 N terminus within the CXCR4 transmembrane binding pocket for activation.

The 1:1 stoichiometry and complex geometry suggested by our study answers a fundamental question regarding CXCR4:CXCL12, and likely most receptor:chemokine complexes. The results add to the accumulating data regarding the role of receptor monomers and not dimers in interactions with the various components of signaling complexes. Studies of rhodopsin (70), β_2 -adrenergic (71), neurotensin (72), and μ -opioid (73) receptors demonstrate that monomeric GPCRs are fully capable of activating G proteins. Monomeric rhodopsin can be phosphorylated by rhodopsin kinases and binds to visual arrestin in native disk membranes (74); and the structures of the β_2 -adrenergic receptor in complex with a heterotrimeric G protein (75) and β -arrestin₁ (76) also suggest a 1:1 interaction. Along with the present work, these studies support receptor monomers as fully competent signaling units.

On the other hand, our results do not dismiss previously observed dimer-mediated phenomena, such as the conformational changes within CXCR4 homodimers upon CXCL12 stimulation

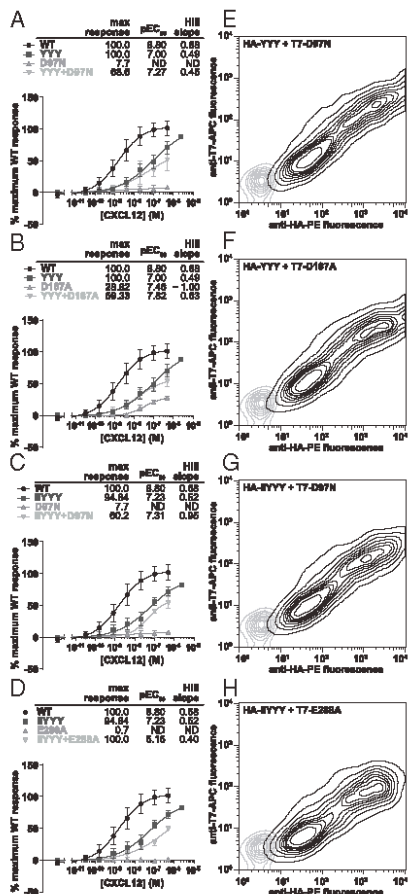


Fig. 4. The absence of functional rescue when coexpressing two complementary mutants of CXCR4 in CHO-G_{α15} cells. (A–D) CHO-G_{α15} cells were transfected with CRS1 mutants, CRS2 mutants, or cotransfected with both and their Ca²⁺ mobilization measured in response to varying concentrations of CXCL12. For all of the mutant pairs tested, the Ca²⁺ mobilization response of cotransfected cells did not exceed that of cells transfected with each of the mutants individually. In each experiment, cells transfected with WT CXCR4 were also tested as a positive control. Four representative mutant pairs are shown. Averages and SDs of all replicates in 2–12 independent experiments are shown. (E–H) Mutant coexpression in CHO-G_{α15} cells was monitored via flow cytometry by costaining cotransfected cells with PE-conjugated anti-HA antibody and APC-conjugated anti-T7 antibody. Two-dimensional contour plots show that in all cases, the mutants were efficiently coexpressed.

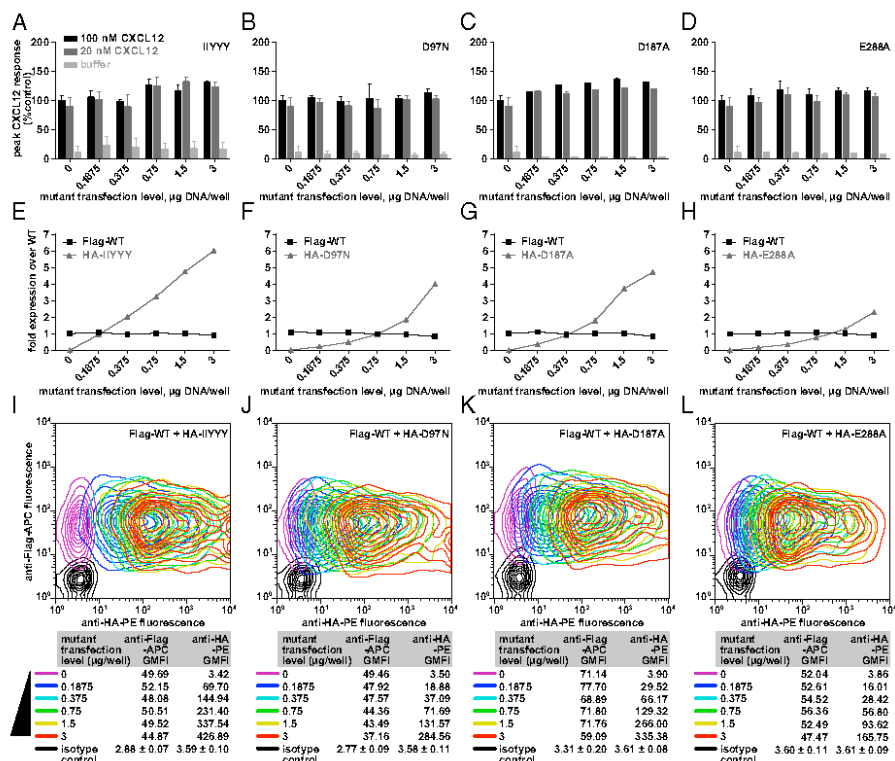


Fig. 5. Diluting WT-WT dimers by increasing transfection of loss-of-function mutants does not lead to a decrease in signaling. (A–D) Peak fluorescence values from Ca^{2+} mobilization experiments in which CXCR4 HEK293 tetraacycline-inducible cells transfected with the indicated amounts of CR51 and CR52 mutants were stimulated with the indicated CXCL12 concentrations. Data for four representative mutants are shown along with averages and SDs of replicates in two to four independent experiments. (E–H) WT and mutant receptor expression levels were monitored by flow cytometry; in all cases, the WT expression was constant and the transfected mutant expression exceeded it two- to sixfold. WT and mutant receptors N-terminally tagged with Flag and HA tags, respectively, were codetected on the cell surface with APC-conjugated anti-Flag antibody and PE-conjugated anti-HA antibody. To normalize geometric mean fluorescence intensity between the two antibodies, a series of samples coexpressing Flag-tagged and HA-tagged WT receptor was coexpressed with these antibodies and also (independently) with anti-CXCR4 antibody (data now shown). (I–L) Coexpression of the two constructs was monitored by flow cytometry.

(23), and ligand binding transinhibition within CXCR4 heterodimers with CCR2 and CCR5 (28, 62). Our data suggest that these phenomena must have other explanations than simultaneous binding of the chemokine to two protomers in the dimer. For example, they may originate from a conformational change that occurs upon 1:1 receptor:chemokine binding that is transmitted across the receptor dimer.

Similarly, our evidence adds to the interpretation of emerging data on regulation of CXCR4: CXCL12 signaling by the atypical chemokine receptor ACKR3 (CXCR7). CXCR4 and CXCR7 not only share CXCL12 as a chemokine ligand, but also heterodimerize in live cells. Such heterodimerization has been reported to negatively regulate CXCL12-mediated G protein signaling (77); for example, dilution of CXCR4: CXCR4 homodimers with CXCR4: CXCR7 heterodimers reduces G protein-mediated cellular responses to CXCL12 (30). Alteration of functional responses of one receptor by selective ligands of another has been reported as well (78–81). Our results suggest that these cross-talk phenomena occur because of propagation of

conformational changes across the heterodimer interface and not because of *in trans* binding of CXCL12 to both receptors in the dimer. It is also possible that a heterodimer presents a new intracellular interface that supports altered signaling responses.

Finally, our data do not exclude the possibility that receptor oligomerization contributes to other processes, such as regulation of pharmacology and trafficking of homo- versus hetero-oligomers (82, 83). It may also contribute to the coordination and efficiency of sequential steps in the GPCR lifecycle.

Materials and Methods

Molecular Modeling. Initial 1:1 and 2:1 receptor:chemokine models were generated by chemical field-guided molecular docking (48) of CXCL12 into the binding pocket of the CXCR4 monomer (for 1:1 model) or dimer (for 2:1 model) using the CXCR4 structures PDB ID codes 3OE0 and 3ODU (7). For the 2:1 models, CXCR4 dimers were derived from both chains in PDB ID code 3ODU or from chain A and its similarly oriented crystallographic neighbor in PDB ID code 3OE0. Chemical fields were generated from the structures of the cocrystallized ligands (IT1 and CX15) as described in refs. 48 and 84

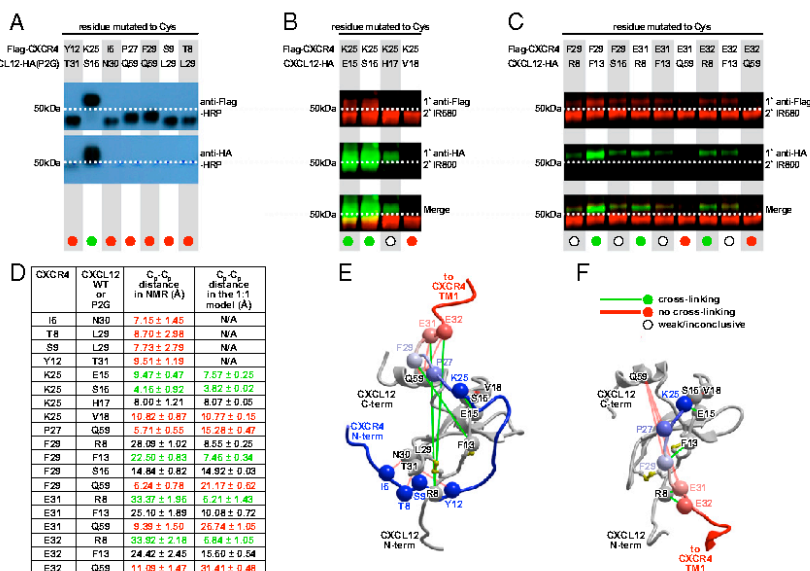


Fig. 6. Cysteine trapping experiment with CXCR4 and CXCL12 coexpressed in insect Sf9 cells. (A–C) Nonreducing Western blot analysis of extracts from Sf9 cells coexpressing single Cys mutants of Flag-tagged CXCR4 with single Cys mutants of HA-tagged CXCL12 or its antagonist version, CXCL12(P2G) (15). Molecular weight shift and positive HA-tag staining in the purified material (green circles) indicates spontaneously formed disulfide bond and suggests spatial proximity of the two cysteine residues in the complex, whereas the absence of a chemokine band (red circles) is indicative of spatially distant position of the probed residues. Open circles indicate weak/inconclusive cross-linking. (A) Coexpression samples were probed with HRP-conjugated anti-FLAG and anti-HA antibodies (top and bottom, respectively). Flag-CXCR4(K25C) efficiently cross-linked with CXCL12-HA(P2G-S16C) as evidenced by the molecular weight shift and by positive staining with both anti-FLAG and anti-HA antibodies; other probed mutant pairs did not cross-link. (B and C) Li-COR IRDye conjugated secondary antibodies were used to differentially identify Flag-CXCR4 and CXCL12-HA on a single blot. (B) Specificity of the cross-linking reaction in the vicinity of CXCR4 K25 and CXCL12 S16. Flag-CXCR4(K25C) forms strong complexes with CXCL12-HA(S16C) and (E15C), a much weaker complex with CXCL12-HA(H17C) and no complex with CXCL12-HA(V18C). (C) Validation of residue proximities observed in the second-generation 1:1 model of the CXCR4:CXCL12 complex. Flag-CXCR4(F29C) forms a medium strength complex with CXCL12-HA(F13C); Flag-CXCR4(E31C) and (E32C) both form weak complexes with CXCL12-HA(R8C) and (F13C), but not at all with CXCL12-HA(Q59C). (D) C_α-C_β distances observed between the probed CXCR4:CXCL12 residue pairs in the NMR structure (39) and second-generation 1:1 complex models. Averages and SDs were calculated using the 20 structures of the NMR ensemble (PDB ID code 2K05) or two top-scoring model conformations. (E and F) Positive and negative cross-links mapped onto 3D structures of CXCR4:CXCL12 complex in the context of the NMR structure (39) (E) or a second-generation 1:1 complex model in Fig. 1D (F). Chemokine orientation is identical between E and F.

and attenuated for ligand atoms that are not in direct contact with the receptor. The ensemble of initial conformations of CXCL12 was generated from all available X-ray and NMR structures in the PDB; in cases where N-terminal residues of CXCL12 were missing from electron density, they were constructed ab initio. The receptor pocket was represented with potential grid maps as described in ref. 50, with the N-terminal residues K25–R30 and the side chains of residues E179–D182, I185, D187, F189, and D193 excluded from the calculations because of the uncertainty of their positions. A full-atom peptide representing CXCR4 residues K25–R30 was generated ab initio. For generation of models compatible with the NMR structure of the CXCL12 complex with the CXCR4 N terminus (39), this peptide was restrained to the C_α atoms of proximal CXCL12 residues in the structure (F14–S16, I51–K56, and I58–E60) using soft harmonic restraints with target distances specified as observed in the structure. For second-generation NMR-independent models, a restraint was introduced in the form of the experimentally validated disulfide bond between CXCR4 K25C and CXCL12 S16C. The C-terminal part of the peptide was restrained to the positions of CXCR4 residues C28–R30 in the crystal structure, which are in turn tethered by a disulfide bond from C28 to C274 in the extracellular loop 3. Multiple orientations of CXCL12 were generated from each starting conformation by systematically flipping it along its principal axes. The system was then extensively sampled with a Biased Probability Monte Carlo search as implemented in the Internal Coordinate Mechanics software (49). During sampling, the backbone of chemokine residues P10–N67 was kept fixed except for switching between the multiple preselected conformations described above, and the side chains of these residues were

sampled explicitly. Both backbone and side chains of the CXCR4 N-terminal peptide (residues K25–R30) and the chemokine N terminus (residues K1–C9) were sampled explicitly.

Ca²⁺ Mobilization Assay in CHO-Gα₁₅ and HEK293 CXCR4 Tet-On Cells for Functional Complementation and Dimer Dilution Experiments, Respectively. Calcium mobilization assays were carried out using the FLIPR Calcium 4 Assay Kit (Molecular Devices). Cells were cultured and transfected with relevant CXCR4 WT and mutant constructs as described in *SI Text*. For functional complementation experiments, CHO-Gα₁₅ cells were lifted from dishes 6–8 h after transfection using sterile PBS containing 5 mM EDTA, plated at a density of 9×10^4 cells/well in poly-D-lysine-coated 96-well black/clear-bottom plates (Becton Dickinson Labware), cultured for another 16–20 h, and then tested using an adherent cell assay format. For dimer dilution experiments in HEK293 cells, cell culture media was replaced with fresh DMEM containing 10% (vol/vol) FBS 6–8 h after transfection, cells were cultured for another 16–20 h, and then tested in a detached cell assay format.

For adherent CHO-Gα₁₅ cell assay, cell culture media in the 96-well plates was replaced with 112.5 μL per well of Ca²⁺ mobilization assay buffer consisting of 1× HBSS (Gibco), 20 mM HEPES, 0.1% BSA, and 4 mM probenecid. For detached HEK293 cell assay, cells were lifted from the culture dishes using PBS containing 5 mM EDTA, washed, resuspended in Ca²⁺ mobilization assay buffer consisting of 1× HBSS, 20 mM HEPES, and 0.1% BSA, and aliquoted into poly-D-lysine-coated 96-well black/clear-bottom plates at a density of 1.5×10^5 cells per well in 112.5 μL buffer. For both assay formats,

112.5 μ L of the calcium indicator was added to the plate and mixed by gentle pipetting; detached cells were evenly settled at the bottom of the wells by centrifuging the plates at 250 \times g for 3 min. Following 75-min incubation of the plates at 37 °C with 5% CO₂, ligand stimulation and response recordings were carried out using a FlexStation 3 plate reader (Molecular Devices). For functional complementation experiments, dose-response curves were generated with CXCL12 concentrations extending beyond the point of signal saturation. For dimer dilution experiments, CXCL12 concentrations of 0 nM, 20 nM, and 100 nM were tested. Triplicate measurements were made for each concentration, and each experiment was performed at least twice on different days. All responses were expressed as percent maximal response elicited by WT in the same experiment. The reported values are averages with SD of all replicates from all experiments for each concentration of CXCL12. Data were analyzed in Prism 6 (GraphPad Software) using a sigmoidal dose-response curve with variable slope as a model.

BRET and Co-Immunoprecipitation Experiments to Assess CXCR4 Mutant Dimerization Propensity. BRET experiments were conducted with CXCR4-*Renilla* luciferase (CXCR4-Rluc) and CXCR4-YFP constructs possessing the same mutations as those used in the functional complementation and dimer dilution experiments. The BRET assay as applied to chemokine receptor dimerization was described previously (23, 59). Briefly, HEK293T cells were transfected with constant amounts of CXCR4-Rluc constructs and increasing amounts of CXCR4-YFP constructs, keeping the total amount of DNA transfected into each sample constant by empty vector complementation. After 48 h, cells were lifted from the culture plates with PBS containing 0.1% D-glucose, cell concentrations were normalized, and 10⁵ cells were plated into each well of a 96-well white clear-bottom tissue-culture assay plate (BD Falcon). Fluorescence readings (excitation: 485 nm, emission: 538 nm) were recorded using a SpectraMax M5 fluorescent plate reader (Molecular Devices). Coelenterazine was then added to a final concentration of 5- μ M, white backing tape (Perkin-Elmer) applied to the bottom of the assay plate, and both unfiltered and filtered luminescence (emission: 460 nm, 535 nm) readings were recorded with a VICTOR X Light 2030 luminometer (Perkin-Elmer). BRET ratios were calculated by dividing the luminescence signal at 535 nm by the signal at 460 nm. BRET_{net} values were calculated by subtracting the BRET ratio of Rluc-only transfected cells from all BRET ratios. BRET_{net} data were graphed as a function of increasing fluorescence/luminescence ratio. Resultant BRET YFP titration data were fit to a one site binding (hyperbolic) model in Prism (GraphPad Software).

For coimmunoprecipitation experiments, Flag-CXCR4-Tet-On and HEK293T cells were plated in a six-well plate and transiently transfected the next day with increasing amounts of HA-tagged WT and mutant CXCR4. Transfection media was replaced 6 h later with fresh culture media. Next, 16–18 h later, the culture media was removed, cells were rinsed with PBS, and lysed directly on

the plate using 400 μ L of cold lysis buffer [20 mM Tris-HCl, pH 7.5, 200 mM NaCl, 10% (vol/vol) glycerol, 1% DDM, 1 \times Protease Inhibitor mixture (Sigma)]. Lysates were transferred to 1.5-mL tubes, incubated with rocking at 4 °C for 1 h, and cleared by centrifugation for 20 min at 20,000 \times g at 4 °C. Cleared lysates were incubated with anti-Flag affinity resin (Sigma) at 4 °C for 2 h with rocking, after which resin was washed four times with fresh lysis buffer, bound proteins were eluted with 150 ng/ μ L of 3 \times Flag peptide (Sigma), and analyzed by Western blot using high-affinity HRP-conjugated rat anti-HA antibody (3F10, Roche).

Analysis of Disulfide-Trapped Complexes Between Cysteine Mutants of Flag-CXCR4 and CXCL12-HA. For the cysteine-trapping experiments, Flag-CXCR4 and CXCL12-HA cysteine mutant proteins were coexpressed in Sf9 insect cells and purified as described in *SI Text*. Purified protein samples were analyzed by nonreducing 10% SDS/PAGE gel where molecular weight shift and the relative band intensity were used as indicators of presence and relative abundance, respectively, of the irreversibly trapped complex. Western blotting was used to confirm the nature of Flag-CXCR4 and CXCL12-HA bands. For that process, ~5 μ L of purified sample was run on a 10% SDS/PAGE and transferred to a nitrocellulose membrane. The membrane was blocked in TBS-T with 5% (wt/vol) milk for 1 h at room temperature. Primary staining was performed using 5 μ L of mouse anti-Flag M2 primary antibody (Sigma) and 5 μ L rat anti-HA 3F10 primary antibody (Roche) for the receptor and chemokine, respectively, in 10 mL of fresh TBS-T with 5% (wt/vol) milk for 1 h at room temperature. Secondary staining was done with 1 μ L of IRDye 680 conjugated donkey anti-mouse IgG and IRDye 800 conjugated goat anti-rat IgG (LI-COR Biosciences) in 10 mL of TBS-T with 5% (wt/vol) BSA for 1 h at room temperature. Following incubation, the membrane was washed three times with 10 mL of fresh TBS-T for 10 min, transferred into 1 \times sterile PBS, and imaged using the Odyssey IR imaging system (LI-COR Bioscience).

ACKNOWLEDGMENTS. We thank B. Volkman (Medical College of Wisconsin) for suggesting the CRS1 mutations; T. Gilliland, M. Gustavsson, Y. Zheng (University of California, San Diego), S. Katritch, and R. Stevens (The Scripps Research Institute) for valuable discussions; M. Bouvier (University of Montreal) for sharing the initial bioluminescence resonance energy transfer cloning vectors; and J. Morseman (Columbia Biosciences) for generously providing test samples of fluorescent antibodies. The work was partially supported by NIH Grants R01 GM071872 and U54 GM094618 (to R.A.), U01 GM094612 (to R.A. and T.M.H.), R01 AI37113, R01 GM081763, and R21 AI101687 (to T.M.H.); Cellular and Molecular Pharmacology Training Grant T32 GM007752 (to B.S.S.); Molecular Biophysics Training Grant T32 GM008326 (to B.S.S.); and 2012 Post Doctoral Fellowship in Pharmacology/Toxicology from the Pharmaceutical Research and Manufacturers of America (PhRMA) Foundation (to L.G.H.).

- Ma Q, et al. (1998) Impaired B-lymphopoiesis, myelopoiesis, and deranged cerebellar neuron migration in CXCR4- and SDF-1-deficient mice. *Proc Natl Acad Sci USA* 95(16):9448–9453.
- Zou Y-R, Kottmann AH, Kuroda M, Taniuchi J, Littman DR (1998) Function of the chemokine receptor CXCR4 in haematopoiesis and in cerebellar development. *Nature* 393(6685):595–599.
- Feng Y, Broder CC, Kennedy PE, Berger EA (1996) HIV-1 entry cofactor: Functional cDNA cloning of a seven-transmembrane, G protein-coupled receptor. *Science* 272(5263):872–877.
- Zlotnik A, Burkhardt AM, Honey B (2011) Homeostatic chemokine receptors and organ-specific metastasis. *Nat Rev Immunol* 11(6):597–606.
- Tanegashima K, et al. (2013) CXCL14 is a natural inhibitor of the CXCL12-CXCR4 signaling axis. *FEBS Lett* 587(12):1731–1735.
- Saini V, Marchese A, Majetschak M (2010) CXC chemokine receptor 4 is a cell surface receptor for extracellular ubiquitin. *J Biol Chem* 285(20):15566–15576.
- Wu B, et al. (2010) Structures of the CXCR4 chemokine GPCR with small-molecule and cyclic peptide antagonists. *Science* 330(6007):1066–1071.
- Tan Q, et al. (2013) Structure of the CCR5 chemokine receptor-HIV entry inhibitor maraviroc complex. *Science* 341(6152):1387–1390.
- Brelot A, Heveker N, Montes M, Allison M (2000) Identification of residues of CXCR4 critical for human immunodeficiency virus coreceptor and chemokine receptor activities. *J Biol Chem* 275(31):23736–23744.
- Zhou H, Tal HH (2000) Expression and functional characterization of mutant human CXCR4 in insect cells: Role of cysteinyl and negatively charged residues in ligand binding. *Arch Biochem Biophys* 373(1):211–217.
- Kofuku Y, et al. (2009) Structural basis of the interaction between chemokine stromal cell-derived factor-1/CXCL12 and its G-protein-coupled receptor CXCR4. *J Biol Chem* 284(50):35240–35250.
- Saini V, et al. (2011) The CXC chemokine receptor 4 ligands ubiquitin and stromal cell-derived factor-1 α function through distinct receptor interactions. *J Biol Chem* 286(38):33466–33477.
- Gupta SK, Pillarsetti K, Thomas RA, Aiyar N (2001) Pharmacological evidence for complex and multiple site interaction of CXCR4 with SDF-1 α : Implications for development of selective CXCR4 antagonists. *Immunol Lett* 78(1):29–34.
- Scholten DJ, et al. (2012) Pharmacological modulation of chemokine receptor function. *Br J Pharmacol* 165(6):1617–1643.
- Crump MP, et al. (1997) Solution structure and basis for functional activity of stromal cell-derived factor-1; Dissociation of CXCR4 activation from binding and inhibition of HIV-1. *EMBO J* 16(23):6996–7007.
- Gerlach LO, Skerlj RT, Bridger GJ, Schwartz TW (2001) Molecular interactions of cycloclam and bicyclam non-peptide antagonists with the CXCR4 chemokine receptor. *J Biol Chem* 276(17):14153–14160.
- Rosenkilde MM, et al. (2004) Molecular mechanism of AMD3100 antagonism in the CXCR4 receptor: Transfer of binding site to the CXCR3 receptor. *J Biol Chem* 279(4):3033–3041.
- Choi W-T, et al. (2005) Unique ligand binding sites on CXCR4 probed by a chemical biology approach: Implications for the design of selective human immunodeficiency virus type 1 inhibitors. *J Virol* 79(24):15298–15404.
- Tian S, et al. (2005) Distinct functional sites for human immunodeficiency virus type 1 and stromal cell-derived factor 1 α on CXCR4 transmembrane helical domains. *J Virol* 79(20):12667–12673.
- Wong RSV, et al. (2008) Comparison of the potential multiple binding modes of bicyclam, monocyclam, and nocydam small-molecule CXCR4 chemokine receptor 4 inhibitors. *Mol Pharmacol* 74(6):1485–1495.
- Milligan G (2013) The prevalence, maintenance, and relevance of G protein-coupled receptor oligomerization. *Mol Pharmacol* 84(1):158–169.
- Babcock GJ, Farzan M, Sodroski J (2003) Ligand-independent dimerization of CXCR4, a principal HIV-1 coreceptor. *J Biol Chem* 278(5):3378–3385.
- Percherancier Y, et al. (2005) Bioluminescence resonance energy transfer reveals ligand-induced conformational changes in CXCR4 homo- and heterodimers. *J Biol Chem* 280(11):9895–9903.

24. Toth PT, Ren D, Miller RJ (2004) Regulation of CXCR4 receptor dimerization by the chemokine SDF-1 α and the HIV-1 coat protein gp120: Fluorescence resonance energy transfer (FRET) study. *J Pharmacol Exp Ther* 310(1):8–17.
25. Luker KE, Gupta M, Luker GD (2009) Imaging chemokine receptor dimerization with firefly luciferase complementation. *FASEB J* 23(3):823–834.
26. Choi W-T, et al. (2012) A novel synthetic bivalent ligand to probe chemokine receptor CXCR4 dimerization and inhibit HIV-1 entry. *Biochemistry* 51(36):7079–7086.
27. Lagane B, et al. (2008) CXCR4 dimerization and beta-arrestin-mediated signaling account for the enhanced chemotaxis to CXCL12 in WHIM syndrome. *Blood* 112(1):34–44.
28. Sohy D, Parmentier M, Springael J-Y (2007) Allosteric transinhibition by specific antagonists in CXCR2/CXCR4 heterodimers. *J Biol Chem* 282(41):30062–30069.
29. Silk N, Herold D, Jin T (2008) Fluorescence resonance energy transfer imaging reveals that chemokine-binding modulates heterodimers of CXCR4 and CCR5 receptors. *PLoS ONE* 3(10):e3242.
30. Décaillot FM, et al. (2011) CXCR7/CXCR4 heterodimer constitutively recruits beta-arrestin to enhance cell migration. *J Biol Chem* 286(37):32188–32197.
31. Kramp BK, Sarabi A, Koenen RR, Weber C (2011) Heterophilic chemokine receptor interactions in chemokine signaling and biology. *Exp Cell Res* 317(5):655–663.
32. Salanga CL, O'Hayre M, Handel T (2009) Modulation of chemokine receptor activity through dimerization and cross-talk. *Cell Mol Life Sci* 66(8):1370–1386.
33. Contento RL, et al. (2008) CXCR4-CCR5: A couple modulating T cell functions. *Proc Natl Acad Sci USA* 105(29):10101–10106.
34. Mellado M, et al. (2001) Chemokine receptor homo- or heterodimerization activates distinct signaling pathways. *EMBO J* 20(10):2497–2507.
35. Szpakowska M, et al. (2012) Function, diversity and therapeutic potential of the N-terminal domain of human chemokine receptors. *Biochem Pharmacol* 84(10):1365–1380.
36. Kufareva I, Abagyan R, Handel TM (2014) Role of 3D structures in understanding, predicting, and designing molecular interactions in the chemokine receptor family. *Chemokines, Top Med Chem*, ed Tschammer N (Springer, Heidelberg), pp 1–45.
37. Drury LJ, et al. (2011) Monomeric and dimeric CXCL12 inhibit metastasis through distinct CXCR4 interactions and signaling pathways. *Proc Natl Acad Sci USA* 108(43):17655–17660.
38. Rajarathnam K, et al. (1994) Neutrophil activation by monomeric interleukin-8. *Science* 264(5155):90–92.
39. Veldkamp CT, et al. (2008) Structural basis of CXCR4 sulfotyrosine recognition by the chemokine SDF-1/CXCL12. *Sci Signal* 1(37):ra4.
40. El-Asmar L, et al. (2005) Evidence for negative binding cooperativity within CCR5-CXCR2b heterodimers. *Mol Pharmacol* 67(2):460–469.
41. Vila-Coro AJ, et al. (1999) The chemokine SDF-1 α triggers CXCR4 receptor dimerization and activates the JAK/STAT pathway. *FASEB J* 13(13):1699–1710.
42. Steel E, Murray VL, Liu AP (2014) Multiplex detection of homo- and heterodimerization of G protein-coupled receptors by proximity biotinylation. *PLoS ONE* 9(4):e93646.
43. Bakker RA, et al. (2004) Domain swapping in the human histamine H1 receptor. *J Pharmacol Exp Ther* 311(1):131–138.
44. Maggio R, Vogel Z, Wess J (1993) Coexpression studies with mutant muscarinic/adrenergic receptors provide evidence for intermolecular “cross-talk” between G-protein-linked receptors. *Proc Natl Acad Sci USA* 90(7):3103–3107.
45. Monnot C, et al. (1996) Polar residues in the transmembrane domains of the type 1 angiotensin II receptor are required for binding and coupling. Reconstitution of the binding site by co-expression of two deficient mutants. *J Biol Chem* 271(3):1507–1513.
46. Rivero-Müller A, et al. (2010) Rescue of defective G protein-coupled receptor function in vivo by intermolecular cooperation. *Proc Natl Acad Sci USA* 107(5):2319–2324.
47. Trettel F, et al. (2003) Ligand-independent CXCR2 dimerization. *J Biol Chem* 278(42):40980–40988.
48. Kufareva I, Chen Y-C, Ilatovskiy AV, Abagyan R (2012) Compound activity prediction using models of binding pockets or ligand properties in 3D. *Curr Top Med Chem* 12(7):1869–1882.
49. Abagyan R, Totrov M (1994) Biased probability Monte Carlo conformational searches and electrostatic calculations for peptides and proteins. *J Mol Biol* 235(3):983–1002.
50. Fernández-Rodríguez J, Totrov M, Abagyan R (2002) Soft protein-protein docking in internal coordinates. *Protein Sci* 11(2):280–291.
51. Våbene J, Nikiforovich GV, Marshall GR (2005) Insight into the binding mode for cyclopeptide antagonists of the CXCR4 receptor. *Chem Biol Drug Des* 67(5):346–354.
52. Hatse S, et al. (2003) Mutations at the CXCR4 interaction sites for AMD3100 influence anti-CXCR4 antibody binding and HIV-1 entry. *FEBS Lett* 546(2–3):300–306.
53. Hatse S, et al. (2001) Mutation of Asp(171) and Asp(262) of the chemokine receptor CXCR4 impairs its coreceptor function for human immunodeficiency virus-1 entry and abrogates the antagonistic activity of AMD3100. *Mol Pharmacol* 60(1):164–173.
54. Zhou N, et al. (2001) Structural and functional characterization of human CXCR4 as a chemokine receptor and HIV-1 co-receptor by mutagenesis and molecular modeling studies. *J Biol Chem* 276(46):42826–42833.
55. Offermanns S, Simon MI (1995) G alpha 15 and G alpha 16 couple a wide variety of receptors to phospholipase C. *J Biol Chem* 270(25):15175–15180.
56. Farzan M, et al. (2002) The role of post-translational modifications of the CXCR4 amino terminus in stromal-derived factor 1 α association and HIV-1 entry. *J Biol Chem* 277(23):29484–29489.
57. Zivarek JJ, et al. (2013) Sulfopeptide probes of the CXCR4/CXCL12 interface reveal oligomer-specific contacts and chemokine allostery. *ACS Chem Biol* 8(9):1955–1963.
58. Hamdan FF, Percherancier Y, Breton B, Bouvier M (2006) Monitoring protein-protein interactions in living cells by bioluminescence resonance energy transfer (BRET). *Curr Protoc Neurosci* Chapter 5:Unit 5.23.
59. Kufareva I, et al. (2013) A novel approach to quantify G-protein-coupled receptor dimerization equilibrium using bioluminescence resonance energy transfer. *Chemokines: Methods and Protocols, Methods Mol Biol*, eds Cardona AE, Uboogu EE (Springer, New York), Vol 1013, pp 93–127.
60. James JR, Oliveira MI, Carmo AM, Iaboni A, Davis SJ (2006) A rigorous experimental framework for detecting protein oligomerization using bioluminescence resonance energy transfer. *Nat Methods* 3(12):1001–1006.
61. Liang Y, et al. (2003) Organization of the G protein-coupled receptors rhodopsin and opsin in native membranes. *J Biol Chem* 278(24):21655–21662.
62. Sohy D, et al. (2009) Hetero-oligomerization of CCR2, CCR5, and CXCR4 and the protean effects of “selective” antagonists. *J Biol Chem* 284(45):31270–31279.
63. May LT, Bridge LJ, Stoddart LA, Bridson SJ, Hill SJ (2011) Allosteric interactions across native adenosine-A3 receptor homodimers: Quantification using single-cell ligand-binding kinetics. *FASEB J* 25(10):3465–3476.
64. Szalai B, et al. (2012) Allosteric interactions within the AT₁ angiotensin receptor homodimer: Role of the conserved DRY motif. *Biochem Pharmacol* 84(4):477–485.
65. Brodk C, et al. (2007) Activation of a dimeric metabotropic glutamate receptor by intersubunit rearrangement. *J Biol Chem* 282(45):33000–33008.
66. Hernandez PA, et al. (2003) Mutations in the chemokine receptor gene CXCR4 are associated with WHIM syndrome, a combined immunodeficiency disease. *Nat Genet* 34(1):70–74.
67. Benkirane M, Jin DY, Chun RF, Koup RA, Jeang KT (1997) Mechanism of trans-dominant inhibition of CCR5-mediated HIV-1 infection by ccr5delta32. *J Biol Chem* 272(49):30603–30606.
68. Xu L, Li Y, Sun H, Li D, Hou T (2013) Structural basis of the interactions between CXCR4 and CXCL12/SDF-1 revealed by theoretical approaches. *Mol Biosyst* 9(8):2107–2117.
69. Liou H-H, et al. (2014) In silico analysis reveals sequential interactions and protein conformational changes during the binding of chemokine CXCL8 to its receptor CXCR1. *PLoS ONE* 9(4):e94178.
70. Whorton MR, et al. (2008) Efficient coupling of transducin to monomeric rhodopsin in a phospholipid bilayer. *J Biol Chem* 283(7):4387–4394.
71. Whorton MR, et al. (2007) A monomeric G protein-coupled receptor isolated in a high-density lipoprotein particle efficiently activates its G protein. *Proc Natl Acad Sci USA* 104(18):7682–7687.
72. Inagaki S, et al. (2012) Modulation of the interaction between neurotensin receptor NTS1 and Gq protein by lipid. *J Mol Biol* 417(1–2):95–111.
73. Kuzak AJ, et al. (2009) Purification and functional reconstitution of monomeric μ -opioid receptors: Allosteric modulation of agonist binding by Gi2. *J Biol Chem* 284(39):26732–26741.
74. Bayburt TH, et al. (2011) Monomeric rhodopsin is sufficient for normal rhodopsin kinase (GRK1) phosphorylation and arrestin-1 binding. *J Biol Chem* 286(2):1420–1428.
75. Rasmussen SGF, et al. (2011) Crystal structure of the β 2 adrenergic receptor-Gs protein complex. *Nature* 477(7366):549–555.
76. Shukla AK, et al. (2014) Visualization of arrestin recruitment by a G-protein-coupled receptor. *Nature* 512(7513):218–222.
77. Levoye A, Balabanian K, Baleux F, Bachelier F, Lagane B (2009) CXCR7 heterodimerizes with CXCR4 and regulates CXCL12-mediated G protein signaling. *Blood* 113(24):6085–6093.
78. Kalatskaya I, et al. (2009) AMD3100 is a CXCR7 ligand with allosteric agonist properties. *Mol Pharmacol* 75(5):1240–1247.
79. Gravel S, et al. (2010) The peptidomimetic CXCR4 antagonist TC14012 recruits beta-arrestin to CXCR7: Roles of receptor domains. *J Biol Chem* 285(49):37939–37943.
80. Zabel BA, et al. (2009) Elucidation of CXCR7-mediated signaling events and inhibition of CXCR4-mediated tumor cell transendothelial migration by CXCR7 ligands. *J Immunol* 183(5):3204–3211.
81. Zabel BA, Lewin S, Berahovich RD, Jaén JC, Schall TJ (2011) The novel chemokine receptor CXCR7 regulates trans-endothelial migration of cancer cells. *Mol Cancer* 10(1):73.
82. Lin H, Trejo J (2013) Transactivation of the PAR1-PAR2 heterodimer by thrombin elicits β -arrestin-mediated endosomal signaling. *J Biol Chem* 288(16):11203–11215.
83. Stephens B, Handel TM (2013) Chemokine receptor oligomerization and allostery. *Prog in Mol Biol Transl Sci* 115:375–420.
84. Totrov M (2008) Atomic property fields: Generalized 3D pharmacophore potential for automated ligand superposition, pharmacophore elucidation and 3D QSAR. *Chem Biol Drug Des* 71(1):15–27.

Supporting Information

Kufareva et al. 10.1073/pnas.1417037111

SI Text

Molecular Cloning. For experiments in mammalian cells, mutations were cloned into Flag-CXCR4, CXCR4-*Renilla* luciferase (CXCR4-Rluc), and CXCR4-YFP using the QuikChange Site-Directed Mutagenesis Kit (Agilent) according to the manufacturer's directions. HA-CXCR4 and T7-CXCR4 mutants were obtained by swapping the Flag tag (M-DYKDDDDK) for an HA tag (M-YPYDVPDYA) or T7 tag (M-ASMTGGQQMGM) using the Flag-CXCR4 constructs, also by QuikChange. For disulfide cross-linking experiments in *Spodoptera frugiperda* (Sf9) insect cells, a Flag-tagged CXCR4 construct [CXCR4-1 in Wu et al. (1)] in pFastBac1 was generated as previously described (1). CXCL12 with its native signal sequence and a C-terminal HA tag (YPYDVPDYA) was also subcloned into pFastBac1 for coexpression in Sf9 cells. Cysteine mutations were introduced into Flag-CXCR4 and CXCL12-HA using QuikChange [referred to below as Flag-CXCR4(Cys), CXCL12-HA(Cys), and CXCL12-HA(P2G-Cys) in the case of a construct that also has a P2G mutation that converts CXCL12 into an antagonist (2)].

Cell Culture and Transfection. CHO-G α_{15} cells were maintained in DMEM/F12 nutrient mixture (Gibco) supplemented with 10% (vol/vol) FBS and 700 μ g/mL G418. CXCR4 Tet-On cells were obtained by transfecting HEK293 cells with pACMV-Tet-On-Flag-CXCR4 and selecting for stably transfected cells with the addition of 700 μ g/mL G418. These cells were maintained in DMEM with Glutamax (Invitrogen), 10% (vol/vol) tetracycline-free FBS (Gibco), and 700 μ g/mL G418. HEK293T cells were maintained in DMEM with Glutamax and 10% (vol/vol) FBS. All mammalian cells were cultured at 37 °C with 5% CO₂.

Transient transfections of CHO-G α_{15} stable cells were carried out using the TransIT CHO transfection kit according to the manufacturer's instructions, with the following modifications: 4- μ L transfection reagent and 0.5 μ L of the CHO Mojo booster reagent were used per every 1 μ g of DNA to be transfected. These cells were plated in DMEM/F12 containing 10% (vol/vol) FBS and 0.25% DMSO 24 h before transfection, and the media was switched to DMEM/F12 with 10% (vol/vol) FBS just before transfection. Transient transfections of both HEK293 CXCR4 stable cells and HEK293T cells were performed using the TransIT-LT1 reagent (Mirus Bio), according to manufacturer's instruction.

Sf9 cells were cultured in ESF 921 media (Expression Systems) in vented Erlenmeyer flasks (Corning) at 27 °C with shaking. High-titer recombinant baculovirus (>10⁹ viral particles per mL) was obtained using the Bac-to-Bac Baculovirus Expression System (Invitrogen). Briefly, recombinant baculoviruses were generated by transfecting 5 μ L of recombinant bacmid containing the target gene sequence into 2.5 mL of Sf9 cells at a density of 1.2 \times 10⁶ cells/mL using 3 μ L of Xtreme Gene Transfection Reagent (Roche) and 100 μ L of Transfection Medium (Expression Systems). Cell suspensions were incubated for 96 h with shaking at 27 °C. P0 viral stocks were then isolated and used to generate P1 viral stocks. Viral titers were quantified by flow cytometry following cell staining with PE-conjugated anti-gp64 antibody (Expression Systems). Sf9 cells at a density of 2–2.6 \times 10⁶ cells/mL were coinfecting with P1 virus of both Flag-CXCR4(Cys) and CXCL12-HA(Cys) or CXCL12-HA(P2G-Cys) at a multiplicity of infection of 5. Biomass was harvested between 44 and 48 h postinfection.

Quantification of Protein Surface Expression by Flow Cytometry. For testing WT and mutant CXCR4 surface expression, mammalian

cells were washed in PBS containing 0.5% BSA (FACS buffer). For Flag-tag detection, staining was carried out in a 50 \times dilution (2 μ g/mL) of anti-DDDDK (Clone M2) conjugated to SureLight APC or mouse IgG1 isotype control conjugated to SureLight APC (Columbia Biosciences) for 45 min on ice. For T7-tag detection, staining was carried out in a 10 \times dilution of anti-T7 conjugated to SureLight APC (Columbia Biosciences). For HA-tag detection, staining was carried out in a 10 \times dilution of anti-HA-APC (Miltenyi Biotec) (Clone GG8-1F3.3.1). For simultaneous tag detection, cells were costained with two antibodies against tags of interest (either Flag and HA, or T7 and HA) using the same concentrations as above, also for 45 min on ice. For endogenous CXCR4 detection, cells were stained in a 50 \times dilution of anti-CXCR4-PE (clone 1D9) or IgG_{2a} isotype control-PE (BD Biosciences), also for 45 min on ice. Cells were then washed 3 \times in FACS buffer before analysis, which was carried out using a Guava bench top miniflow cytometer (Millipore).

Generation of Stable CHO-G α_{15} Cell Line for CXCR4 Mutant Characterization. Plasmid vector for human G $\alpha_{15/16}$ in pcDNA3.1⁺ was purchased from the Missouri S&T cDNA Resource Center and transfected into Chinese hamster ovary cells (CHO-K1, ATCC) using the TransIT-CHO transfection kit (Mirus Bio). After 24 h, cells were transferred into selection media containing 600 μ g/mL G418 (Gibco). After 1 wk of selection, the surviving cells were reseeded into a 96-well plate at a density of \sim 1 cell per well, and single-cell colonies were allowed to grow for 2 wk, with fresh G418-containing cell culture media supplemented every 2 d. Colonies were analyzed by Western blot using rabbit polyclonal antibody against G $\alpha_{15/16}$ (Abcam) and HRP-conjugated goat anti-rabbit antibody (Thermo) (Fig. S1M), and by Ca²⁺ mobilization upon transient transfection with CXCR4 (Fig. S1N–P), for G α_{15} expression. The clone with the highest expression and best signal-to-noise ratio (L12) was chosen for all experiments (referred to as CHO-G α_{15}).

Protein Purification for Disulfide Cross-Linking Experiments. For screening of cross-linked species between Flag-CXCR4 and CXCL12-HA cysteine mutants, biomass was thawed and lysed in hypotonic buffer [10 mM Hepes pH 7.5, 10 mM MgCl₂, 20 mM KCl, and EDTA-free protease inhibitor mixture (Roche)] followed by 40 strokes of Dounce homogenization and centrifugation at 50,000 \times g at 4 °C for 30 min. Purified membranes were subjected to two additional rounds of Dounce homogenization and centrifugation in a high salt buffer (10 mM Hepes pH 7.5, 10 mM MgCl₂, 20 mM KCl, 1 M NaCl, and EDTA-free protease inhibitor mixture). Following the last centrifugation, membrane pellets were resuspended and homogenized in hypotonic buffer supplemented with 30% glycerol (vol/vol) and flash-frozen at –80 °C until further use. Purified membranes were thawed on ice and mixed with an equal volume of 2 \times solubilization buffer [100 mM Hepes pH 7.5, 800 mM NaCl, 1.5% (wt/vol) n-dodecyl- β -D-maltopyranoside (DDM, Anatrace), 0.3% cholesteryl hemisuccinate (CHS, Sigma)], incubated for 3 h at 4 °C, and then centrifuged at 25,000 \times g for 30 min. The supernatant was incubated overnight at 4 °C with TALON IMAC resin (Clontech) and 20 mM imidazole. After binding, the resin was washed with twenty column volumes of wash buffer [25 mM Hepes pH 7.5, 400 mM NaCl, 0.025% DDM, 0.005% CHS, 10% (vol/vol) glycerol]. Complexes were eluted in six column volumes of wash buffer supplemented with 250mM Imidazole pH 8.0.

1. Wu B, et al. (2010) Structures of the CXCR4 chemokine GPCR with small-molecule and cyclic peptide antagonists. *Science* 330(6007):1066–1071.
2. Crump MP, et al. (1997) Solution structure and basis for functional activity of stromal cell-derived factor-1; Dissociation of CXCR4 activation from binding and inhibition of HIV-1. *EMBO J* 16(23):6996–7007.

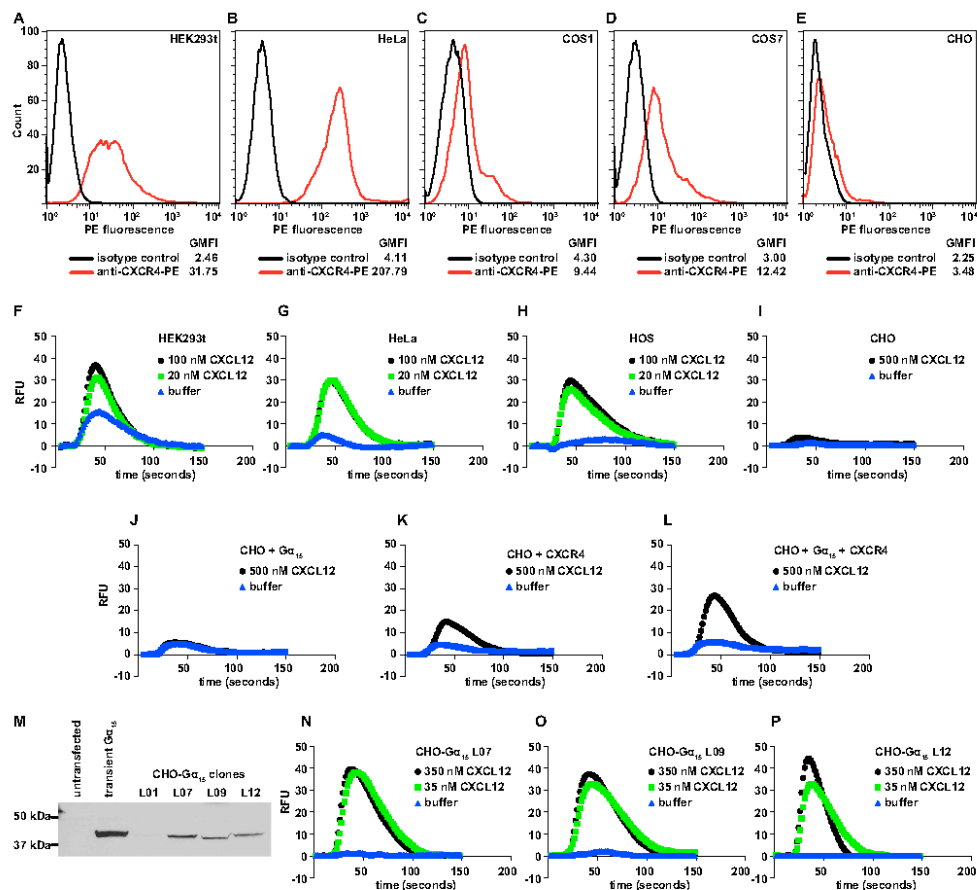


Fig. S1. Design of CXCR4-free cell line for CXCR4 mutant functionality testing. (**A–E**) Endogenous expression of CXCR4 was detected via flow cytometry following surface staining with anti-CXCR4-PE (clone 1D9; BD Biosciences). Endogenous CXCR4 was detected on the surface of (**A**) HEK293t cells, (**B**) HeLa cells, (**C**) COS1, and (**D**) COS7 cells, but not (**E**) CHO cells. (**F–I**) Ca^{2+} mobilization elicited by the indicated CXCL12 concentrations was also measured for several cell types. CXCL12 caused Ca^{2+} mobilization in untransfected (**F**) HEK293t, (**G**) HeLa, and (**H**) HOS cells, but not in (**I**) CHO cells. (**J–L**) CHO cells displayed robust CXCL12-induced Ca^{2+} mobilization after transfection with both $G_{\alpha_{15}}$ and CXCR4. CHO cells that were transfected with (**J**) $G_{\alpha_{15}}$ alone showed no appreciable Ca^{2+} mobilization, and those transfected with (**K**) CXCR4 showed an improved but still low response, whereas transfection with (**L**) both $G_{\alpha_{15}}$ and CXCR4 produced robust CXCL12-induced Ca^{2+} mobilization. (**M–P**) Clone selection of stably $G_{\alpha_{15}}$ -transfected CHO cells and resultant Ca^{2+} mobilization data. (**M**) Western blot detection of human $G_{\alpha_{15}}$ in clonally selected populations of stably transfected CHO cells. Cells were harvested, normalized, pelleted by centrifugation, and lysed in G protein-specific lysis buffer [20 mM HEPES, pH 8.8, 100 mM NaCl, 5 mM MgCl₂, 1% sodium cholate, 1× Protease inhibitor (Sigma), 2 mM GTP, and 1 mM DTT]. Cell lysates were separated by SDS/PAGE, transferred to nitrocellulose membranes, blocked overnight, and probed with rabbit polyclonal antibody against $G_{\alpha_{15}}$ (Abcam) followed by HRP-conjugated goat anti-rabbit antibody (Thermo) according to the manufacturer's instructions. (**N–P**) Three separate clones of CHO- $G_{\alpha_{15}}$ stable cells all display robust CXCL12-induced Ca^{2+} mobilization upon transfection with CXCR4.

Table S1. Properties of the cell lines tested and generated to identify a background-free CXCR4 mutant testing system

Cell line	Endogenous CXCR4 expression*	Transfection efficiency [†]	Ca ²⁺ mobilization [‡] : untransfected	Ca ²⁺ mobilization: CXCR4 transfected
HEK293T	+++	+++	+++	+++
HeLa	+++	NT	++	NT
COS-1	++	NT	NT	NT
COS-7	++	NT	NT	NT
HOS	+	—	++	++
CHO-K1	—	++	—	+
CHO-Gα ₁₅	—	++	—	++
Target properties	—	+++	—	+++

*Quantified by anti-CXCR4-PE staining and flow cytometry.

[†]Efficiency tested by screening a panel of transfection reagents: Roche X-tremeGene, Mirus TransIT-LT1, TransIT-2020, or TransIT-CHO, Fermentas ExGen-500, Invitrogen Lipofectamine 2000, LP9.

[‡]Tested by FLIPR4 Ca²⁺ mobilization assay. +++, excellent/highest among the cell lines tested; ++, good; +, moderate; —, poor/none; NT, not tested.

Acknowledgement

Chapter three, in full, is a reprint of a published research article as it appears in Proceedings of the National Academy of Sciences of the USA. (Kufareva, I., **B. S. Stephens**, L. G. Holden, L. Qin, C. Zhao, T. Kawamura, R. Abagyan and T. M. Handel (2014). "Stoichiometry and geometry of the CXC chemokine receptor 4 complex with CXC ligand 12: molecular modeling and experimental validation." Proc Natl Acad Sci U S A **111**(50): E5363-5372.) The dissertation author was a co-primary researcher and author of this material.

Chapter 4

What Do Structures Tell Us About Chemokine Receptor Function and Antagonism?



ANNUAL REVIEWS **Further**

Click [here](#) to view this article's online features:

- Download figures as PPT slides
- Navigate linked references
- Download citations
- Explore related articles
- Search keywords

What Do Structures Tell Us About Chemokine Receptor Function and Antagonism?

Irina Kufareva, Martin Gustavsson, Yi Zheng, Bryan S. Stephens, and Tracy M. Handel

Skaggs School of Pharmacy and Pharmaceutical Sciences, University of California, San Diego, La Jolla, California 92093; email: ikufareva@ucsd.edu, thandel@ucsd.edu

Annu. Rev. Biophys. 2017. 46:175–98

The *Annual Review of Biophysics* is online at biophys.annualreviews.org

<https://doi.org/10.1146/annurev-biophys-051013-022942>

Copyright © 2017 by Annual Reviews. All rights reserved

Keywords

G protein–coupled receptor, crystallography, molecular modeling, receptor activation, allostery, druggability

Abstract

Chemokines and their cell surface G protein–coupled receptors are critical for cell migration, not only in many fundamental biological processes but also in inflammatory diseases and cancer. Recent X-ray structures of two chemokines complexed with full-length receptors provided unprecedented insight into the atomic details of chemokine recognition and receptor activation, and computational modeling informed by new experiments leverages these insights to gain understanding of many more receptor:chemokine pairs. In parallel, chemokine receptor structures with small molecules reveal the complicated and diverse structural foundations of small molecule antagonism and allostery, highlight the inherent physicochemical challenges of receptor:chemokine interfaces, and suggest novel epitopes that can be exploited to overcome these challenges. The structures and models promote unique understanding of chemokine receptor biology, including the interpretation of two decades of experimental studies, and will undoubtedly assist future drug discovery endeavors.

Contents

INTRODUCTION	176
CHEMOKINES: STRUCTURE AND BIOLOGY	177
THE STRUCTURAL BASIS OF CHEMOKINE RECEPTOR INTERACTIONS WITH CHEMOKINES	178
Early Studies: The Two-Site Model of Receptor Activation	178
The Architecture of Receptor:Chemokine Complexes as Elucidated by Crystallography and Experimentally Guided Modeling	179
Repurposing of Chemokine Interfaces	182
INSIGHTS INTO RECEPTOR ACTIVATION FROM EXPERIMENTS INTERPRETED IN THE CONTEXT OF STRUCTURES AND MODELS ..	182
Intramolecular Signal Transmission Network in CXCR4	183
Activation of an Atypical Chemokine Receptor	185
ON THE ALLOSTERY OF CHEMOKINE RECEPTORS	185
Upside-Down and Downside-Up Allostery	185
“Orthosteric Allostery” of Chemokine Receptor Antagonists	186
“Allosteric Allostery” of Chemokine Receptor Antagonists	187
ON THE DRUGGABILITY OF CHEMOKINE RECEPTORS	189
The Physicochemical Challenges of Receptor:Chemokine Interfaces	189
The Ultimate Pharmacodynamic–Pharmacokinetic Conflict in Small Molecule Antagonists of Chemokine Receptors	190
Biologics and Biomimetics	190
Allosterics	190
CONCLUSIONS	191

INTRODUCTION

As master regulators of cell migration, chemokines and chemokine receptors are critical to fundamental biological processes, including embryonic development early in life, immune surveillance, host defense and wound repair throughout life, and disease that comes with age (3, 41, 46). The receptors belong to the class A family of G protein–coupled receptors (GPCRs) and are expressed on migrating cells. The ligands (chemokines) are small proteins that are secreted by most cell types either constitutively or inducibly in response to a wide variety of stimuli and environmental cues (111). By forming gradients on cell surfaces and extracellular matrices in tissues, chemokines serve as the directional signals for cell migration (82, 112).

Because they control leukocyte migration, chemokines and chemokine receptors were initially recognized as fundamental mediators of inflammation. In 1996, two chemokine receptors were identified as the coreceptors that facilitate HIV entry into cells (38) and in 2001, a link between chemokines and cancer metastasis was made (87). Today, chemokines and chemokine receptors have been identified as important mediators in an unusually large number of diseases, many of which were anticipated based on the roles of these molecules in cell migration and inflammation, and some of which were unexpected, such as AIDS (121). By analogy with other members of the class A GPCR family, chemokine receptors were initially considered highly druggable targets, which inspired more than two decades of drug discovery efforts. However, progress has often been described as slow (102, 115), and only two small molecules against the chemokine receptor system

are currently approved for use: the CCR5 antagonist, maraviroc (31) and a CXCR4 antagonist, plerixafor (26). Additionally, two antibody-based drugs, the anti-CCR4 monoclonal antibody, Mogamulizumab (33), and the anti-CXCL8 antibody, Abcream (146), have been approved in, respectively, Japan and China.

Factors contributing to clinical failures have been attributed to both deficiencies of the therapeutic candidates and the complexities of receptor:chemokine biology (54, 103, 115, 121). As for other GPCRs, important properties of drug candidates include the target residence time for ensuring adequate receptor occupancy and receptor selectivity for minimizing off-target effects (22, 140). However, chemokine receptors pose additional challenges that may be less problematic for other GPCRs. For example, their sequences, expression patterns, and function differ markedly between species, which complicates the design and interpretation of animal studies (54, 121). Other factors include the apparent redundancy of the chemokine system (which provides a rationale for developing multitargeted antagonists) and the limited understanding of the complexities of diseases in which multiple chemokine receptors and cell types are involved (115). Additionally, the overall druggability of class A GPCRs may not translate as easily to chemokine receptors because their endogenous ligands are proteins and the interaction interfaces are extensive (15, 104). Finally, the difficulties of competing with abundant levels of endogenous chemokines compared with, for example, hormone receptors, call for the development of insurmountable or allosteric antagonists.

Fortunately, the recent plethora of GPCR structures is providing new insights into ligand binding modes, binding locations, binding kinetics, and associated ligand pharmacology, all of which can address the above issues and contribute to the design of more efficacious drugs (21). In this review, we describe recent breakthroughs in understanding receptor interactions with chemokines and small molecules, as well as receptor activation mechanisms, all based on findings from structural biology and experiment-guided molecular modeling. We also discuss the implications of this information for developing drugs targeting chemokine receptors.

CHEMOKINES: STRUCTURE AND BIOLOGY

In humans, there are approximately 45 chemokines (116) that have been classified into four families (CC, CXC, CX3C, and XC) based on the pattern of Cys residues in their N termini (**Figure 1a,b**). Unlike most GPCR ligands, chemokines are proteins, approximately 8–12 kDa in size. They have a highly conserved tertiary structure defined by an N-terminal unstructured domain that is critical for receptor activation, an irregular N loop, a three-stranded β -sheet connected by loops (e.g., the 30s and 40s loops), and a C-terminal helix (**Figure 1a,b**) (68, 69).

The 22 chemokine receptors share the canonical topology of most GPCRs. They have seven transmembrane (TM) helices, three extracellular and three intracellular loops, an unstructured extracellular N terminus, and an intracellular C terminus. Chemokine binding at the extracellular side of the receptor triggers a conformational change that transmits the signal toward the intracellular side where direct coupling to G proteins and β -arrestins activates cell migration pathways. Receptors are classified as CC, CXC, CX3C, or XC according to the subfamily of their preferred ligands (116).

Most chemokines dimerize or form higher order oligomers (69). The elongated structure of CC chemokine dimers is stabilized by interactions between the CC motifs and preceding N-terminal residues of the monomers (**Figure 1c**). Dimerization of CXC chemokines is driven by interactions between their β_1 strands (**Figure 1d**). Some chemokines form higher order oligomers (**Figure 1e**) (74), many of which utilize both CC and CXC dimerization interfaces (72, 89).

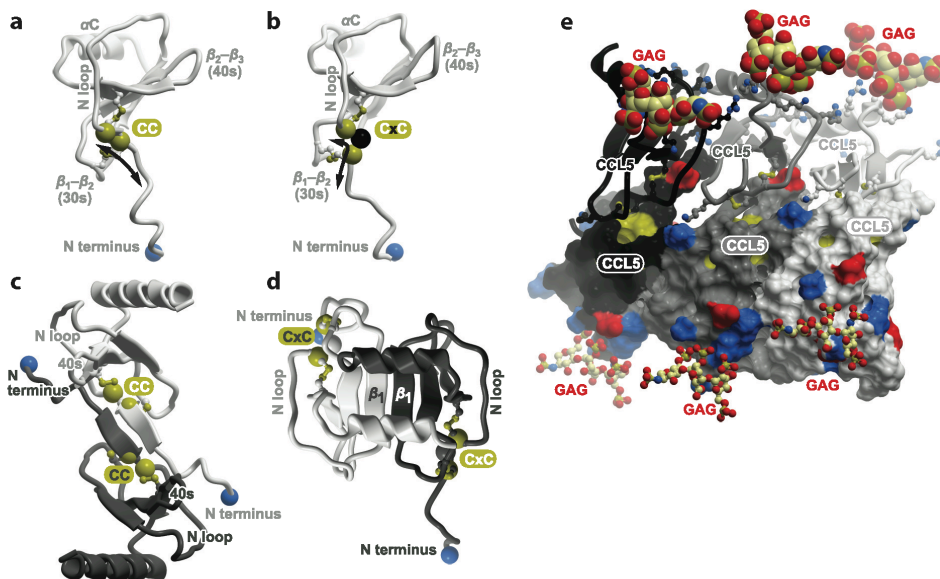


Figure 1

Topology and oligomerization behavior of chemokines. (a,b) Typical structures of CC (a) and CXC (b) chemokines. (c,d) Typical dimerization geometry of CC (c) and CXC (d) chemokines. (e) CC chemokines bind GAGs (glycosaminoglycans) through extensive, positively charged interfaces formed through chemokine oligomerization. The oligomers are formed by polymerization of dimers that have a geometry consistent with that seen in panel c.

Despite the propensity of chemokines to oligomerize, studies with constitutively monomeric chemokine variants have demonstrated that monomers are sufficient, and generally required, for receptor activation (58, 97, 106, 129). By contrast, oligomerization is required for high affinity binding of chemokines to their other receptors, the glycosaminoglycans (GAGs), which are found on cell surfaces and the extracellular matrix (34). These GAG interactions are important for immobilizing chemokines and facilitating the formation of haptotactic chemokine gradients that effectively provide a path for chemokine receptor-bearing cells to follow (49, 82, 112, 117). Thus, in the multistep process of cell migration, chemokine oligomers bound to GAGs must reversibly dissociate to fully engage receptors as monomers.

THE STRUCTURAL BASIS OF CHEMOKINE RECEPTOR INTERACTIONS WITH CHEMOKINES

Early Studies: The Two-Site Model of Receptor Activation

Prior to the recent crystallographic studies of intact receptor:chemokine complexes, structural information was derived from mutagenesis experiments, structures of chemokines alone, and from nuclear magnetic resonance (NMR) studies of chemokines bound to N-terminal peptides from the receptors (reviewed in 68, 69). Mutagenesis studies revealed that chemokine N termini

largely control receptor activation: Even subtle modification of the N termini can alter ligand pharmacology by converting agonists into partial agonists, antagonists, or even super agonists. By contrast, mutation of the globular core domain of chemokines usually produces effects on potency proportional to effects on receptor binding affinity. Because of the disproportionate control of signaling by the two chemokine domains, a two-site model became the paradigm for the interaction (85, 98). In this model, the receptor N terminus binds to the chemokine core (an interaction often referred to as chemokine recognition site 1, or CRS1) while the chemokine N terminus binds in the pocket of the receptor TM helical domain (chemokine recognition site 2, or CRS2) (**Figure 2a**) (116). The affinity of the CRS1 interaction is enhanced by posttranslational sulfation of Tyr residues in the receptor N termini (37, 77, 83, 107, 137, 138, 150, 151), which may regulate selective chemokine binding (150).

When considered in light of the two recent structures of chemokines complexed to intact receptors, the two-site model is clearly oversimplified (68). Nevertheless, it captured the essential roles of the chemokine domains, and guided numerous efforts toward engineering chemokines with altered pharmacology for proof-of-concept studies of the efficacy of antagonizing specific receptors in various diseases (44, 50, 135) or for probing the value of the engineered chemokines as therapeutic candidates. One of the best examples of the latter is a series of N-terminally modified CCL5 (RANTES) variants that show a superior ability to inhibit HIV entry into cells compared with wild-type CCL5 (10, 39).

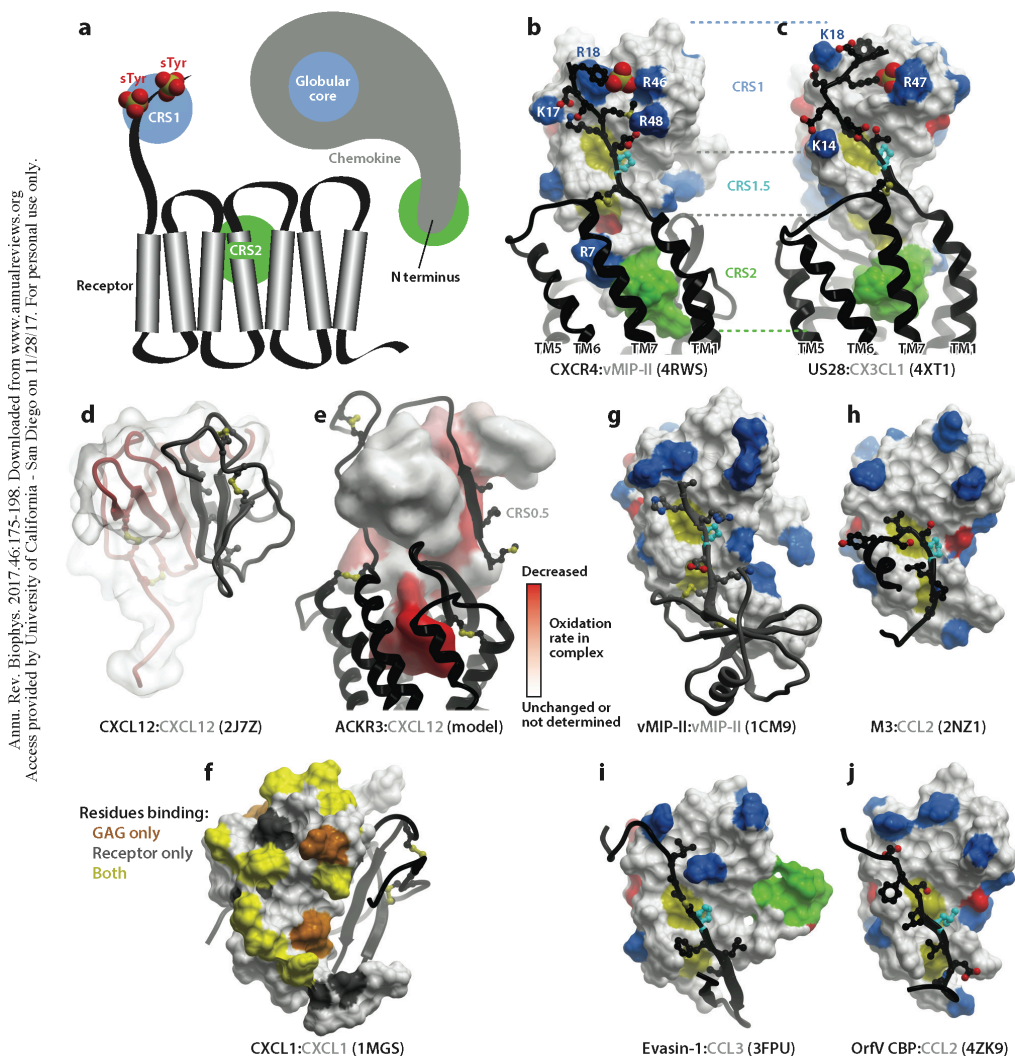
The Architecture of Receptor:Chemokine Complexes as Elucidated by Crystallography and Experimentally Guided Modeling

Apart from earlier structures of rhodopsin (99), breakthroughs in structural studies of GPCRs with intact TM domains started with the 2007 structure of the β_2 -adrenergic receptor (β_2 AR) (19, 110) and were followed by structures of other GPCRs, including chemokine receptors (131, 143). In 2015, the first structure of a chemokine receptor in complex with a chemokine was solved: that of human CXCR4 in complex with a viral chemokine antagonist vMIP-II (104). Shortly thereafter, the structure of the viral chemokine receptor US28 was solved in complex with the human chemokine agonist CX3CL1 (15). Both the CXCR4:vMIP-II and US28:CX3CL1 structures demonstrated the CRS1 and CRS2 interactions of the two-site model; however, in both structures density was missing for much of the receptor N termini, including Tyr residues known to be sulfated. The observed parts of the receptor N termini were bound in pockets defined by the chemokine N and 40s loops (CRS1). Modeling of sulfotyrosines proximal to the observed N termini of the receptors allowed their placement in favorable positions in the N loop/40s loop groove for interaction with basic residues of the chemokines (**Figure 2b,c**). Although more structures will be needed for confirmation, it seems likely that the N loop/40s loop interaction with receptor N termini will be a common CRS1 feature of most complexes. For example, the binding of a small inhibitor to this pocket in CXCL12 (119) validated it as a hot spot and closely paralleled the predicted interactions of the CXCR4 N terminus in a model of the CXCR4:CXCL12 complex (68, 104).

As expected, the N terminus of each chemokine was observed to bind in a large, wide-open polar pocket defined by the 7TM bundle (CRS2) of its receptor (**Figure 2b,c**). In this pocket, the chemokines directly contact residues at key positions involved in signal initiation in many other GPCRs. Despite this trend, the features of CRS2 interactions appear to be receptor- and chemokine-specific, in line with the variation of the binding pockets for small molecule ligands in GPCRs (63).

A surprising observation in both receptor:chemokine structures was how extensive, in fact virtually contiguous, the interaction interface was, which prompted the naming of an intermediate

interaction site as CRS1.5 (Figure 2b,c) (104). Located between CRS1 and CRS2, this region is centered on a conserved Pro-Cys motif of the receptor N terminus that packs against the conserved disulfide of the chemokines. Interestingly, these interactions result in the formation of an antiparallel β -sheet similar to those observed in the respective chemokine dimer interfaces (Figure 1c), and this explains in part, why CC chemokines cannot bind receptors as dimers



(58, 129). In contrast, the geometry of CXC chemokine dimers permits them to bind and activate receptors (104), although they tend to have lower affinity and altered pharmacology compared with the respective monomeric chemokines (32, 91, 106, 137). When the receptors from the CXCR4:vMIP-II and the US28:CX3CL1 structures are superimposed, the root mean square deviation of the chemokines is as large as 8.3 Å, suggesting that CRS1.5 acts as a pivot that allows chemokines to differentially engage the extracellular loops of the receptor (known as ECL2 and ECL3) while maintaining the CRS1 and CRS2 interactions. This may be important for the structural adaptability that enables promiscuous receptor:chemokine interactions, including the binding of a single receptor to multiple ligands that have very low sequence homology.

Other experimental data and modeling studies have suggested additional unanticipated receptor:chemokine interaction epitopes (68). In addition to CRS1 and CRS1.5 interactions involving the N terminus of the receptor proximal to the first conserved Cys, several reports have suggested involvement of the receptor distal N terminus. For example, mutation or deletion of amino acids within the first 10 residues of the receptor has been shown to affect chemokine binding or receptor activation in the case of CXCR4:CXCL12 (12, 142) and CXCR2 with CXCL1, CXCL7, and CXCL8 (62). An NMR structure of CXCL12 in complex with an N-terminal peptide (residues 1–38) from CXCR4 suggests that the distal end pairs with the β_1 -strand of CXCL12 (120), a region also implicated by cross-saturation NMR experiments (67). Mutagenesis and chemical shift perturbation studies of CXCR1:CXCL8 also support a role for the CXCL8 β_1 -strand (59, 78), as well as a potential direct interaction of the chemokine β_1 -strand with the receptor N terminus (59). Finally, a recent radiolytic footprinting, disulfide cross-linking, and molecular modeling study of ACKR3:CXCL12 suggested interactions between the ACKR3 distal N terminus and the CXCL12 β_1 -strand (48). The constraints imposed by the TM domain of the receptor, as well as disulfide cross-links between ACKR3 and CXCL12, suggest that the interaction results in the formation of an antiparallel β -sheet between receptor and chemokine (Figure 2*d,e*) in contrast to the parallel β -sheet suggested by NMR studies (120). The compatibility of this antiparallel orientation with earlier models of CXCR4:CXCL12 (70, 104) also prompted the proposal of a similar extended model for CXCR4:CXCL12 (not shown). Although structures of additional receptor:chemokine complexes will be required to obtain precise details, it is interesting to note that an antiparallel β -sheet would mimic the interface of CXC chemokine dimers (Figure 2*d*), analogous to the CRS1.5 region of the CXCR4:vMIP-II and US28:CX3CL1 structures that mimics the dimer interfaces of CC and CX3C chemokines. Regardless of orientation, this interaction has sufficient support to deserve a name, and we refer to it as CRS0.5, in line with the CRS1, 1.5, and 2 nomenclature.

The extent and distributed nature of receptor:chemokine interfaces explain why mutation of individual receptor or chemokine residues, particularly those involving CRS1, rarely has a dramatic

←

Figure 2

Chemokine interaction with receptors and other binding partners. (*a*) Canonical two-site model of receptor:chemokine recognition. (*b,c*) Structures of receptor:chemokine complexes solved in 2015 (CXCR4:vMIP-II and US28:CX3CL1) are consistent with the two-site model. Important basic residues on the chemokines are highlighted in blue. The chemokine N terminus is highlighted in green. The Pro residue of the receptor Pro-Cys motif is colored cyan and packs up against the conserved disulfide of the chemokine (yellow). Proximal sulfonyl residues from the receptor N terminus were modeled and are shown with the sulfate colored red and yellow. (*d,e*) The CXC chemokine dimerization geometry (*d*) is closely mimicked by the hypothetical interaction of the distal receptor N terminus with the β_1 -strand of the chemokine in the modeled ACKR3:CXCL12 complex (*e*). The prediction is supported by radiolytic footprinting data. (*f*) The binding interface of CXCL1, consisting of the proximal N terminus of the chemokine and its N loop/40s loop groove, is shared by GAGs and the receptor. (*g-j*) CC chemokine dimers and pathogen chemokine binding proteins share receptor binding interfaces and geometry. Protein Data Bank identification numbers are given in parentheses. Abbreviations: CBP, chemokine binding protein; CRS, chemokine recognition site; GAGs, glycosaminoglycans; OrfV, Orf virus.

impact on binding or signaling (142). Unless the mutated residue is an interaction hot spot (9), multiple mutations or truncations are typically required to produce a significant effect.

Repurposing of Chemokine Interfaces

Regions of chemokines corresponding to CRS1.5 and CRS0.5 represent interfaces that are repurposed for interactions with chemokine receptors versus other binding partners. These interfaces facilitate, respectively, CC and CXC chemokine oligomerization, which is critical for their high affinity binding to GAGs. However, when chemokine oligomers dissociate, these oligomerization interfaces become available, and given their propensity to mediate protein:protein interactions (68), it is not surprising that they are repurposed for binding receptors and other proteins.

Chemokine dimer interfaces are not the only repurposed regions. Many chemokines, such as CCL2 and CXCL1 show significant overlap between residues important for receptor binding and those important for GAG binding, where both sets map to the N loop/40s loop groove (Figure 2*f*). For both CCL2 and CXCL1, the groove features a number of basic residues and the receptor N termini feature acidic residues and validated (CCR2) or predicted (CXCR1) sulfated Tyr residues (51, 75, 118, 130). Similar to receptor N termini, GAGs are rich in acidic moieties and they must be sulfated to bind virtually all chemokines with high affinity (34). Thus, interface repurposing contributes to the ability of some chemokines (especially CC) to bind both receptors and GAGs, but in a mutually exclusive manner.

Interface repurposing is also prevalent in complexes of chemokines with chemokine binding proteins (CBPs) from viruses and ticks (23, 76, 144) that target and neutralize chemokines to suppress the immune response. For example, a dimer of the γ -herpesvirus CBP M3 features a cleft where chemokines bind (1). In the case of an M3:CCL2 complex, the C-terminal domain of M3 interacts with the chemokine by positioning a Pro against the conserved chemokine disulfide (Figure 2*b*), similar to the interaction observed in chemokine:chemokine dimers (Figure 2*g*) and receptor:chemokine complexes (Figure 2*b,c*). The M3 N-terminal domain binds to the N loop/40s loop groove; and similar to receptor N termini or GAGs, this domain is highly acidic and complementary to the basic surfaces of chemokines (not shown). Thus the M3:chemokine interaction mimics both receptor:chemokine and GAG:chemokine interactions, and as such, effectively blocks the chemokine from its two main functions. Moreover, a comparison of a panel of CBPs from multiple viruses and ticks showed universal targeting of the variable chemokine N loop and the invariant disulfide (Figure 2*i,j*) (76). The repurposing of these interfaces and motifs in multiple unrelated complexes suggests they have a role as fundamental determinants of chemokine interactions and can serve as reliable guides for future computational docking studies.

INSIGHTS INTO RECEPTOR ACTIVATION FROM EXPERIMENTS INTERPRETED IN THE CONTEXT OF STRUCTURES AND MODELS

GPCRs exist in equilibrium between multiple conformational states that can be defined as active or inactive based on their ability to couple to downstream effectors (G proteins or β -arrestins) (29, 80). Ligand binding shifts the equilibrium toward one of the states, which effectively defines ligand pharmacology. The chemokine receptor structures solved thus far represent a wide range of conformational states: the CX3CL1-complexed US28 is in an active state; the maraviroc-bound CCR5 and all structures of CXCR4 are inactive; and a recent double antagonist-bound CCR2 structure has the conformational signature of a deep inactive state (15, 104, 148). However,

these static structures do not reveal the intricate and dynamic details of the residue network that couples agonist binding at the extracellular side to the intracellular conformational changes. Recent mutagenesis and radiolytic footprinting efforts, in combination with structural models, have provided important residue-specific clues into the mechanism of activation in the context of CXCR4 and ACKR3 (48, 142).

Intramolecular Signal Transmission Network in CXCR4

Using a high-throughput shotgun mutagenesis approach covering every amino acid of CXCR4, Wescott and coworkers (142) identified residue positions where mutations disrupted CXCL12-induced receptor signaling. The mutations may exert their effect through several mechanisms, such as biasing the receptor's conformational equilibrium, disrupting chemokine or G protein binding, or disrupting the intramolecular communication network. Interestingly, when mapped onto active- and inactive-state models of CXCR4: CXCL12 (104), about one-half of the identified residues formed a continuous chain connecting CXCL12 binding residues in the receptor extracellular pocket to the intracellular G protein-coupling residues. These residues were clustered into five functional layers and their roles tentatively assigned as (a) chemokine engagement, (b) signal initiation, (c) signal propagation, (d) activation microswitches, and (e) G protein coupling (Figure 3a-f) (142).

The residues in the chemokine engagement layer form a solvent-accessible ring in the receptor CRS2 (Figure 3a) and are predicted to capture the proximal N terminus of the chemokine while directing the distal N terminus toward signal initiator residues in the base of the binding pocket (Figure 3b). The initiator residue E288^{7,39} [superscript denotes Ballesteros-Weinstein numbering of residues in GPCRs (4)] engages the side chain of CXCL12 residue K1, which orients CXCL12 P2 for interaction with other initiator residues, W94^{2,60} and Y116^{3,32} (Figure 3c). K1 and P2 in CXCL12 are critical activation determinants, as deletion or mutation of K1 or substitution of P2 by Gly results in complete loss of agonist activity (24). The models suggest that K1 deletion or substitution leads to a loss of contact with, respectively, the engagement residue D97^{2,63} or the initiator residue E288^{7,39}. The antagonism of the P2G mutant may be due to loss of steric contact with initiator residues W94^{2,60} and Y116^{3,32} (Figure 3c).

Along with binding to the distal N terminus of the chemokine, the initiator residues contact the signal propagation residues in the TM7 part of the receptor core (Figure 3d). These, in turn, make contact with W252^{6,48} of the CWxP rotamer motif and could thereby communicate structural shifts to helix VI, which is known to undergo the largest conformational changes upon activation (36, 42, 64, 109). Within the signal propagation group, a sequential cluster of residues (V242^{6,38}-ILLLA-F248^{6,44}) in the intracellular half of helix VI appears to act as a bridge connecting W252^{6,48} to the key intracellular GPCR signaling motifs, including the DRY box and NPxxY and Y(x)₅KL microswitch motifs (Figure 3d) (64). The results of the Wescott et al. mutagenesis study (142) suggest that the bridge region must be hydrophobic and strictly helical; moreover, evaluation in the context of active- and inactive-state models demonstrates that the bridge undergoes significant repacking with respect to the conserved signaling microswitches. Therefore, its helical hydrophobic nature may enable it to serve as a lubricant for helix and side chain repacking during the conformational transition.

To transition from an inactive to active state, the conserved microswitch residues Y219^{5,58} and Y302^{7,53} [parts of, respectively, the Y(x)₅KL and NPxxY motifs, and both identified in the study by Wescott et al. (142)] undergo major repositioning that brings them in close proximity inside the TM bundle to support a G protein-compatible interface (Figure 3e) (43). Finally, R134^{3,50} and

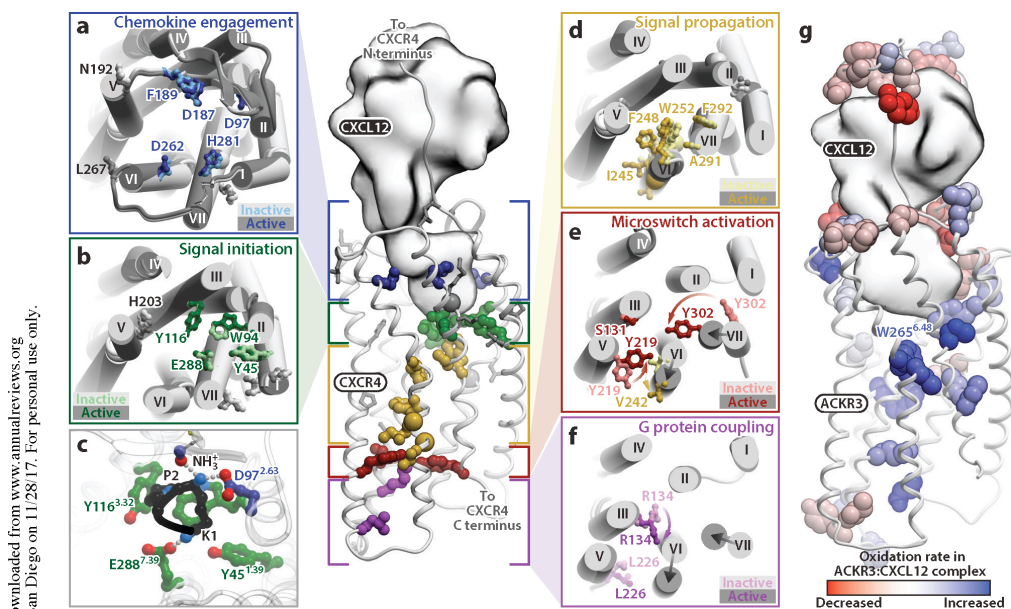


Figure 3

Insights into chemokine receptor activation. (a–f) Residues critical for CXCL12-induced activation of CXCR4 were identified and mapped onto inactive- and active-state models of the CXCR4: CXCL12 complex. (a, b, d–f) Five structural and functional layers are shown in the context of the full structure (center) and enlargements: (a) chemokine engagement (blue), (b) signal initiation (green), (d) signal propagation (yellow), (e) microswitch activation (red), and (f) G protein coupling (purple). Predicted residue conformations in the inactive and active states are shown in lighter and darker colors, respectively. (c) The proposed geometry of the interaction between the CXCL12 distal N terminus (a critical signaling domain, black) and chemokine-engagement (blue) and signal-initiation (green) residues of CXCR4. (g) Radiolytic footprinting mapping of residue solvent exposure in the atypical chemokine receptor ACKR3. Residues protected by the chemokine (as compared with a small molecule-bound state) are shown in shades of red. These residues are mostly located in the N terminus and the extracellular loops of the receptor. However, numerous residues within the transmembrane domain become less protected in the chemokine-bound state; these residues report on increased solvent exposure of the transmembrane core due to conformational changes upon chemokine-induced full activation of ACKR3. In the residue numbering, superscript denotes Ballesteros-Weinstein numbers for residues in G protein-coupled receptors. Roman numerals indicate helices.

L226 were identified as critical by the screen and likely represent G protein interaction hotspots because their coupling role is conserved across several GPCRs (Figure 3f) (8, 109).

The interconnected chain of propagation, microswitch, and G protein-coupling residues is likely conserved across all class A GPCRs. This is in agreement with the fact that in multiple GPCRs, activation has been shown to involve uniform conformational changes of evolutionarily conserved structural elements (63, 139). By contrast, the engagement and initiator residues are likely to be most relevant to the chemokine receptor family (63) and even within this family, may be chemokine- and receptor-specific.

Activation of an Atypical Chemokine Receptor

The findings regarding CXCR4 activation are especially interesting when compared with the activation mechanism of the atypical chemokine receptor ACKR3. ACKR3 shares its ligands CXCL11 and CXCL12 with, respectively, CXCR3 and CXCR4 (16) but unlike these receptors, it does not couple to G proteins and signals exclusively through β -arrestin-mediated pathways (92, 105). Thus, ACKR3 provides a unique opportunity to determine the contribution of receptor structure to the activation of one specific intracellular signaling pathway. A recent study of ACKR3 (48) collected more than 100 structural restraints from radiolytic footprinting, disulfide-trapping, and mutagenesis, and utilized molecular modeling to produce experimentally driven models of ACKR3:ligand complexes (**Figure 3g**). By comparing ACKR3 complexes with the small molecule partial agonist CCX777 and with the chemokine full agonist CXCL12, radiolytic footprinting identified two classes of residues: those directly involved in chemokine binding and those undergoing structural transitions during the course of ACKR3 activation. The conformational change upon full agonist binding led to an increased exposure of intracellular residues, reconfiguration of the highly conserved W265^{6,48} residue (of the CWxP rotamer motif), and increased solvent accessibility of the TM region. A number of similarities are apparent between this study involving an atypical receptor and previous studies of GPCRs; for example, the reorientation of W265^{6,48} is consistent with a conformational transition, and the increased solvent accessibility of the intracellular region is consistent with the opening of a binding cleft to accommodate intracellular effectors (60, 109). Furthermore, the results corroborate the hypothesis of activation being mediated by an extensive water-mediated intramolecular polar network in GPCRs (8, 55). Taken together, these results suggest that although ACKR3 exclusively activates β -arrestin-dependent pathways, its active conformation is similar to that of canonical GPCRs.

ON THE ALLOSTERY OF CHEMOKINE RECEPTORS

Upside-Down and Downside-Up Allostery

As detailed in the previous section, GPCRs are fundamentally allosteric machines because their intracellular action (G protein coupling) is controlled by the binding of ligands on the extracellular side (**Figure 4a**) (133). For the most comprehensively studied receptors, it has been demonstrated that allosteric communication works both upside down (i.e., from the extracellular ligand binding site to the intracellular G protein-coupling interface) and downside up. For example, the addition of an extracellular agonist to β_2 AR results in conformational changes at the intracellular ends of receptor TM helices (45, 71, 108) and enhances the stability of receptor:G protein complexes (upside down) (145). Similarly, the addition of either G protein or a G protein-mimicking nanobody Nb80 (125), both of which bind intracellularly, affects the affinity and binding kinetics of extracellular agonists (downside up) (30, 108). The bidirectional communication works not only in the context of receptor activation but also in inactivation: Inactive-state-specific intracellularly binding nanobodies and antibodies reduce receptor affinity for extracellular agonists and increase affinity for inverse agonists (52, 124).

These insights were obtained for β_2 AR and the adenosine A_{2A} receptor ($AA_{2A}R$), but they likely apply to most other GPCRs, including chemokine receptors. For CCR5 and CXCR4, high affinity chemokine agonist binding cannot be achieved without receptor coupling to a nucleotide-free G protein α -subunit (**Figure 4a**) (20, 94, 123). On the contrary, for CCR2, intracellularly binding synthetic antagonists inhibit the binding of the chemokine agonist CCL2, while increasing the binding of extracellularly acting antagonists (152, 153). All of these observations are consistent with the idea of chemokine receptors being allosterically regulated upside down and downside up, similar to β_2 AR and the $AA_{2A}R$ (**Figure 4a**).

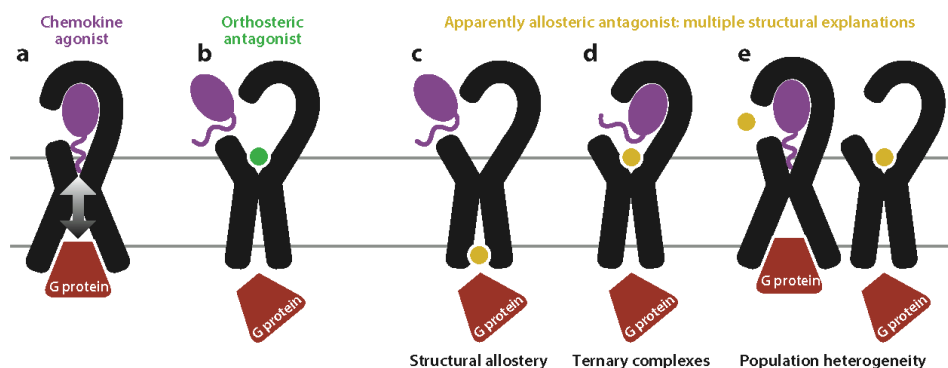


Figure 4

The allosteric nature of chemokine receptor activation and inhibition. (a) Extracellular chemokine binding translates into intracellular G protein coupling, and communication also works in reverse, with G protein binding enhancing the affinity of chemokines. (b) Orthosteric antagonists directly block the binding of chemokines in the CRS2 (chemokine recognition site 2) ligand binding pocket. (c–e) The apparently allosteric behavior of chemokine receptor antagonists can have multiple explanations, including binding at a site distinct from the chemokine (c), occupying a part of the extensive chemokine interaction interface while allowing the formation of a ternary complex (d), or binding to a distinct subpopulation of receptors (e). The latter can happen in heterogeneous receptor populations in which the G protein–coupled subpopulation preferentially binds the chemokine agonist while the uncoupled subpopulation binds small molecule antagonists.

“Orthosteric Allostery” of Chemokine Receptor Antagonists

Small molecule antagonists of chemokine receptors interfere with chemokine binding, G protein coupling, or both, and it is now clear that they can do so by binding intracellularly or extracellularly (Figure 4b–e). Intracellular antagonists are, by definition, allosteric with respect to chemokines (Figure 4c). However, even extracellularly binding small molecules that (presumably) spatially overlap with the bound chemokine can also demonstrate apparent allosteric behavior (Figure 4d,e). Many small molecule antagonists of CCR5 [e.g., TAK-779, SCH-C (126), SCH-D (vicriviroc), or aplaviroc] inhibit chemokine [e.g., CCL3 (MIP-1 α) and CCL4 (MIP-1 β)] binding and chemokine-induced Ca²⁺ mobilization in an insurmountable manner (88, 141). By contrast, chemokine inhibition of antagonist binding is surmountable with increasing concentrations of antagonist. For other chemokines [e.g., CCL5 (RANTES)], antagonists may allow residual binding (e.g., maraviroc and SCH-D) or may not inhibit chemokine binding at all (aplaviroc) (141). The small molecule CCR1 antagonist UCB-35625 has been shown to effectively disrupt receptor function with minimal effects on chemokine binding (113). An allosteric, non-competitive mechanism has also been demonstrated for DF1681Y (repertaxin or reparixin) (5), an antagonist of CXCR1 and CXCR2 that is currently in clinical trials (ClinicalTrials.gov identifiers: NCT01817959, NCT01967888, and NCT02370238).

Such complicated, probe-dependent inhibition mechanisms often lead to the classification of small molecule antagonists (including maraviroc for CCR5, UCB-35625 for CCR1, and DF1681Y for CXCR1 and CXCR2) as allosteric (40). Nevertheless, the X-ray structure of the CCR5:maraviroc complex (131) and subsequent structures of chemokine-bound complexes of homologous receptors (15, 104) suggest that the binding site of maraviroc overlaps with CRS2—that is, with the TM domain pocket of the receptor that also accommodates the N terminus of the

chemokines (Figure 5a,b). Similarly, mutational studies have suggested that UCB-35625 binds in the orthosteric pocket of CCR1 (28) and that DF1681Y binds in the orthosteric pocket of CXCR1 and CXCR2 (6).

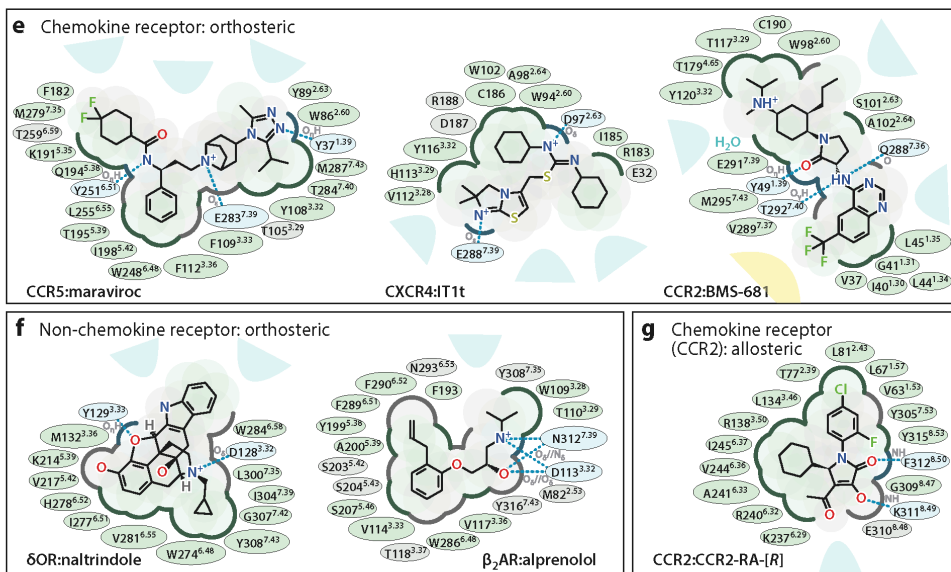
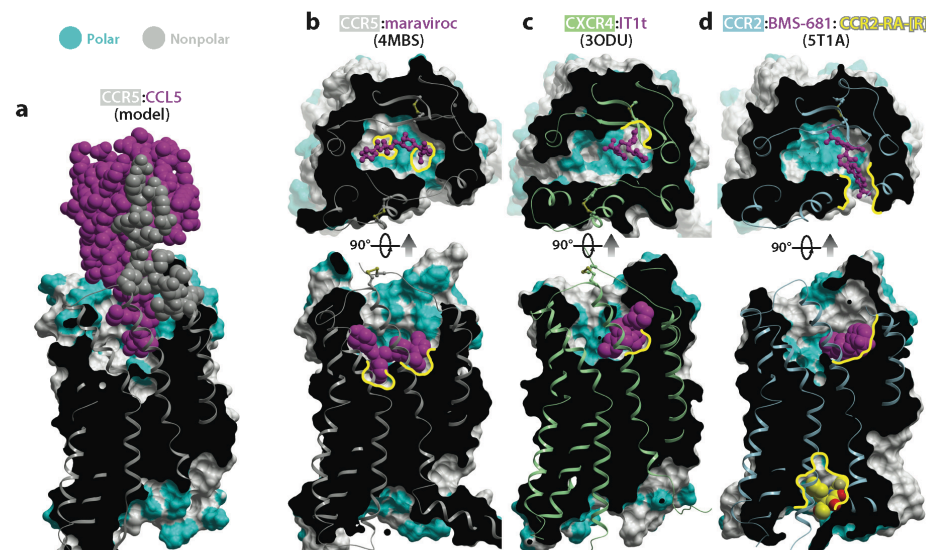
Based on these findings, the noncompetitive behavior of such antagonists must have a different explanation than simply binding at an alternative, nonoverlapping site of the receptor. One possibility is related to the distributed nature of receptor:chemokine interfaces: Receptors that mostly depend on CRS1 for chemokine binding could conceivably allow simultaneous binding of chemokines at CRS1 and small molecules at CRS2, resulting in the formation of ternary complexes (Figure 4d) (79). This phenomenon has been recently described in great detail for heterobivalent ligands and is also sometimes referred to as partial competition (134). The large volume and flexibility of the receptor pocket (CRS2) may also make it permissive to ternary complex formation. Alternatively, these effects may be explained by the presence of a mixed population of receptors in cells: Receptors that are coupled to G protein have different ligand preferences compared with uncoupled receptors (20), allowing for the apparent simultaneous binding of both types of ligands (Figure 4e). Apart from a structural explanation, unusually slow dissociation kinetics of the chemokine probe or the test compound can translate into what appears as insurmountable inhibition on the timescale of a typical experiment.

“Allosteric Allostery” of Chemokine Receptor Antagonists

By contrast with the apparently allosteric antagonists that bind in the extracellular, orthosteric pocket of the receptors, a number of chemokine receptor antagonists have been unambiguously demonstrated to bind elsewhere. For CCR4, antagonists of the pyrazinyl sulfonamide series require intracellular access for activity and lose efficacy when the intracellular part of helix VII and the C terminus of CCR4 are replaced with homologous regions from CCR5 (2). For CXCR2, several compounds [Pteridone-1, Navarixin (SCH 527123 or MK-7123), and the diarylurea SB265610] have been demonstrated via site-directed mutagenesis to depend on intracellular residues (114). For the diarylurea SB265610, mapping of the intracellular binding site followed the discovery of its ability to inhibit binding of [¹²⁵I]-CXCL8 as well as the functional response to multiple chemokines in a noncompetitive, insurmountable manner (11).

For CCR2, numerous chemotypes of acidic antagonists have been described (13, 14, 25, 66, 84, 100). The potency and efficacy of these antagonists are not affected by mutations in the orthosteric pocket (84); their presence does not interfere with the binding of canonical orthosteric antagonists (152, 153) but their ability to inhibit function is insurmountable (153). For several compounds, the binding site was directly mapped to an intracellular pocket contacting helices VI, VII, and VIII (152). Finally, a recent crystallographic study of CCR2 confirmed that one of these antagonists, CCR2-RA-[R] (25), does indeed bind intracellularly (Figures 4c and 5d) (148).

The binding of small molecules to the intracellular side of CCR2 is possible because this receptor has a sufficiently large cavity between the intracellular ends of helices I, II, VI, and VII. Crystallography suggests that CCR2-RA-[R] binds through a balanced combination of nonpolar and polar interactions within the cavity, the latter through hydrogen bonding with the exposed backbone amides of CCR2 helix VIII. Both the volume and the hydrogen bonding capacity of this cavity depend on the Gly residue at position 8.47 (G309^{S.47} in CCR2). The residues lining the cavity are characterized by moderate to high conservation within the chemokine receptor family, and G^{S.47} is conserved in most of them. The fact that some of the intracellularly binding CCR2 antagonists have only moderately weaker potencies against CCR1 (100) and CCR5 (152) supports the existence of a homologous cavity in these receptors. The binding site of several CXCR1 and CXCR2 antagonists was also mapped to a homologous region through mutagenesis (93, 114) and



competition binding studies (27). Moreover, an X-ray structure has recently been solved for CCR9 with an allosteric antagonist vercirnon bound at a homologous site (96).

The numerous structural mechanisms for the apparent allostery of chemokine receptor antagonists (Figure 4c–e) have important implications for the design of receptor-targeting therapeutics, as does deciphering these mechanisms by means of structural biology and molecular modeling.

ON THE DRUGGABILITY OF CHEMOKINE RECEPTORS

Given the prominent roles of chemokine receptors in disease and the extensive drug discovery efforts that have been deployed to develop drugs targeting the chemokine system, the success stories of approved therapeutics have been disproportionately low. The biological challenges of targeting these receptors have been described in many reviews, as summarized in the Introduction (54, 103, 115, 121). A challenge that has received less consideration is related to the nuances of the chemokine receptors as targets where recent structures have been particularly revealing.

The Physicochemical Challenges of Receptor:Chemokine Interfaces

Even though chemokine receptors belong to the superfamily of GPCRs (targeted by a huge fraction of approved small molecule drugs), they have evolved to bind proteins such as chemokines (Figure 5a). As for many other protein:protein interfaces, receptor interfaces with chemokines are extensive, comparatively flat, flexible, and excessively polar; they lack hydrophobicity and enclosure: the two features associated with the concept of druggability (21). As such, they are conceptually challenging targets for small molecules.

Only three orthosteric small molecule antagonists have been crystallized with chemokine receptors so far: the CXCR4 antagonist isothiourrea IT1t (132, 143); the above-mentioned HIV-entry CCR5 inhibitor maraviroc (131); and BMS-681, a potent dual affinity CCR2 and CCR5 antagonist (Figure 5b–d) (17, 148). Owing to the conformational plasticity of the respective receptor pockets, each crystallized antagonist finds and utilizes a unique enclosed nonpolar subpocket. Nevertheless, the high degree of solvent exposure for all three crystallized antagonists, as well as their scarce hydrophobic anchoring to the pocket surface (Figure 5b–e), are in stark contrast with other GPCR antagonists, for example naltrindole (an opioid receptor antagonist) and aprenolol (a β_2 AR antagonist) (Figure 5f). It surely is not by chance that most disclosed chemokine receptor antagonist series consist of large, polar, flexible molecules, which may negatively impact their oral bioavailability, metabolic stability, and other pharmacokinetic properties (101).

Figure 5

Structural basis of small molecule antagonism of chemokine receptors. (a) Receptors (grey) interact with chemokines (magenta) via extensive interfaces with numerous polar contacts (cyan); the interaction is additionally reinforced by the flexible N terminus of the receptor (CRS1, or chemokine recognition site 1) essentially wrapping around the chemokine. Like most protein:protein interactions, chemokine:receptor interactions are conceptually difficult to inhibit with small molecules. (b–d) Structures of chemokine receptors with small molecule antagonists: (b) CCR5:maraviroc, (c) CXCR4:IT1t, and (d) CCR2 in a ternary complex with BMS-681 and CCR2-RA-[R]. Each molecule explores a unique nonpolar subpocket (yellow) within the overall large and polar (i.e., poorly druggable) binding pocket. (e) All three crystallized orthosteric small molecule antagonists of chemokine receptors demonstrate a low degree of enclosure and a high degree of solvent exposure. (f) This is in stark contrast with small molecule antagonists of non-chemokine G protein-coupled receptors. (g) The crystallized allosteric antagonist of CCR2 binds in an intracellular pocket with favorable druggability properties and demonstrates a high degree of enclosure. Protein Data Bank identification numbers are given in parentheses. In the residue numbering, superscript denotes Ballesteros–Weinstein numbers for residues in G protein-coupled receptors.

The Ultimate Pharmacodynamic–Pharmacokinetic Conflict in Small Molecule Antagonists of Chemokine Receptors

To aggravate the challenges even further, several studies have suggested that achieving therapeutic endpoints in inflammatory and autoimmune diseases requires that an unusually large fraction of the target receptor (90–95%) is occupied (and inhibited) at all times during the course of treatment (115). This imposes constraints on the potency, residence time (140), selectivity, and toxicity parameters of chemokine receptor drug candidates that far exceed typical ranges for other targets. In combination with the inherently poor druggability of the receptor:chemokine interfaces, it creates a conflict between the requirements of pharmacodynamics and pharmacokinetics and makes the discovery and development of successful, competitive, small molecule chemokine receptor antagonists a daunting task.

Biologics and Biomimetics

Because of the small molecule challenge, biologics and biomimetics have attracted attention as alternative chemotypes for inhibiting receptor:chemokine interactions. For example, in the case of CXCR4, a series of cyclized peptides originating from the horseshoe crab antimicrobial peptide polyphemusin II [T22 and T140 series (127, 128)] has been well characterized (73, 86, 147). CVX15, a member of this series, was crystallized with CXCR4 in 2010 (143), demonstrating a much better fit with the binding pocket than could ever be achieved with a small molecule. Other biologic scaffolds used for antagonist development include engineered chemokines (10, 50, 122), as well as nanobodies and antibodies (47, 56, 57, 61, 81, 136). Mogamulizumab, a monoclonal antibody targeting CCR4, recently became the first biologic to be approved for cutaneous T cell lymphoma (33). In a complementary effort, antibodies (7, 149) and therapeutic nucleotides (35, 53, 95) are pursued as agents targeting chemokines. With all of these agents, oral availability is out of the question; however, various approaches to improving metabolic stability have been successful (18, 95). In combination with the ample potential for optimizing receptor inhibition properties, this suggests that biologics and biomimetics may become a promising next-generation class of therapeutics targeting the chemokine receptor system.

Allosterics

Fortunately, competitive inhibition of receptor:chemokine interactions is not the only way to counteract receptor signaling. As described in the previous section, mechanisms of chemokine receptor activation suggest possibilities for allosteric regulation and, indeed, numerous allosterically acting small molecules have been reported. The recent structure of CCR2 simultaneously bound to two antagonists (148) provided for the first time the opportunity to directly compare the physicochemical and druggability properties of the orthosteric pocket with those of an allosteric site in a chemokine receptor. The comparison is clearly in favor of the allosteric pocket! Unlike the orthosteric site, it is of a favorable size (not too large and not too small), well enclosed, and possesses a balanced combination of hydrophobic and polar features. The degree to which the cocrystallized allosteric antagonist CCR2-RA-[R] is buried from solvent (**Figure 5d,g**) is more reminiscent of the close-to-ideal case of β_2 AR antagonists (**Figure 5f**) than of the orthosteric antagonists of chemokine receptors (**Figure 5e**). A similar trend is observed with vercirnon, the crystallized allosterically acting antagonist of CCR9 (not shown) (96).

Of course, an additional challenge posed by the allosteric inhibition approach is that intracellularly acting antagonists must be cell permeable. Nevertheless, the favorable druggability properties

of the allosteric pocket, and the fact that it appears to be present in other receptors, may open a new avenue for chemokine receptor inhibition. The structures of CCR2:BMS-681:CCR2-RA-[R] (148) and CCR9:vercimon (96) complexes will undoubtedly facilitate rational drug discovery efforts for these and possibly for other chemokine receptors through ligand-informed homology modeling (65, 90).

CONCLUSIONS

Although chemokine receptors are promising targets for inflammatory conditions, autoimmune diseases, and cancer, targeting them has so far delivered only a small number of successful therapeutics. Drug discovery failures are caused in part by the complex and poorly understood biology of receptors and chemokines, and in part by the inherently challenging nature of receptor:chemokine interactions as targets for small molecule development. Recent years have brought several breakthroughs in understanding of the structural basis of receptor interactions with chemokines and small molecules, as well as receptor activation, antagonism, and allosteric regulation. Structures and models may help address the major drug discovery hurdles, and accelerate the discovery of drugs targeting the chemokine receptor axis.

DISCLOSURE STATEMENT

The authors are not aware of any affiliations, memberships, funding, or financial holdings that might be perceived as affecting the objectivity of this review.

ACKNOWLEDGMENTS

This work was partially supported by grants from the US National Institutes of Health (R01 GM071872, R01 AI118985, R21 AI121918, R21 AI122211, and R01 GM117424).

LITERATURE CITED

- Alexander-Brett JM, Fremont DH. 2007. Dual GPCR and GAG mimicry by the M3 chemokine decoy receptor. *J. Exp. Med.* 204:3157–72
- Andrews G, Jones C, Wreggett KA. 2008. An intracellular allosteric site for a specific class of antagonists of the CC chemokine G protein-coupled receptors CCR4 and CCR5. *Mol. Pharmacol.* 73:855–67
- Baggiolini M. 1998. Chemokines and leukocyte traffic. *Nature* 392:565–68
- Ballesteros JA, Weinstein H. 1995. Integrated methods for the construction of three-dimensional models and computational probing of structure-function relations in G protein-coupled receptors. In *Methods in Neurosciences: Receptor Molecular Biology*, ed. SC Sealfon, pp. 366–428. San Diego: Academic
- Bertini R, Allegretti M, Bizzarri C, Moriconi A, Locati M, et al. 2004. Noncompetitive allosteric inhibitors of the inflammatory chemokine receptors CXCR1 and CXCR2: prevention of reperfusion injury. *PNAS* 101:11791–96
- Bertini R, Barcelos LS, Beccari AR, Cavalieri B, Moriconi A, et al. 2012. Receptor binding mode and pharmacological characterization of a potent and selective dual CXCR1/CXCR2 non-competitive allosteric inhibitor. *Br. J. Pharmacol.* 165:436–54
- Blanchetot C, Verzijl D, Mujić-Delić A, Bosch L, Rem L, et al. 2013. Neutralizing nanobodies targeting diverse chemokines effectively inhibit chemokine function. *J. Biol. Chem.* 288:25173–82
- Blankenship E, Vahedi-Faridi A, Lodowski DT. 2015. The high-resolution structure of activated opsin reveals a conserved solvent network in the transmembrane region essential for activation. *Structure* 23:2358–64
- Bogan AA, Thorn KS. 1998. Anatomy of hot spots in protein interfaces. *J. Mol. Biol.* 280:1–9

10. Bönsch C, Munteanu M, Rossitto-Borlat I, Fürstenberg A, Hardley O. 2015. Potent anti-HIV chemokine analogs direct post-endocytic sorting of CCR5. *PLoS ONE* 10:e0125396
11. Bradley ME, Bond ME, Manini J, Brown Z, Charlton SJ. 2009. SB265610 is an allosteric, inverse agonist at the human CXCR2 receptor. *Br. J. Pharmacol.* 158:328–38
12. Brelot A, Heveker N, Montes M, Alizon M. 2000. Identification of residues of CXCR4 critical for human immunodeficiency virus coreceptor and chemokine receptor activities. *J. Biol. Chem.* 275:23736–44
13. Brown GD, Shi Q, Delucca GV, Batt DG, Galella MA, et al. 2016. Discovery and synthesis of cyclohexenyl derivatives as modulators of CC chemokine receptor 2 activity. *Bioorg. Med. Chem. Lett.* 26:662–66
14. Buntinx M, Hermans B, Goossens J, Moechars D, Gilissen RAHJ, et al. 2008. Pharmacological profile of JNJ-27141491 [(S)-3-[3,4-Difluorophenyl]-propyl]-5-isoxazol-5-yl-2-thioxo-2,3-dihydro-1H-imidazole-4-carboxyl acid methyl ester], as a noncompetitive and orally active antagonist of the human chemokine receptor CCR2. *J. Pharmacol. Exp. Ther.* 327:1–9
15. Burg JS, Ingram JR, Venkatakrishnan AJ, Jude KM, Dukkipati A, et al. 2015. Structural basis for chemokine recognition and activation of a viral G protein-coupled receptor. *Science* 347:1113–17
16. Burns JM, Summers BC, Wang Y, Melikian A, Berahovich R, et al. 2006. A novel chemokine receptor for SDF-1 and I-TAC involved in cell survival, cell adhesion, and tumor development. *J. Exp. Med.* 203:2201–13
17. Carter PH, Brown GD, Cherney RJ, Batt DG, Chen J, et al. 2015. Discovery of a potent and orally bioavailable dual antagonist of CC chemokine receptors 2 and 5. *ACS Med. Chem. Lett.* 6:439–44
18. Cerini F, Landay A, Gichinga C, Lederman MM, Flyckr R, et al. 2008. Chemokine analogues show suitable stability for development as microbicides. *J. Acquir. Immune. Defic. Syndr.* 49:472–76
19. Cherezov V, Rosenbaum DM, Hanson MA, Rasmussen SGF, Thian FS, et al. 2007. High-resolution crystal structure of an engineered human β_2 -adrenergic G protein-coupled receptor. *Science* 318:1258–65
20. Colin P, Benureau Y, Staropoli I, Wang Y, Gonzalez N, et al. 2013. HIV-1 exploits CCR5 conformational heterogeneity to escape inhibition by chemokines. *PNAS* 110:9475–80
21. Cooke RM, Brown AJ, Marshall FH, Mason JS. 2015. Structures of G protein-coupled receptors reveal new opportunities for drug discovery. *Drug Discov. Today* 20:1355–64
22. Copeland RA. 2016. The drug-target residence time model: a 10-year retrospective. *Nat. Rev. Drug Discov.* 15:87–95
23. Couñago RM, Knapp KM, Nakatani Y, Fleming SB, Corbett M, et al. 2015. Structures of orf virus chemokine binding protein in complex with host chemokines reveal clues to broad binding specificity. *Structure* 23:1199–213
24. Crump MP, Gong JH, Loetscher P, Rajarathnam K, Amara A, et al. 1997. Solution structure and basis for functional activity of stromal cell-derived factor-1; dissociation of CXCR4 activation from binding and inhibition of HIV-1. *EMBO J.* 16:6996–7007
25. Dasse O, Evans J, Zhai H-X, Zou D, Kintigh J, et al. 2007. Novel, acidic CCR2 receptor antagonists: lead optimization. *Lett. Drug Des. Discov.* 4:263–71
26. De Clercq E. 2010. Recent advances on the use of the CXCR4 antagonist plerixafor (AMD3100, MozobilTM) and potential of other CXCR4 antagonists as stem cell mobilizers. *Pharmacol. Ther.* 128:509–18
27. de Kruijf P, van Heteren J, Lim HD, Conti PGM, van der Lee MMC, et al. 2009. Nonpeptidergic allosteric antagonists differentially bind to the CXCR2 chemokine receptor. *J. Pharmacol. Exp. Ther.* 329:783–90
28. de Mendonca FL, da Fonseca PCA, Phillips RM, Saldanha JW, Williams TJ, Pease JE. 2005. Site-directed mutagenesis of CC chemokine receptor 1 reveals the mechanism of action of UCB 35625, a small molecule chemokine receptor antagonist. *J. Biol. Chem.* 280:4808–16
29. Deupi X, Kobilka BK. 2010. Energy landscapes as a tool to integrate GPCR structure, dynamics, and function. *Physiology* 25:293–303
30. DeVree BT, Mahoney JP, Vélez-Ruiz GA, Rasmussen SGF, Kuszak AJ, et al. 2016. Allosteric coupling from G protein to the agonist-binding pocket in GPCRs. *Nature* 535:182–86

31. Dorr P, Westby M, Dobbs S, Griffin P, Irvine B, et al. 2005. Maraviroc (UK-427,857), a potent, orally bioavailable, and selective small-molecule inhibitor of chemokine receptor CCR5 with broad-spectrum anti-human immunodeficiency virus type 1 activity. *Antimicrob. Agents Chemother.* 49:4721–32
32. Drury LJ, Ziarek JJ, Gravel SP, Veldkamp CT, Takekoshi T, et al. 2011. Monomeric and dimeric CXCL12 inhibit metastasis through distinct CXCR4 interactions and signaling pathways. *PNAS* 108:17655–60
33. Duvic M, Pinter-Brown LC, Foss FM, Sokol L, Jorgensen JL, et al. 2015. Phase 1/2 study of mogamulizumab, a defucosylated anti-CCR4 antibody, in previously treated patients with cutaneous T-cell lymphoma. *Blood* 125:1883–89
34. Dyer DP, Salanga CL, Volkman BF, Kawamura T, Handel TM. 2016. The dependence of chemokine-glycosaminoglycan interactions on chemokine oligomerization. *Glycobiology* 26:312–26
35. Eulberg D, Purschke W, Anders H-J, Selve N, Klusmann S. 2008. Spiegelmer NOX-E36 for renal diseases. In *Therapeutic Oligonucleotides*, ed. J Kurreck, pp. 200–25. Cambridge, UK: Royal Soc. Chem.
36. Farrens DL, Altenbach C, Yang K, Hubbell WL, Khorana HG. 1996. Requirement of rigid-body motion of transmembrane helices for light activation of rhodopsin. *Science* 274:768–70
37. Farzan M, Babcock GJ, Vasilieva N, Wright PL, Kiprilov E, et al. 2002. The role of post-translational modifications of the CXCR4 amino terminus in stromal-derived factor 1 α association and HIV-1 entry. *J. Biol. Chem.* 277:29484–89
38. Feng Y, Broder CC, Kennedy PE, Berger EA. 1996. HIV-1 entry cofactor: functional cDNA cloning of a seven-transmembrane, G protein-coupled receptor. *Science* 272:872–77
39. Gaertner H, Cerini F, Escola J-M, Kuenzi G, Melotti A, et al. 2008. Highly potent, fully recombinant anti-HIV chemokines: reengineering a low-cost microbicide. *PNAS* 105:17706–11
40. Geny PR, Sexton PM, Christopoulos A. 2015. Novel allosteric modulators of G protein-coupled receptors. *J. Biol. Chem.* 290:19478–88
41. Gerard C, Rollins BJ. 2001. Chemokines and disease. *Nat. Immunol.* 2:108–15
42. Gether U, Lin S, Ghanouni P, Ballesteros JA, Weinstein H, Kobilka BK. 1997. Agonists induce conformational changes in transmembrane domains III and VI of the β_2 adrenoceptor. *EMBO J.* 16:6737–47
43. Goncalves JA, South K, Ahuja S, Zaitseva E, Opefi CA, et al. 2010. Highly conserved tyrosine stabilizes the active state of rhodopsin. *PNAS* 107:19861–66
44. Gong JH, Ratkay LG, Waterfield JD, Clark-Lewis I. 1997. An antagonist of monocyte chemoattractant protein 1 (MCP-1) inhibits arthritis in the MRL-*lpr* mouse model. *J. Exp. Med.* 186:131–37
45. Granier S, Kim S, Shafer AM, Ratnala VRP, Fung JJ, et al. 2007. Structure and conformational changes in the C-terminal domain of the β_2 -adrenoceptor: insights from fluorescence resonance energy transfer studies. *J. Biol. Chem.* 282:13895–905
46. Griffith JW, Sokol CL, Luster AD. 2014. Chemokines and chemokine receptors: positioning cells for host defense and immunity. *Annu. Rev. Immunol.* 32:659–702
47. Griffiths K, Dolezal O, Cao B, Nilsson SK, See HB, et al. 2016. I-bodies, human single domain antibodies that antagonize chemokine receptor CXCR4. *J. Biol. Chem.* 291:12641–57
48. Gustavsson M, Wang L, van Gils N, Stephens BS, Zhang P, et al. 2017. Structural basis of ligand interaction with atypical chemokine receptor 3. *Nature Commun.* 8:14135–49
49. Haessler U, Pisano M, Wu M, Swartz MA. 2011. Dendritic cell chemotaxis in 3D under defined chemokine gradients reveals differential response to ligands CCL21 and CCL19. *PNAS* 108:5614–19
50. Hanes MS, Salanga CL, Chowdry AB, Comerford I, McColl SR, et al. 2015. Dual targeting of the chemokine receptors CXCR4 and ACKR3 with novel engineered chemokines. *J. Biol. Chem.* 290:22385–97
51. Hemmerich S, Paavola C, Bloom A, Bhakra S, Freedman R, et al. 1999. Identification of residues in the monocyte chemoattractant protein-1 that contact the MCP-1 receptor, CCR2. *Biochemistry* 38:13013–25
52. Hino T, Arakawa T, Iwanari H, Yurugi-Kobayashi T, Ikeda-Suno C, et al. 2012. G-protein-coupled receptor inactivation by an allosteric inverse-agonist antibody. *Nature* 482:237–40
53. Hoellenriegel J, Zboralski D, Maasch C, Rosin NY, Wierda WG, et al. 2014. The Spiegelmer NOX-A12, a novel CXCL12 inhibitor, interferes with chronic lymphocytic leukemia cell motility and causes chemosensitization. *Blood* 123:1032–39

54. Horuk R. 2009. Chemokine receptor antagonists: overcoming developmental hurdles. *Nat. Rev. Drug Discov.* 8:23–33
55. Huang W, Manglik A, Venkatakrisnan AJ, Laeremans T, Feinberg EN, et al. 2015. Structural insights into μ -opioid receptor activation. *Nature* 524:315–21
56. Jacobson JM, Lalezari JP, Thompson MA, Fichtenbaum CJ, Saag MS, et al. 2010. Phase 2a study of the CCR5 monoclonal antibody PRO 140 administered intravenously to HIV-infected adults. *Antimicrob. Agents Chemother.* 54:4137–42
57. Jahnichen S, Blanchetot C, Maussang D, Gonzalez-Pajuelo M, Chow KY, et al. 2010. CXCR4 nanobodies (VHH-based single variable domains) potently inhibit chemotaxis and HIV-1 replication and mobilize stem cells. *PNAS* 107:20565–70
58. Jin H, Shen X, Baggett BR, Kong X, Li Wang PJ. 2007. The human CC chemokine MIP-1 β dimer is not competent to bind to the CCR5 receptor. *J. Biol. Chem.* 282:27976–83
59. Joseph PRB, Rajarathnam K. 2015. Solution NMR characterization of WTCXCL8 monomer and dimer binding to CXCR1 N-terminal domain. *Protein Sci.* 24:81–92
60. Kang Y, Zhou XE, Gao X, He Y, Liu W, et al. 2015. Crystal structure of rhodopsin bound to arrestin by femtosecond X-ray laser. *Nature* 523:561–67
61. Kashyap MK, Amaya-Chanaga CI, Kumar D, Choi MY, Rassenti LZ, et al. 2015. Targeting the CXCR4–CXCL12 pathway using an anti-CXCR4IgG1 antibody (PF-06747143) in chronic lymphocytic leukemia. *Blood* 126:4162–62
62. Katancik JA, Sharma A, de Nardin E. 2000. Interleukin 8, neutrophil-activating peptide-2 and GRO- α bind to and elicit cell activation via specific and different amino acid residues of CXCR2. *Cytokine* 12:1480–88
63. Kautrich V, Cherezov V, Stevens RC. 2012. Diversity and modularity of G protein-coupled receptor structures. *Trends Pharmacol. Sci.* 33:17–27
64. Kautrich V, Cherezov V, Stevens RC. 2013. Structure–function of the G protein-coupled receptor superfamily. *Annu. Rev. Pharmacol. Toxicol.* 53:531–56
65. Kautrich V, Rueda M, Abagyan R. 2012. Ligand-guided receptor optimization. *Methods Mol. Biol.* 857:189–205
66. Kettle JG, Faull AW, Barker AJ, Davies DH, Stone MA. 2004. *N*-benzylindole-2-carboxylic acids: potent functional antagonists of the CCR2b chemokine receptor. *Bioorg. Med. Chem. Lett.* 14:405–8
67. Kofuku Y, Yoshiura C, Ueda T, Terasawa H, Hirai T, et al. 2009. Structural basis of the interaction between chemokine stromal cell–derived factor-1/CXCL12 and its G-protein-coupled receptor CXCR4. *J. Biol. Chem.* 284:35240–50
68. Kufareva I. 2016. Chemokines and their receptors: insights from molecular modeling and crystallography. *Curr. Opin. Pharmacol.* 30:27–37
69. Kufareva I, Salanga CL, Handel TM. 2015. Chemokine and chemokine receptor structure and interactions: implications for therapeutic strategies. *Immunol. Cell Biol.* 93:372–83
70. Kufareva I, Stephens BS, Holden LG, Qin L, Zhao C, et al. 2014. Stoichiometry and geometry of the CXC chemokine receptor 4 complex with CXC ligand 12: molecular modeling and experimental validation. *PNAS* 111:E5363–E72
71. Lamichhane R, Liu JJ, Pljevaljcic G, White KL, van der Schans E, et al. 2015. Single-molecule view of basal activity and activation mechanisms of the G protein-coupled receptor β_2 AR. *PNAS* 112:14254–59
72. Lau EK, Paavola CD, Johnson Z, Gaudry JP, Geretti E, et al. 2004. Identification of the glycosaminoglycan binding site of the CC chemokine, MCP-1: implications for structure and function in vivo. *J. Biol. Chem.* 279:22294–305
73. Lefrançois M, Lefebvre M-R, Saint-Onge G, Boulais PE, Lamothe S, et al. 2011. Agonists for the chemokine receptor CXCR4. *ACS Med. Chem. Lett.* 2:597–602
74. Liang WG, Triandafillou CG, Huang T-Y, Zulueta MML, Banerjee S, et al. 2016. Structural basis for oligomerization and glycosaminoglycan binding of CCL5 and CCL3. *PNAS* 113:5000–5
75. Liu J, Louie S, Hsu W, Yu KM, Nicholas HB, Rosenquist GL. 2008. Tyrosine sulfation is prevalent in human chemokine receptors important in lung disease. *Am. J. Respir. Cell Mol. Biol.* 38:738–43
76. Lubman OY, Fremont DH. 2016. Parallel evolution of chemokine binding by structurally related herpesvirus decoy receptors. *Structure* 24:57–69

77. Ludeman JP, Stone MJ. 2014. The structural role of receptor tyrosine sulfation in chemokine recognition. *Br. J. Pharmacol.* 171:1167–79
78. Lusi-Narasimhan M, Power CA, Allet B, Alouani S, Bacon KB, et al. 1995. Mutation of Leu²⁵ and Val²⁷ introduces CC chemokine activity into interleukin-8. *J. Biol. Chem.* 270:2716–21
79. Maeda K, Nakata H, Koh Y, Miyakawa T, Ogata H, et al. 2004. Spirodiketopiperazine-based CCR5 inhibitor which preserves CC-chemokine/CCR5 interactions and exerts potent activity against R5 human immunodeficiency virus type 1 in vitro. *J. Virol.* 78:8654–62
80. Manglik A, Kim TH, Masureel M, Altenbach C, Yang Z, et al. 2015. Structural insights into the dynamic process of β_2 -adrenergic receptor signaling. *Cell* 161:1101–11
81. Maussang D, Mujic-Delic A, Descamps FJ, Stortelers C, Vanlandschoot P, et al. 2013. Llama-derived single variable domains (nanobodies) directed against chemokine receptor CXCR7 reduce head and neck cancer cell growth in vivo. *J. Biol. Chem.* 288:29562–72
82. Middleton J, Neil S, Wintle J, Clark-Lewis I, Moore H, et al. 1997. Transcytosis and surface presentation of IL-8 by venular endothelial cells. *Cell* 91:385–95
83. Millard CJ, Ludeman JP, Canals M, Bridgford JL, Hinds M, et al. 2014. Structural basis of receptor sulfotyrosine recognition by a CC chemokine: the N-terminal region of CCR3 bound to CCL11/eotaxin-1. *Structure* 22:1571–81
84. Mirzadegan T, Benko G, Filipek S, Palczewski K. 2003. Sequence analyses of G-protein-coupled receptors: similarities to rhodopsin. *Biochemistry* 42:2759–67
85. Monteclaro FS, Charo IF. 1996. The amino-terminal extracellular domain of the MCP-1 receptor, but not the RANTES/MIP-1 α receptor, confers chemokine selectivity: evidence for a two-step mechanism for MCP-1 receptor activation. *J. Biol. Chem.* 271:19084–92
86. Montpas N, Cabana J, St-Onge G, Gravel S, Morin G, et al. 2015. Mode of binding of the cyclic agonist peptide TC14012 to CXCR7: identification of receptor and compound determinants. *Biochemistry* 54:1505–15
87. Muller A, Homey B, Soto H, Ge N, Catron D, et al. 2001. Involvement of chemokine receptors in breast cancer metastasis. *Nature* 410:50–56
88. Muniz-Medina VM, Jones S, Maglich JM, Galardi C, Hollingsworth RE, et al. 2009. The relative activity of “function sparing” HIV-1 entry inhibitors on viral entry and CCR5 internalization: Is allosteric functional selectivity a valuable therapeutic property? *Mol. Pharmacol.* 75:490–501
89. Murphy JW, Yuan H, Kong Y, Xiong Y, Lolis EJ. 2010. Heterologous quaternary structure of CXCL12 and its relationship to the CC chemokine family. *Proteins* 78:1331–37
90. Mysinger MM, Weiss DR, Ziarek JJ, Gravel S, Doak AK, et al. 2012. Structure-based ligand discovery for the protein-protein interface of chemokine receptor CXCR4. *PNAS* 109:5517–22
91. Nasser MW, Raghuvanshi SK, Grant DJ, Jala VR, Rajarathnam K, Richardson RM. 2009. Differential activation and regulation of CXCR1 and CXCR2 by CXCL8 monomer and dimer. *J. Immunol.* 183:3425–32
92. Nibbs RJB, Graham GJ. 2013. Immune regulation by atypical chemokine receptors. *Nat. Rev. Immunol.* 13:815–29
93. Nicholls DJ, Tomkinson NP, Wiley KE, Brammall A, Bowers L, et al. 2008. Identification of a putative intracellular allosteric antagonist binding-site in the CXC chemokine receptors 1 and 2. *Mol. Pharmacol.* 74:1193–202
94. Nijmeijer S, Leurs R, Smit MJ, Vischer HF. 2010. The Epstein-Barr virus-encoded G protein-coupled receptor BILF1 hetero-oligomerizes with human CXCR4, scavenges G α proteins, and constitutively impairs CXCR4 functioning. *J. Biol. Chem.* 285:29632–41
95. Oberthur D, Achenbach J, Gabdulhakov A, Buchner K, Maasch C, et al. 2015. Crystal structure of a mirror-image L-RNA aptamer (Spiegelmer) in complex with the natural L-protein target CCL2. *Nat. Commun.* 6:6923
96. Oswald C, Rappas M, Kean J, Doré AS, Errey JC, et al. 2016. Intracellular allosteric antagonism of the CCR9 receptor. *Nature* 540:462–65
97. Paavola CD, Hemmerich S, Grunberger D, Polsky I, Bloom A, et al. 1998. Monomeric monocyte chemoattractant protein-1 (MCP-1) binds and activates the MCP-1 receptor CCR2B. *J. Biol. Chem.* 273:33157–65

98. Pakianathan DR, Kuta EG, Artis DR, Skelton NJ, Hebert CA. 1997. Distinct but overlapping epitopes for the interaction of a CC-chemokine with CCR1, CCR3 and CCR5. *Biochemistry* 36:9642–48
99. Palczewski K, Kumasaka T, Hori T, Behnke CA, Motoshima H, et al. 2000. Crystal structure of rhodopsin: a G protein-coupled receptor. *Science* 289:739–45
100. Peace S, Philp J, Brooks C, Piercy V, Moores K, et al. 2010. Identification of a sulfonamide series of CCR2 antagonists. *Bioorg. Med. Chem. Lett.* 20:3961–64
101. Pease J, Horuk R. 2012. Chemokine receptor antagonists. *J. Med. Chem.* 55:9363–92
102. Proudfoot AEI, Power CA, Schwarz MK. 2010. Anti-chemokine small molecule drugs: a promising future? *Expert Opin. Investig. Drugs* 19:345–55
103. Proudfoot AEI. 2002. Chemokine receptors: multifaceted therapeutic targets. *Nat. Rev. Immunol.* 2:106–15
104. Qin L, Kufareva I, Holden LG, Wang C, Zheng Y, et al. 2015. Crystal structure of the chemokine receptor CXCR4 in complex with a viral chemokine. *Science* 347:1117–22
105. Rajagopal S, Kim J, Ahn S, Craig S, Lam CM, et al. 2010. β -arrestin- but not G protein-mediated signaling by the “decoy” receptor CXCR7. *PNAS* 107:628–32
106. Rajarathnam K, Sykes B, Kay C, Dewald B, Geiser T, et al. 1994. Neutrophil activation by monomeric interleukin-8. *Science* 264:90–92
107. Rapp C, Snow S, Laufer T, McClendon CL. 2013. The role of tyrosine sulfation in the dimerization of the CXCR4:SDF-1 complex. *Protein Sci.* 22:1025–36
108. Rasmussen SGF, Choi H-J, Fung JJ, Pardon E, Casarosa P, et al. 2011. Structure of a nanobody-stabilized active state of the β_2 adrenoceptor. *Nature* 469:175–80
109. Rasmussen SGF, DeVree BT, Zou Y, Kruse AC, Chung KY, et al. 2011. Crystal structure of the β_2 adrenergic receptor-Gs protein complex. *Nature* 477:549–55
110. Rosenbaum DM, Cherezov V, Hanson MA, Rasmussen SGF, Thian FS, et al. 2007. GPCR engineering yields high-resolution structural insights into β_2 -adrenergic receptor function. *Science* 318:1266–73
111. Rossi D, Zlotnik A. 2000. The biology of chemokines and their receptors. *Annu. Rev. Immunol.* 18:217–42
112. Russo E, Teixeira A, Vaahomeri K, Willrodt AH, Bloch JS, et al. 2016. Intralymphatic CCL21 promotes tissue egress of dendritic cells through afferent lymphatic vessels. *Cell Rep.* 14:1723–34
113. Sabroe I, Peck MJ, Van Keulen BJ, Jorritsma A, Simmons G, et al. 2000. A small molecule antagonist of chemokine receptors CCR1 and CCR3: potent inhibition of eosinophil function and CCR3-mediated HIV-1 entry. *J. Biol. Chem.* 275:25985–92
114. Salchow K, Bond ME, Evans SC, Press NJ, Charlton SJ, et al. 2010. A common intracellular allosteric binding site for antagonists of the CXCR2 receptor. *Br. J. Pharmacol.* 159:1429–39
115. Schall TJ, Proudfoot AEI. 2011. Overcoming hurdles in developing successful drugs targeting chemokine receptors. *Nat. Rev. Immunol.* 11:355–63
116. Scholten DJ, Canals M, Maussang D, Roumen L, Smit MJ, et al. 2011. Pharmacological modulation of chemokine receptor function. *Br. J. Pharmacol.* 165:1617–43
117. Schwarz J, Sixt M. 2016. Quantitative analysis of dendritic cell haptotaxis. *Methods Enzymol.* 570:567–81
118. Sepuru KM, Rajarathnam K. 2016. CXCL1/MGSA is a novel glycosaminoglycan (GAG)-binding chemokine: structural evidence for two distinct non-overlapping binding domains. *J. Biol. Chem.* 291:4247–55
119. Smith EW, Liu Y, Getschman AE, Peterson FC, Ziarek JJ, et al. 2014. Structural analysis of a novel small molecule ligand bound to the CXCL12 chemokine. *J. Med. Chem.* 57:9693–99
120. Smith EW, Nevins AM, Qiao Z, Liu Y, Getschman AE, et al. 2016. Structure-based identification of novel ligands targeting multiple sites within a chemokine-G-protein-coupled-receptor interface. *J. Med. Chem.* 59:4342–51
121. Solari R, Pease JE, Begg M. 2015. “Chemokine receptors as therapeutic targets: Why aren’t there more drugs?” *Eur. J. Pharmacol.* 746:363–67
122. Spiess K, Jeppesen MG, Malmgaard-Clausen M, Krzykowski K, Dulal K, et al. 2015. Rationally designed chemokine-based toxin targeting the viral G protein-coupled receptor US28 potently inhibits cytomegalovirus infection in vivo. *PNAS* 112:8427–32

123. Springael J-Y, Le Minh PN, Urizar E, Costagliola S, Vassart G, Parmentier M. 2006. Allosteric modulation of binding properties between units of chemokine receptor homo- and hetero-oligomers. *Mol. Pharmacol.* 69:1652–61
124. Staus DP, Strachan RT, Manglik A, Pani B, Kahsai AW, et al. 2016. Allosteric nanobodies reveal the dynamic range and diverse mechanisms of G-protein-coupled receptor activation. *Nature* 535:448–52
125. Steyaert J, Kobilka BK. 2011. Nanobody stabilization of G protein-coupled receptor conformational states. *Curr. Opin. Struct. Biol.* 21:567–72
126. Strizki JM, Xu S, Wagner NE, Wojcik L, Liu J, et al. 2001. SCH-C (SCH 351125), an orally bioavailable, small molecule antagonist of the chemokine receptor CCR5, is a potent inhibitor of HIV-1 infection in vitro and in vivo. *PNAS* 98:12718–23
127. Tamamura H, Omagari A, Oishi S, Kanamoto T, Yamamoto N, et al. 2000. Pharmacophore identification of a specific CXCR4 inhibitor, T140, leads to development of effective anti-HIV agents with very high selectivity indexes. *Bioorg. Med. Chem. Lett.* 10:2633–37
128. Tamamura H, Xu Y, Hattori T, Zhang X, Arakaki R, et al. 1998. A low-molecular-weight inhibitor against the chemokine receptor CXCR4: a strong anti-HIV peptide T140. *Biochem. Biophys. Res. Commun.* 253:877–82
129. Tan JHY, Canals M, Ludeman JP, Wedderburn J, Boston C, et al. 2012. Design and receptor interactions of obligate dimeric mutant of chemokine monocyte chemoattractant protein-1 (MCP-1). *J. Biol. Chem.* 287:14692–702
130. Tan JHY, Ludeman JP, Wedderburn J, Canals M, Hall P, et al. 2013. Tyrosine sulfation of chemokine receptor CCR2 enhances interactions with both monomeric and dimeric forms of the chemokine monocyte chemoattractant protein-1 (MCP-1). *J. Biol. Chem.* 288:10024–34
131. Tan Q, Zhu Y, Li J, Chen Z, Han GW, et al. 2013. Structure of the CCR5 chemokine receptor–HIV entry inhibitor maraviroc complex. *Science* 341:1387–90
132. Thoma G, Streiff MB, Kovarik J, Glickman F, Wagner T, et al. 2008. Orally bioavailable isothiouracil block function of the chemokine receptor CXCR4 in vitro and in vivo. *J. Med. Chem.* 51:7915–20
133. Tschammer N, Christopoulos A, Kenakin T. 2015. Allosteric modulation of chemokine receptors. In *Chemokines*, ed. N Tschammer, pp. 87–117. Basel, Switz.: Springer
134. Vauquelin G, Hall D, Charlton SJ. 2015. ‘Partial’ competition of heterobivalent ligand binding may be mistaken for allosteric interactions: a comparison of different target interaction models. *Br. J. Pharmacol.* 172:2300–15
135. Veillard NR, Kwak B, Pelli G, Mulhaupt F, James RW, et al. 2004. Antagonism of RANTES receptors reduces atherosclerotic plaque formation in mice. *Circ. Res.* 94:253–61
136. Vela M, Aris M, Llorente M, Garcia-Sanz JA, Kremer L. 2015. Chemokine receptor-specific antibodies in cancer immunotherapy: achievements and challenges. *Front. Immunol.* 6:12
137. Veldkamp CT, Seibert C, Peterson FC, De la Cruz NB, Haugner JC III, et al. 2008. Structural basis of CXCR4 sulfotyrosine recognition by the chemokine SDF-1/CXCL12. *Sci. Signal.* 1:ra4
138. Veldkamp CT, Seibert C, Peterson FC, Sakmar TP, Volkman BF. 2006. Recognition of a CXCR4 sulfotyrosine by the chemokine stromal cell-derived factor-1 α (SDF-1 α /CXCL12). *J. Mol. Biol.* 359:1400–9
139. Venkatakrishnan AJ, Deupi X, Lebon G, Heydenreich FM, Flock T, et al. 2016. Diverse activation pathways in class A GPCRs converge near the G-protein-coupling region. *Nature* 536:484–87
140. Vilums M, Zweemer AJM, Yu Z, de Vries H, Hillger JM, et al. 2013. Structure–kinetic relationships—an overlooked parameter in hit-to-lead optimization: a case of cyclopentylamines as chemokine receptor 2 antagonists. *J. Med. Chem.* 56:7706–14
141. Watson C, Jenkinson S, Kazmierski W, Kenakin T. 2005. The CCR5 receptor-based mechanism of action of 873140, a potent allosteric noncompetitive HIV entry inhibitor. *Mol. Pharmacol.* 67:1268–82
142. Wescott MP, Kufareva I, Paes C, Goodman JR, Thaker Y, et al. 2016. Signal transmission through the CXCR4 chemokine receptor 4 (CXCR4) transmembrane helices. *PNAS* 113:9928–33
143. Wu B, Chien EYT, Mol CD, Fenalti G, Liu W, et al. 2010. Structures of the CXCR4 chemokine GPCR with small-molecule and cyclic peptide antagonists. *Science* 330:1066–71
144. Xue X, Lu Q, Wei H, Wang D, Chen D, et al. 2011. Structural basis of chemokine sequestration by CrmD, a poxvirus-encoded tumor necrosis factor receptor. *PLoS Pathog.* 7:e1002162

145. Yao XJ, Velez Ruiz G, Whorton MR, Rasmussen SGF, DeVree BT, et al. 2009. The effect of ligand efficacy on the formation and stability of a GPCR-G protein complex. *PNAS* 106:9501–6
146. Zhang M-Y, Lu J-J, Wang L, Gao Z-C, Hu H, et al. 2015. Development of monoclonal antibodies in China: overview and prospects. *BioMed. Res. Int.* 2015:10
147. Zhang W-B, Navenot J-M, Haribabu B, Tamamura H, Hiramatu K, et al. 2002. A point mutation that confers constitutive activity to CXCR4 reveals that T140 is an inverse agonist and that AMD3100 and ALX40-4C are weak partial agonists. *J. Biol. Chem.* 277:24515–21
148. Zheng Y, Qin L, Ortiz Zacarias NV, de Vries H, Han GW, et al. 2016. Structure of CC chemokine receptor 2 with orthosteric and allosteric antagonists. *Nature* 540:458–61
149. Zhong C, Wang J, Li B, Xiang H, Ultsch M, et al. 2013. Development and preclinical characterization of a humanized antibody targeting CXCL12. *Clin. Cancer Res.* 19:4433–45
150. Zhu JZ, Millard CJ, Ludeman JP, Simpson LS, Clayton DJ, et al. 2011. Tyrosine sulfation influences the chemokine binding selectivity of peptides derived from chemokine receptor CCR3. *Biochemistry* 50:1524–34
151. Ziarek JJ, Getschman AE, Butler SJ, Taleski D, Stephens B, et al. 2013. Sulfopeptide probes of the CXCR4/CXCL12 interface reveal oligomer-specific contacts and chemokine allostery. *ACS Chem. Biol.* 8:1955–63
152. Zweemer AJM, Bunnik J, Veenhuizen M, Miraglia F, Lenselink EB, et al. 2014. Discovery and mapping of an intracellular antagonist binding site at the chemokine receptor CCR2. *Mol. Pharmacol.* 86:358–68
153. Zweemer AJM, Nederpelt I, Vrieling H, Hafith S, Doornbos MLJ, et al. 2013. Multiple binding sites for small-molecule antagonists at the CC chemokine receptor 2. *Mol. Pharmacol.* 84:551–61

Acknowledgement

Chapter four, in full, is a reprint of a published review article as it appears in Annual Review of Biophysics. This was a collaboratively written review relying on each experimentalist author's area of expertise. (Kufareva, I., M. Gustavsson, Y. Zheng, **B. S. Stephens** and T. M. Handel (2017). "What Do Structures Tell Us About Chemokine Receptor Function and Antagonism?" Annu Rev Biophys **46**: 175-198.) The dissertation author was among several independent contributors to this material.

Chapter 5

Anatomy of the CXC chemokine receptor 4 signaling complex with CXCL12

Introduction

Chemokine receptors enable cells to migrate in response to directional cues provided by chemokine gradients, and are key mediators of immune cell homeostasis and surveillance as well as recruitment and organization of immune cells in acute inflammation (Sokol and Luster 2015). In humans the chemokine signaling network involves at least 45 receptors and 22 ligands (Scholten, Canals et al. 2012). The chemokines are ~10 kDa secreted proteins, and the chemokine receptors are members of the class A subfamily of G protein-coupled receptors (GPCRs).

Given the migratory function of chemokine signaling, it is not surprising that multiple cancers express high levels of chemokine receptors and are thought to exploit them for metastasis (Scholten, Canals et al. 2012). This is especially true for blood borne cancers (of hematopoietic origin). CXCR4 and CXCL12 in particular are expressed by a large number of different cancers and participate in the migration underlying both metastasis and tumor-supporting stromal cell recruitment (Guo, Wang et al. 2016). CXCR4 signaling is also often directly important for cancer cell survival (Guo, Wang et al. 2016), which is not surprising as CXCR4 signaling contributes to the maintenance of undifferentiated hematopoietic stem cells in the bone marrow (Sokol and Luster 2015). CXCR4 is also a principal co-receptor for the fusion of HIV to T cell membranes (Scholten, Canals et al. 2012).

The involvement of CXCR4 in various disease states provides the biomedical impetus for studying the structure of CXCR4, and the first crystal structures of CXCR4, in separate complexes with a small molecule and a cyclic peptide antagonist,

were reported in 2010 (Wu, Chien et al. 2010). More recently, a crystal structure was reported for the receptor in complex with the viral mimic chemokine vMIP-II (Qin, Kufareva et al. 2015), and in that report we submitted an early docking-based model of the CXCL12:CXCR4 complex that was produced using the solved complex structure as a template. Crystal structures have also been solved for CCR5 bound by the antagonist maraviroc (Tan, Zhu et al. 2013), CCR5 covalently secured to the antagonist CCL5 variant [5P7]-CCL5 (Zheng, Han et al. 2017), and CCR2 simultaneously bound by an orthosteric antagonist and an allosteric antagonist that binds to the receptor intracellularly where G proteins and arrestin molecules couple (Zheng, Qin et al. 2016). The structure of the virally encoded receptor US28 in complex with CX3CL1 was also solved in 2015 (Burg, Ingram et al. 2015).

At the same time, a large body of functional evidence has accumulated through various signaling studies of receptors, beginning long before any structural details of any chemokine receptors were available. Since 1997, a “two-site” model of interaction has been used to describe the binding of CXCL12 to CXCR4, and this model has broadened to describe chemokine:receptor interactions in general (Crump, Gong et al. 1997). In this model, there are two functionally distinct regions of the receptor, known as chemokine recognition site 1 and 2 (CRS1 and CRS2). CRS1 consists of the receptor N-terminus, which binds the globular domain of the chemokine, and CRS2 refers to the transmembrane domain of the receptor, which interacts with the N-terminus of the chemokine. The CRS1 interaction is described as occurring first and contributing to the formation of the chemokine:receptor complex strictly through the contribution of binding affinity. The CRS2 interaction with the chemokine N-terminus

is in turn considered the interaction that is responsible for the conformational change that leads to receptor activation, and ultimately the activation of signaling proteins coupled to the intracellular surface of the receptor.

Observing the recent handful of chemokine:receptor complex crystal structures and the CXCL12:CXCR4 model that accompanied the vMIP-II:CXCR4 structure, a conserved central point in the interaction for all of the complexes seems to exist in the hydrophobic packing interaction between the CC/CXC/CX3C cysteines of the chemokine and the –PC- motif of the receptor, which we have labeled CRS1.5 as it bridges the CRS1 and CRS2 “regions” of what is actually a contiguous interaction interface. As would be expected to allow for the correct recognition between cognate chemokine-receptor pairs, the diversity between the complexes is seen in both the CRS1 and CRS2 regions of the interaction on either side of the strikingly conserved CRS1.5 interaction (Kufareva, Gustavsson et al. 2017). (It should be noted that most of the CRS1 interaction is missing from the crystal structures as only the most C-terminal residues of the receptor N-termini have been solved.) Among the crystal structures, only CX3CL1:US28 is between an activating chemokine and a competent receptor. However, a recent large study of mutations throughout CXCR4 led to major advances in understanding how the CRS2 region of the CXCL12:CXCR4 interaction gives rise to receptor activation, which was accomplished by interpreting LOF mutagenesis signaling data with the aid of another computational model we derived for the CXCL12:CXCR4 complex (Wescott, Kufareva et al. 2016).

A crystal structure of the CXCR4:CXCL12 has remained elusive, at least in part due to the instability of agonist-bound GPCRs in the absence of a coupled

signaling protein such as a G protein. At the same time, numerous computationally derived models of the complex between CXCR4 and CXCL12 (or related derivative agonists) complex have emerged from various groups (Huang, Shen et al. 2003, Xu, Li et al. 2013, Kufareva, Stephens et al. 2014, Mona, Besserer-Offroy et al. 2016, Cutolo, Basdevant et al. 2017, Ziarek, Kleist et al. 2017). There is, however, a large degree of variation in the orientation proposed in these structural models, which highlights the need for caution in interpretation of any given model. It also highlights the need for better testing of such models, particularly testing that goes beyond LOF evidence, as the highly acidic receptor orthosteric pocket, along with the highly basic chemokine receptor-interacting domain, virtually ensures that key interaction residues in the receptor will be sampled even if the particular interactions in the model are incorrect.

It is not surprising that CXCR4 is the focus of multiple attempts in drug development, including cancer treatment, HIV infection, and treatment of WHIM syndrome (Pozzobon, Goldoni et al. 2016). To date, however, the only successful drug targeting CXCR4 is plerixafor, which is used in combination with granulocyte colony-stimulating factor (G-CSF) to mobilize CXCR4-bearing hematopoietic stem cells for re-implantation into the bone marrow of patients with non-Hodgkin lymphoma or myeloma (Danylesko, Sareli et al. 2016). There is clearly a need for better understanding the nature of chemokine:receptor complexes so that more potent and efficacious drugs can be rationally designed. A clear understanding of how chemokines bind and activate their receptors generally is only now emerging (Kufareva, Gustavsson et al. 2017), and we are far from understanding the unique

details of how each chemokine/receptor complex enables the receptors to adopt their G protein-activating state.

Here, we introduce the latest model of the CXCR4: CXCL12 complex derived from docking studies of CXCL12 binding to CXCR4 that were undertaken using the crystal structure of CXCR4: vMIP-II as a template. The model contains a proposed orientation of the full receptor N-terminus, which as mentioned has not been resolved in any chemokine receptor crystal structure to date, and replicates the prediction of a new CRS0.5 region of the chemokine:receptor interaction we previously made for ACKR3 (Gustavsson, Wang et al. 2017). We provide particularly strong evidence for the accuracy of this new model in the form of reciprocal charge swap rescue of function data, which goes beyond the limits of loss of function mutagenesis data in supporting the proposed receptor-interactions. We also present a substantial amount of novel data demonstrating β arrestin-2 recruitment changes resulting from mutations placed throughout CXCR4. Interestingly, discovered diminished CXCR4 signaling efficacy upon removal of the CRS1 interaction. We also discovered unexpected signaling bias resulting from several different receptor perturbations.

Materials and Methods

Modeling

A full length atomic resolution model of the CXCR4: CXCL12 complex was produced using the CXCR4: vMIP-II crystal structure (Qin, Kufareva et al. 2015) as a template. The core of CXCL12 was overlaid with that of vMIP-II, and the N-terminus of CXCL12 was subsequently re-docked *ab initio* using a chemical fields approach.

The CXCR4 N-terminal region spanning residues 21-26 was also re-docked *ab initio* with constraints provided by cysteine mutant disulfide trapping data (Kufareva, Stephens et al. 2014, Kufareva, Handel et al. 2015). Finally, the remaining 20 N-terminal residues of CXCR4 were modeled manually relying in part on insights provided in private communication with the Brian Volkman lab.

BRET-based recruitment assay

β arrestin-2 recruitment was measured with a bioluminescence resonance energy transfer 2 (BRET2) assay (Bonnetterre, Montpas et al. 2016). Four days prior to each assay, HEK293T cells, cultured in Dulbecco's Modified Eagle Media (DMEM) + 10% fetal bovine serum (FBS), were passaged and plated at 425,000 cells per well in 6-well tissue culture plates. Two days later, the cells were transfected with two separate pcDNA vectors containing (1) the gene for N-terminally HA-tagged human CXCR4 fused C-terminally to the renilla luciferase 3 gene and (2) the gene for β arrestin-2 fused N-terminally to the GFP10 gene. CXCR4-Rluc3 and GFP10- β arrestin-2 containing vectors were kindly donated by Nicolaus Heveker, Université de Montréal, Montreal, Quebec, Canada. The N-terminal HA tag was added after receipt of the CXCR4-Rluc3 vector, followed by the production of our mutant library. All mutations, as well as the N-terminal HA tag, were introduced into the CXCR4 coding region of the HA-CXCR4-Rluc3 vector using the quikchange site-directed mutagenesis method (Stratagene). Vector amounts used in the transfections, 0.1 and 2.4 μ g for HA-CXCR4-Rluc3 and GFP10- β arrestin-2 respectively, were selected to meet three criteria. First, the expression of GFP10- β arrestin-2 relative to HA-CXCR4-Rluc3 was high enough to ensure all saturation of HA-CXCR4-Rluc3

according to the acceptor/donor BRET2 titration curve relationship (Figure 5.S1). Experiments were designed in this way to avoid, to the extent possible, misinterpretations of efficacy changes resulting from the variation in BRET_{max} that is observed at different points along this titration curve (Bonneterre, Montpas et al. 2016). The second criterion met was that a sufficient level of Rluc3 must be expressed in order to yield an analyzable signal for both wavelengths of luminescence measured in the BRET assay, and the third was that a maximum of 2.5 ug of DNA per well was transfected into the cells. Transfections were carried out, according to the manufacturer's recommended protocol, using TransIT-LT1 transfection reagent (MirusBio). On the day of the assay, cells were washed while still adherent with PBS, then re-suspended through manual pipetting in PBS + 0.1% D-glucose (BRET buffer) and diluted to obtain a final concentration of 1.5 million cells per mL of suspension. Ninety uL of cell suspension was then dispensed into each well of a white, clear bottom, tissue culture treated 96-well plate (Corning) before the plate was placed into a CO₂ conditioned incubator for 30 minutes to allow the cells to reach 37 degrees C. GFP10-β arrestin-2 fluorescence levels were then measured with a SpectraMax M5 fluorescent plate reader (Molecular Devices). Ten uL of BRET buffer containing 10 times the final intended concentration of CXCL12 (WT or mutant) was then added to each well before an additional 10 minute waiting period, during which the plate was placed in a VictorX Light multilabel plate reader (PerkinElmer Life Sciences) pre-warmed to 37 degrees C. Finally, coelenterazine-200A (also known as Deep Blue C) was added to each well in order to obtain a final concentration of 5 uM immediately before measuring the luminescence at both 410 and 515 nm in the VictorX Light

luminometer. BRET ratios (515 nm luminescence/410 nm luminescence) were calculated in excel. In order to compare WT and mutant signaling assay results, as well as the results of different combinations of CXCL12 and CXCR4 mutants, results on each day were normalized to 100% WT efficacy, and mean values from independent experiments (each performed in duplicate) for each CXCL12 concentration were plotted together. Curve fitting was carried out with GraphPad PRISM using 4-parameter agonist concentration response equation.

Calcium mobilization-based G protein signaling assay

Ca²⁺ mobilization experiments were carried with the aid of the FLIPR4 calcium assay dye kit (Molecular Devices). As detailed previously (Kufareva, Stephens et al. 2014), we use a modified CHO K1 cell line for these experiments that stably expresses the promiscuously coupling G alpha subunit G alpha 15. These cells were cultured in 1:1 DMEM/F12 nutrient mixture supplemented with 10% FBS and 700 ug/mL active G418 mammalian antibiotic. Three days prior to each assay, the cells were passaged and plated at 2 million cells per dish into 10 cm diameter tissue culture dishes, in 1:1 DMEM/F12 nutrient mixture supplemented with 10% FBS and further supplemented with 0.25% DMSO to aid in transfection efficiency (Ye, Kober et al. 2009). The next day, the media was removed and replaced with 1:1 DMEM/F12 nutrient mixture supplemented with 10% FBS immediately prior to transfection with. In this case, Trans-IT CHO transfection kit is used according to the manufacturer's recommended protocol, with the uL reagent: ug DNA ratio adjusted to 4:1. For the current study, 24 ug of either WT or mutant HA-CXCR4-rluc3 DNA were transfected into the cells in each dish. While we were first reticent to use the C-terminally Rluc3

fused form of CXCR4 for these assays, we discovered that this procedure provided the advantage of equalizing the expression between WT and mutant forms of the receptor, thus reducing the uncertainty in interpretations of efficacy differences that result from frequently altered expression of mutants. The next day, the cells were washed with PBS before re-suspension using PBS + 5 mM EDTA, then centrifuged and re-suspended in 1:1 DMEM/F12 nutrient mixture supplemented with 10% FBS before replating at 90,000 cells/well in black, clear bottom, poly-D-lysine coated 96-well plates (Corning). The following day, media was carefully removed from the adherent cells before 200 μ L of a 1:1 mixture of HBSS + 20 mM HEPES + 0.1% BSA and FLIPR4 dye was added to each well. After a 75 minute incubation at 37 degrees C, the assay was carried out in a FlexStation 3 multi-mode plate reader (Molecular Devices) using the instruments automated injection function to introduce CXCL12 at the final indicated concentrations. Fluorescence was measured at 525 nm after excitation at 485 nm repeatedly (with 1.52 second intervals) over the course of 150 seconds. Reduced peak fluorescence values were calculated in excel by subtraction of baseline fluorescence from peak values, and reduced peak fluorescence versus CXCL12 concentration response curve fitting was carried out using GraphPad PRISM. In order to compare WT and mutant signaling assay results, as well as the results of different combinations of CXCL12 and CXCR4 mutants, results on each day were normalized to 100% WT efficacy, and mean values from independent experiments (each performed in duplicate) for each CXCL12 concentration were plotted together. Curve fitting was carried out with GraphPad PRISM using 4-parameter agonist concentration response equation.

Flow cytometry-based expression testing

For both HEK293Ts and CHO G α 15 stable cells transfected with WT and mutant versions of CXCR4, expression testing was carried out using the same method. Cells were resuspended in PBS + 5 mM EDTA, centrifuged, and re-suspended in PBS + 0.5% PBS (FACS buffer) to a final concentration of between 0.1-1 million cells per mL of buffer. For anti-HA staining, fluorophore conjugated anti-HA antibody (Miltenyi Biotec) was added to obtain an 11X dilution, and cells were stained on ice in the dark for 10 min, according to the procedure recommended by the antibody manufacturer. For anti-CXCR4 staining, fluorophore conjugated anti-CXCR4 antibody (either 12G5 or 1D9, both BD) was added to obtain a 50X dilution, and cells were stained on ice in the dark for 45 min, according to the procedure recommended by the antibody manufacturer. Cells were then washed three times with FACS buffer and then fixed with a final concentration of 0.8% PFA. Flow cytometric analysis of the antibody-stained and fixed cells was carried out using a GUAVA benchtop flow cytometer (EMD Millipore). Flow cytometry data analysis was performed using FlowJo software.

Statistical comparison of WT and mutant signaling parameters

Statistical comparisons between WT and mutant CXCR4 concentration response parameters were carried out on the same combined dataset in prism using the extra sum-of-squares F test model (with significance determined by $P < 0.05$).

Bias calculations

We used an established method for estimation of bias in results from different signaling pathways that does not require independently derived binding data. The

equation for what Rajagopal and colleagues (2011) termed the equiactive comparison method of bias calculation, adapted to our situation of comparing WT CXCR4 signaling to that of a mutant or receptor truncation, is:

$$\text{Bias factor } (\beta) = \log \left\{ \frac{[(E_{\max 1} \times EC50_2) / (EC50_1 \times E_{\max 2})]_{\text{mutant}}}{[(E_{\max 1} \times EC50_2) / (EC50_1 \times E_{\max 2})]_{\text{WT}}} \right\}$$

where 1 and 2 designate parameters for signaling through pathways 1 and 2, designated arbitrarily.

This equation yields a logarithmic estimation of the relative activity in one pathway versus another, e.g. when the bias factor is 1, mutant A is ten times more active in pathway X than in pathway Y.

Results

A full length model of the CXCR4: CXCL12 signaling complex

In the model of the CXCL12: CXCR4 interaction (Figure 5.1), the orientation of CXCL12 with respect to CXCR4 is globally consistent with the orientation of vMIP-II in the co-crystallized CXCR4: vMIP-II complex. The CRS2 region of the interaction is also quite similar to a previous model of the CXCL12: CXCR4 complex that we derived before the vMIP-II: CXCR4 crystal structure was available (Kufareva et al. 2014). As was the case with the CXCR4: vMIP-II structure, the CRS1 and CRS2 regions of the complex interaction are not discretely divisible, but rather part of a large contiguous interface between the chemokine and receptor (Figure 5.1).

Novel to this model is the complete N-terminus of CXCR4, as this region was not resolved N-terminal to CXCR4 residue Y21 in the CXCR4: vMIP-II structure, and

moreover no distal chemokine receptor N-terminus has been solved in any structure to date (Kufareva, Gustavsson et al. 2017). Within this previously unknown region of the CRS1 component of the complex, residues 1-7 of the receptor are engaged in a β sheet interaction with the first β strand of the intramolecular CXCL12 β sheet, thereby extending the sheet (Figure 5.1). This interaction is strikingly similar to the β sheet portion of the CXC chemokine homodimerization interface. We previously predicted the same interaction in the case of the ACKR3: CXCL12 interaction, and we have labeled this interaction region CRS0.5 to maintain consistency with the existing CRS1/CRS nomenclature (Gustavsson et al. 2017). Proximal to this interaction, the CXCR4 N-terminus (CRS1) wraps all the way around the top of CXCL12, descending into the conserved PC domain that displays hydrophobic packing against cysteines 9 and 11 of CXCL12 in the now familiar CRS1.5 interaction (Kufareva et al. 2017). The N-terminus of CXCL12 contacts both conserved class A GPCR signal initiation residues (e.g. W94, Y116, and E288) and chemokine receptor-specific engagement residues such as D97, D187, and D262. (Wescott et al. 2016).

When the CXCL12: CXCR4 model is compared with crystallized receptor chemokine complexes, which to date include vMIP-II: CXCR4 (Qin et al. Science 2015, PDB ID 4RWS), CX3CL1: US28 (Burg et al. Science 2015, PDB ID 4XT1, 4XT3), and [5P7]CCL5: CCR5 (Zheng et al. 2017, PDB ID 5UIW), several similarities and differences are apparent. For one, the CXCL12: CXCR4 model is similar to the vMIP-II: CXCR4 crystal structure in the loose engagement of receptor extracellular loops by the chemokines, whereas in the CX3CL1: US28 structure clear contacts between the chemokine core and the receptor extra-cellular loops (ECLs) are made,

and in the [5P7]CCL5:CCR5 crystal structure there is even more extensive engagement, so much so that the buried surface area is 1700 Å² compared to 1300 Å² for vMIP-II:CXCR4 and C3XCL1:US28 (Zheng et al. 2017). Previously, we noted that when the three co-crystallized structures are compared, the CRS1.5 interaction with the CC/CXC motif cysteines of the chemokine seems to be a conserved “pivot point” around which diversity is seen in the CRS1 and CRS2 interactions between different chemokine:receptor complexes (Kufareva et al. 2017). This trend is continued with the CXCR4:CXCL12 model, as the conserved CRS1.5 interaction is clearly seen, but the CRS1 interaction (to the extent it is solved in the crystal structures), and even more so the CRS2 interaction, is different in this new model than in any of the three co-crystallized complex structures.

Establishing reliable and clearly interpretable assays to validate the new CXCR4:CXCL12 complex model

Mutagenesis studies of CXCR4 have previously focused on G protein signaling (Doranz, Orsini et al. 1999, Brelot, Heveker et al. 2000), so information specific to CXCR4’s alternative signaling pathway, originating with β arrestin-2 recruitment to the receptor (Orsini, Parent et al. 1999), is lacking. Using our model as a guide, we tested multiple CRS2 CXCR4 mutants to assess their effects on β arrestin-2 recruitment, using a BRET2-based β arrestin-2 recruitment assay. In particular cases where the G protein signaling data is relevant and either missing, incomplete, or unclear due to conflicting previous reports, we also tested mutants in our established G protein signaling assay (Kufareva, Stephens et al. 2014), which relies on measurement

of calcium as a second messenger in G protein activation. Signaling parameters for all mutants tested are listed comprehensively in tables 5.1 and 5.2.

In order to enable valid comparisons between WT and mutant signaling parameters, in particular efficacy, we took care to ensure mutant expression as close as possible to WT levels. In the case of BRET, we first ensured that the parameters derived from our experiments do not vary substantially within a wide range of WT CXCR4-rluc3 expression levels (Figure 5.S1). All of the mutants tested in this study expressed well within this range except for a large N-terminal truncation, Δ 1-26, and D133N, which were severely compromised in expression but just outside the range of confirmed expression flexibility for the assay (Figures 5.S2 & 5.S3). We also tested the surface expression of all mutants along with WT HA-CXCR4-rluc3 to determine whether the ratio of surface to total expression was equivalent. The only mutants with major deficits in surface expression are Δ 1-26 and D133N, and it appears from comparison with WT CXCR4 expression that the low surface expression for these mutants is simply a result of low overall expression (Figures 5.S2 & 5.S3).

In the case of Ca^{2+} mobilization, several mutants expressed at lower levels than WT CXCR4. Unlike BRET experiments, Ca^{2+} mobilization comparisons are subject to misinterpretation when mutant receptors being tested are not expressed at levels similar to WT expression. We therefore adjusted the WT expression levels used for comparison with mutants in order to accurately determine their effects on G protein signaling parameters (Figure 5.S4). This strategy allowed us to obtain signaling data to analyze using control data from WT CXCR4 expressed at mutant-comparable levels

for all but one mutant, D133N, which expressed too poorly in the CHO Galpha15 expressing cell line used in the assay to yield analyzable data.

Residues directly contacting the extreme CXCL12 N-terminus are critical for β arrestin-2 recruitment to CXCR4

The interaction between CRS2 and the disordered N-terminus of CXCL12 has long been held to be directly responsible for CXCR4 activation. In our model, CXCL12 K1 is revealed to be interacting with CXCR4 D97 through the N-terminal amine group, and with CXCR4 E288 through the lysine side chain (Figure 5.2A). This concurs with the previous mutagenesis data, as it has already been demonstrated that mutating or removing CXCL12's N-terminal lysine (Crump, Gong et al. 1997, Ziarek, Kleist et al. 2017), or mutating either D97 or E288 of CXCR4 (Brelot, Heveker et al. 2000, Kufareva, Stephens et al. 2014), abolishes G protein signaling. We tested both D97N and E288Q mutations of CXCR4 in BRET-based β arrestin-2 recruitment assays, and both eliminated CXCL12-mediated β arrestin-2 recruitment (Figure 5.2B). Residue D187, near the base of the CXCR4 ECL2 hairpin, appears in our model positioned to interact with the backbone amines of CXCL12 V3 and S4, and has long been known to be important for G protein signaling (Brelot, Heveker et al. 2000, Kufareva, Stephens et al. 2014). We observed that D187A mutation rendered CXCR4 almost completely inactive in β arrestin-2 recruitment as well (Figure 5.2B). Y116 sits just underneath CXCL12 and is thought to couple CXCL12: CXCR4 engagement to the further intracellular conformational changes within the receptor that ultimately allow for G protein coupling and activation. It is well established that Y116A mutation abrogates CXCR4's G protein signaling (Thiele, Mungalpara et al. 2014, Wescott,

Kufareva et al. 2016), and we found the same results in the case of β arrestin-2 recruitment (Figure 5.2B).

CXCR4 D262 directly engages R8 of CXCL12 in an interaction critical to CXCR4 activation

D262 of CXCR4 is clearly interacting with R8 of CXCL12 in the CXCL12:CXCR4 model (Figure 5.3A), and D262 has previously been reported to be important for CXCR4 binding and activation by CXCL12 based on mutagenesis data (Zhou and Tai 2000, Wescott, Kufareva et al. 2016). We tested a series of D262 (TM6) mutants (D262A, D262N, D262K, D262R) in the β arrestin-2 recruitment assay (Figure 5.3B). D262A, D262K and D262R are nearly abolished in CXCL12-mediated β arrestin-2 recruitment, while D262N shows a more modest but still severe effect (Figure 5.3B). The varying potency effects seen for these mutants is difficult to interpret reliably, as the severely compromised efficacy prevents accurate determination of EC50 values for all but the D262N mutation. As the existing data relevant to G protein signaling effects of D262 mutation is not entirely clear, we also tested D262N and D262K in our established G protein signaling assay (Ca^{2+} mobilization) in order to compare results between the two CXCR4 signaling pathways. The potency of CXCR4 G protein activation was reduced for D262N and even more so for D262K (Figure 5.3C). While both mutants did show reductions in the efficacy of G protein signaling, the efficacy effects were not as great as in β arrestin-2 recruitment (Figure 5.3C).

In an alternative model of CXCR4:CXCL12 complex recently published by Ziarek et al. (2017), E32 (TM1) was purported to interact directly with R8 of

CXCL12. In our model, E32 is not pointed toward CXCL12 at all. To help address this discrepancy, we produced E32Q, E32R, and E32K CXCR4 mutations and tested them in our β arrestin-2 recruitment assay. E32Q and E32K mutations both displayed slight but significant decreases in E_{max} values, whereas E32R mutation displayed slight but significant decreases in both potency and efficacy (Figure 5.3D).

In order to test the accuracy of our model in such a way as to provide stronger evidence than is possible through loss of function mutagenesis studies alone, we undertook a strategy of reciprocal charge reversal (Figure 5.4). The goal was to not only confirm the importance of the mutated residues through loss of function, but to further demonstrate that the pairwise interactions in our model are correct through rescue of function when reciprocally charge-reversing mutations of chemokine and receptor are combined. We first mutated arginine 8 of CXCR12 to glutamate. This CXCL12 mutation dramatically reduced the chemokine's capacity for activating CXCR4, as measured in BRET-based β arrestin-2 recruitment assays (Figure 5.4A&B). Stimulating cells expressing D262K or D262R CXCR4 with R8E CXCL12, however, substantially rescues the miniscule CXCR4 activation seen with R8E CXCL12 in combination with WT CXCR4 (Figure 5.4A). While the potency of activation for the R8E:D262K/R combinations is weaker than that of the WT interaction, it is striking that the efficacy observed approaches full efficacy seen for WT CXCL12: CXCR4 signaling.

In order to address the alternative orientation suggested by Ziarek et al., as well as obtain an additional specificity control, we tested the effects of combining E32K/R CXCR4 with R8E CXCL12. We observed no rescue of R8E CXCL12 signaling when

combined with E32K or E32R CXCR4 (Figure 5.4B). To further rule out the possibility that our results were nonspecific and arose solely from changing the net charge of the chemokine and receptor binding pocket, we combined R8E CXCL12 with E277K and E277R CXCR4, but we saw no rescue of R8E signaling for this combination (Figure 5.4B).

CXCR4 E277 directly engages R12 of CXCL12 in an interaction that is important for CXCR4 signaling

CXCR4 residue E277 has also been reported to be important for CXCL12 binding to CXCR4 (Zhou and Tai 2000), but it should be noted that in the original report, expression of mutants was not quantitatively compared to WT CXCR4 expression, so there was considerable uncertainty in this case. Nevertheless, E277 clearly interacts with R12 of CXCL12 in the model, thus supporting the importance of this residue in forming the CXCL12:CXCR4 complex (Figure 5.4A). Two other glutamate residues, E275 in TM7 and E268 in ECL3, also appear close enough to R12 of CXCL12 to warrant testing for a direct interaction, although E277 is closer. When we mutated each of these residues, we observed that neither E275 nor E268 mutation (to Q, K, or R) has any major negative effect on β arrestin-2 recruitment, although there is a slight deficit in the efficacy observed for E275Q and E275R mutations (Figure 5.5A&B). Interestingly, E277 mutation to Q has no significant effect on signaling, and E277A shows a slight increase in efficacy, whereas E277K and E277R show clear potency and efficacy deficits (Figure 5.5C). When E268 and E275 are mutated to arginine along with E277 in the same CXCR4 construct, no additional effect is observed beyond that observed with E277 mutation alone (Figure 5.5C).

Altogether, these data strongly suggest that E277 alone is important for the interaction with CXCL12 R12. At the same time, no effect is seen until the charge of E277 is reversed, suggesting this interaction is actually dispensable, and that introducing a repulsive interaction in its place destabilizes the chemokine:receptor complex. Again, we sought to compare the effects of E277 mutation on β arrestin-2 recruitment to those on G protein signaling, as previous G protein signaling data is not clear. The effect of E277R mutation in Ca^{2+} mobilization G protein signaling assay is similar but smaller than that seen in β arrestin-2 recruitment experiments (Figure 5.5D).

In our model, R30 (TM1) extends toward CXCL12 near the CXC motif and appears positioned to coordinate CXCR4 TM7 residue E277 as well as to interact with the CXCL12 backbone between residue 8 and 9. In order to test the importance of R30, we mutated it to both alanine and glutamine, and both mutants demonstrate major efficacy deficits in β arrestin-2 recruitment (Figure 5.5E). In Ca^{2+} mobilization G protein signaling assays, signaling is compromised but again the effects, especially on efficacy, are much smaller than seen in β arrestin-2 recruitment experiments (Figure 5.5F).

We again employed the charge swap strategy to confirm the pairwise interaction between CXCL12 R12 and CXCR4 E277. R12E CXCL12 greatly decreases the potency and efficacy of activation, although not to the same extent as R8E (Figure 5.6A&B). Similar to the effects of combining D262K/R CXCR4 with R8E CXCL12, E277K CXCR4 rescues the signaling of R12E CXCL12 substantially (Figure 5.6A). E277R also rescues some of the potency effect of R12E, though interestingly, displays a much lower efficacy than E277K when stimulated by R12E

CXCL12, and even seems to be less efficacious than WT CXCR4 stimulated with R12E CXCL12 (Figure 5.6A). In the alternative model of Ziarek and colleagues, R12 interacts with CXCR4 D181, so we also tested combinations of R12E with D181K and D181R. The D181K/R:R12E combinations further served as a good test of alternative orientations in that D181 is on the opposite side of the CXCR4 binding pocket from E277. We found no rescue of function when either D181K or D181R were combined with R12E CXCL12 (Figure 5.6B). Reversing the additional specificity control used before, we also tested the combination of R12E CXCL12 with D262R and D262K CXCR4, and again saw no rescue of R12E activity (Figure 5.6B).

Negatively charged residues in the CXCR4 ECL2 hairpin are collectively important for β arrestin-2 recruitment efficacy

Extra-cellular loop 2 (ECL2) of CXCR4 contains three negatively charged residues (E179, D181, and D182) in the β hairpin region, which in our model are proximal to K27 and R41 of CXCL12 (Figure 5.7A). It has been previously reported that a charge-neutralizing mutation of the β hairpin region of CXCR4 ECL2 has a major negative effect on receptor G protein signaling (Doranz, Orsini et al. 1999). In order to assess the importance of ECL2 for receptor activation, and to determine the contribution of each ECL2 hairpin residue to the interaction, we mutated E179, D181, and D182 of the CXCR4 ECL2 hairpin to alanine, lysine, and arginine. No significant effects were observed for any of the E179 mutations (Figure 5.7B). Of three D182 mutants (A,K,R) only D182R showed an effect, in this case purely on efficacy (Figure 5.7C). Three D181 mutations (A,N,K) produce very similar but small effects on

efficacy, and D181K shows a slight but significant effect on potency as well (Figure 5.7D). The most impactful single point mutation was D181R, which reduced efficacy by 34%. Combined hairpin mutations, in which E179, D181, and D182 are all mutated to either lysine or arginine, severely impaired the efficacy of β arrestin-2 recruitment, reducing it to just 39 and 25 percent of WT Emax respectively (Figure 5.7D). Interestingly, G protein signaling for the combined hairpin lysine mutant is only slightly reduced in efficacy but shows a greater potency effect than in β arrestin-2 recruitment, while D181K alone shows no significant effect at all in Ca²⁺ mobilization (Figure 5.7E).

There have also been reports that N176, also present in ECL2, is glycosylated and that this modification is important for CXCL12 binding affinity (Zhou and Tai 1999). It is not apparent from the model how such a receptor modification would aid in CXCL12 recognition. We found that the N176A mutation has no effect on β arrestin-2 recruitment to CXCR4 (Figure 5.7F).

Mutating CXCR4 residues involved in G protein coupling results in opposite effects on G protein activation and β arrestin-2 recruitment

The conserved DRY motif in the intracellular region of TM3 is well known for its importance in the G protein coupling of class A GPCRs generally, and the central R3.50 residue was revealed to participate directly in G protein coupling when the structure of the β_2 adrenergic receptor-Gs complex was solved (Rasmussen, DeVree et al. 2011). We tested R134A and D133N mutations of CXCR4 in both β arrestin-2 recruitment and G protein signaling assays. R134A showed clear constitutive activity in β arrestin-2 recruitment, and nevertheless displayed a higher CXCL12-mediated

efficacy and stronger potency than WT CXCR4 (Figure 5.8A&B). In Ca^{2+} mobilization experiments, the efficacy of R134A signaling was reduced but not abrogated (Figure 5.8C). D133N on the other hand showed an approximately 50% reduction in β arrestin-2 recruitment efficacy and interestingly, an increase in potency (Figure 5.8A). As noted we were unable to obtain analyzable Ca^{2+} mobilization data for D133N due to extremely low expression in the cells utilized for the assay.

Transmembrane helix V mutations cause impaired β arrestin-2 recruitment through unknown mechanisms

We tested the effects on β arrestin-2 recruitment of mutating W195 and Q200 (TM5), as we previously discovered that the corresponding residues in the related CXCL12-binding atypical chemokine receptor ACKR3 (W208 and E213 respectively) are important for both the potency and efficacy of CXCL12-mediated arrestin recruitment (Gustavsson, Wang et al. 2017). In the CXCL12: CXCR4 model, neither residue appears to interact with any region of CXCL12 in the model, and are pointed away from the receptor core entirely, as they are in the model of the ACKR3: CXCL12 complex we reported (Gustavsson et al. 2017) (Figure 5.9A). In the case of CXCR4, W195A and Q200D mutations both impair efficacy in β arrestin-2 recruitment, with W195A reducing it by >50% (Figure 5.9B). The potency of W195A CXCR4 activation is also impaired.

Proximal charged residues in the N-terminus of CXCR4 are important for the potency CXCL12-mediated β arrestin-2 recruitment to CXCR4

According to the CRS1/CRS2 hypothesis, the N-terminus of CXCR4 has long been thought to be crucial solely for CXCL12 affinity. In this longstanding model of

chemokine receptor activation, the receptor N-termini are involved purely in chemokine binding, and not in the activation of the receptor directly. In the CXCL12: CXCR4 model, clear charge complementarity can be seen for the proximal region of CRS1 as it wraps around the CXCL12 globular domain, contacting residues from the N-loop, the 40s loop, and the C-terminal helix of the chemokine, while the distal N-terminus (CRS0.5) forms a β strand extending the intramolecular CXCL12 β sheet (Figures 5.10A & 5.11A). Specifically, CXCR4 E26 interacts with CXCL12 R47, K25 interacts with CXCL12 E15 (of the RFFESH motif, long thought to be involved in binding the CXCR4 N-terminus), CXCR4 D22 interacts with CXCL12 H17 (also of the RFFESH motif), the putative sulfate group attached to CXCR4 Y21 interacts with CXCL12 R20, and CXCR4 D20 interacts with K56 of CXCL12 (Figure 5.10A). We tested mutations of each of these CXCR4 residues, as well as a combined mutant with all of these residues mutated to alanine, for their effects in β arrestin-2 recruitment. Consistent with the CRS1/CRS2 hypothesis as well as previous G protein signaling results of CXCR4 N-terminal mutation, all of the mutated residues showed effects on potency (Figure 5.10B-G). Although there were slight reductions in efficacy (none greater than 20%), it is difficult to be certain that failure to reach saturation was the cause of slight apparent efficacy deficits in these cases, as testing higher concentrations of CXCL12 than those used is complicated by CXCL12 homodimerization. Specifically, dimeric CXCL12 does not recruit β arrestin-2 to CXCR4, so reduced β arrestin-2 recruitment is seen at super-saturating CXCL12 concentrations as significant amounts of CXCL12 dimer is formed (Ziarek et al. *Sci Signal.* 2017). The one notable partial exception to the pattern for these residues was

K25. K25A showed a slight and reproducible but insignificant increase in potency compared to WT, and K25D showed a clear reduction in efficacy to ~70% WT level (Figure 5.10E). In the case of D20 and E26, alanine mutation alone did not suffice to significantly affect observed EC50 values, and charge-reversing mutations were required to significantly shift the EC50 (Figure 5.10B&F), whereas in the case of Y21 and D22, alanine mutations did significantly affect EC50 values, and charge-reversing mutations [Y21 is considered a negatively charged residue in this context as it has been demonstrated to be tyrosine phosphorylated (Farzan, Babcock et al. 2002)] shifted the observed EC50s to an equal or greater extent (Figure 5.10C&D).

When all of the alanine mutations are combined, the potency effect is greater than that of any one mutation alone, and there is no effect on efficacy (Figure 5.10G). Interestingly, the effects are not additive, and the effect of mutating all of the residues to alanine is not much greater than for Y21A mutation alone. These results are consistent with the large contiguous chemokine:receptor interface in that even disrupting all of the proximal CRS1 interaction is limited in its effect. It should also be noted that CXCR4 can be activated even when the CRS1 interaction is absent (Loetscher, Gong et al. 1998), so it is difficult to predict what the maximum effect of combining CRS1 mutants should be in any particular assay.

The full N-terminus of CXCR4, including CRS0.5, is important for the efficacy of β arrestin-2 recruitment

In order to definitively assess the contribution of the CRS1 interaction to CXCL12-mediated β arrestin-2 recruitment to CXCR4, we truncated the first 26 residues of the CXCR4 N-terminus, eliminating all residues N-terminal to the PC

CRS1.5 motif that divides CRS1 from CRS2. Surprisingly, we observed an almost complete elimination of signaling efficacy when the N-terminus of CXCR4 was truncated, along with the expected potency shift on the same order as the combined CRS1 alanine mutant (Figure 5.11B).

The CRS0.5 β sheet-extending interaction present in the model is very similar to the CRS0.5 interaction we predicted for the CXCL12:ACKR3 interaction, but we did not at the time ascertain its functional significance. In light of the surprising efficacy depletion upon CRS1 truncation, and as the proximal charged CRS1 residues do not seem to be involved in efficacy when the point mutation data is considered, we decided to test the functional importance of this newly hypothesized CRS0.5 interaction. When only the first seven residues of CXCR4 were truncated, a lesser but still significant reduction in efficacy was observed for this narrow CRS0.5 truncation, with no potency change in this case (Figure 5.11B). To investigate further, we created several additional N-terminally truncated CXCR4 constructs beginning at residues 11, 16, 20, and 26. We observed a clear trend towards increasingly reduced efficacy for longer CXCR4 truncations, with nearly all of the decrease in efficacy observed by truncation to residue 15 (Figure 5.11B). At the same time, the potency changes seen with the full CRS1 (residues 1-26) truncation do not begin to appear until truncation beyond residue 15. Not surprisingly for large N-terminal truncations, we noted that the Δ 1-19 and Δ 1-26 CXCR4 constructs were impaired in their expression (Figure 5.S3), and Δ 1-26 in particular was severely impaired. Nevertheless, as discussed above, Δ 1-19 expressed well within a range for which our assay yields reliable signaling parameter determinations, and Δ 1-26 was just at the edge of this range. In any case if

Δ 1-26 is excluded from consideration out of caution, the clear pattern in the truncation results is just as emergent.

In order to assess the effects of truncating the CXCR4 N-terminus on G protein signaling, we tested CXCR4 Δ 1-10, Δ 1-15, and Δ 1-25 in our Ca^{2+} mobilization G protein signaling assay. The Δ 1-15 and Δ 1-25 truncations of CXCR4 were impaired in expression in the CHO Ga15 cells, but we were able to adjust WT expression levels to similar levels for comparison. After adjusting WT expression levels to match the impaired expression seen for the truncations, we observed only potency effects for all three truncations (Figure 5.11C). The discrepancy between efficacy in G protein signaling and β arrestin-2 recruitment is particularly striking in the case of Δ 1-15 and Δ 1-25 CXCR4.

Quantifying the apparent bias seen when visually comparing β arrestin-2 recruitment and G protein signaling results

Given the discrepancy in efficacy determinations for the truncations of CXCR4 between the two assays, it was essential to determine whether the unpredicted effects of removing the CRS1 component of the CXCL12: CXCR4 interaction were in fact biased, i.e. whether they reflect an effect selective to one signaling pathway over the other, in this case β arrestin-2 recruitment. While the results appear clearly biased for Δ 1-15 and Δ 1-25 CXCR4, an essential consideration is that our BRET-based β arrestin-2 recruitment assay is a 1:1 quantification of the extent of receptor:arrestin interaction, whereas Ca^{2+} mobilization is a measurement of an amplified second messenger downstream of the receptor in its signaling pathway. Often when assaying an amplified second messenger, the maximal signal achievable in the assay is reached

before all receptors are activated, which can obscure from analysis the true receptor-intrinsic efficacy (Ehlert, Griffin et al. 1999, Rajagopal, Ahn et al. 2011). In the case of bias calculations when ligands are compared to a reference agonist, or when mutants are compared to WT receptor, a simple method has been developed to account for amplification effects (Ehlert, Griffin et al. 1999, Griffin, Figueroa et al. 2007, Ehlert 2008, Rajagopal, Ahn et al. 2011), and we took advantage of this method in order to estimate bias for all mutants for which we had both arrestin recruitment and G protein signaling data.

When the signaling parameters derived from our data are used to quantify signaling bias caused by mutation (relative to WT signaling) by the equiactive bias estimation method, the $\Delta 1-25$ CXCR4 truncation does indeed appear to be weakly biased toward G protein activation, or in other words selectively compromised in β arrestin-2 recruitment (Table 5.3). However, the $\Delta 1-10$ and $\Delta 1-15$ truncations are not quantitatively biased by this estimation. Interestingly, when reconsidering all mutants from which both G protein and arrestin signaling data were derived, both D262N and D262K are quantitatively biased toward G protein activation, even more so than $\Delta 1-25$ CXCR4. E277R also displays bias toward G protein activation, though the bias factor is smaller in this case. The ECL2 mutant D181K and the EADD-KAKK ECL2 hairpin combined mutant both appear to be weakly biased, with bias factor value of 0.19 towards G protein activation, but the uncertainty in the determination makes confidence impossible here. As is apparent from visual inspection of the signaling results, and therefore serving as a sort of positive control for the bias determinations, R134A mutation renders CXCR4 strongly β arrestin-2 recruitment-biased, with the

largest bias factor value of any mutant tested (and the only one that is appreciably β arrestin-2-biased at all). The remaining CXCR4 mutations tested in both assays, R30Q, Y21R, and the combined D20,Y21,D22,K25,E26 alanine mutant all yielded near-zero bias factors. The full results of bias calculations are listed in table 5.3.

Discussion

The model presented herein is among the first full length CXCR4: CXCL12 complex models, and has the strongest support in the form of reciprocal charge reversal rescue of function data. Given the well-established set of inactivating mutations known for CXCR4, it is not surprising that several models implicate these residues in interactions with CXCL12. Obviously, the multiple models that all purport to describe the interaction between CXCR4 and CXCL12 cannot all be correct, given their wide variation in the orientation of CXCL12 with respect to CXCR4. The uncertainty inherent in this situation of multiple conflicting models necessitates holding the models up to more stringent testing with methods that provide stronger evidence than traditional loss of function mutagenesis. Here, we use a “charge swap” strategy to go beyond loss of function, and demonstrate not just that the residues engaged in our model are important, but that they interact in the pairwise manner suggested by our model. In the case of both R8E and R12E CXCL12 mutations, activation of WT CXCR4 is severely impaired, and charge-reversing mutation of the interacting CXCR4 residue from the model was able to rescue receptor activation remarkably. Not all interaction residues in CXCR4 are amenable to such a strategy, such as deeper residues that when mutated render CXCR4 permanently inactive and

CRS1 residues that when mutated don't produce signaling deficits great enough to rescue. Thus we argue that our two interacting pairs, D262:R8 and E277:R12, provide the strongest support possible for our model in the form of functional data, especially for the CRS2 region of the interaction.

As expected, key CXCL12 engagement and receptor activation initiation residues known to be crucial to orienting CXCL12 N-terminus in the CXCR4 binding pocket and translating its binding to receptor activation (Wescott et al. 2016) all render CXCR4 dead or near dead when mutated. For all of these residues, there was existing evidence their mutation critically impaired G protein signaling. With the new charge swap validated CXCL12: CXCR4 model, we are able for the first time to confidently rationalize these results in terms of the particular interactions within the complex that are perturbed when each residue is mutated. The critical N-terminal lysine of CXCL12, for example, is an absolute requirement for CXCR4 activation, and so it is not surprising to see that it likely engages both D97 and E288 of CXCR4 in activating the receptor, as both residues are also absolute requirements for receptor activation, with even neutral mutation completely inactivating CXCR4. Nearly two decades ago, a seminal report on CXCL12 by Crump and colleagues (1997), glycine addition to the CXCL12 N-terminus was found to increase the potency of receptor activation rather than diminish activity, and the authors concluded that the CXCL12 K1 side chain, and not its N-terminal amine group, is critical for CXCR4 activation. Indeed, in the present model, D97 is a chemokine receptor-specific "engagement residue" that binds to the N-terminal amine of CXCL12 K1 directly and positions its side chain for interaction

with E288, which in turn is directly involved in initiating the activation of CXCR4 (Wescott et al. 2016).

The proline at position 2 of CXCL12 is interesting in that its mutation to glycine creates an antagonist variant of CXCL12 with near-WT affinity (Crump et al. 1997). In the model we can see that CXCL12 P2 engages in interactions with W94^{2.60} and Y116, both of which are involved in initiating the activation of CXCR4 upon CXCL12 binding along with E288 (Wescott et al. 2016). Again, returning to the original report of CXCL12 mutation effects, V3I mutation did not disrupt and in fact aided in CXCL12-mediated CXCR4 activation. We can now see that the critical D187 interaction with the CXCL12 N-terminal backbone at V3 allows for this flexibility in residue 3 side chain size. The side chain of V3 itself reaches toward an area of the CXCR4 major binding pocket with relatively neutral charge created by residues I259 and I284. From this region of the model it is very understandable that the V3I mutation would lead to an even better fit for the CXCL12 N-terminus.

The chemokine engagement structural role of CXCR4 D262, including its binding to CXCL12 R8 specifically, has been argued previously (Wescott et al. 2016). Here, we present what is to our knowledge the most clearly interpretable signaling data for D262 mutant CXCR4 from β arrestin-2 association experiments. The effect of D262 mutation is less severe, when considering the charge-eliminating asparagine mutation, than that of the core CRS2 signal initiation residues E288 and Y116, or even the other chemokine engagement residues D97 and D187, both of which eliminate signaling when mutated to uncharged residues. Nevertheless the chemokine-engagement interaction between CXCR4 D262 and CXCL12 R8 is clearly important,

as a large potency shift and drop in efficacy are seen for D262N and both alanine and charge-reversing mutations do eliminate the vast majority of receptor signaling. The D262N and D262K mutations also produced significant negative effects on both potency and efficacy in G protein signaling, with D262K again displaying a much larger effect.

Both the similarities and differences between the charge swap pair results are interesting. In the case of both R8E and R12E, swapping the charge of the interacting CXCR4 residue substantially rescues the severe potency deficit of the chemokine mutant, but the mutant combination is still less potent than the rescuing CXCR4 mutant alone (i.e. stimulated with WT CXCL12). Considering the relative sizes of the CXCR4 binding pocket and the CXCL12 N-terminus, the disproportionate effect on the effectiveness of either binding interface upon single residue charge reversal seems reasonable. The apparent differences between the two charge swap pairs are seen in the efficacy effects. Mutating D262 of CXCR4 to a basic residue produces a major efficacy deficit, eliminating receptor activation almost entirely, and the R8E CXCL12 mutation rescues this loss of efficacy remarkably, perhaps entirely to 100% of WT levels, though we cannot be sure due to the failure to achieve full saturation for the combination. This supports the critical “engagement” role for the R8:D262 interaction in orienting the CXCL12 N-terminus correctly for receptor activation deeper within CRS2. In the case of E277 mutation, only a minor efficacy deficit is observed to begin with, and it doesn't seem to be rescued substantially by chemokine mutation, though the modeled E_{max} for E277K:R12E combination is 79% of WT, which is slightly higher than 74% for E277K mutation alone. Making interpretation even more difficult,

the efficacy determination for E277K:R12E combination is questionable as the interaction again does not quite reach saturation. In fact, due to the severity of the potency effects, we cannot be certain as to the nature of either CXCL12 mutation on efficacy. As neither mutant was able to achieve saturation of CXCR4 even at the highest concentrations used, and we are limited in exploring this further, as testing higher CXCL12 concentrations in β arrestin-2 recruitment assays leads to artificially lower efficacy due to CXCL12 homodimerization (Ziarek et al. 2017), it is entirely possible that one or both mutants primarily or even solely affect(s) potency (although that seems highly unlikely for the R8E mutant given the D262K and D262R results). It is notable that even charge-eliminating R30 mutation has a greater effect on CXCR4 efficacy than E277 charge-reversing mutation. In the model, R30 appears positioned to interact with both E277 of CXCR4 and with the carbonyl group of CXCL12 R8. Therefore, while the charge swap results strongly support the R8:D262 and R12:E277 pairwise interactions, the position of R30 in the complex may provide for additional stabilization that is important to both CXCL12 N-terminal engagement interactions. Returning to the charge swap results, if the efficacy effect of E277 charge-reversing mutation primarily results from disrupting R30 coordination, it would make sense that R12E CXCL12 does not substantially reverse this effect (i.e. R12E CXCL12 does not rescue the efficacy of E277K CXCR4 signaling) even if the interaction with CXCR4 residue 277 is rescued, while at the same time E277K CXCR4 mutation would still be expected to rescue the severe potency deficit seen for R12E CXCL12. In any case, it seems clear that the R12:E277 interaction itself is more dedicated toward potency of

the interaction than efficacy when compared to the other chemokine engagement interactions discussed so far.

The second extracellular loop of CXCR4 is not close enough to CXCL12 in the model to warrant assignment of specific interactions, but the three acidic residues of the ECL2 beta hairpin, E179, D181, and D182, are proximate to the beta sheet region of CXCL12 and are closest, in terms of oppositely charged residues, to K27 and R41 of CXCL12. When each residue is mutated in isolation, only D181 mutants are consistently impaired in signaling, and only D181R mutation leads to a >25% reduction in efficacy. However, when all three residues are charge reversed together, a major effect in efficacy is observed (>60% reduction for lysine mutations and 75% reduction for arginine). Considered along with the distance between CXCL12 and the ECL2 hairpin region in the model, these data seem to suggest an important but flexible region of the CXCL12: CXCR4 interaction, in which the stretch of acidic residues in the CXCR4 ECL2 hairpin provide somewhat redundant and somewhat additive affinity for CXCL12, allowing for some compensation when only one is mutated. Finally, although ECL2 has been reported to undergo a glycosylation event that is important for CXCL12 binding (Zhou and Tai 1999), we find no evidence for the importance of N176 in CXCL12-mediated CXCR4 activation.

The conserved DRY motif within class A GPCRs has long been known to be important to their activation. The aspartate (133) and arginine (134) of the DRY motif in CXCR4 may engage in an interaction analogous to the Asp3.49-Arg3.50-Glu6.30 salt bridge originally discovered in rhodopsin (Palczewski, Kumasaka et al. 2000) and suspected for B2AR (Valentin-Hansen, Groenen et al. 2012) in order to maintain the

receptor in the inactive state. While the corresponding TM6 residue is not acidic in CXCR4, and therefore the interaction cannot be a true “ionic lock”, water-mediated interaction may allow for a polar version of the interaction. The conserved arginine, R3.50, is directly involved in G protein binding in the crystal structure of β_2 adrenergic receptor in complex with Gs (Rasmussen et al. 2011). Mutation of the conserved TM2/ICL3 arginine in many class A GPCRs renders them inactive, and a reduction in G protein signaling has been reported for CXCR4 R134 mutation specifically (Berchiche, Chow et al. 2007, Wescott, Kufareva et al. 2016) (Berchiche et al. JBC 2006, Wescott et al. Proc Natl Acad Sci U S A. 2016). Aspartate 3.49 mutation to asparagine was also tested previously and resulted in no change compared to WT G protein signaling (Berchiche et al. JBC 2006).

Here, we observe that R134A mutation in CXCR4 actually produces a highly constitutively active receptor, and in some way also allows for potent and efficacious CXCL12-mediated β arrestin-2 recruitment in addition to the observed steady state constitutive association. At the same time, G protein activation as measured by Ca^{2+} signaling is impaired but not abrogated. The simplest explanation here seems to be one in which R134A mutation selectively impairs G protein coupling (due to the direct role of R3.50 in G protein binding) while also rendering the receptor constitutively active (due to its role in maintaining inactive state), thus generating a β arrestin-biased form of constitutive activity. However, it is in fact difficult to experimentally distinguish a β arrestin-2 biased constitutively active receptor from a generally constitutively active one, as β arrestin-2 recruitment is a later and longer lasting step in receptor signaling and would thus predominate in observation in either case. This is

especially true given the Ca²⁺ mobilization method we are using to measure G protein signaling, which is not well designed to detect constitutive activity. Our results here may reflect an inaccessibility of constitutively active R134A CXCR4 to G proteins due to preoccupation with other steps in signaling (as well as the transient nature of Ca²⁺ mobilization) more than a reduction in G protein coupling competency. It is also particularly difficult to interpret the BRET results in this case as the large CXCL12-mediated BRET change may actually represent conformational changes within pre-associated receptor:arrestin complexes. Although we are not able to fully interpret these results, we are currently undertaking follow-up studies to understand the structure and interactions of the constitutively active R134A CXCR4 mutant.

Two residues in TMV, W195 and Q200, show substantial effects on signaling when mutated. As we mentioned in Gustavsson et al. (2017), in which the same residues had large effects when mutated in ACKR3, these findings suggest allosteric involvement of residues at these positions in chemokine receptor activation, as they are not directly involved in the binding pocket or the signaling core of the receptor. It is interesting that both residues are present in the vicinity of the crystallographic CXCR4 homodimer interface, and W195 is directly involved in the interface (Wu, Chien et al. 2010). In a study of the effects of various mutations on CXCR4 homodimerization, W195A was the sole single residue mutation that yielded effects on dimerization affinity as observed by BRET-based GPCR dimerization assays (Kufareva, Stephens et al. 2013). While evidence for functional significance of class A GPCR homodimerization has remained elusive, and we do not suggest any firm conclusions here, our data are nonetheless consistent with the homodimerization

interface of chemokine receptors being allosterically involved in their activation in some way.

The large effects on efficacy in β arrestin-2 recruitment of the N-terminal CXCR4 truncations are both unexpected and intriguing. Given that CRS1 is unlikely to be directly involved in the intra-molecular conformational change corresponding to CXCR4 activation, it is possible that CRS1 functions to enwrap CXCL12 and extend the lifetime of the active complex. Similar explanations have been discovered to underlie varying efficacies of agonists of other GPCRs (Sykes, Dowling et al. 2009, Sykes, Riddy et al. 2014). At the very least, our data reveal that the functional assumptions made about the CRS1 component of the CXCL12: CXCR4 interaction, namely that CRS1 only contributes purely binding affinity to the complex and is uninvolved in signaling efficacy, is overly simplistic when all of receptor signaling is considered. We are currently preparing several complementary experimental strategies, including equilibrium and kinetic radio-ligand binding experiments and single molecule receptor conformation experiments, in order to understand the structural basis for this surprising functional role of CRS1 and the newly modeled CRS0.5 region of the CXCL12: CXCR4 complex.

We were intrigued by the multiple cases of mutants and truncations that seemed to show more pronounced effects in arrestin signaling experiments. One complicating factor in interpreting these findings is the possibility of “receptor reserve” in our calcium mobilization assays of G protein activation (Rajagopal et al. 2011). Put simply, these assays rely on the measurement of a greatly amplified second messenger (Ca^{2+}), so efficacy changes may not be observed because the maximal

signal achievable in the assay is reached without activating all receptors on the cell surface, obscuring intrinsic receptor activation efficacy differences from experimental observation. Nevertheless, we took advantage of a bias estimation method known as the “equiactive” comparison method, which corrects for varying levels of signal amplification between assays (Ehlert et al. 1999, Griffin et al. 2007, Ehlert 2008, Rajagopal et al. 2011). When bias is estimated using the signaling parameters for all of the mutants that we tested in both β arrestin-2 and G protein signaling activities, several mutants appear to be biased, i.e. are impaired in one signaling pathway more than the other. Obviously R134A is a β arrestin-2 biasing mutation in CXCR4, so it is reassuring that it is estimated to be the most strongly biased of the mutants we tested. Among the CXCR4 truncations 1-10, 1-15, and 1-25, only 1-25 is quantitatively biased, indeed towards G protein signaling (i.e. away from arrestin association). In addition, D262N, D262K, and E277R all appear to be biased toward G protein signaling as well, whereas ECL2 mutants D181K and EADD-KAKK may be weakly biased in the same direction, though it is impossible to be sure due to the large error inherent in the estimation. There are both structural (Reiter, Ahn et al. 2012, Wacker, Wang et al. 2013) and temporal (Sykes, Riddy et al. 2014, Klein Herenbrink, Sykes et al. 2016) explanations that are possible in the case of bias signaling, and we are currently preparing experiments in pursuit of the explanation for the biased effect of these CXCR4 perturbations on arrestin engagement.

References

Berchiche, Y. A., K. Y. Chow, B. Lagane, M. Leduc, Y. Percherancier, N. Fujii, H. Tamamura, F. Bachelierie and N. Heveker (2007). "Direct assessment of

CXCR4 mutant conformations reveals complex link between receptor structure and G(α)i activation." J Biol Chem **282**(8): 5111-5115.

Bonnetterre, J., N. Montpas, C. Boularan, C. Galés and N. Heveker (2016). "Analysis of Arrestin Recruitment to Chemokine Receptors by Bioluminescence Resonance Energy Transfer." Methods Enzymol **570**: 131-153.

Brelot, A., N. Heveker, M. Montes and M. Alizon (2000). "Identification of residues of CXCR4 critical for human immunodeficiency virus coreceptor and chemokine receptor activities." J Biol Chem **275**(31): 23736-23744.

Burg, J. S., J. R. Ingram, A. J. Venkatakrishnan, K. M. Jude, A. Dukkupati, E. N. Feinberg, A. Angelini, D. Waghray, R. O. Dror, H. L. Ploegh and K. C. Garcia (2015). "Structural biology. Structural basis for chemokine recognition and activation of a viral G protein-coupled receptor." Science **347**(6226): 1113-1117.

Crump, M. P., J. H. Gong, P. Loetscher, K. Rajarathnam, A. Amara, F. Arenzana-Seisdedos, J. L. Virelizier, M. Baggiolini, B. D. Sykes and I. Clark-Lewis (1997). "Solution structure and basis for functional activity of stromal cell-derived factor-1; dissociation of CXCR4 activation from binding and inhibition of HIV-1." EMBO J **16**(23): 6996-7007.

Cutolo, P., N. Basdevant, G. Bernadat, F. Bachelerie and T. Ha-Duong (2017). "Interaction of chemokine receptor CXCR4 in monomeric and dimeric state with its endogenous ligand CXCL12: coarse-grained simulations identify differences." J Biomol Struct Dyn **35**(2): 399-412.

Danylesko, I., R. Sareli, N. Varda-Bloom, R. Yerushalmi, N. Shem-Tov, A. Shimoni and A. Nagler (2016). "Plerixafor (Mozobil): A Stem Cell-Mobilizing Agent for Transplantation in Lymphoma Patients Predicted to Be Poor Mobilizers - A Pilot Study." Acta Haematol **135**(1): 29-36.

Doranz, B. J., M. J. Orsini, J. D. Turner, T. L. Hoffman, J. F. Berson, J. A. Hoxie, S. C. Peiper, L. F. Brass and R. W. Doms (1999). "Identification of CXCR4 domains that support coreceptor and chemokine receptor functions." J Virol **73**(4): 2752-2761.

Ehlert, F. J. (2008). "On the analysis of ligand-directed signaling at G protein-coupled receptors." Naunyn Schmiedebergs Arch Pharmacol **377**(4-6): 549-577.

Ehlert, F. J., M. T. Griffin, G. W. Sawyer and R. Bailon (1999). "A simple method for estimation of agonist activity at receptor subtypes: comparison of native and cloned M3 muscarinic receptors in guinea pig ileum and transfected cells." J Pharmacol Exp Ther **289**(2): 981-992.

Farzan, M., G. J. Babcock, N. Vasilieva, P. L. Wright, E. Kiprilov, T. Mirzabekov and H. Choe (2002). "The role of post-translational modifications of the CXCR4 amino terminus in stromal-derived factor 1 alpha association and HIV-1 entry." J Biol Chem **277**(33): 29484-29489.

Griffin, M. T., K. W. Figueroa, S. Liller and F. J. Ehlert (2007). "Estimation of agonist activity at G protein-coupled receptors: analysis of M2 muscarinic receptor signaling through Gi/o,Gs, and G15." J Pharmacol Exp Ther **321**(3): 1193-1207.

Guo, F., Y. Wang, J. Liu, S. C. Mok, F. Xue and W. Zhang (2016). "CXCL12/CXCR4: a symbiotic bridge linking cancer cells and their stromal neighbors in oncogenic communication networks." Oncogene **35**(7): 816-826.

Gustavsson, M., L. Wang, N. van Gils, B. S. Stephens, P. Zhang, T. J. Schall, S. Yang, R. Abagyan, M. R. Chance, I. Kufareva and T. M. Handel (2017). "Structural basis of ligand interaction with atypical chemokine receptor 3." Nat Commun **8**: 14135.

Huang, X., J. Shen, M. Cui, L. Shen, X. Luo, K. Ling, G. Pei, H. Jiang and K. Chen (2003). "Molecular dynamics simulations on SDF-1alpha: binding with CXCR4 receptor." Biophys J **84**(1): 171-184.

Klein Herenbrink, C., D. A. Sykes, P. Donthamsetti, M. Canals, T. Coudrat, J. Shonberg, P. J. Scammells, B. Capuano, P. M. Sexton, S. J. Charlton, J. A. Javitch, A. Christopoulos and J. R. Lane (2016). "The role of kinetic context in apparent biased agonism at GPCRs." Nat Commun **7**: 10842.

Kufareva, I., M. Gustavsson, Y. Zheng, B. S. Stephens and T. M. Handel (2017). "What Do Structures Tell Us About Chemokine Receptor Function and Antagonism?" Annu Rev Biophys **46**: 175-198.

Kufareva, I., T. M. Handel and R. Abagyan (2015). "Experiment-Guided Molecular Modeling of Protein-Protein Complexes Involving GPCRs." Methods Mol Biol **1335**: 295-311.

Kufareva, I., B. Stephens, C. T. Gilliland, B. Wu, G. Fenalti, D. Hamel, R. C. Stevens, R. Abagyan and T. M. Handel (2013). "A novel approach to quantify G-protein-coupled receptor dimerization equilibrium using bioluminescence resonance energy transfer." Methods Mol Biol **1013**: 93-127.

Kufareva, I., B. S. Stephens, L. G. Holden, L. Qin, C. Zhao, T. Kawamura, R. Abagyan and T. M. Handel (2014). "Stoichiometry and geometry of the CXC chemokine receptor 4 complex with CXC ligand 12: molecular modeling and experimental validation." Proc Natl Acad Sci U S A **111**(50): E5363-5372.

Loetscher, P., J. H. Gong, B. Dewald, M. Baggiolini and I. Clark-Lewis (1998). "N-terminal peptides of stromal cell-derived factor-1 with CXC chemokine receptor 4 agonist and antagonist activities." *J Biol Chem* **273**(35): 22279-22283.

Mona, C. E., É. Besserer-Offroy, J. Cabana, M. Lefrançois, P. E. Boulais, M. R. Lefebvre, R. Leduc, P. Lavigne, N. Heveker, É. Marsault and E. Escher (2016). "Structure-Activity Relationship and Signaling of New Chimeric CXCR4 Agonists." *J Med Chem* **59**(16): 7512-7524.

Orsini, M. J., J. L. Parent, S. J. Mundell, A. Marchese and J. L. Benovic (1999). "Trafficking of the HIV coreceptor CXCR4. Role of arrestins and identification of residues in the c-terminal tail that mediate receptor internalization." *J Biol Chem* **274**(43): 31076-31086.

Palczewski, K., T. Kumasaka, T. Hori, C. A. Behnke, H. Motoshima, B. A. Fox, I. Le Trong, D. C. Teller, T. Okada, R. E. Stenkamp, M. Yamamoto and M. Miyano (2000). "Crystal structure of rhodopsin: A G protein-coupled receptor." *Science* **289**(5480): 739-745.

Pozzobon, T., G. Goldoni, A. Viola and B. Molon (2016). "CXCR4 signaling in health and disease." *Immunol Lett* **177**: 6-15.

Qin, L., I. Kufareva, L. G. Holden, C. Wang, Y. Zheng, C. Zhao, G. Fenalti, H. Wu, G. W. Han, V. Cherezov, R. Abagyan, R. C. Stevens and T. M. Handel (2015). "Structural biology. Crystal structure of the chemokine receptor CXCR4 in complex with a viral chemokine." *Science* **347**(6226): 1117-1122.

Rajagopal, S., S. Ahn, D. H. Rominger, W. Gowen-MacDonald, C. M. Lam, S. M. Dewire, J. D. Violin and R. J. Lefkowitz (2011). "Quantifying ligand bias at seven-transmembrane receptors." *Mol Pharmacol* **80**(3): 367-377.

Rasmussen, S. G., B. T. DeVree, Y. Zou, A. C. Kruse, K. Y. Chung, T. S. Kobilka, F. S. Thian, P. S. Chae, E. Pardon, D. Calinski, J. M. Mathiesen, S. T. Shah, J. A. Lyons, M. Caffrey, S. H. Gellman, J. Steyaert, G. Skiniotis, W. I. Weis, R. K. Sunahara and B. K. Kobilka (2011). "Crystal structure of the β 2 adrenergic receptor-Gs protein complex." *Nature* **477**(7366): 549-555.

Reiter, E., S. Ahn, A. K. Shukla and R. J. Lefkowitz (2012). "Molecular mechanism of β -arrestin-biased agonism at seven-transmembrane receptors." *Annu Rev Pharmacol Toxicol* **52**: 179-197.

Scholten, D. J., M. Canals, D. Maussang, L. Roumen, M. J. Smit, M. Wijtmans, C. de Graaf, H. F. Vischer and R. Leurs (2012). "Pharmacological modulation of chemokine receptor function." *Br J Pharmacol* **165**(6): 1617-1643.

Sokol, C. L. and A. D. Luster (2015). "The chemokine system in innate immunity." Cold Spring Harb Perspect Biol **7**(5).

Sykes, D. A., M. R. Dowling and S. J. Charlton (2009). "Exploring the mechanism of agonist efficacy: a relationship between efficacy and agonist dissociation rate at the muscarinic M3 receptor." Mol Pharmacol **76**(3): 543-551.

Sykes, D. A., D. M. Riddy, C. Stamp, M. E. Bradley, N. McGuinness, A. Sattikar, D. Guerini, I. Rodrigues, A. Glaenzel, M. R. Dowling, F. Mullershausen and S. J. Charlton (2014). "Investigating the molecular mechanisms through which FTY720-P causes persistent S1P1 receptor internalization." Br J Pharmacol **171**(21): 4797-4807.

Tan, Q., Y. Zhu, J. Li, Z. Chen, G. W. Han, I. Kufareva, T. Li, L. Ma, G. Fenalti, W. Zhang, X. Xie, H. Yang, H. Jiang, V. Cherezov, H. Liu, R. C. Stevens, Q. Zhao and B. Wu (2013). "Structure of the CCR5 chemokine receptor-HIV entry inhibitor maraviroc complex." Science **341**(6152): 1387-1390.

Thiele, S., J. Mungalpara, A. Steen, M. M. Rosenkilde and J. Våbenø (2014). "Determination of the binding mode for the cyclopentapeptide CXCR4 antagonist FC131 using a dual approach of ligand modifications and receptor mutagenesis." Br J Pharmacol **171**(23): 5313-5329.

Valentin-Hansen, L., M. Groenen, R. Nygaard, T. M. Frimurer, N. D. Holliday and T. W. Schwartz (2012). "The arginine of the DRY motif in transmembrane segment III functions as a balancing micro-switch in the activation of the β 2-adrenergic receptor." J Biol Chem **287**(38): 31973-31982.

Wacker, D., C. Wang, V. Katritch, G. W. Han, X. P. Huang, E. Vardy, J. D. McCorvy, Y. Jiang, M. Chu, F. Y. Siu, W. Liu, H. E. Xu, V. Cherezov, B. L. Roth and R. C. Stevens (2013). "Structural features for functional selectivity at serotonin receptors." Science **340**(6132): 615-619.

Wescott, M. P., I. Kufareva, C. Paes, J. R. Goodman, Y. Thaker, B. A. Puffer, E. Berdougo, J. B. Rucker, T. M. Handel and B. J. Doranz (2016). "Signal transmission through the CXC chemokine receptor 4 (CXCR4) transmembrane helices." Proc Natl Acad Sci U S A **113**(35): 9928-9933.

Wu, B., E. Y. Chien, C. D. Mol, G. Fenalti, W. Liu, V. Katritch, R. Abagyan, A. Brooun, P. Wells, F. C. Bi, D. J. Hamel, P. Kuhn, T. M. Handel, V. Cherezov and R. C. Stevens (2010). "Structures of the CXCR4 chemokine GPCR with small-molecule and cyclic peptide antagonists." Science **330**(6007): 1066-1071.

Xu, L., Y. Li, H. Sun, D. Li and T. Hou (2013). "Structural basis of the interactions between CXCR4 and CXCL12/SDF-1 revealed by theoretical approaches." *Mol Biosyst* **9**(8): 2107-2117.

Ye, J., V. Kober, M. Tellers, Z. Naji, P. Salmon and J. F. Markusen (2009). "High-level protein expression in scalable CHO transient transfection." *Biotechnol Bioeng* **103**(3): 542-551.

Zheng, Y., G. W. Han, R. Abagyan, B. Wu, R. C. Stevens, V. Cherezov, I. Kufareva and T. M. Handel (2017). "Structure of CC Chemokine Receptor 5 with a Potent Chemokine Antagonist Reveals Mechanisms of Chemokine Recognition and Molecular Mimicry by HIV." *Immunity* **46**(6): 1005-1017.e1005.

Zheng, Y., L. Qin, N. V. Zacarias, H. de Vries, G. W. Han, M. Gustavsson, M. Dabros, C. Zhao, R. J. Cherney, P. Carter, D. Stamos, R. Abagyan, V. Cherezov, R. C. Stevens, A. P. IJzerman, L. H. Heitman, A. Tebben, I. Kufareva and T. M. Handel (2016). "Structure of CC chemokine receptor 2 with orthosteric and allosteric antagonists." *Nature* **540**(7633): 458-461.

Zhou, H. and H. H. Tai (1999). "Characterization of recombinant human CXCR4 in insect cells: role of extracellular domains and N-glycosylation in ligand binding." *Arch Biochem Biophys* **369**(2): 267-276.

Zhou, H. and H. H. Tai (2000). "Expression and functional characterization of mutant human CXCR4 in insect cells: role of cysteinyl and negatively charged residues in ligand binding." *Arch Biochem Biophys* **373**(1): 211-217.

Ziarek, J. J., A. B. Kleist, N. London, B. Raveh, N. Montpas, J. Bonnetterre, G. St-Onge, C. J. DiCosmo-Ponticello, C. A. Koplinski, I. Roy, B. Stephens, S. Thelen, C. T. Veldkamp, F. D. Coffman, M. C. Cohen, M. B. Dwinell, M. Thelen, F. C. Peterson, N. Heveker and B. F. Volkman (2017). "Structural basis for chemokine recognition by a G protein-coupled receptor and implications for receptor activation." *Sci Signal* **10**(471).

Figures and Tables

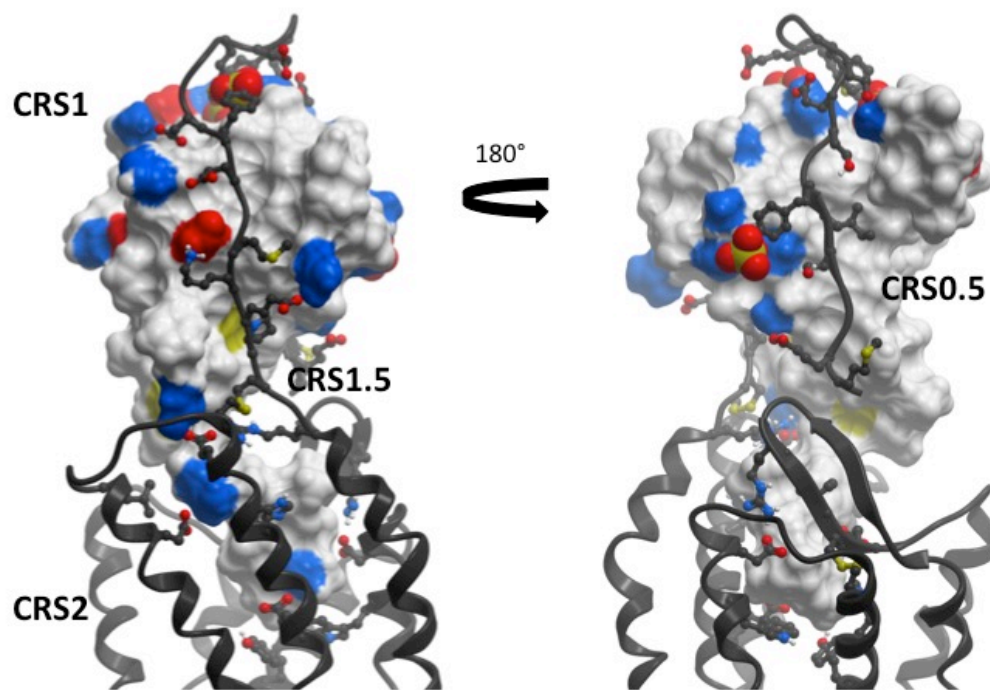


Figure 5.1. A full length model of the CXCL12:CXCR4 signaling complex. General regions of CRS1, CRS1.5, and CRS2 are labeled along with the more recently predicted CRS0.5 interaction component.

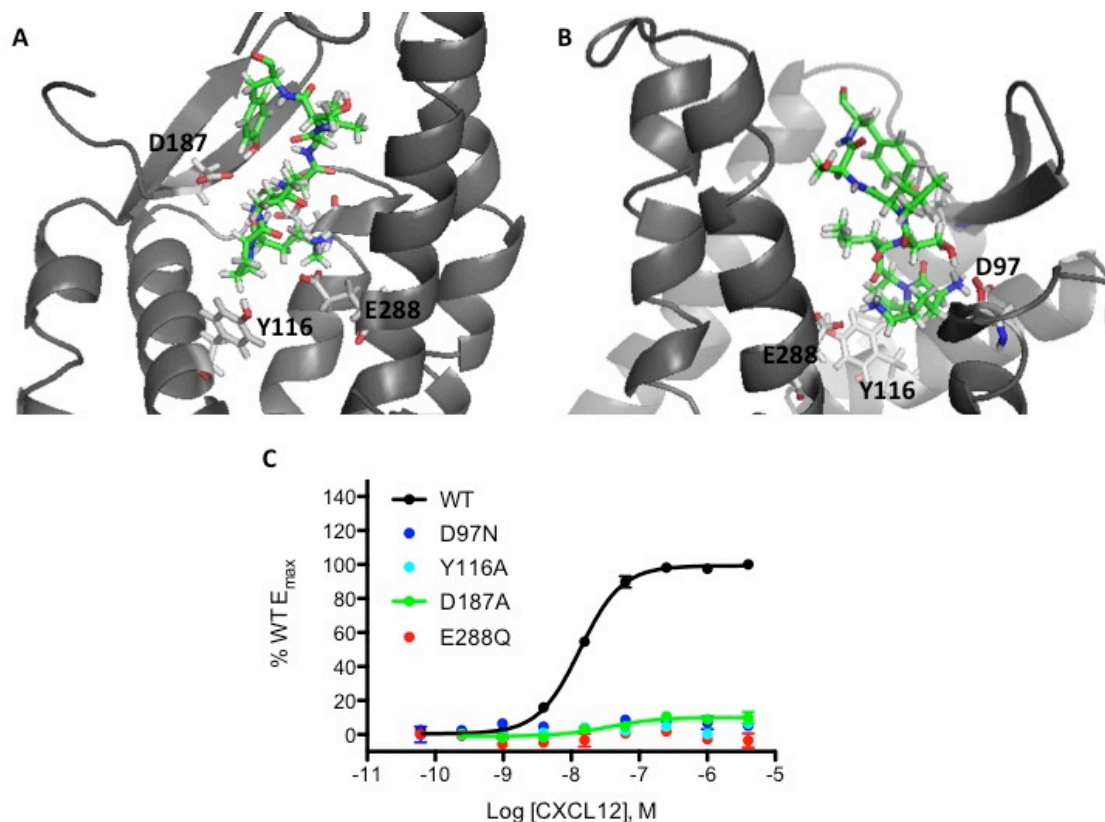


Figure 5.2. Mutating CRS2 residues known to be critical to G protein signaling abrogates β arrestin-2 recruitment as well. (A) Close-up and isolated view of the extreme CXCL12 N-terminus engaged with the CXCR4 binding pocket. The chemokine N-terminus (green) is shown as sticks and the receptor (grey) are shown with cartoon rendering for simplicity. The signal initiation residues Y116 and E288 as well as the engagement residues D97 and D187 are highlighted by additional stick rendering to emphasize their interactions with the CXCL12 N-terminus. (B) CXCL12 concentration response BRET-based β arrestin-2 recruitment data for D97N, Y116A, D187A, and E288Q. Cells co-expressing either WT or mutant CXCR4 fused C-terminally to RLuc3 along with GFP10- β arrestin-2 were exposed to varying concentrations of WT CXCL12 for 30 minutes before their luminescence at both donor (RLuc3) and acceptor (GFP10) emission maxima measured. WT CXCR4 was included in every experiment to allow for normalization. Data represent the normalized mean values from at least three independent experiments (\pm SEM), each performed in duplicate. Curves were modeled using the four-parameter agonist response equation available in GraphPad PRISM.

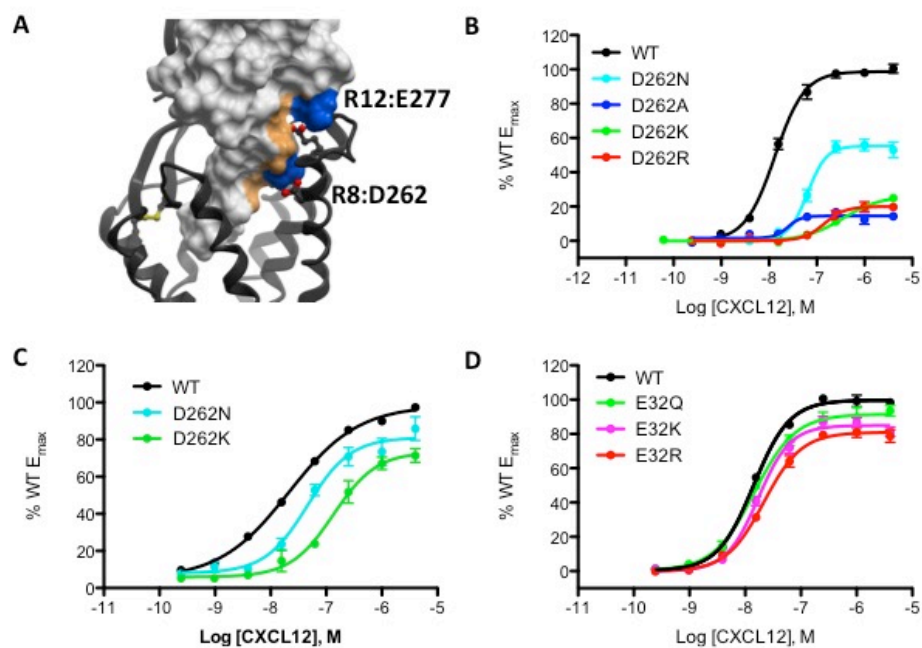


Figure 5.3. Residue D262 of CXCR4 is important for potent and efficacious CXCL12-mediated receptor activation. (A) Close-up view of the modeled interaction between CXCL12 R8 and CXCR4:D262. CXCR4 residue E277R is also shown in its nearby interaction with CXCL12 R12. (B) CXCL12 concentration response BRET-based β arrestin-2 recruitment data for a series of D262 mutations, shown alongside WT results. (C) CXCL12 concentration response Ca^{2+} mobilization data shown alongside WT results. Cells expressing mutant receptors were tested alongside cells expressing comparable levels of WT CXCR4 to allow for normalization and correct interpretation. CHO $\text{G}\alpha_{15}$ stable cells expressing WT, D262N, or D262K CXCR4 were stimulated with varying concentrations of CXCL12 in the presence of FLIPR4 Ca^{2+} -sensitive fluorescent dye immediately before fluorescence reading were taken. Cells expressing mutant receptors were tested alongside cells expressing comparable levels of WT CXCR4 to allow for normalization and correct interpretation. Data represent the normalized mean values from at least three independent experiments (\pm SEM), each performed in triplicate. Curves were modeled using the four-parameter agonist response equation available in GraphPad PRISM. (D) CXCL12 concentration response BRET-based β arrestin-2 recruitment data for Q, K, and R mutations of CXCR4 E32 shown with WT data for comparison. Only minor effects are seen for these mutants.

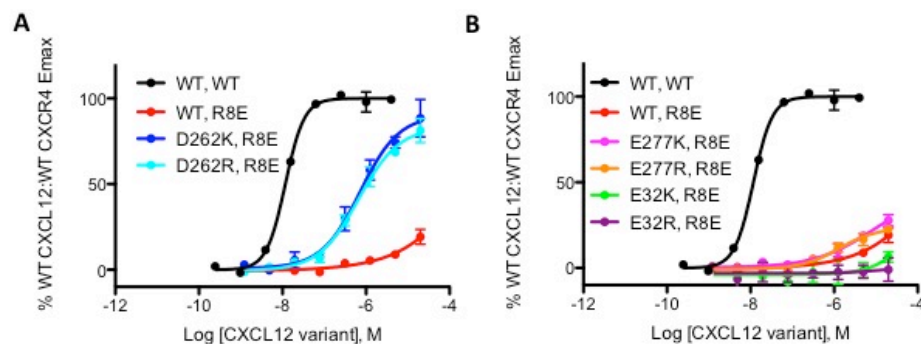


Figure 5.4. R8E mutation in CXCL12 severely impairs β arrestin-2 recruitment, and recruitment is greatly rescued by both D262K and R mutations in CXCR4. (A) β arrestin-2 recruitment data obtained by stimulating (red) WT CXCR4 with R8E CXCL12, (black) WT CXCR4 with WT CXCL12, (dark blue) D262K CXCR4 with R8E CXCL12, and (light blue) D262K CXCR4 with R8E CXCL12. (B) β arrestin-2 recruitment data obtained by stimulating (black) WT CXCR4 with WT CXCL12 or (red) WT CXCR4, (purple) E32R CXCR4, (green) E32K CXCR4, (magenta) E277K CXCR4, and (orange) E277R with R8E CXCL12. The data throughout represent the normalized mean values from at least three independent experiments (\pm SEM), each performed in triplicate, and are plotted as normalized to maximal WT:WT activity in the assay. The same combined WT:WT and R8E CXCL12:WT CXCR4 datasets are shown in both panels.

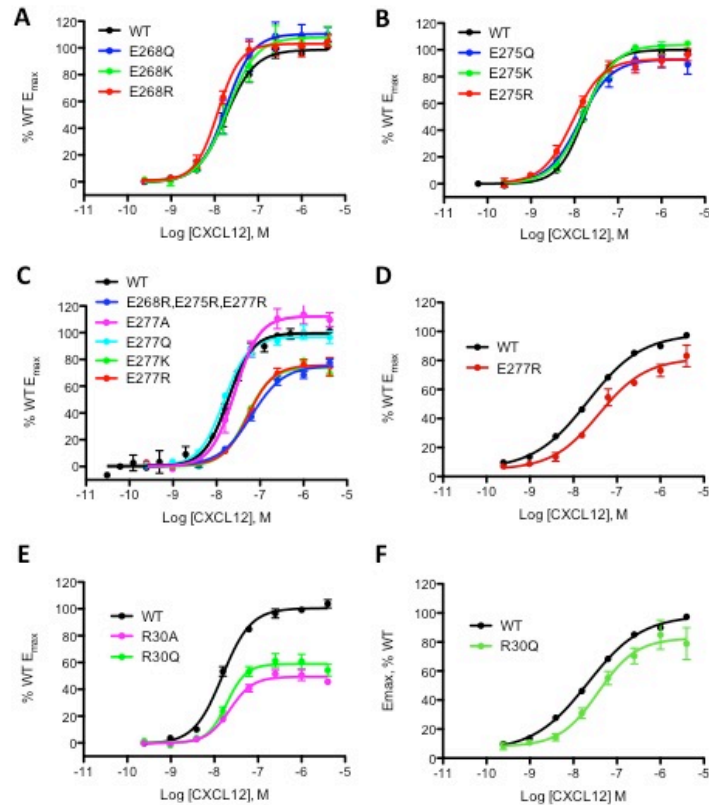


Figure 5.5. Mutagenesis targeting both R30 and E277 impairs CXCR4 signaling, supporting the engagement of both residues with the CXCL12 N-terminus as predicted in the model. CXCL12 concentration response BRET-based β arrestin-2 recruitment data showing that mutating either E268 (A) or E275 (B) (both proximal to R12 of CXCL12 in the model) produces no notable differences in signaling. (D) β arrestin-2 recruitment data demonstrates that charge-reversing mutation of CXCR4 E277 reduces signaling. Mutating glutamates 268, 275, and 277 in the same receptor construct produced no additional decrease in signaling. (E) CXCL12 concentration response Ca^{2+} mobilization data for E277R CXCR4 shown alongside WT results. CHO Ga15 stable cells expressing WT or E277R mutant CXCR4 were stimulated with varying concentrations of CXCL12 in the presence of FLIPR4 Ca^{2+} -sensitive fluorescent dye immediately before fluorescence reading were taken. Cells expressing mutant receptors were tested alongside cells expressing comparable levels of WT CXCR4 to allow for normalization and correct interpretation. (F) β arrestin-2 recruitment data for R30A and R30Q mutants of CXCR4. Both mutations have a major effect on efficacy whereas only R30A seems to affect potency. (G) CXCL12 concentration response Ca^{2+} mobilization data for R30Q CXCR4 shown alongside WT results. In the case of β arrestin-2 recruitment experiments, Data represent the normalized mean values from at least three independent experiments (\pm SEM), each performed in duplicate. In the case of Ca^{2+} mobilization data, data represent the normalized mean values from at least three independent experiments (\pm SEM), each performed in triplicate. In both cases curves were modeled using the four-parameter agonist response equation available in GraphPad PRISM.

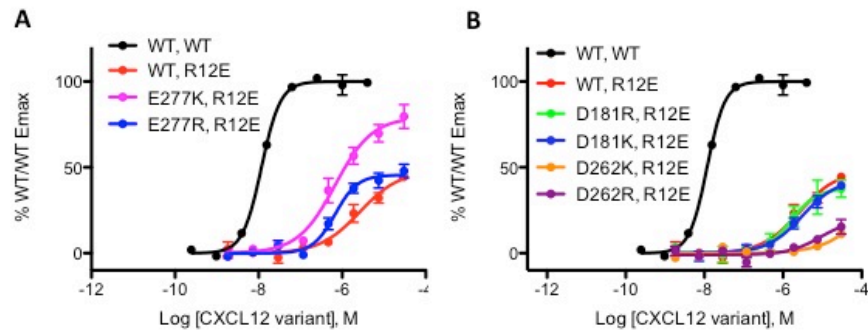


Figure 5.6. Mutating R12 of CXCL12 to glutamate severely impairs its activation of CXCR4, and this effect is substantially reversed by charge-reversing mutation of CXCR4 residue E277. (A) CXCL12 concentration response BRET-based β arrestin-2 recruitment data obtained by stimulating (black) WT CXCR4 with WT CXCL12 or (red) WT CXCR4, (magenta) E277K CXCR4, and (blue) E277R CXCR4 with R12E CXCL12. (B) β arrestin-2 recruitment data obtained by stimulating (black) WT CXCR4 with WT CXCL12 or (red) WT CXCR4, (blue) D181K CXCR4, (green) D181R CXCR4, (orange) D262K CXCR4, and (maroon) D262R CXCR4 with R12E CXCL12. The data throughout represent the normalized mean values from at least three independent experiments (\pm SEM), each performed in triplicate, and are plotted as normalized to maximal WT:WT activity in the assay. The same combined WT/WT and R12E CXCL12/WT CXCR4 datasets are shown in both panels.

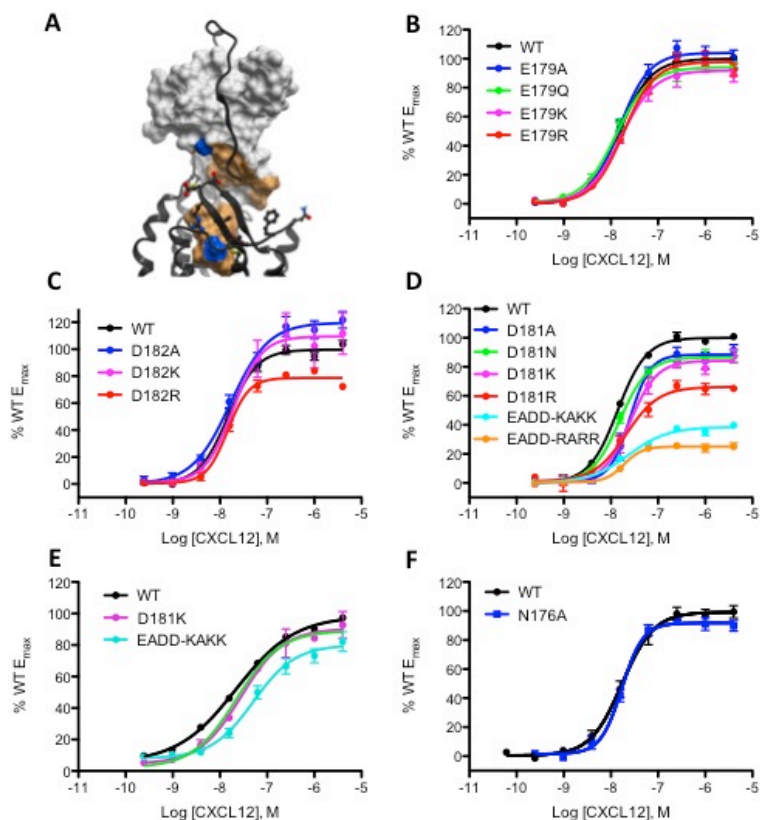


Figure 5.7. Negatively charged residues in ECL2 of CXCR4 are important for the efficacy of arrestin recruitment. (A) Close-up of the CXCL12: CXCR4 model where ECL2 engages with CXCR4. The interactions here are not clear as this region of CXCR4 does not closely engage CXCL12 in the model, but the basic residues K27 and R41 present in the β -sheet domain of CXCL12 may attract the negative charge at the tip of CXCR4 ECL2. (B) β arrestin-2 recruitment CXCL12 concentration response data for mutants of CXCR4 residue E179, showing no differences in signaling from WT CXCR4 even when E179 is charge-reversed. (C) β arrestin-2 recruitment concentration response data for mutants of CXCR4 residue D182. D182A appears to have slightly improved efficacy, whereas D182K shows no effect and D182R is slightly impaired in efficacy. (D) β arrestin-2 recruitment CXCL12 concentration response BRET data for mutants of CXCR4 residue D181 as well as combined charge-reversing mutations of E179, D181, and D182. Effects on efficacy are seen for all D181 mutations, with D181R showing a particularly strong effect. The combined charge-reversing mutations both severely impaired the efficacy of β arrestin-2 recruitment. (E) Ca^{2+} mobilization CXCL12 concentration response data for D181K and the combined triple lysine mutant reveal much milder effects on G protein signaling (F) β arrestin-2 recruitment CXCL12 concentration response data for N176A CXCR4 mutant, which shows no difference from WT signaling. Data represent the normalized mean values from at least three independent experiments (\pm SEM), each performed in duplicate in the case of β arrestin-2 recruitment experiments and in triplicate in the case of Ca^{2+} mobilization. Curves were modeled using the four-parameter agonist response equation available in GraphPad PRISM.

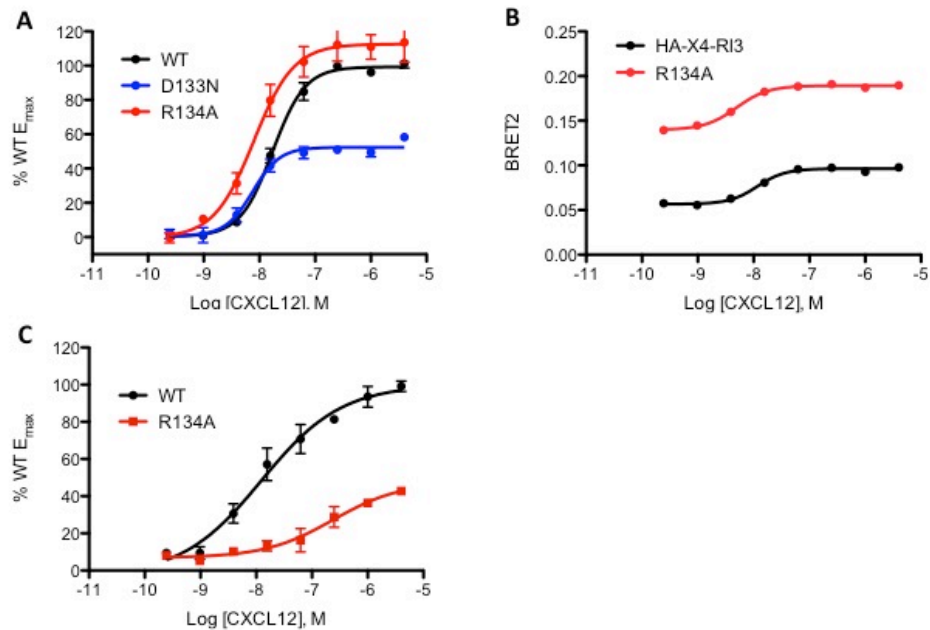


Figure 5.8. Mutation of the DRY motif residue R134A produces a constitutively active β arrestin-2 recruiting form of CXCR4. (A) Normalized CXCL12 concentration response β arrestin-2 recruitment data for D133N and R134A CXCR4 mutations. R134A is improved in both potency and efficacy over WT signaling, whereas D133N allows for slightly more potent CXCL12-mediated β arrestin-2 recruitment but is reduced by half in efficacy compared to WT signaling. (B) The raw BRET ratio data from the same experiments. The large increase in basal BRET in the case of R134A indicates a constitutive engagement with β arrestin-2. (C) Ca^{2+} mobilization data for the R134A CXCR4 mutant shown along with WT results. R134A is severely impaired in both potency and efficacy. For β arrestin-2 recruitment experiments, data represent the normalized mean values from at least three independent experiments (\pm SEM), each performed in duplicate. For Ca^{2+} mobilization data, data represent the normalized mean values from at least three independent experiments (\pm SEM), each performed in triplicate. In both cases curves were modeled using the four-parameter agonist response equation available in GraphPad PRISM.

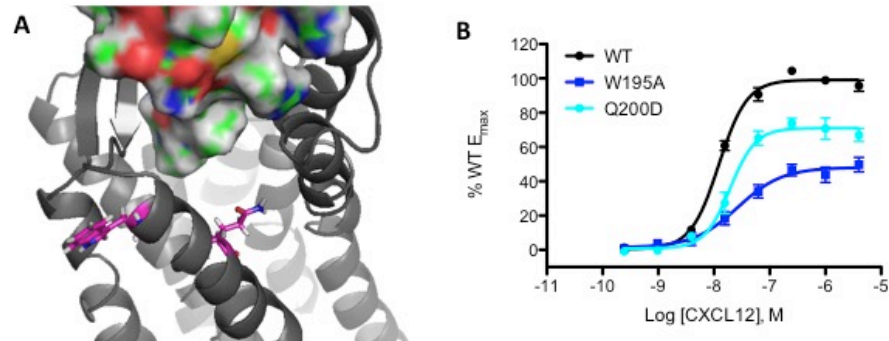


Figure 5.9. Mutating TM5 residues W195 and Q200 causes deficits in signaling that are not easily explained by the CXCL12: CXCR4 model. (A) Close-up of view of the positions of W195 and Q200 in TM5 of CXCR4. CXCL12 is shown with space-filling surface rendering to emphasize its occupation of the CXCR4 binding pocket, which is opposite these TM5 residues. (B) Normalized CXCL12 concentration response β arrestin-2 recruitment BRET data for W195A and Q200D CXCR4 mutants. Data represent the normalized mean values from at least three independent experiments (\pm SEM), each performed in duplicate. Curves were modeled using the four-parameter agonist response equation available in GraphPad PRISM.

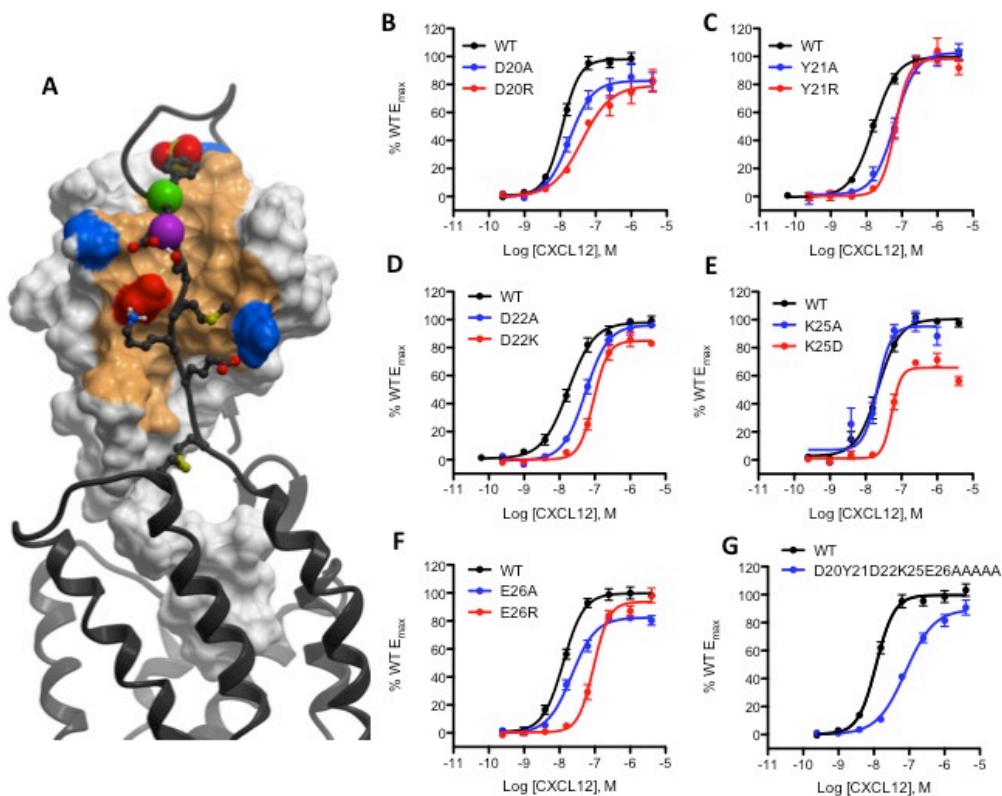


Figure 5.10. The effects of mutating charged residues (as well as the putatively sulfated Y21 residue) in the most proximal region of CRS1 reinforce the role of this region in providing for potent CXCL12 association. (A) Close-up of the interaction of the C-terminal portion of CRS1 with CXCL12, with charged residues D20, D22, K25, and E26 along with Y21 highlighted as spheres. (B-G) β arrestin-2 recruitment CXCL12 concentration response data for alanine (cyan) and charge-reversing (magenta) mutations of (B) D20, (C) Y21, (D) D22, (E) K25, (F) E26, and (G) all of these residues combined led overwhelmingly to effects on potency as expected. K25A seems to be the least consistent with the pattern. K25A was the only mutant to have no effect on signaling and K25D was the only mutant to have a clear effect on the efficacy of signaling. The combined alanine mutant shows the largest potency effect.

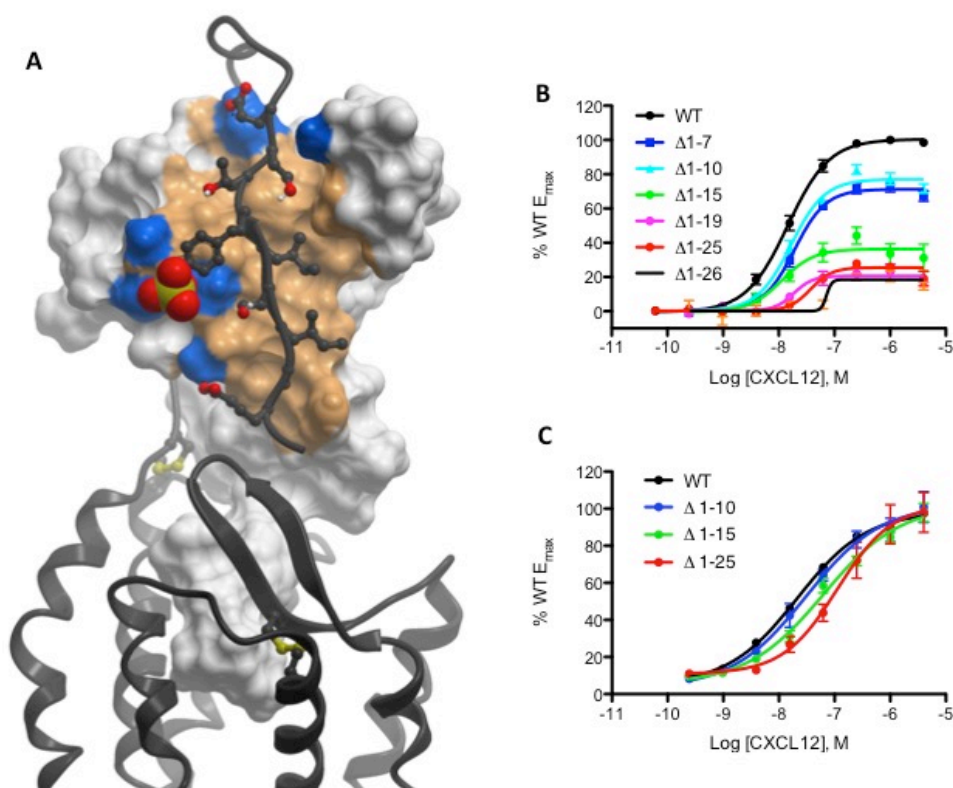


Figure 5.11. Successively larger truncations of CRS0.5 and CRS1 produce surprising progressive deficits in β arrestin-2 recruitment efficacy that are not seen in Ca^{2+} mobilization results. (A) Close-up view of the predicted CRS0.5 interaction between the extreme CXCR4 N-terminus and CXCL12. (B) β arrestin-2 recruitment CXCL12 concentration response data for truncations ranging from all of CRS0.5 (1-7) to all of CRS1 (1-26) show clear impairments in efficacy that generally increase with truncation size. (C) CXCL12 concentration response Ca^{2+} mobilization data for the 1-10, 1-15, and 1-25 length CXCR4 truncations.

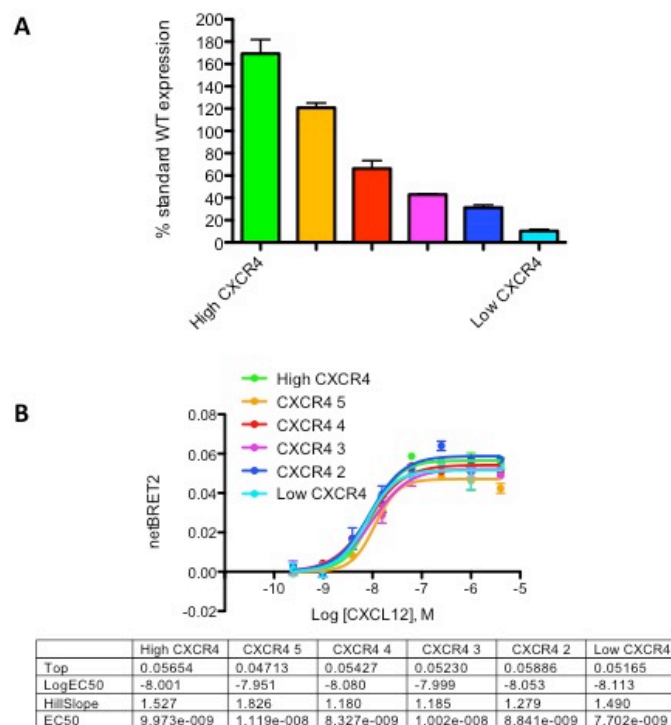


Figure 5.S1. BRET results are unaffected by changes in receptor-RLuc3 expression level within a wide range. Cells were transfected with seven different amounts of WT CXCR4-RLuc3 along with GFP10- β arrestin-2 and assayed for both surface expression and CXCL12-mediated β arrestin-2 recruitment via BRET. (A) Receptor surface expression was quantified via flow cytometry with a PE-conjugated anti-CXCR4 antibody (clone 12G5). The geometric mean of PE fluorescence for each sample was normalized to that observed in cells transfected with the usual amount of WT CXCR4-RLuc3 DNA used in our CXCL12-mediated β arrestin-2 recruitment BRET assay. Data are means from two independent experiments (\pm SEM), each performed in duplicate.

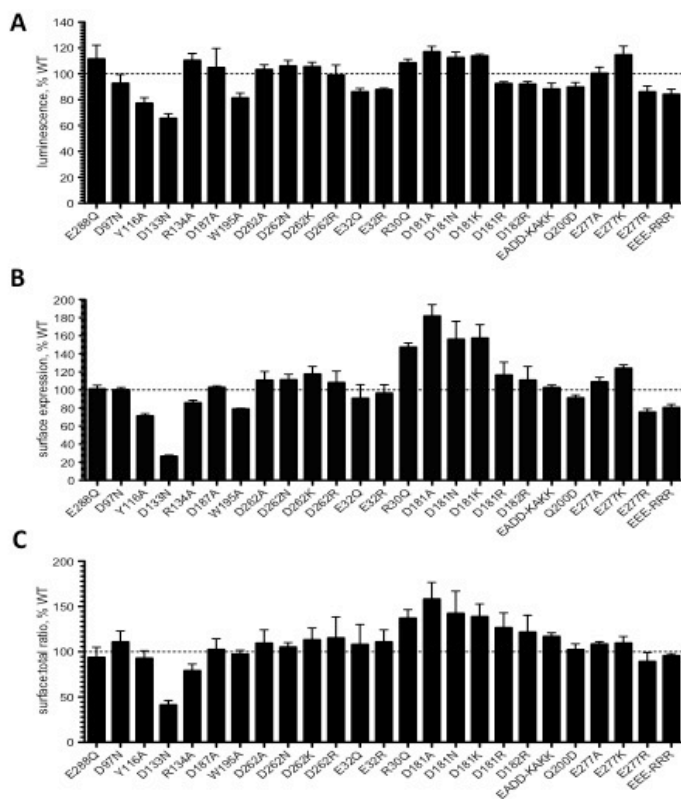


Figure 5.S2. Expression of trans-membrane domain mutant forms of CXCR4 that show differences in signaling from WT receptor. (A) Total unfiltered Rluc3 luminescence, normalized to the luminescence of WT CXCR4-Rluc3, always measured in the same experiment. (B) Surface expression as determined by flow cytometry after staining with fluorophore-conjugated anti-CXCR4 antibody. To ensure the mutations did not interfere with antibody recognition of CXCR4 we used the 1D9 anti-CXCR4 monoclonal antibody, which targets the CXCR4 N-terminus. (C) The ratio of surface (from B) to total (from A) expression, again normalized to WT CXCR4. Data are means of three independent experiments \pm SEM, each performed in duplicate.

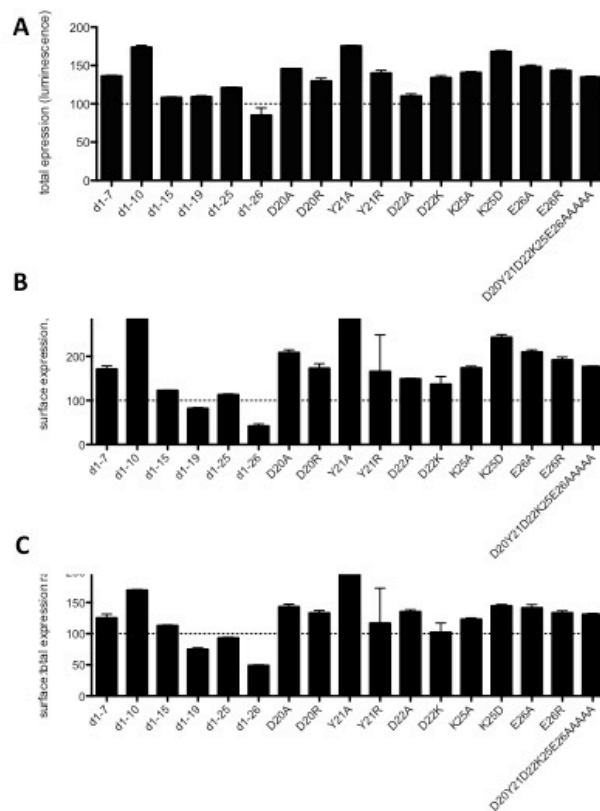


Figure 5.S3. Expression of N-terminal domain mutant and truncated forms of CXCR4 that show differences in signaling from WT receptor. (A) Total unfiltered Rluc3 luminescence, normalized to the luminescence of WT CXCR4-Rluc3, always measured in the same experiment. (B) Surface expression as determined by flow cytometry after staining with fluorophore-conjugated anti-CXCR4 antibody. To ensure the mutations did not interfere with antibody recognition of CXCR4 we used the 12G5 anti-CXCR4 monoclonal antibody, which targets the CXCR4 trans-membrane domain. (C) The ratio of surface (from B) to total (from C) expression, again normalized to WT CXCR4. Data are means of two independent experiments \pm SEM, each performed in duplicate.

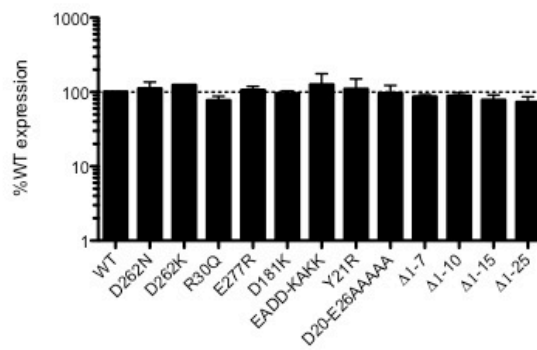


Figure 5.S4. Expression of all mutants tested in Ca²⁺ mobilization signaling assays relative to WT receptor tested on the same day, after adjustment of WT receptor DNA amount according to the observed mutant expression range. As shown by dotted lines in the linear Y-axis graph (top), we were able to express all mutants within +/- 30% of WT levels used for comparison.

Table 5.1. Signaling parameters derived from β arrestin-2 recruitment experiments.
NS = no analyzable signaling detected

<i>CXCR4 mutant</i>	β arrestin-2 recruitment	
	<i>E_{max} (% WT, +/- SE)</i>	<i>pEC₅₀ (+/- SE)</i>
D97N	NS	NS
Y116A	NS	NS
D187A	10.0 ± 1.8	7.44 ± 0.34
E288Q	NS	NS
D262N	55.3 ± 1.9	7.19 ± 0.05
D262A	14.5 ± 1.2	7.61 ± 0.22
D262K	27.0 ± 3.4	6.45 ± 0.16
D262R	20.0 ± 1.4	6.84 ± 0.10
E32Q	91.5 ± 2.1	7.84 ± 0.05
E32K	84.9 ± 1.5	7.77 ± 0.03
E32R	80.9 ± 1.5	7.66 ± 0.04
E268Q	110.5 ± 4.9	7.74 ± 0.09
E268K	108.0 ± 4.7	7.70 ± 0.09
E268R	103.1 ± 2.7	7.93 ± 0.05
E275Q	92.9 ± 3.5	7.88 ± 0.09
E275K	103.8 ± 2.4	7.78 ± 0.05
E275R	92.9 ± 2.3	8.04 ± 0.06
E277A	112.3 ± 3.6	7.57 ± 0.06
E277Q	96.9 ± 2.0	7.83 ± 0.04
E277K	74.1 ± 1.5	7.31 ± 0.03
E277R	75.7 ± 2.5	7.27 ± 0.05
E268R,E275R,E277R	75.3 ± 2.3	7.20 ± 0.05
R30A	49.3 ± 1.5	7.65 ± 0.05
R30Q	58.8 ± 2.1	7.72 ± 0.06
E179A	104.0 ± 2.7	7.83 ± 0.05
E179Q	94.1 ± 2.1	7.89 ± 0.05
E179K	91.8 ± 2.8	7.79 ± 0.07
E179R	97.8 ± 2.3	7.73 ± 0.05
D181A	88.4 ± 2.8	7.59 ± 0.05

Table 5.1. Signaling parameters derived from β arrestin-2 recruitment experiments. (cont.)

<i>CXCR4 mutant</i>	β arrestin-2 recruitment	
	<i>E_{max} (% WT, +/- SEM)</i>	<i>pEC₅₀ (+/- SE)</i>
D181K	84.2 ± 2.7	7.59 ± 0.06
D181R	66.2 ± 2.5	7.67 ± 0.08
D182A	119.7 ± 3.6	7.77 ± 0.07
D182K	109.5 ± 6.7	7.72 ± 0.12
D182R	78.7 ± 1.6	7.83 ± 0.03
E179K,D181K,D182K	38.6 ± 1.6	7.62 ± 0.09
E179R,D181R,D182R	25.0 ± 1.1	7.72 ± 0.07
D133N	52.3 ± 1.7	8.12 ± 0.07
R134A	112.6 ± 4.5	8.10 ± 0.10
W195A	48.1 ± 2.6	7.57 ± 0.12
Q200D	71.0 ± 2.3	7.71 ± 0.05
D20A	82.6 ± 3.6	7.73 ± 0.03
D20R	79.3 ± 4.2	7.38 ± 0.10
Y21A	93.5 ± 2.8	7.08 ± 0.03
Y21R	98.2 ± 3.4	7.18 ± 0.04
D22A	96.0 ± 2.3	7.26 ± 0.04
D22K	84.9 ± 2.3	7.03 ± 0.04
K25A	95.3 ± 5.1	7.67 ± 0.08
K25D	65.7 ± 2.1	7.27 ± 0.06
E26A	82.7 ± 1.7	7.72 ± 0.04
E26R	93.6 ± 2.6	7.03 ± 0.04
D20A,Y21A,D22A,K25A,E26A	89.6 ± 2.9	7.10 ± 0.06
Δ 1-7	73.6 ± 1.7	7.74 ± 0.08
Δ 1-10	79.3 ± 1.6	7.80 ± 0.06
Δ 1-15	37.1 ± 2.7	8.01 ± 0.23
Δ 1-19	21.8 ± 1.8	7.74 ± 0.23
Δ 1-25	27.2 ± 1.5	7.44 ± 0.13
Δ 1-26	19.6 ± 2.3	7.13 ± 0.25

Table 5.2. Signaling parameters derived from Ca²⁺ mobilization experiments.

<i>CXCR4 mutant</i>	Ca²⁺ mobilization	
	<i>E_{max} (% WT, +/- SE)</i>	<i>pEC₅₀ (+/- SE)</i>
D262N	81.1 ± 3.6	7.33 ± 0.09
D262K	73.3 ± 3.6	6.87 ± 0.08
E277R	81.4 ± 4.5	7.41 ± 0.12
R30Q	82.7 ± 5.1	7.43 ± 0.14
D181K	90.5 ± 3.7	7.54 ± 0.09
E179K,D181K,D182K	80.1 ± 3.7	7.29 ± 0.09
R134A	53.3 ± 5.0	6.77 ± 0.10
D20A,Y21A,D22A,K25A,E26A	74.1 ± 4.1	7.06 ± 0.11
Δ 1-10	94.7 ± 3.2	7.52 ± 0.10
Δ 1-15	92.0 ± 2.4	7.29 ± 0.07
Δ 1-25	99.8 ± 2.4	6.96 ± 0.13

Table 5.3. Equiactive bias factors calculated for select mutants. Bias is calculated such that a negative value indicates bias toward G protein activation and a positive value indicates bias toward arrestin association.

*PSE=propagated SEM

<i>CXCR4 mutant</i>	<i>Bias factor (+/- PSE*)</i>
D262N	-0.51 ± 0.13
D262K	-1.09 ± 0.20
E277R	-0.38 ± 0.15
R30Q	-0.07 ± 0.17
D181K	-0.19 ± 0.13
E179K,D181K,D182K	-0.19 ± 0.15
R134A	1.44 ± 0.17
Y21R	0.05 ± 0.19
D20A,Y21A,D22A,K25A,E26A	0.08 ± 0.15
d1-10	0 ± 0.14
d1-15	0.13 ± 0.25
d1-25	-0.29 ± 0.13

Acknowledgement

Chapter five is adapted from a manuscript currently in preparation for submission for publication. (**Stephens, B. S.**; I. Kufareva and T. M. Handel (2017). “Anatomy of the CXC chemokine receptor 4 signaling complex with CXCL12.” in preparation for submission to Science Signaling.) The dissertation author was the primary researcher and author of this material.

Chapter 6

Speculative discussion and future
experimental directions

On the need for cautious interpretation of Ca²⁺ signaling data in chemokine receptor research, and the value of relatively direct measurements of receptor activity

Largely because of the expanding known repertoire of GPCR signaling pathways (Shukla, Xiao et al. 2011) and the phenomenon of biased signaling (Strachan, Sun et al. 2014), there is growing recognition that GPCR signaling must involve both temporal and spatial organization of multiple different signaling effector activation events. This makes it important to independently study the different signaling pathways activated by a receptor. In the case of chemokine receptors in general, G protein activation experiments are almost solely relied on in the literature for testing the effects of mutations on receptor-mediated signaling, with only a few recent exceptions (Benredjem, Girard et al. 2017, Gustavsson, Wang et al. 2017). Moreover, studies have relied overwhelmingly on Ca²⁺ mobilization experiments, which are likely to often be subject to receptor reserve effects that can obscure the true effects of mutations, as discussed in the next section. At present, there are no studies that we are aware of in which CXCR4 mutations were tested for effects in arrestin recruitment using full concentration-response curves. Throughout the majority of the literature, CXCR4 activation is at least tacitly defined without regard for the multiple intracellular activities of the receptor, so that the effects of mutations on G protein signaling (again usually measured through amplified second messenger assays) have always been assumed to fully reveal the underlying effects on receptor function. This likely reflects the relatively recent recognition of the important non-G protein aspects

of GPCR signaling, and the even more recent understanding that different signaling pathways activated by GPCRs may be activated differentially (signaling bias). In any case, we now know that this is certainly not the case, and in fact several CXCR4 mutations and truncations cause much larger apparent effects in arrestin signaling due to both assay sensitivity issues as well as some as of yet unexplained genuinely biased results in certain cases.

The general tendency of CXCR4 mutants to show more pronounced effects in our BRET2 arrestin recruitment assay is a cause for concern when considering the wider body of CXCR4 mutagenesis results. While it is obvious from our data that relying on Ca^{2+} mobilization as a general measure of G protein activation by CXCR4 will (and almost certainly has) lead to underestimation of mutational effects, the problem is even worse in that until quite recently, many CXCR4 mutagenesis experiments were carried out using a single CXCL12 concentration. This is largely due to historical reasons of feasibility, but the cause for caution is nonetheless significant. Considering our data here, in cases with extreme effects such as D262 mutation, the effects are large enough that they are observable in either assay, regardless of the quantified bias. However, in the case of CRS0.5 truncations and ECL2 hairpin charge-reversing mutations, the effects in Ca^{2+} mobilization are so minor by visual inspection that the mutants would be interpreted as essentially ineffectual if only this form of signaling data were available.

When equiactive bias calculation methods (Rajagopal, Ahn et al. 2011) are applied, much of the apparent discrepancy between the two signaling pathway assays turns out to be artificial, as indicated by near-zero bias factors. This result means that

the efficacy differences seen in arrestin recruitment experiments are “exchanged” for potency differences in Ca^{2+} mobilization experiments, which are not as visually obvious due to the logarithmic plotting of ligand concentration when analyzing concentration-response data. The simplest reasonable explanation for this is that the Ca^{2+} mobilization assay is subject to receptor reserve, or in other words that the amplified second messenger levels reach a maximum before all receptors expressed by the experimental cells are activated (Ehlert, Griffin et al. 1999, Griffin, Figueroa et al. 2007, Ehlert 2008).

In light of our results, it seems advisable for researchers in the field to use the most direct, non-amplified signaling readouts available, and BRET-based methods are very advantageous in this regard. They provide a real-time, 1:1 measurement of donor/acceptor proximity. In addition to the elimination of the concern of receptor reserve, this also allows for the design of experiments in which closely comparable receptor expression levels are not critical to reliable interpretation. The unexpected findings of major efficacy effects for CRS1 truncations in particular highlights the need for cautious re-interpretation of the mutagenesis results throughout the existing literature, especially those data derived using second messenger assays such as cAMP and Ca^{2+} -measuring assays. Chapter 5 herein, currently in preparation for publication, features full concentration-response curve arrestin signaling data for an extensive set of CXCR4 mutations, and should make a major contribution to catching up on our understanding of the established CXCR4 signaling pathway that has not been unexplored via mutagenesis.

Extended interpretation of N-terminal truncations and other CXCR4 perturbations that cause unexpectedly large efficacy deficits in arrestin recruitment

As our arrestin recruitment data make clear, the traditional functional implications of the CRS1/CRS2 model, specifically that CRS1 is involved in initial binding but not in receptor activation efficacy after binding, is at least partly oversimplified. The standard interpretation of such a large decrease in efficacy, whether biased or not, would be that the receptor is unable to achieve the fully active conformation in the absence of the full CRS1 interaction. This interpretation seems to be structurally unrealistic given the distance between the CRS1: CXCL12 globular domain interaction and critical activation-causing interactions between CRS2 and the CXCL12 N-terminus are somewhat understood (Wescott, Kufareva et al. 2016). It also contradicts the long held and reasonably well evidenced CRS1/CRS2 two-site model. Nevertheless, it is conceivable that the enwrapping of the CXCL12 globular domain is necessary for receptor activation in an indirect way. Perhaps this CRS1 engagement is necessary to induce/stabilize an intra-molecular CXCL12 orientation that is required for the CXCL12 N-terminus to activate CXCR4. The similar finding of apparently arrestin-specific loss of efficacy resulting from charge-reversing mutation of the CXCR4 ECL2 hairpin would concord with this explanation. In the model, the ECL2 hairpin is extended toward CXCL12 just under the CXCR4 N-terminus, so such a “CXCL12-priming” requirement of CRS1 may also involve this region of ECL2.

An interesting alternative explanation lies in the role of agonist binding kinetics in receptor activation efficacy. In a recent series of publications, Charlton and colleagues have renewed interest in a long-neglected role of dissociation rates in the efficacy measured in GPCR activity assays (Sykes, Dowling et al. 2009, Sykes, Riddy et al. 2014). In the seminal study (Sykes, Dowling and Charlton 2009), the researchers observed that varying off-rates for a series of M3 muscarinic receptor agonists closely correlated with the observed efficacy in G protein signaling. Their interpretation was that as multiple cycles of G protein activation are possible for any given receptor:agonist binding event, faster dissociation would lead to fewer cumulative G protein activation events and thus lower efficacy.

A similar explanation would make sense in the case of our findings here. In speculatively extending this paradigm to arrestin association, it was critically noted in the M3 receptor study (Sykes, Dowling et al. 2009) that there is support for this possible explanation in a previous study of the β_2 adrenergic receptor (B2AR), in which it was demonstrated that continuous agonist occupancy is required in order to maintain arrestin association (Krasel, Bünemann et al. 2005). Given the structural role observed in the CXCL12:CXCR4 model for CRS0.5 and CRS1 overall, it seems reasonable to speculate that the distal region of CRS1 (approximately residues 1-20) would serve as a molecular “cap”, securing CXCL12 once it is bound to extend the lifetime of the signaling complex. Removal of this cap may experimentally reduce the efficacy of receptor signaling, independently of any effect on the active receptor conformation, by simply reducing the lifetime of each productive (and in the case of most of our experimental data, arrestin-recruiting) CXCL12:CXCR4 complex.

Furthermore, it may also be that a greatly increased dissociation rate of CXCL12 from CXCR4 resulting from truncation of the CXCR4 N-terminus leads to lower efficacy specifically for arrestin recruitment. Here the data are unclear, as only the longer 1-25 truncation is quantitatively biased. This suggests that CRS1 removal does indeed affect the intrinsic efficacy for both G protein and arrestin recruitment, but at the same time that removing the entirety of the CRS1 interaction is particularly compromising to arrestin recruitment.

It has recently been discovered that differential kinetics can give rise to apparent bias in the absence of genuine differences in receptor activation mechanisms between different agonists (Klein Herenbrink, Sykes et al. 2016). While G protein signaling in our calcium mobilization assay is very rapid and transient, the arrestin recruitment measured in our BRET assay does not reach a maximal plateau until 7-10 minutes after receptor stimulation, so it would stand to reason that an off-rate-specific effect would have a more significant effect in arrestin recruitment experiments.

The equiactive bias estimates reported in chapter 5 are subject to large error in the cases of severely compromised mutants, so the quantifications of bias in our results can only be tentatively interpreted. However much the effects of the mildly biasing ECL2 mutations and CRS1 truncation reflect genuine differences in the receptors efficacy of coupling to the different effectors, a kinetic explanation for the effect of the CXCR4 N-terminal truncations would provide a clear structural explanation for the case of G protein-biased activation of CXCR4 by the dimeric form of CXCL12 (Veldkamp, Seibert et al. 2008). As the CRS0.5 interaction features a β sheet in an identical region to part of the CXCL12 homodimer interface, it is

impossible for the dimeric form of CXCL12 to engage in this particular interaction with CXCR4. The result of this according to our speculation here would be a rapid dissociation rate for the CXCL12 dimer: CXCR4 complex, which would in turn would yield little to no arrestin recruitment.

The charge-reversed mutation of all ECL2 hairpin acidic residues produces a surprisingly large efficacy reduction in β arrestin-2 recruitment given its relative superficiality in the CXCR4 binding pocket and that it binds in the model to the globular domain of CXCL12 (and therefore at least not directly involved in the orientation of the CXCL12 N-terminus). It is also conspicuously mild in its effect in G protein signaling assays, similar to the CRS1 truncation data, although the bias factor determined for the EADD-KAKK mutant is low ($\beta = 0.19 \pm 0.15$ towards G protein activation). With the CRS1 cap hypothesis in mind, the β hairpin of ECL2 seems positioned to provide an additional stabilizing interaction along with the CRS1 cap, helping to enwrap CXCL12 directly opposite CRS1 (CRS1 and the tip of ECL2 nearly meet in the model) and provide for an overall enclosing of the complex. The function of such a “clamping” mechanism between the extreme N-terminus of CXCR4 and the ECL2 β hairpin would be to secure CXCL12 in the CXCR4 binding pocket long enough to allow for full agonism. Any clamping mechanism along these lines would likely be influenced by arrestin and G protein coupling, analogous to the recent seminal findings for the B2AR (DeVree, Mahoney et al. 2016).

Again recalling the homodimeric form of CXCL12, it is interesting to note here that when the crystal structure of the CXCL12 homodimer is overlaid with CXCL12 in the present model, the only area (other than the precise overlap between

CRS0.5 and the CXCL12 dimer interface) where it is apparent that there may be steric hindrance in the ECL2 region. The dimeric form of CXCL12 may be impaired in two different stabilizing interactions with CXCR4, rendering it an extremely short lifetime and therefore ineffective (and perhaps effectively G protein-biased) agonist. In other words, the near-zero arrestin recruitment reported for homodimeric CXCL12 (Veldkamp, Seibert et al. 2008) might represent a case of a seemingly biased dimeric agonist that ultimately differs from the monomeric form of CXCL12 only in the kinetics of its receptor interaction.

Though kinetic explanations for the CRS0.5/CRS1 truncation and ECL2 charge reversal effects are still speculative, they would seem to be the most in line with the current and long-standing CRS1/CRS2 model of chemokine receptor activation, as opposed to the straightforward traditional alternative interpretation discussed above, that the CRS1 and ECL2 interactions are important in enabling transitioning to the active receptor state. If our kinetic interpretation is correct, it suggests an important novel function for the newly modeled CRS0.5 region of chemokine:receptor complexes (Gustavsson, Wang et al. 2017), in that the interactions in this region of the complex are key in maintaining CXCL12 association with CXCR4 long enough to allow for efficacious CXCR4 signaling.

While there is no strong evidence in either direction, it is entirely possible that purely kinetic differences in chemokine oligomer/variant binding to receptors, which ultimately cause large differences in the activation of particular CXR4-mediated pathways, are yet another layer of complexity utilized for fine tuning of the chemokine system's role in immune cell migration. Either way, this would enable novel thinking

in drug development efforts targeting CXCR4. One strategy that may be enabled if there is indeed a manipulable link between CXCL12 occupancy duration and efficacy would be to extend the lifetime of the complex in order to effectively convert endogenous CXCL12 into a “super-agonist” that goes beyond competitive inhibition and effectively down-regulates receptor surface expression. The result sought would be similar to that achieved with recently generated CCL5 super-agonist derivatives that effectively sequester CCR5 for supra-physiological time periods and thereby provide strong resistance to infection by HIV-tropic HIV strains (Hartley, Dorgham et al. 2003). Indeed, it is interesting to ask in light of our results whether the reportedly biased super-agonists developed for CCR5 stabilize truly distinct biased receptor states or simply possess much longer receptor engagement half-lives.

Interestingly, the most quantitatively biased CXCR4 mutations were actually that of D262, followed by E277R mutation. Both of these residues, we can now confidently conclude, are CXCL12-engagement residues that we previously interpreted as critical to binding and orienting the CXCL12 N-terminus for receptor activation (Wescott, Kufareva et al. 2016). If there is an underlying kinetic basis for our findings of bias herein, this suggests that chemokine engagement interactions are particularly critical to maintaining the complex, at least in fully engaged active-receptor form. Obviously it is also possible, according to the more traditional interpretation of biased signaling, that the more superficial chemokine engagement interactions are specifically involved in orienting the receptor for arrestin engagement. As it is entirely possible that these deeper residues do participate in the conformational change of CXCR4 activation, either explanation seems plausible, and we are excited

to address this question along with our other hypotheses as described in the following two sections.

Understanding the coupling of G protein, arrestin, and other effectors to CXCR4

An important aspect of chemokine receptor signaling just now becoming amenable to precise modeling and study are the precise structural mechanisms of signaling effector engagement and activation. With the recent solution of both G protein-coupled (Rasmussen, DeVree et al. 2011) and arrestin-coupled (Kang, Zhou et al. 2015) states of model class A GPCRs, homology-based models of CXCR4 and other chemokine receptors engaged with G_i and β arrestin-2 are feasible, and we are currently preparing for such efforts. The interesting β arrestin-2-biased and constitutive effects of R134A mutation will help to guide and interpret these modeling attempts. We can now rapidly test new mutations in our arrestin recruitment assay, as well as potentially carry out more definitive charge swap experiments, so that we are able to generate data towards supporting and refining models of both the arrestin and G protein coupled CXCR4 ternary complexes.

This avenue of research is particularly interesting and important to understand in light of the differential effects observed for the two different signaling pathways. While the possibility of a purely temporal explanation for functionally G protein-biasing receptor perturbations makes prediction impossible, modeling the full ternary complex between CXCL12: CXCR4 and both G protein and arrestin may well reveal clear reasons for the selective effect of D262, E277, ECL2, and CRS1 perturbation on

arrestin recruitment. Even in the case that no significant differences in receptor state when engaged with the different effectors is predicted, this may contribute to explaining what appears to be an intrinsic difference in the activation of the two relevant signaling pathways when considered along with data derived from the experimental efforts described in the next section.

Future experiments

In order to gain confidence that receptor reserve is the explanation for the frequently apparent discrepancies between our Ca^{2+} mobilization and BRET results, we are currently developing simple experiments that will allow us to confirm receptor reserve by comparing the results of irreversibly inhibiting a small proportion of cell surface CXCR4 in both of our experimental systems. Moving forward, in order to more definitively the question of bias, we will implement alternative measurements of G protein signaling such as luciferase fragment complementation-based direct G protein activation assays and BRET-based direct receptor:G protein association assays.

In order to directly observe real-time transitioning of CXCR4 between active and inactive states, as well as the effect of agonist addition to this process, we are currently in the preliminary stages of developing single molecule experiments that rely on signaling-competent chemokine receptors stabilized in nanodiscs. Studying the mutants via this method would allow direct testing of our speculative explanations for impaired signaling based in chemokine:receptor complex lifetime. The single molecule fluorescence receptor labeling sites successfully used so far for the B2AR

were such that distinguishable activation signatures for G protein activation versus arrestin recruitment/activation were observed, and this may aid in understanding any true structural bias underlying our results.

We will also independently determine equilibrium binding as well as kinetic parameters for the binding of CXCL12 to WT, mutant, and truncated CXCR4 constructs in our experimental cells, with the ultimate goal of quantitatively assessing bias using the most rigorous and reliable method available, direct operational model calculations (Rajagopal, Ahn et al. 2011). The kinetic and equilibrium binding assays can also be used in combination to determine whether there is an increase in the rate of CXCL12 dissociation from CXCR4 when, for example, CRS1 is truncated.

References

Benredjem, B., M. Girard, D. Rhainds, G. St-Onge and N. Heveker (2017). "Mutational Analysis of Atypical Chemokine Receptor 3 (ACKR3/CXCR7) Interaction with Its Chemokine Ligands CXCL11 and CXCL12." *J Biol Chem* **292**(1): 31-42.

DeVree, B. T., J. P. Mahoney, G. A. Vélez-Ruiz, S. G. Rasmussen, A. J. Kuszak, E. Edwald, J. J. Fung, A. Manglik, M. Masureel, Y. Du, R. A. Matt, E. Pardon, J. Steyaert, B. K. Kobilka and R. K. Sunahara (2016). "Allosteric coupling from G protein to the agonist-binding pocket in GPCRs." *Nature* **535**(7610): 182-186.

Ehlert, F. J. (2008). "On the analysis of ligand-directed signaling at G protein-coupled receptors." *Naunyn Schmiedebergs Arch Pharmacol* **377**(4-6): 549-577.
Ehlert, F. J., M. T. Griffin, G. W. Sawyer and R. Bilon (1999). "A simple method for estimation of agonist activity at receptor subtypes: comparison of native and cloned M3 muscarinic receptors in guinea pig ileum and transfected cells." *J Pharmacol Exp Ther* **289**(2): 981-992.

Griffin, M. T., K. W. Figueroa, S. Liller and F. J. Ehlert (2007). "Estimation of agonist activity at G protein-coupled receptors: analysis of M2 muscarinic receptor signaling through Gi/o, Gs, and G15." *J Pharmacol Exp Ther* **321**(3): 1193-1207.

Gustavsson, M., L. Wang, N. van Gils, B. S. Stephens, P. Zhang, T. J. Schall, S. Yang, R. Abagyan, M. R. Chance, I. Kufareva and T. M. Handel (2017). "Structural basis of ligand interaction with atypical chemokine receptor 3." Nat Commun **8**: 14135.

Hartley, O., K. Dorgham, D. Perez-Bercoff, F. Cerini, A. Heimann, H. Gaertner, R. E. Offord, G. Pancino, P. Debré and G. Gorochov (2003). "Human immunodeficiency virus type 1 entry inhibitors selected on living cells from a library of phage chemokines." J Virol **77**(12): 6637-6644.

Kang, Y., X. E. Zhou, X. Gao, Y. He, W. Liu, A. Ishchenko, A. Barty, T. A. White, O. Yefanov, G. W. Han, Q. Xu, P. W. de Waal, J. Ke, M. H. Tan, C. Zhang, A. Moeller, G. M. West, B. D. Pascal, N. Van Eps, L. N. Caro, S. A. Vishnivetskiy, R. J. Lee, K. M. Suino-Powell, X. Gu, K. Pal, J. Ma, X. Zhi, S. Boutet, G. J. Williams, M. Messerschmidt, C. Gati, N. A. Zatsepin, D. Wang, D. James, S. Basu, S. Roy-Chowdhury, C. E. Conrad, J. Coe, H. Liu, S. Lisova, C. Kupitz, I. Grotjohann, R. Fromme, Y. Jiang, M. Tan, H. Yang, J. Li, M. Wang, Z. Zheng, D. Li, N. Howe, Y. Zhao, J. Standfuss, K. Diederichs, Y. Dong, C. S. Potter, B. Carragher, M. Caffrey, H. Jiang, H. N. Chapman, J. C. Spence, P. Fromme, U. Weierstall, O. P. Ernst, V. Katritch, V. V. Gurevich, P. R. Griffin, W. L. Hubbell, R. C. Stevens, V. Cherezov, K. Melcher and H. E. Xu (2015). "Crystal structure of rhodopsin bound to arrestin by femtosecond X-ray laser." Nature **523**(7562): 561-567.

Klein Herenbrink, C., D. A. Sykes, P. Donthamsetti, M. Canals, T. Coudrat, J. Shonberg, P. J. Scammells, B. Capuano, P. M. Sexton, S. J. Charlton, J. A. Javitch, A. Christopoulos and J. R. Lane (2016). "The role of kinetic context in apparent biased agonism at GPCRs." Nat Commun **7**: 10842.

Krasel, C., M. Bünemann, K. Lorenz and M. J. Lohse (2005). "Beta-arrestin binding to the beta2-adrenergic receptor requires both receptor phosphorylation and receptor activation." J Biol Chem **280**(10): 9528-9535.

Rajagopal, S., S. Ahn, D. H. Rominger, W. Gowen-MacDonald, C. M. Lam, S. M. Dewire, J. D. Violin and R. J. Lefkowitz (2011). "Quantifying ligand bias at seven-transmembrane receptors." Mol Pharmacol **80**(3): 367-377.

Rasmussen, S. G., B. T. DeVree, Y. Zou, A. C. Kruse, K. Y. Chung, T. S. Kobilka, F. S. Thian, P. S. Chae, E. Pardon, D. Calinski, J. M. Mathiesen, S. T. Shah, J. A. Lyons, M. Caffrey, S. H. Gellman, J. Steyaert, G. Skinotis, W. I. Weis, R. K. Sunahara and B. K. Kobilka (2011). "Crystal structure of the β_2 adrenergic receptor-Gs protein complex." Nature **477**(7366): 549-555.

Shukla, A. K., K. Xiao and R. J. Lefkowitz (2011). "Emerging paradigms of β -arrestin-dependent seven transmembrane receptor signaling." Trends Biochem Sci **36**(9): 457-469.

Strachan, R. T., J. P. Sun, D. H. Rominger, J. D. Violin, S. Ahn, A. Rojas Bie Thomsen, X. Zhu, A. Kleist, T. Costa and R. J. Lefkowitz (2014). "Divergent transducer-specific molecular efficacies generate biased agonism at a G protein-coupled receptor (GPCR)." J Biol Chem **289**(20): 14211-14224.

Sykes, D. A., M. R. Dowling and S. J. Charlton (2009). "Exploring the mechanism of agonist efficacy: a relationship between efficacy and agonist dissociation rate at the muscarinic M3 receptor." Mol Pharmacol **76**(3): 543-551.

Sykes, D. A., D. M. Riddy, C. Stamp, M. E. Bradley, N. McGuinness, A. Sattikar, D. Guerini, I. Rodrigues, A. Glaenzel, M. R. Dowling, F. Mullershausen and S. J. Charlton (2014). "Investigating the molecular mechanisms through which FTY720-P causes persistent S1P1 receptor internalization." Br J Pharmacol **171**(21): 4797-4807.

Veldkamp, C. T., C. Seibert, F. C. Peterson, N. B. De la Cruz, J. C. Haugner, H. Basnet, T. P. Sakmar and B. F. Volkman (2008). "Structural basis of CXCR4 sulfotyrosine recognition by the chemokine SDF-1/CXCL12." Sci Signal **1**(37): ra4.

Wescott, M. P., I. Kufareva, C. Paes, J. R. Goodman, Y. Thaker, B. A. Puffer, E. Berdougo, J. B. Rucker, T. M. Handel and B. J. Doranz (2016). "Signal transmission through the CXC chemokine receptor 4 (CXCR4) transmembrane helices." Proc Natl Acad Sci U S A **113**(35): 9928-9933.